

LOCALIZATION OF SOURCES OF
HUMAN EVOKED RESPONSES

Thesis by
Robert Nicholas Kavanagh

In Partial Fulfillment of the Requirements
for the Degree of
Doctor of Philosophy

California Institute of Technology
Pasadena, California

1972

(Submitted July 6, 1971)

ACKNOWLEDGEMENT

I would like to sincerely thank my advisor, Dr. Derek H. Fender for his guidance throughout this research. Besides being my tutor and source of inspiration, he also spent many hours helping me to make this thesis as readable as possible.

Fellow students are also to be relied upon for encouragement and technical assistance. I have been fortunate to know at least one physicist, Stewart Loken; one wizard of all things optical, Cary Lu; one healer of psychological lesions, Bill Dodson; and two gentlemen who were always willing to listen and suggest reasonable things, Bill Hill and Gaetan St-Cyr. I wish to give special thanks to Tony Goodwin, my office mate, who shared many technical discussions and also proofread the thesis.

Individual thanks also go to Dr. W. R. Smythe for his many helpful suggestions in developing the theoretical models; to Roberta Duffy and Dee Van Ingen who typed the final copy and finally to my wife Carol, who never complained about subordinating her needs to the production of this thesis.

This work was supported by NIH Grant GM 01335, which also provided a Traineeship for my own financial support during the time I spent at Caltech.

ABSTRACT

The evoked response, a signal present in the electroencephalogram when specific sense modalities are stimulated with brief sensory inputs, has not yet revealed as much about brain function as it apparently promised when first recorded in the late 1940's. One of the problems has been to record the responses at a large number of points on the surface of the head; thus in order to achieve greater spatial resolution than previously attained, a 50-channel recording system was designed to monitor experiments with human visually evoked responses.

Conventional voltage versus time plots of the responses were found inadequate as a means of making qualitative studies of such a large data space. This problem was solved by creating a graphical display of the responses in the form of equipotential maps of the activity at successive instants during the complete response. In order to ascertain the necessary complexity of any models of the responses, factor analytic procedures were used to show that models characterized by only five or six independent parameters could adequately represent the variability in all recording channels.

One type of equivalent source for the responses which meets these specifications is the electrostatic dipole. Two different dipole models were studied: the dipole in a homogeneous sphere and the dipole in a sphere comprised of two spherical shells (of different conductivities) concentric with and enclosing a homogeneous

sphere of a third conductivity. These models were used to determine nonlinear least squares fits of dipole parameters to a given potential distribution on the surface of a spherical approximation to the head. Numerous tests of the procedures were conducted with problems having known solutions. After these theoretical studies demonstrated the applicability of the technique, the models were used to determine inverse solutions for the evoked response potentials at various times throughout the responses. It was found that reliable estimates of the location and strength of cortical activity were obtained, and that the two models differed only slightly in their inverse solutions. These techniques enabled information flow in the brain, as indicated by locations and strengths of active sites, to be followed throughout the evoked response.

TABLE OF CONTENTS

Chapter	Title	Page
I	Introduction	1
II	Experimental Methods and Preliminary Data Presentation	26
III	The Dimensionality of the Human Visual Evoked Response	62
IV	Models of Evoked Response Generators as Dipoles in Homogeneous and Non-homogeneous Spheres	111
V	Equivalent Dipoles for Human Visually Evoked Responses	155
VI	Discussion	218
	Appendices	
	A. The Dipole in a Homogeneous Sphere	239
	B. The Dipole in a Homogeneous Sphere Surrounded by Two Concentric Shells of Different Conductivities	253
	C. Details of Preliminary Data Re-Formatting	274

I. INTRODUCTION

As an undergraduate, the author once attended a physics lecture during which elementary electronics was discussed. During the lecture the instructor mentioned some of the more common electronic devices, including the capacitor. At this point one of the students raised his hand and said he had never seen nor heard of such a device, and could the instructor please describe one in more detail. The rather perplexed lecturer asked if it was really true that the student had no idea of the nature of a capacitor and was quite apparently disappointed when the student reaffirmed his lack of experience. Perhaps to recover his confidence by passing the whole affair off lightly, the instructor quickly drew the standard representation of a capacitor, 2 parallel lines, on the blackboard and said as sincerely as was possible to the troublesome student "If you have indeed never seen one before, THERE'S ONE!".

The foregoing anecdote is somewhat allegorical, for just as the beginning student of physics had difficulty in ascertaining what possible functional information concerning the capacitor is related by two parallel lines on a blackboard, so the modern student of neurophysiology is uncertain about the meaning of the biological signal whose analysis is discussed in this thesis, the evoked response. Just as the schematic representation of the capacitor is only a symbol for all of the properties ascribed to the device,

the evoked response is in many ways only symbolic of processes and properties not at all revealed by the tracing of the response itself. The motivation for this thesis was to search out some of the hidden meaning; some of the generic make-up of the human visual evoked response. To begin, a brief outline of some of the neurophysiological milestones which led to the discovery of evoked responses is given.

1. The Beginnings of Recording Brain Activity

The study of neurophysiology in its broadest sense has a long history; excellent summaries have been written and are recommended reading for neophytes in almost all scientific disciplines. Two articles by Brazier (1, 2) in particular, provide insight into some of the early concepts of neurological structures and processes.

Electroencephalography itself is a comparatively young branch of neurophysiology. Probably the first man to record neurological signals which would be called EEG activity was Richard Caton (6), who in 1875 described his observations of electrical phenomena in exposed rabbit brain. That he chose the rabbit was fortuitous, for the recording instruments of the day had such a low frequency response that the slow waves of the rabbit brain were more likely to be sensed than the higher frequency activity of other animals. Caton's work was especially prophetic in that not only did he record the spontaneous activity of the rabbit brain but also probably elicited that which we now refer to as

evoked responses, since he did excite the visual system with brief stimuli, in attempting to locate specific sensory areas.

Fifteen years later, in Krakow Poland, Adolf Beck (4) independently discovered spontaneous activity in dogs, apparently not knowing of the work of Caton in 1875. Along with other investigators, Beck nurtured the growing science of brain wave recording into the twentieth century and beyond, but the literature was conspicuously quiescent for some thirty years.

In 1929 Hans Berger (5) became the first to record, from the intact skull, electroencephalographic potentials in normal man and gave the names alpha and beta to its two principal rhythms. His work began what is now called clinical electroencephalography.

The recording of the EEG is now common practice. Clinical electroencephalographers use these traces as diagnostic tools in the detection of epilepsy and some tumor development. Even in this age of mechanization, however, EEG recording does not enjoy a large degree of formalism and rigorous interpretation techniques. The EEG signal, or spontaneous activity as it shall be referred to, is a very complex process. It is greatly influenced by the psychic as well as the physical state of an individual. Some very marked abnormalities in the spontaneous activity can be correlated with pathological conditions, but in general the clinician's subjective analysis is not capable of detecting the plethora of subtle events in a human EEG.

This is not to say that rigorous analyses have not been successfully attempted. Spectral analysis of the EEG has revealed much information about the basic rhythms present. While there are some cautions to be observed concerning possible errors caused by inadequate sample length (18), it seems certain that this type of time series analysis will continue to be useful in EEG studies. Other analytical tools such as correlation theory and factor analysis have also been used, but most of these more objective analyses of spontaneous activity are in their "formative" stages.

An example of spontaneous activity is shown in Figure 1-1. It is characterized by relatively large amplitude, low frequency activity when the attention of the subject is low, and lower amplitude, higher frequency activity as the level of alertness increases. Recordings made from the scalp typically lie in the range $\pm 50 \mu v$, with very little measurable energy above 50 Hz in frequency.

In this study no attempt will be made to analyze spontaneous EEG, and in fact it will be regarded as "noise." The focus of attention is rather on a particular event in the EEG which can be elicited in a relatively controlled fashion, the evoked response.

2. What is an Evoked Response and how is it Recorded?

Before mentioning some of the early work in evoked potentials, let us define what is meant by the term. Briefly one

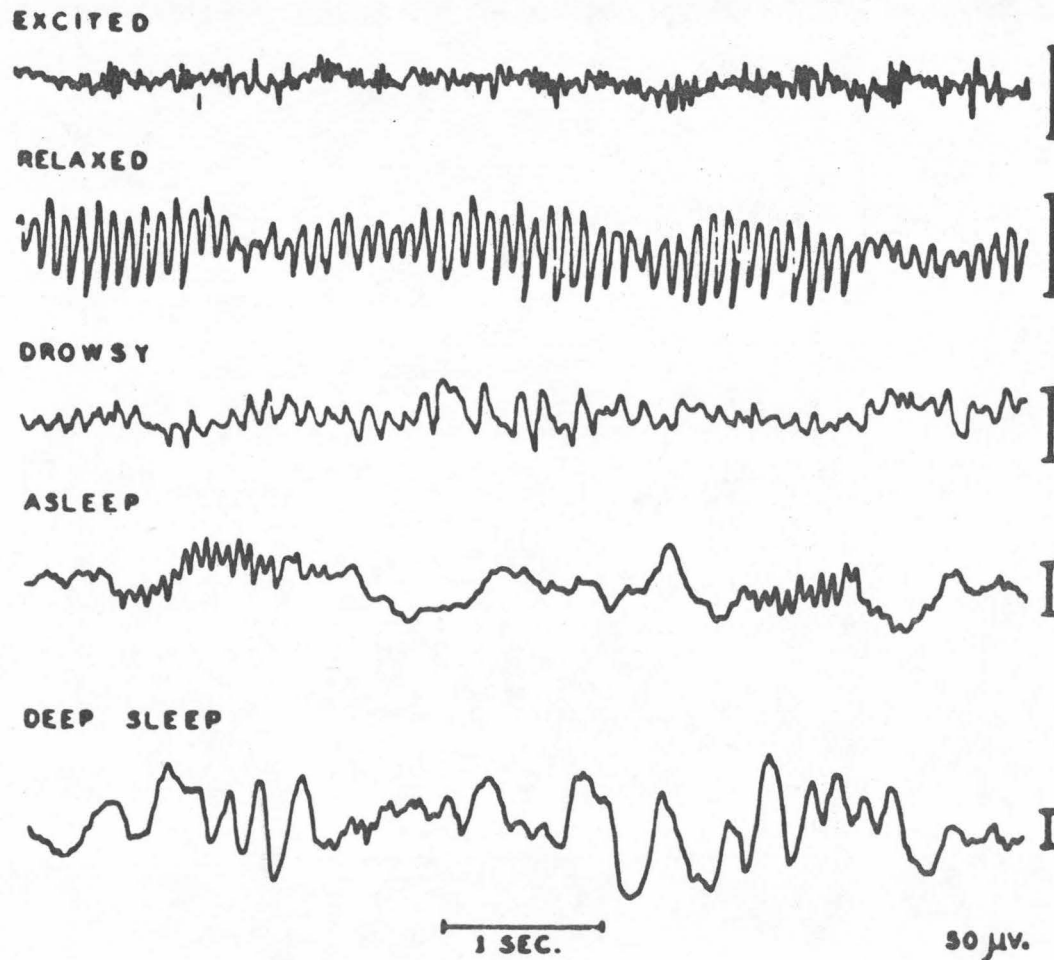


Figure 1-1. Spontaneous EEG activity in the human at different levels of alertness. From Jasper (13).

could say that an evoked potential, or evoked response, is that component of the EEG which can reliably be identified as the response to a brief stimulus to one of the sense modalities. Further, this response is definitely time-locked to the occurrence of the stimulus.

This definition says many things. Obviously it suggests that the evoked response is recorded with much the same equipment used to record spontaneous EEG. Secondly, one must emphasize the qualification regarding the cause and effect relationship with the stimulus. Successive presentations of a given stimulus should produce identical responses. It will be seen that in actual experimental conditions the average of many responses to the same stimulus is in fact identified as the evoked response. Our experience suggests that generally there is little difference between the average of the first half of say 100 responses and the average of the second half, hence this stimulus-response relationship seems to be an experimentally verified aspect of the definition.

Note that practically one can record evoked responses from only three sense modalities. Since it is difficult to arrange a brief stimulus of either smell or taste, we are left with the so-called visual evoked response or visual evoked potential (VER or VEP), the acoustic evoked response (AER or AEP) and the somatosensory evoked response (SER) which is obtained by direct electrical stimulation of a peripheral sensory nerve.

The spontaneous activity constitutes the background from which the evoked response must be extracted. If a 2-3 μ sec light flash is presented to a subject, an electrical event lasting some 300 ms occurs in the EEG. The detection problem is that evoked responses recorded from the scalp usually do not exceed $\pm 5 \mu$ v, and hence are almost impossible to "see" because of the larger amplitude spontaneous activity. The responses are more easily seen of course when recordings are taken from exposed cortex, but detection through the intact skull has had to await the improvement of recording techniques, Dawson (7), in 1947, was the first to use signal averaging techniques to improve the signal to noise ratio. His technique was to superimpose the activity immediately following several stimuli on an oscilloscope screen and thus achieve enhancement of the signal.

Today the same principal is used in a slightly different manner. Many stimuli are presented and a trigger signal at stimulus onset time is used to initiate the "sweep" of a small computer specially designed to do signal averaging. The computer then samples the signal (spontaneous background activity plus evoked response) at regular intervals (say one ms) for the expected duration of the evoked response (say 250 ms). The samples taken during the first sweep are stored in some digital storage medium and the sampled responses to successive stimuli are then summated with all previous samples. In this way activity which is correlated in time with the stimulus (the evoked response) tends to be

additively enhanced while non-correlated activity (the spontaneous EEG) averages to zero for a sufficiently large number of stimuli (usually 80 to 100 for visually evoked responses).

In order to see this, consider that the response recorded after a single stimulus is composed of two parts, the "signal" (the evoked response) and the "noise" (the background spontaneous activity); i. e., let

$$f(t) = s(t) + n(t)$$

be the recorded signal, where $s(t)$ is the evoked response and $n(t)$ is the noise. The noise term can be considered to be Gaussian, with mean zero and variance σ^2 . After averaging the responses to several stimuli, however, consider the expected value of $f(t)$:

$$\begin{aligned} E[f(t)] &= E[s(t) + n(t)] \\ &= E[s(t)] + E[n(t)] \end{aligned}$$

It is assumed that the evoked response is constant over successive stimuli, hence, since $E[n(t)] = 0$,

$$E[f(t)] = s(t)$$

Moreover, define the signal to noise ratio to be the r. m. s. value of the signal divided by the r. m. s. value of the noise. For some sample time, say t_i , the r. m. s. value of the signal is simply $s(t_i)$, while that for the noise is σ . Therefore, at each point t_i of the response to a single stimulus, the signal to noise ratio is $s(t_i)/\sigma$. After averaging say n responses, however, the noise r. m. s. value is decreased by a factor $1/\sqrt{n}$ while the r. m. s.

value of the signal is still $s(t_1)$. Hence, the signal to noise ratio after averaging is $s(t_1) \cdot \sqrt{n}/\sigma$, an improvement of \sqrt{n} .

The spontaneous EEG is probably not Gaussian distributed over short intervals, but over several successive stimuli this assumption becomes more and more acceptable. Slight departures from these assumptions are not, however, sufficient to negate the validity of this averaging technique.

3. The Challenge of the Evoked Response

The above and similar techniques have led many investigators, in the score of years since Dawson refined his techniques, to an exciting yet frustrating conclusion. Recordings on many human subjects have shown unquestionably that a given subject in a constant experimental condition will give evoked responses of high repeatability. Experiments repeated over a period of perhaps weeks show this enticing reliability of the response of a given subject to the same stimulus. Figure 1-2 exemplifies this fact: the responses for each subject are presented as the mean response over consecutive sessions closely bracketed by the mean plus or minus one standard deviation. There is a noticeable difference between subjects, yet the appeal of the evoked response lay in its within-subject reliability. It seemed certain that it must provide some tool for understanding the processes of the brain. Some of the diverse experimental results to date have been that certain characteristics of the evoked response can be correlated with visual stimulus complexity (15); that latencies of

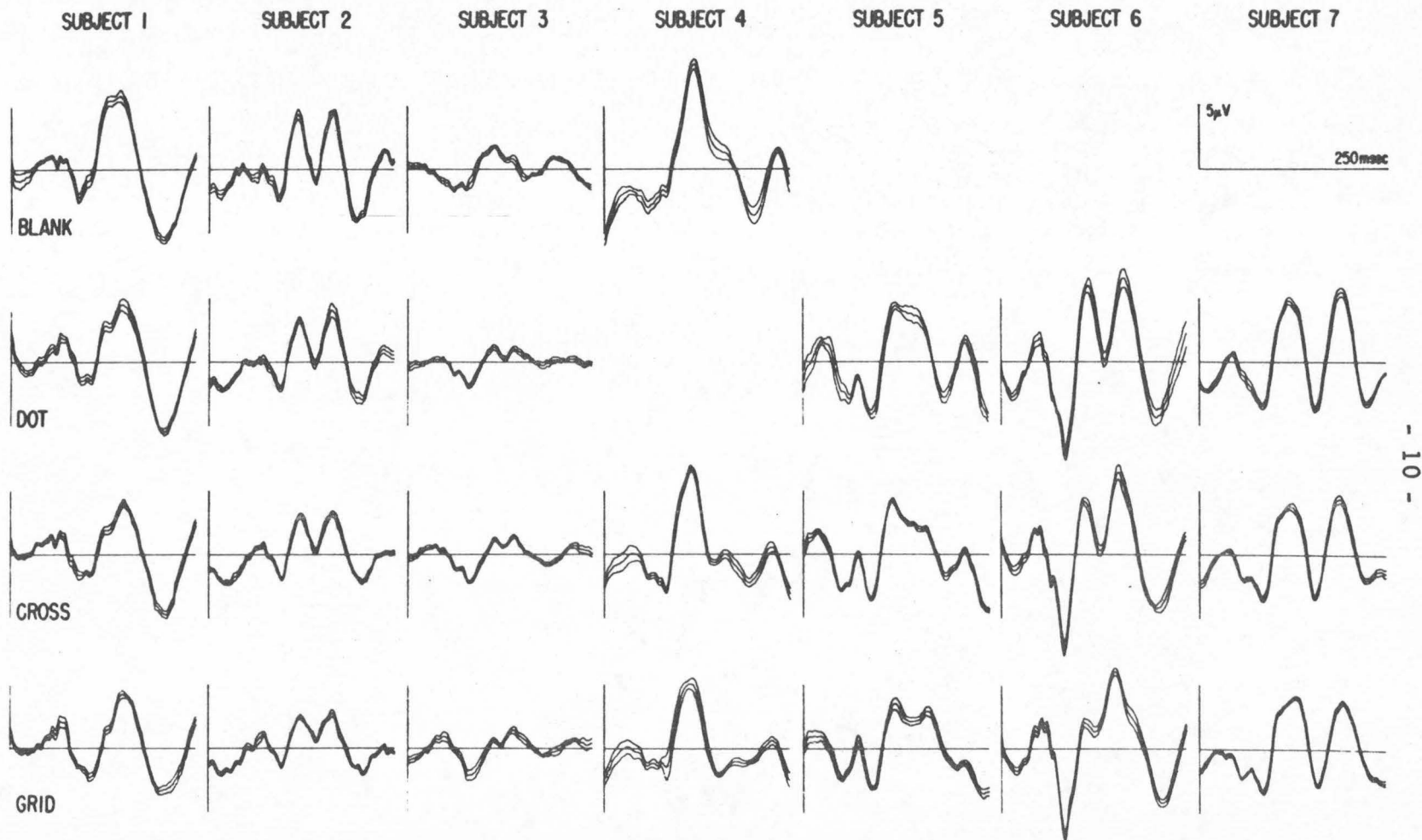


Figure 1-2. Evoked responses of 7 subjects to 4 different visual stimuli. Curves shown are the mean responses to several replications of the same stimulus, plus and minus one standard deviation. From Lehmann and Fender (15).

certain peaks in the response are dependent upon decision-making by the subject (23); and even that the shape of the visual evoked response in cats is directly related to the probability of firing of single cells in the visual cortex (9). Despite these and other valuable building blocks, however, a recent review by Lindsley (17) realistically admits that evoked response research has thus far failed to open any doors to great neurological insights.

There are many reasons for the slow advance of understanding in this area. Some are technical in nature, such as the difficulty in comparing results from one experimenter with those of another. Many investigators still consider upward deflections on an oscilloscope to denote negativity, making it necessary to mentally "flip" their recording to agree with normal polarity conventions. In addition, it is very difficult to report precisely the locations of recording electrodes. The so-called 10-20 electrode system (12) is an attempt to produce a standard reference system, but it still remains for the experimenter to place his electrodes accurately according to this or any other reference scheme. What is desired perhaps is some form of stereotaxic instrument for electrode placement. In short, variations in recording technique have somewhat confused the evoked response literature.

Besides these instrumentation problems, the subject himself is a source of considerable variation in results. It has been stated that there is great variability between subjects for a

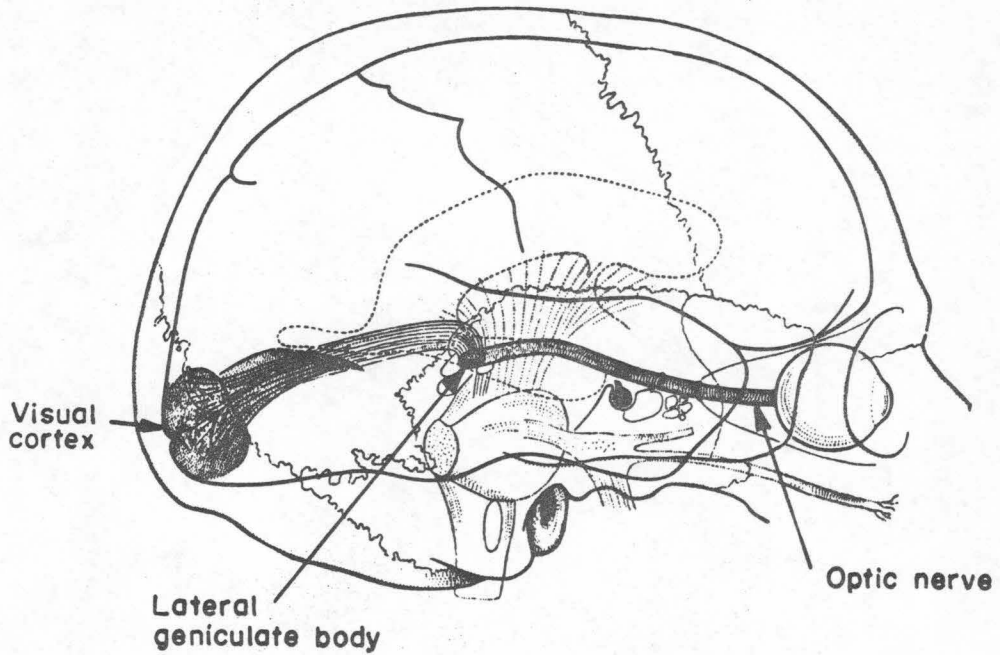
given experiment. A human is such a profusion of neurological responses to his environment that obviously the psychological and neurological states of different subjects cannot be expected to be identical even in the same experimental environments. It would seem that very often the evoked response is as individual as the subject's signature, and these large differences between subjects could obscure any common facets of the response pattern.

There are thus a myriad of confusing features of an evoked response. Even after attempting to eliminate the spontaneous EEG from the recording, what remains is a very complex signal. In spite of the repeatability of the signal, there are today very few inferences that can be made concerning the relationship between the evoked response and the cortical processes underlying it.

4. Neuro-anatomical Origin of the Evoked Response

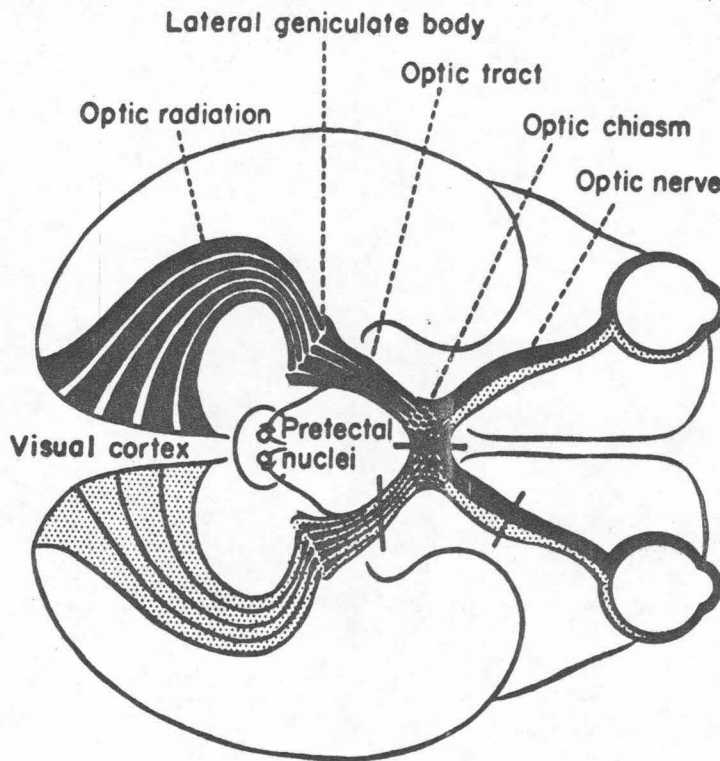
The gross features of the human visual nervous system are shown in Figure 1-3. Briefly, we see that afferent information passes from the retina to the primary visual cortex, passing on the way through a sub-cortical relay station, the lateral geniculate body. A partial bifurcation of the optic nerve occurs at the optic chiasm, where fibers originating from the nasal retinae cross one another, resulting in representation of the left visual field in the right half of the brain and vice-versa. This reversal of topology is common in many nervous systems.

Innervation from the retina is conducted as shown to the primary visual cortex, so-called area 17. Activity in this area



(a)

Figure 1-3. Gross anatomy of visual nervous system
(a) Right side view (b) Top view



(b)

does influence the "visual association areas"---areas 18 and 19, but precise description of the spatial and temporal connections along this path are of course difficult to obtain. Similarly it seems certain that information is shared between the hemispheres across the corpus collosum, but again the histological tracing of this sensory route is slow to obtain.

In addition to not knowing the total spread of visually excited pathways, the function of each site along the way will not be completely described until many more studies are done. The optic tracts quite apparently pass through the lateral geniculate bodies and make synaptic contacts there, but the role of this intermediate station is understood only up to the point of being some type of "relay" center.

Finally, the temporal course of events in the visual nervous system is again unclear. Studies of retinal delay time have shown that parameter to be dependent upon stimulus intensity, ranging from 20 to 35 ms at low stimulus levels to about 5 ms at higher levels (22). The overall delay time from stimulus to appearance of correlated activity in the cortex has been estimated at 35 - 40 ms (22). Beyond these gross features, however, the timing of events along the visual pathway also appeals to further experimentation.

The other extreme of organization of the visual nervous system, at the neuronal level is shown in Figure 1-4. Histological evidence here tells us that the cortex is organized in columns of cells, perpendicular to the surface of the cortex. Information-

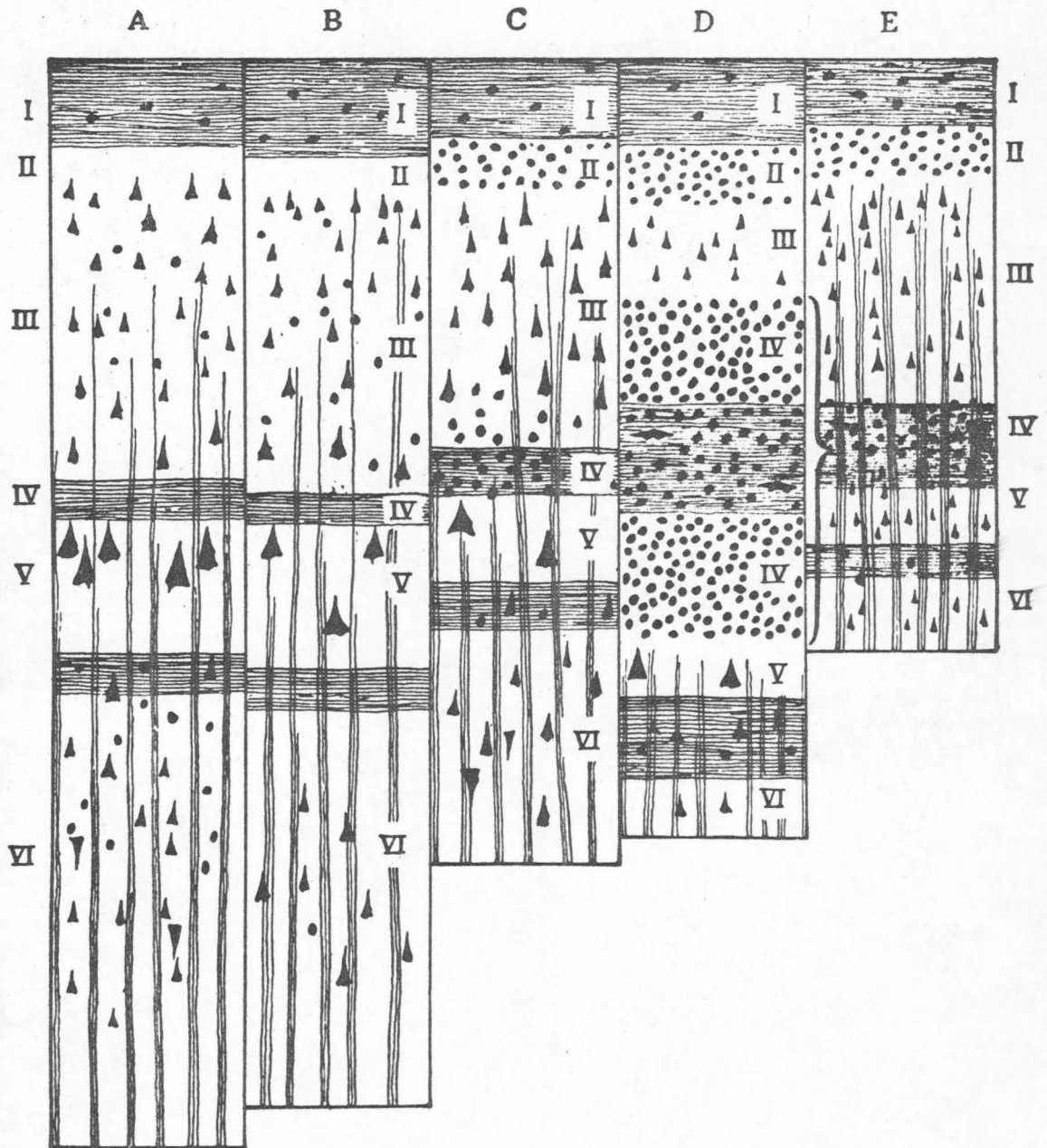


Figure 1-4. Organization at the neuronal level in various types of cortex. A. Motor cortex, B. Pre-motor cortex, C. Sensory cortex, D. Sensory visual cortex, E. Visual association cortex. From Duke-Elder (8).

carrying connections are made both parallel to the axis of the columns and transverse to it (parallel to the surface of the cortex). The problem at this stage of course is to adequately catalogue even a small number of neurones, complete with a careful mapping of their origins and destinations within the brain.

Thus there are two anatomical extremes presented by Figures 1-3 and 1-4. Neither level of organization is adequately understood, and of course knowledge of the neuronal level is precursory to filling in gaps at the gross level. On the one hand, studies of the properties of single neurones continue to define the basic properties of these fundamental neural building blocks. The classic work of Hubel and Weisel (11) and Lettvin et al. (16) are good examples of this methodical study of single cells. Work on the gross features, on the other side of the problem, also continues with gross EEG recordings and similar studies. The conceptual problem is to be able to extrapolate gross behavior from single neurone properties or vice-versa. Certainly models of nervous networks, based on known cellular properties, have been made and are viable tools. These models, however, seldom include more than say 100 neurones, and it is difficult to imagine even the largest of computers being capable of extending these "synthetic" studies to any reasonable fraction of the entire nervous system. Similarly, it is very unlikely that current studies of gross activity will shed very much more light on single cell properties. The spontaneous EEG is such a cacaphony of activity, and as measured

the activity is the averaged or lumped effects of so many cells, that it seems ludicrous to think of identifying the effect of any single neurone.

It is not the purpose of this thesis to demonstrate that these two approaches to studying the nervous system can be brought to collide head-on. Rather it is hoped that the studies here will suggest a method of bridging in some small part this gap in interpretation of available data. The method by which this will be attempted is to study the activity of some restricted but still large population of neurones. The visual evoked response is after all quite specific to visual activity. By studying this event at many more sites on the scalp than previously attempted it is hoped that some new interpretive skills can be developed.

The difficulty in understanding the causal relationships between complicated nervous structures and their external electrical manifestations cannot be overstated. The question is: what really is measured by a gross electrode which records transcranial electrical activity? To be sure millions of individual neurones are active at any one time, and the manner in which the activity of each is combined, distorted, attenuated and otherwise manipulated before being sensed by a single electrode on the scalp is complex to say the least. There are many controversies which have sprung from this enormous interpretive difficulty. Space and time permit only those of direct significance to the present work to be discussed.

Firstly, does the scalp EEG represent the summated effects of neuronal action potentials, or does it arise from the multitude of post-synaptic or generator potentials in the cortex? Observe that most arguments that support one of these two hypotheses must also support the other - an increase in post synaptic potential activity must of necessity engender an increase in the number of action potentials and vice-versa. Even if influence in the brain is much more inhibitory than excitatory, a strong correlation still prevails except it is negative. A report by Fox and O'Brien (9) has considerable import in this matter. These authors recorded single unit activity with a microelectrode, then destroyed the neurone being studied and subsequently recorded average evoked responses within the same region of the cortex with the same electrode. Their results showed that the shape of the post-stimulus histogram of single unit activity was practically identical to the shape of the average evoked response. These conclusions were made quite subjectively; the authors did not in fact test in any statistical manner the hypothesis that the two curves were linearly related. It is perhaps fortunate that the two curves appeared so similar: if say, the evoked response was actually proportional to the logarithm of single spike activity, the curves would not be so similar and an important result might be overlooked. In any event, however, a correlation between single spike activity and the evoked response can reinforce either of the two hypotheses.

There are two observations which could perhaps buoy up the idea that EEG activity comes from synaptic potentials. First it has already been mentioned that very little energy is found above 50 Hz in a typical EEG. Since action potentials have rise times less than a millisecond long one could say that the very absence of high frequency activity rules out the influence of single spike activity on EEG. Also it is said (21) that over 90 percent of the average neuronal surface area is dendritic, hence by virtue of such a large number of synaptic sites the greater component of the EEG must arise from these generator potentials.

Countering the idea that single spike activity is absent from the scalp activity is again the realization that millions of neurones are likely to be firing closely upon one another. The human nervous system probably does not rely on smaller populations of neurones than say 10^5 to process sensory inputs. No matter how insignificant the stimulus, many thousands of neurones are likely to be regimented into activity. Hence, it is still perhaps the "envelope" of all such action potentials that is recorded and it only remains for recording techniques to improve in order to resolve the individual neural spikes omnipresent in the EEG.

The presence of dendritic contributions to the electric potentials measured on the scalp is almost inescapable. While smaller in magnitude than fully developed action potentials, a great deal of summation of these small potentials is possible. Whether these generator potentials predominate in EEG activity is still,

however, a subject requiring further study. What is undertaken in this thesis does not depend on the details of ascribing the makeup of the EEG signal to the two processes above. It is sufficient that in the case of the evoked response there is some repetitive, synchronized activation of a certain population or populations of neurons during the time following the stimulus. These features are sufficient to study the evoked response from the standpoint of localizing these neurone populations within the brain.

5. Attempts at Localization of EEG Generators

As will be seen, the principal thrust of this thesis is to develop some techniques to localize equivalent cortical sites of evoked response activity. This is one of the most tantalizing prospects in electroencephalographic research. Generators of both the spontaneous activity as well as evoked responses are sought; clinical work has frequently been motivated in this direction and neurophysiologists in general have joined in the pursuit. Brazier (3) has made some attempts to locate sources of spontaneous EEG, and some tentative studies of localization of evoked response activity have appeared (e. g. Paicer, Sances and Larson (19)). These localization studies are not of course free of either conceptual or analytical problems.

One of the problems concerns the applicability of "volume conduction" to EEG phenomena. A very detailed and complete description of this theory - essentially a consideration of this electromagnetic properties of single and group neuronal activity

in their normal environments - is available in Plonsey (20). The essence of the theory is very simple: even though the current density associated with either an action potential or a synapse is maximal close to the excited site on the neurone, the current must be continuous throughout all conducting media enclosing the activity. Hence, an electrode even remote from the neural event can, by the properties of electromagnetic fields, be sensitive to the event.

The validity of the theory of volume conduction for all types of EEG activity has been questioned, as discussed in a recent report by Vaughn (21). Specifically, it is said to be difficult to apply the theory to localization of cortical generators when these generators are large in number, as is apparently the case with spontaneous activity. When study is confined to evoked responses, however, the situation is described as much ameliorated, since there is evidence (14) to suggest that the scalp potentials recorded at sites remote from primary projection areas arise from volume conduction. The caution, as correctly stated, is not that increasing the number of generators invalidates the theory of volume conduction --- only that the interference between all these generators clouds any attempts to localize any or all of these active sites. In the extreme case of most spontaneous activity it seems inescapable that the cortical generators are so profuse that no existing techniques could possibly effect any localization. Since in

this thesis I am in fact dealing with only evoked response activity I embrace the applicability of the theory, along with certain other assumptions discussed in Chapter Four.

A very important instrumentation problem is apparent in localization studies. If one is to determine the most probable focus of activity giving rise to the scalp potentials it is important to record these scalp potentials over a large number of sites. In other words, one must be equipped to "map" the distribution of potentials on the head. This is not a trivial consideration by any means, and most laboratories are restricted in this regard by recording systems capable of registering fewer than ten channels.

Many more difficulties will be encountered as attempts to localize cortical generators become more and more refined, but it now appears that a certain momentum is developing toward discovering the elusive sources of EEG and evoked responses.

6. The Goals Set for this Research

In this chapter most of the salient obstacles to knowing the relationship between cortical activity and scalp EEG phenomena have been raised. In short, the neuroanatomical origin of most such phenomena is unknown. The question of synaptic activity predominating over action potentials is unresolved and requires more extensive study. As to the localization of cortical generators, it seems that at present little can be done with spontaneous activity, due to the predominantly intuitive idea that many generators are simultaneously active. Evoked responses, however,

seem to hold some promise. It will hopefully be shown that by mapping the potential field on the head and applying the volume conduction theory it is possible to locate equivalent generators for visual evoked responses.

The point is well taken that this analysis is a formidable task. This study was not undertaken in expectation of stumbling upon some chance correlation of the evoked response activity with other neurophysiological evidence. At all times the author has attempted to keep firmly in mind the actual physical constraints of the problem. Certainly some simplifying assumptions will be made, but these assumptions (concerning head shape, conductivity discontinuities, etc.) are at least consistent with as much available data as possible. The methodology is a compromise between extending rigorous mathematical treatment of the localization problem on the one hand and gathering meaningful neurological insight on the other.

REFERENCES FOR CHAPTER I

1. Brazier, M.A.B., "Rise of Neurophysiology in the 19th Century," J. Neurophysiol. 20(1957), pp. 212-226.
2. Brazier, M.A.B., "The Historical Development of Neurophysiology," Handbook of Physiology, Sec. 1 Neurophysiology 1 (1959), pp. 1-58.
3. Brazier, M.A.B., "A Study of the Electrical Fields at the Surface of the Head," Electroenceph. clin. Neurophysiol. Suppl. 2 (1949), pp. 38-52.
4. Beck, A., "Die Bestimmung der Localisation der Gehirn und Ruchenmarksfunktionin vermittelst der elektrischen Erscheinungen," Centralbl. Physiol. 4 (1890), p. 473.
5. Berger, H., "Uber das Elektrekephalogramm des Menschen," Arch. Psychiat. Nervenkr., 87 (1929), pp. 527-270.
6. Caton, R., "The Electric Currents of the Brain," Brit. Med. J. 2 (1875), p. 278.
7. Dawson, G.D., "Cerebral Responses to Electrical Stimulation of Peripheral Nerve in Man," J. Neurol. Neurosurg. Psychiat. 10 (1947), pp. 134-140.
8. Duke-Elder, S. (ed.) System of Ophthalmology Vol. II The Anatomy of the Visual System, C.V. Mosby Co., St. Louis, (1961), pp. 585-694.
9. Fox, S.S. and O'Brien, I.H., "Duplication of Evoked Potential Waveform by Curve of Probability of Firing of a Single Cell," Science 147 (1965), pp. 888-890.
10. Guyton, A. C., Textbook of Medical Physiology, W.B. Saunders Co., Philadelphia (1967), p. 746.
11. Hubel, D.H. and Wiesel, T.N., "Receptive Fields of Single Neurones in the Cat's Striate Cortex," J. Physiol. 148 (1959), pp. 574-591.
12. Jasper, H.H., "Report of the Committee on Methods of Clinical Examination in Electroencephalography," Electroenceph. clin. Neurophysiol. 10 (1958), pp. 371-375.
13. Jasper, H.H., in Penfield, W. and Erickson, T.C. (eds.), Epilepsy and Cerebral Localization, Thomas Co. Springfield (1941).

14. Kelley, D.L., Goldring, S. and O'Leary J.L., "Averaged Evoked Somatosensory Responses from Exposed Cortex in Man," Arch. Neurol. 13 (1965), pp. 1-9.
15. Lehmann, D. and Fender, D.H., "Component Analysis of Human Averaged Evoked Potentials: Dichoptic Stimuli Using Different Target Structure," Electroenceph. clin. Neurophysiol., 24 (1968), pp. 542-553.
16. Lettvin, J.Y., Maturana, H.R., Pitts, W.H. and McCulloch, W.S., "What the Frog's Eye Tells the Frog's Brain," Proc. Inst. Radio Engrs. 47 (1959), pp. 1940-1951.
17. Lindsley, D.B., "Average Evoked Potentials - Achievements, Failures and Prospects," in Donchin, C. and Lindsley, D.B. (eds.) Average Evoked Potentials -- Methods, Results, and Evaluations, NASA publ. SP-191 (1969), pp. 1-43.
18. Meshalkin, L.D. and Efremova, T.M., "Estimation of the Spectra of Physiological Processes over Short Intervals of Time," in Livanov, M.N. and Rusinov, V.S. (eds.) Mathematical Analysis of the Electrical Activity of the Brain, Harvard Univ. Press. Cambridge Mass. (1968), pp. 37-44.
19. Paicer, P.L., Sances, A. and Larson, S.J., "Theoretical Evaluation of Cerebral Evoked Potentials," Proc. 20th Ann. Conf. Engrg. in Med. and Biol. (1967), p. 14.1.
20. Plonsey, R., Bioelectric Phenomena, McGraw-Hill, New York (1969).
21. Vaughn, H.G., "The Relationship of Brain Activity to Scalp Recordings of Event-Related Potentials," in Donchin, D. and Lindsley, D.B. (eds.) Average Evoked Potentials -Methods, Results and Evaluations, NASA publ. SP-191 (1969), pp. 45-94.
22. Walter, W.G., in Hill, D. and Parr. G. (eds) Electroencephalography -- A Symposium on its Various Aspects, Macmillan Co., New York (1963), p
23. Walter, W.G., Cooper, R., Aldridge, V.J., McCallum, W.C. and Winter, A.L., "Contingent Negative Variation: And Electrical Sign of Sensorimotor Association and Expectancy in the Human Brain," Nature, 203 (1964), pp. 380-384.

II. EXPERIMENTAL METHODS AND PRELIMINARY DATA PRESENTATION

1. An Overview of the Experimental Environment

The data analyzed in this study were recorded at the Smith-Kettlewell Institute of Visual Sciences, Pacific Medical Center, in San Francisco. Much specialized equipment is necessary to record human visual evoked responses, and a cooperative effort with Dr. Dietrich Lehmann and Mr. Jules Madey at the institute was undertaken in order to acquire the necessary data.

Figure 2-1 shows the essential features of a typical experiment. The subject, stimulation apparatus and pre-amplification equipment are all situated in a shielded, darkened, sound-attenuating chamber. A troposcope display device delivers visual stimuli binocularly to the subject, and in this way various combinations of steady illumination of one or both eyes, structured patterns shown to one or both eyes and light flashes shown to one or both eyes can be achieved. Light stimuli were derived from a Grass type PS-2 photostimulator, at an intensity setting of 8.

EEG activity is monitored from Grass gold plated cup electrodes held in place with Grass type EC-2 electrode cream. Mr. Madey designed and constructed a fifty channel system for data recording; the signals are amplified and then analogue samples of each channel are multiplexed onto a seven channel, FM tape

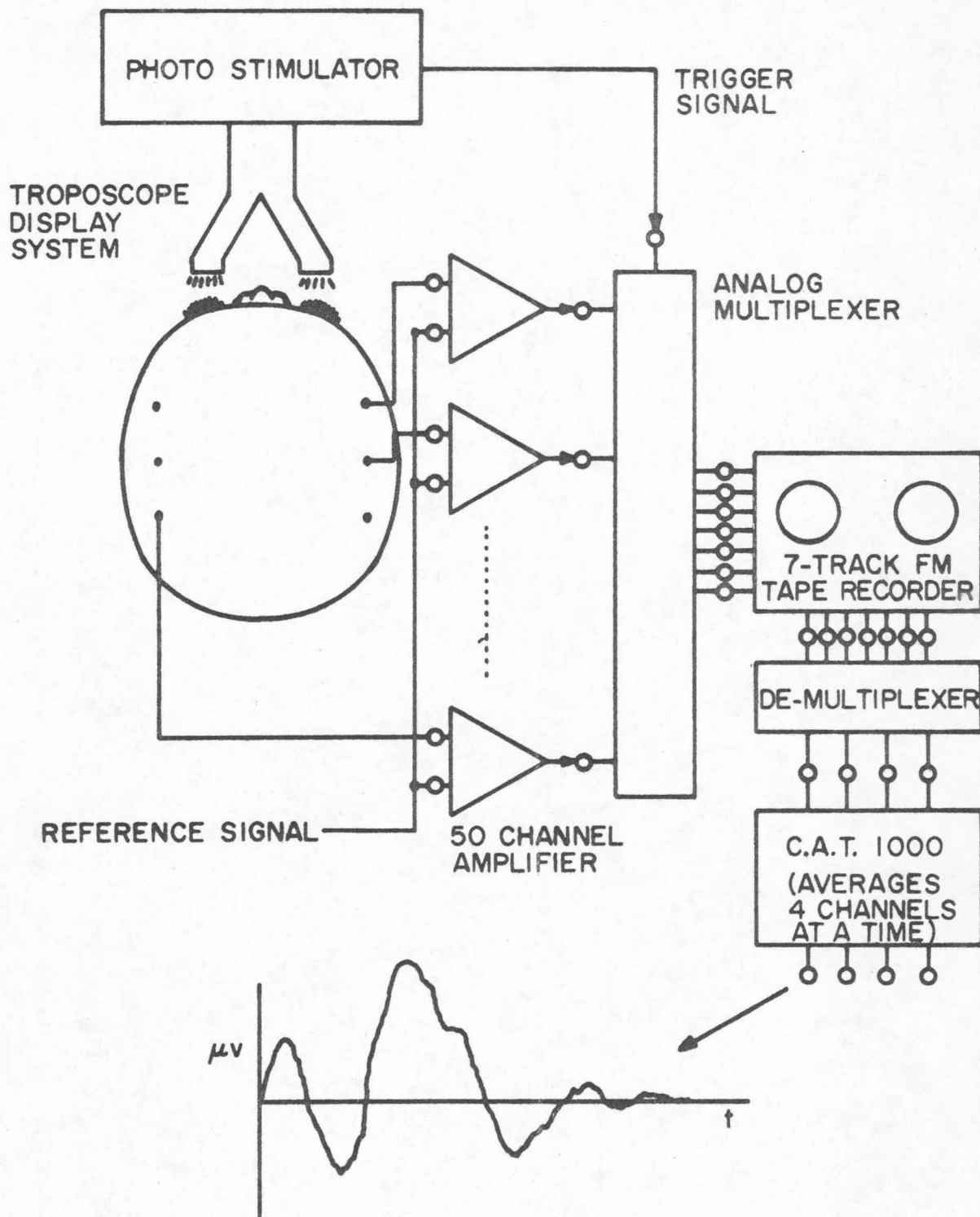


Figure 2-1. The evoked response recording system.

recorder. An entire experiment, consisting of perhaps several replications of several experimental conditions, is recorded continuously in the form of EEG data on the recorder. Also retained are signals denoting stimulus onset times and other timing information necessary to recover and average the responses from individual channels. After the data have been recorded in this way there follows a long process of averaging from stimulus onset time, for a given channel, the responses to each of eighty to one hundred flashes. This is derived by playing back the FM tape, demultiplexing the data samples and averaging in a signal averager (in this case a Computer of Average Transients, model 1000). The CAT averages four channels at a time, sampling each channel every one ms for a total of 256 ms. Finally the visual evoked responses, now in digital form, are punched onto paper tape for analysis.

In the experiments used in this study, two subjects were used: an adult male (KW) and an adult female (DALO). Both subjects were normal. Data have been recorded from more subjects (in the order of ten) than the two used here, but the results from this larger group have not yet been analyzed.

The experimental conditions were very simple--unstructured light flashes to left, right or both eyes. In the case of subject KW, 41 (monopolar) channels were recorded against a 42nd electrode

used as reference, while the DALO data were derived from thirty-eight monopolar channels using a "phantom" reference electrode to be described later.

In chapter I it was mentioned that there are many sources of variability in evoked response experiments that can be identified with the psychic and physical states of the subjects. There are some steps to be taken to head off excessive problems in this respect (3). The subject should be comfortable in the apparatus; he should be well adapted to the low ambient illumination. Dilation of the pupils is desirable in order to standardize retinal illumination by the stimuli. Recording time should be both short and constant and some fixation procedure should be used to insure stimulating identical retinal areas.

There are also many instrumentation problems involved in this type of research. How many recording channels are necessary to characterize an evoked response? What can be used as the reference or indifferent electrode for a given channel? Can all channels use the same indifferent electrode? In addition to these and other aspects of the recording environment, there are always the problems of deciding how the data can be summarized in the most meaningful manner. Some of these problems will be discussed in the remainder of this chapter.

2. The Recording System --- Why fifty Channels?

Historically, EEG data have been recorded from a relatively small number of channels, usually twelve or fewer. The influence of clinical work is quite significant, since few diagnosticians can adequately analyze by eye a large number of channels.

During the study undertaken here, however, it was possible to record up to fifty channels inexpensively, and the question of ease of analysis was not a limiting factor since a large computer was available to do all of the drudgery.

Finding inexpensive systems to record up to fifty channels of EEG was not, however, the goal of this research. The real motivation for recording from so many channels was that it was necessary to accurately map out the potential distribution over the surface of the head in order to use the analytical techniques derived in this thesis. The visual evoked response desired was not just a single channel nor even a small number of channels, but sufficient channels to define a "surface" of potential readings over a large portion of the skull.

At this point it is constructive to ask just how close two electrodes on the scalp can be and still measure different signals. The shunting effect caused by the relatively high conductivity of the scalp is important, so there must be a certain minimal spacing below which no real gain in resolution occurs. In a recent paper

by Rush and Driscoll (10) it is stated that a spacing of five cm is this lower limit, for a surface electrode. This conclusion came about in a study of reciprocal relationships in the brain and its surrounding tissues. Current was passed through surface electrodes and fields were measured inside the skull. When the source and sink electrodes were placed closer than five cm, the shunting in the scalp between the electrodes caused very little current to be passed through the low conductivity skull into the brain. Observe that this does not say that electrodes placed closer than five cm and used to record EEG will measure the same signal strengths --- the scalp does after all have a finite resistivity. A source within the skull will produce a continuous voltage distribution on the surface and electrodes at any spacing will still be sensitive to differences between recording sites. Thus an average electrode spacing was chosen which seemed reasonable both from the point of view of placing the electrodes on the head of the subject and also from considerations of resolution of the surface field. That spacing is three cm, and one can empirically satisfy himself that in order to place an electrode at a spacing of three cm over the area frominion to just forward of the vertex and roughly from ear to ear of an adult human, about fifty electrodes are required.

Clinical people will immediately realize the difficulty in placing this number of electrodes on the subject. An experienced person (Dr. Lehmann) requires about two hours to properly place

all electrodes on the head. Note also that the electrode placement scheme cannot possibly conform to the so-called 10-20 EEG electrode scheme (2), offered as a standard system for describing electrode placement. These experiments, however, are a considerable departure from the considerations which motivated the establishment of 10-20 system, since it was intended to be a clinical scheme.

Eventually it was decided that in order to alleviate the problem of electrode placement, as well as to be able to accurately locate for later analysis the position of each electrode, a special recording helmet could be used. This helmet moulded to the head of a subject, would be lightly sucked onto the head with a vacuum system. The recording helmet, however, was still under development at the time the present results were taken. While the idea shows promise for future recordings, the data herein analyzed were recorded from electrodes attached in the normal manner. As closely as possible the electrodes were placed on the head of the subject in the pattern shown in Figure 2-2. In this way specification of a small number of parameters located the electrode array with satisfactory accuracy. The KW array was composed of six rows by seven columns, while the DALO data were taken from a matrix of six rows by five columns plus four additional electrodes on each side of the head, near the ears.

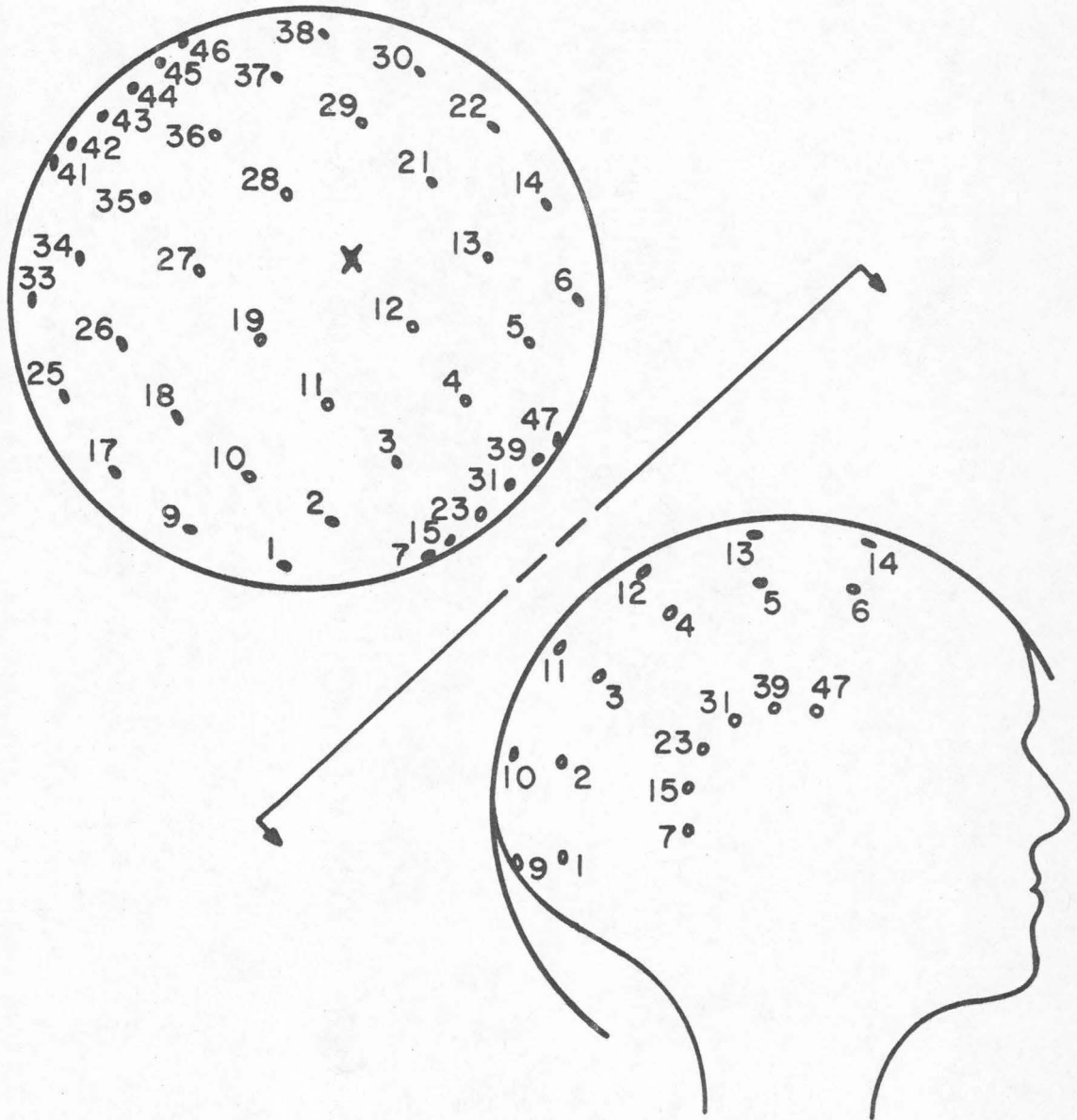


Figure 2-2 (a). Top and right side views of electrode placement for subject KW. Reference electrode was located at site marked by "x" near vertex.

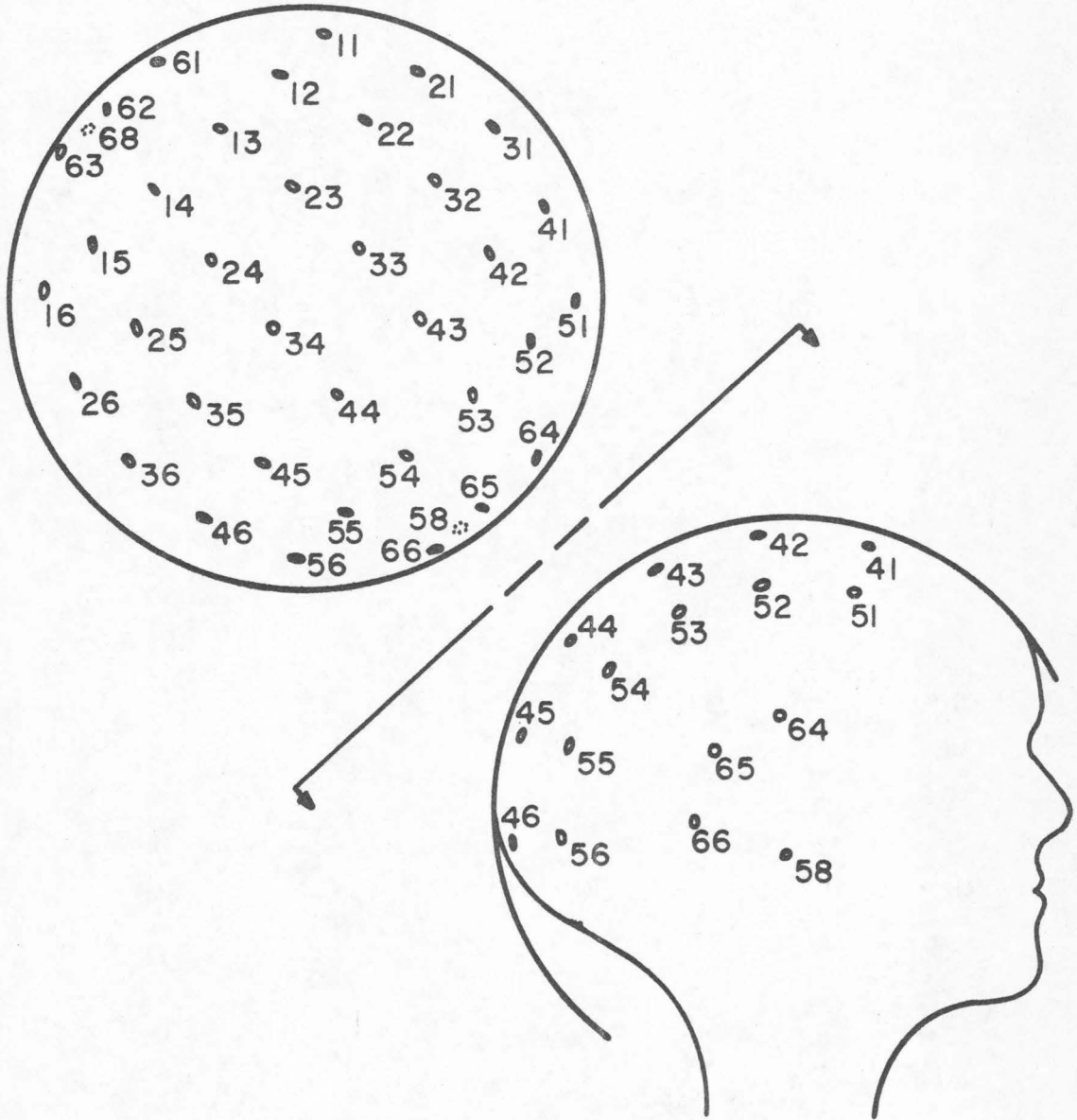


Figure 2-2 (b). Top and right side views of electrode placement for subject DALO. Reference electrode was "phantom" described in text.

3. The Problem of a True Reference Electrode

In the EEG literature today two problems still seem to be given more attention than seems reasonable. Further, the diverse opinions as to their solutions give rise in many cases to observations which cannot be compared with data from other experimenters with different recording techniques.

The first problem is to find a truly indifferent electrode for recording EEG data, and the second, really a variation of the same problem, is whether monopolar or bipolar recordings should be used.

Monopolar recordings are those in which the reference inputs to all amplifiers are connected to a common point, most likely some site on the head where EEG activity is expected to be small (mastoid process, ear lobe etc.) Bipolar recordings on the other hand are made with each amplifier connected to its own "active" and "reference" electrodes.

Most clinical EEG recordings are made from bipolar leads, that is, a differential amplifier is connected to two electrodes on the head and thus measures the difference in voltage between this pair of electrodes. Each amplifier is connected this way, and thus if four channels are recorded, a total of four pairs of electrodes are used, either by placing eight electrodes on the head or by placing fewer than eight and using some electrodes more than once to form a new pair.

To an electrical engineer this is an extremely confusing method. The scheme is carried to its extreme as Grey-Walter (11), in a book on clinical methods, actually gives a formula for computing the number of differential amplifiers "necessary" to "exploit" a given number of electrodes!

One immediately recognizes that the formula is that for combinations of N things taken two at a time. The point is of course that many of these "necessary" channels are derivable from combinations of others, and nothing is gained by adding more amplifiers.

To illustrate the difference between monopolar and bipolar recordings, consider Figure 2-3. In (a) we see four bipolar leads and the responses therein to flashes in either the left or right eyes. Note that there is an apparent polarity reversal from homolateral to heterolateral hemispheres, a fact which many investigators would consider to be intrinsic to the response and probably functionally meaningful. Inspection of the four bipolar leads shows that it is possible to derive monopolar leads from the same data, and thus refer four of the electrodes to one common reference. When the arithmetic is done, ie.

$$E_5 - E_1 = (E_5 - E_3) + (E_3 - E_1), \text{ etc.},$$

we derive (b) in Figure 2-3. Now there is no polarity reversal across the mid-line, only a monotonic change in amplitude of the signals. The data are exactly equivalent to that of (a), but presented

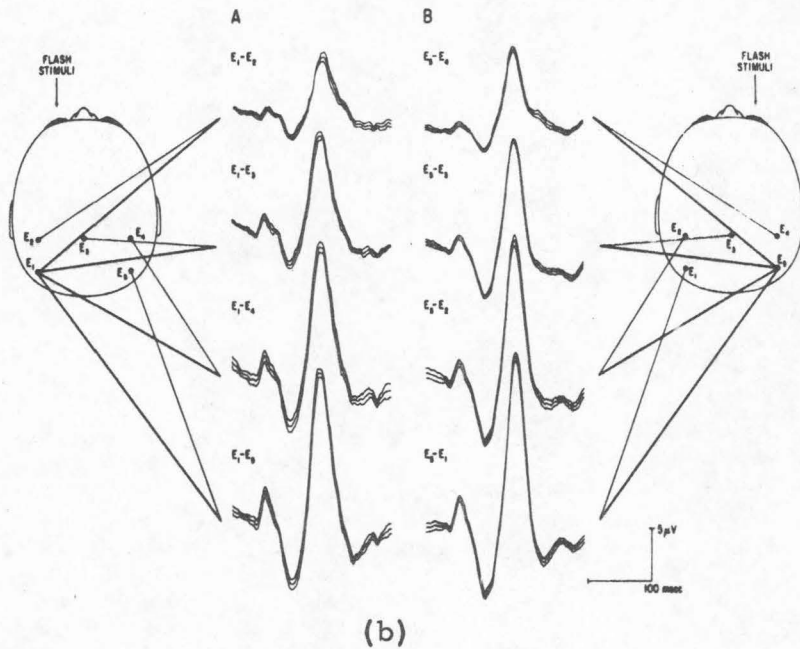
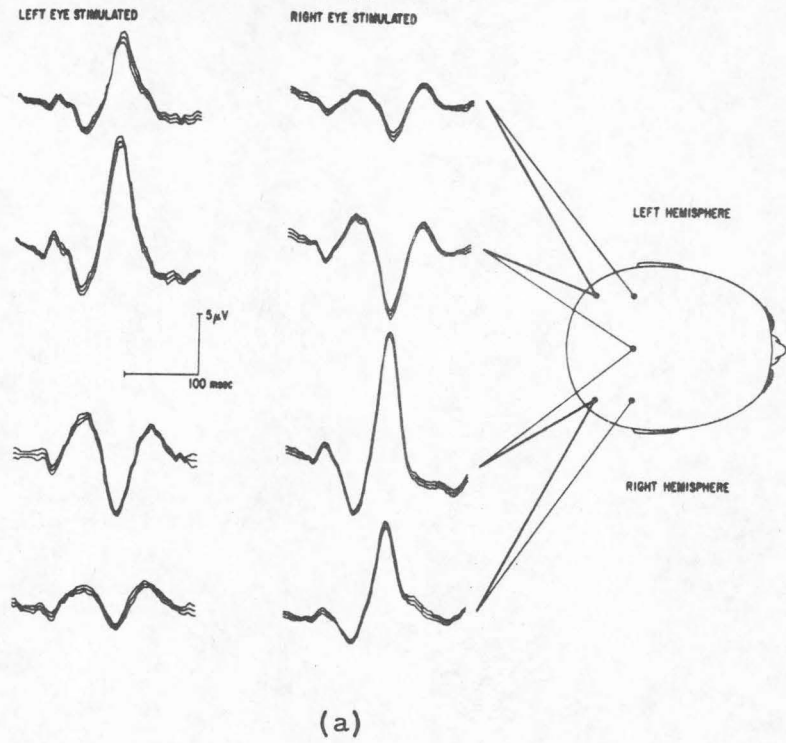


Figure 2-3. Difference between monopolar and bipolar recordings. (a) Bipolar recordings of visual evoked responses for either left or right eye flashed. (b) Transformation of traces in (a) to monopolar leads.

in a different manner. The apparently significant polarity reversal is merely the result of different reference systems!

Ideally one wants to measure monopolar potentials --- the activity of each electrode compared to some common, indifferent reference point. Should bipolar potentials be desired it is simple to find differences between pairs of monopolar potentials.

The problem is of course, where does one find an electrode truly indifferent to the EEG signals? Those authors who have attempted monopolar recordings have used many different sites: ear, vertex, mastoid process, etc. as the location of one electrode against which all others are compared. It is credible to say that these locations are usually relatively indifferent to EEG activity, but one can almost always demonstrate that some small potentials ascribed to the EEG are present even at these sites. It must also be pointed out that any single reference electrode must summate the ground return current from all active electrodes at that point. For a recording system such as is used here, however, the large number of electrodes spread over a considerable portion of the head most probably carry signal currents whose ground returns sum almost to zero.

Note that systems with only one reference electrode are preferentially sensitive to those electrodes which, taken with the reference point are co-linear with the field vector producing the EEG activity (McFee and Johnston)(6). Consider Figure 2-4.

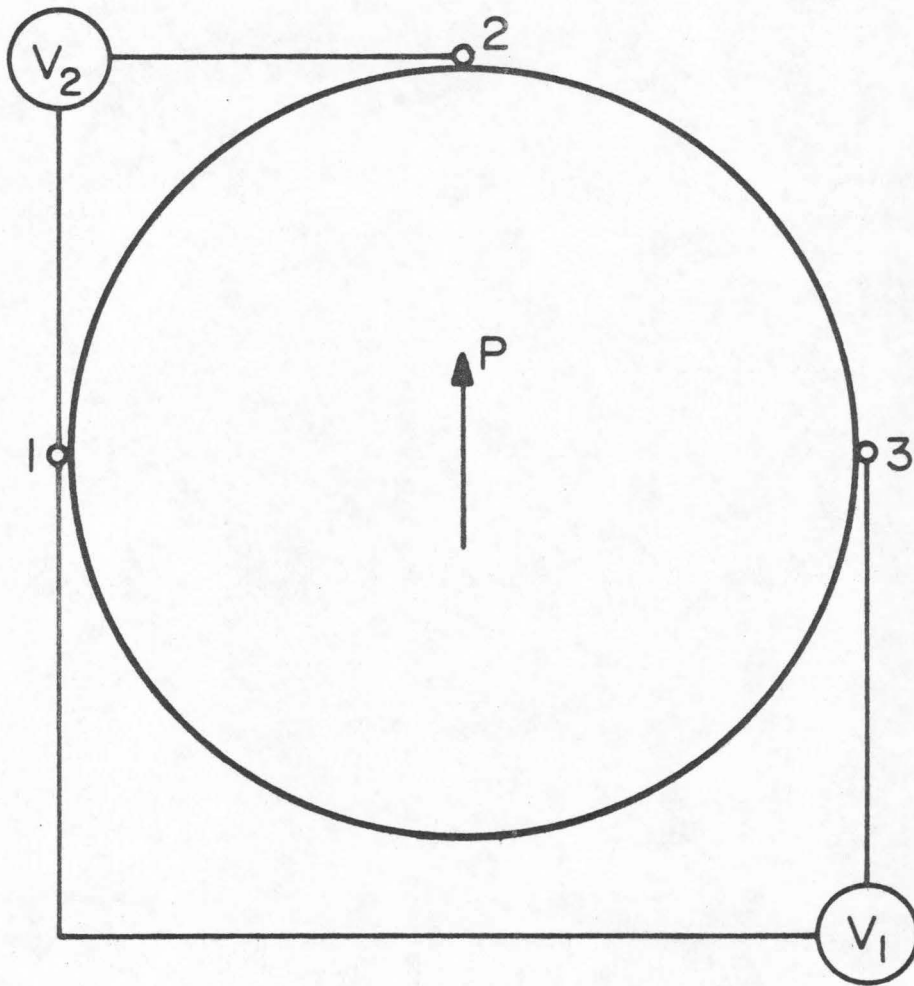


Figure 2-4. Sensitivity differences between electrode pairs. V_1 is insensitive to any changes in strength of dipole P since electrodes 1 and 3 are on equipotential lines. V_2 however is sensitive to changes in strength of P .

A voltmeter connected between electrodes 1 and 3 will measure zero potential difference since these two electrodes lie on the same equipotential line which would be caused by a dipole source at the origin as shown. An instrument connected between electrodes 1 and 2, however, will measure a deflection since electrode 2 is situated where the maximum potential will be attained. In our recording system with a large number of electrodes, there are electrodes which at some moment are at the same potential as the reference site while others are not. A little reflection should convince the reader that this is an acceptable and in fact perfectly workable arrangement.

This author suggests that too many hours have been spent in emotional support of one scheme or another, none of which is really different from the others. Any single electrode placed on the body will be of necessity sensitive to line voltage interference, muscle artifacts and EKG signals (whose magnitude is roughly 1000 times that of the EEG). Furthermore the several sites mentioned above are, for most purposes, electrically equivalent. Think of the problem in a topographical manner: at any point in time the voltages on the surface of the head trace out some potential "surface", with peaks over the high amplitudes and troughs over the low amplitudes. A "man" standing on this surface somewhere can trace out the "shape" of the activity relative to him no matter where he is on the surface. As long as he is not on some spot which is influenced by signals other

than the EEG signals, and in a way not equal to the influence at other points (in other words, if some larger background activity like the EKG shifts the entire surface up or down uniformly, the relative shape is unchanged) his vantage is a viable one.

We have found experimentally that placement of one reference electrode at a site even surrounded by the active monopolar electrodes did not significantly change the shape of the responses as compared with those using any other single reference point. For subject KW this was the case; all forty-one electrodes being measured relative to a forty-second electrode located at the vertex.

As our theoretical work entered this area, however, we arrived at a different system by the time data were taken for subject DALO. For this subject and subjects following, a pseudo-electrode was created and used as the reference point for all channels.

The creation of this electrode is dependent upon some assumptions regarding the electromagnetic aspects of the system. First, as is very lucidly discussed in Plonsey (8), the EEG signals can be considered at each point in time as electrostatic in nature - the recordings do not show large components at frequencies sufficiently high to demand inclusion of electromagnetic effects (the vector potential terms in Maxwells' equations can be ignored). Treating the scalp potentials in this way leads to a second assumption which can be made. Since the diffuse ionic activity

which gives rise to the potentials involves electronic charges which sum to zero (or at least a constant), the sum of the electrostatic potentials measured over a closed surface bounding the charges must also be zero or a constant.

Note that some portions of this supposed surface enclosing the cortex are not normally recording sites (the face, frontal surface, below the chin and ears, etc.). It is our observation however that these sites show little if any activity which can be identified with any portion of the evoked response recorded over the more active areas of the skull. Therefore, to a first approximation, if the electrode array extends to those sites beyond which the signal amplitude is below the system noise level, then the sum of the potentials which exist over this unsampled area will be a small and relatively constant level.

Thus it is reasonable to create a "phantom" reference electrode by the scheme shown in Figure 2-5, due to Madey (5). Each electrode is connected to a summing network which weighs each channel equally in deriving an "average" electrode with respect to which all channels are measured. The equivalent local generators and their associated resistance are denoted by the e_k and R_{e_k} respectively. Assume $R_e \ll R_s \ll R_i$ where R_i represents the amplifier input impedance and is greater than $10^8 \Omega$. Then if this condition is satisfied,

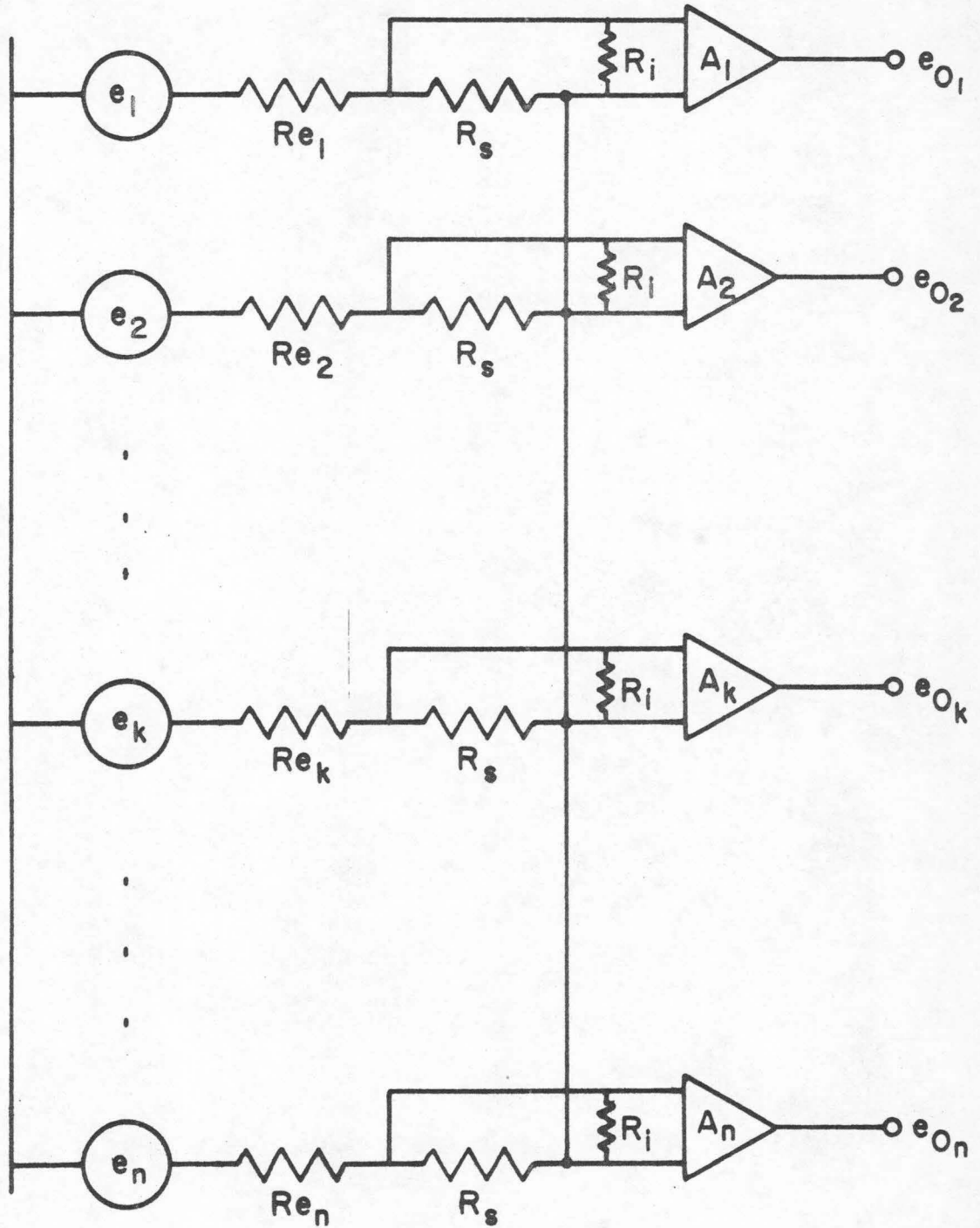


Figure 2-5. Circuit diagram for averaged reference electrode. Due to Madey (5).

$$e_{o_k} = A \cdot (e_k - \frac{1}{n} \sum_{k=1}^n e_k)$$

with small error. Thus if all A_k are assumed equal

$$\sum_{k=1}^n e_{o_k} = 0$$

This idea is not new, since similar reference derivations have been used in EKG recordings, and some systems even use non-uniform weighting in the summing network to achieve electrode sensitivities to certain cardiac events (6). In fact it is interesting to note that Offner (7), who has had considerable influence in the design of EEG recording systems, proposed such a scheme in 1950. Perhaps the fact that large numbers of electrodes are required has slowed acceptance of the principle.

Before leaving this discussion, observe an opportunity exists to test the validity of the "phantom" reference electrode with the KW data. If the assumptions are correct, then the sum of the forty-one potentials at each sample time, weighted equally to produce the equivalent of the summing network shown in Figure 2-5, should be a small number. The results of performing this operation are shown in Figure 2-6. Over the duration of the response we see that the assumptions are reasonably justified -- the sum is small if only piecewise constant.

One can test the hypothesis that the phantom electrodes thus derived are not correlated with each other or with the active

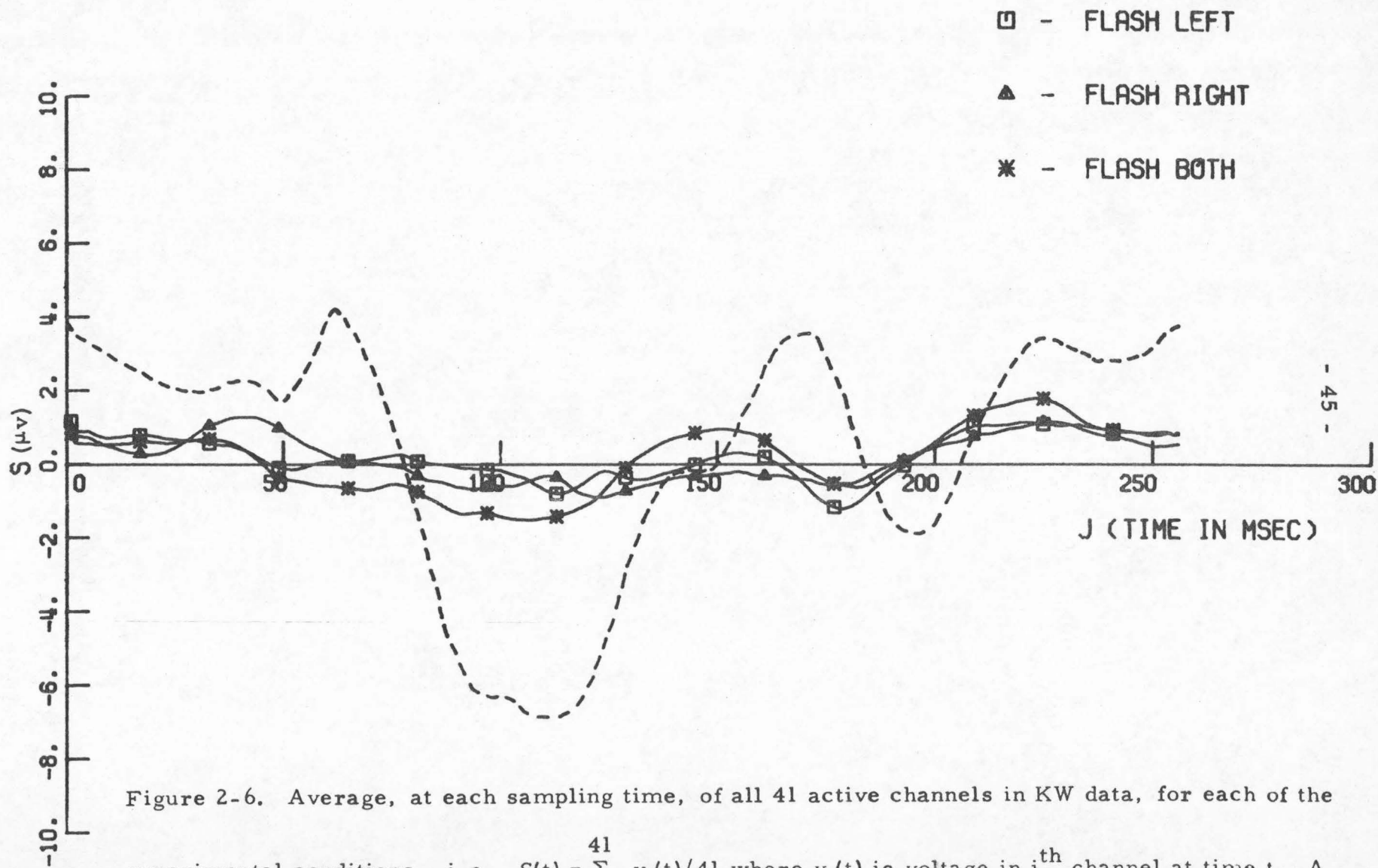


Figure 2-6. Average, at each sampling time, of all 41 active channels in KW data, for each of the

experimental conditions. i. e., $S(t) = \sum_{i=1}^{41} v_i(t)/41$ where $v_i(t)$ is voltage in i^{th} channel at time t . A

typical evoked response is shown as dotted.

electrode recordings. The average correlation (by the Pearson product-moment method) among all channels for all three conditions is 0.573. The average correlation between active channels and the phantom channels of Figure 2-6 is 0.526 and the average correlation between the phantom channels is 0.732. At the 5% significance level the critical level of the correlation coefficients is approximately 0.304, hence all correlations are significant. Moreover, there is a higher correlation between the three traces (.732) of Figure 2-6 than would seem apparent by eye.

These high correlations do not condemn the use of the averaged reference electrode. One would in fact anticipate a certain degree of significant correlation by virtue of the fact that this average electrode is a linear combination of the active channels, hence it must be related to them. The high correlation between the three averaged electrodes is perhaps only a further indication of something which can be seen in the data -- the responses to the three different stimuli are very similar.

This process would only have an adverse effect on the recordings if the averaged traces of Figure 2-6 were highly oscillatory. This would mean that at one point all potential readings would be elevated and then shortly thereafter all would be depressed. This would of course alter the shape of the evoked responses obtained. It would appear that this would not have been a problem here, since the averaged reference is quite flat over a

considerable portion, from about 50 ms to 130 ms (a very significant interval, as will be seen) and again relatively flat from about 130 ms to 170 ms (another interesting interval).

In any event, the magnitudes of the averaged reference potentials for the most part lie within the standard errors of most of the evoked responses. It may be that further investigation will demonstrate how to more closely approach an average level of zero or a small constant, but in the aggregate, this one test of the scheme seems to support its continued use.

4. Data Reduction and Display Methods

The paper tape records produced by the laboratory in San Francisco were removed to Caltech for all subsequent analysis. Figure 2-7 shows an outline of the preliminary data re-formatting done. Each of the three stimulus conditions reported here was presented a total of three times for each subject, allowing extraction of a mean response for each condition. The data were then smoothed to remove any maverick sample errors. The final tape containing the "raw" data contains the mean responses, standard deviations, smoothed mean response and first time derivative of the mean response for each channel for each condition. Details of this process can be found in the appendix.

It would be an understatement to say that the experimenter is impressed at this point by the abundance of data which exist

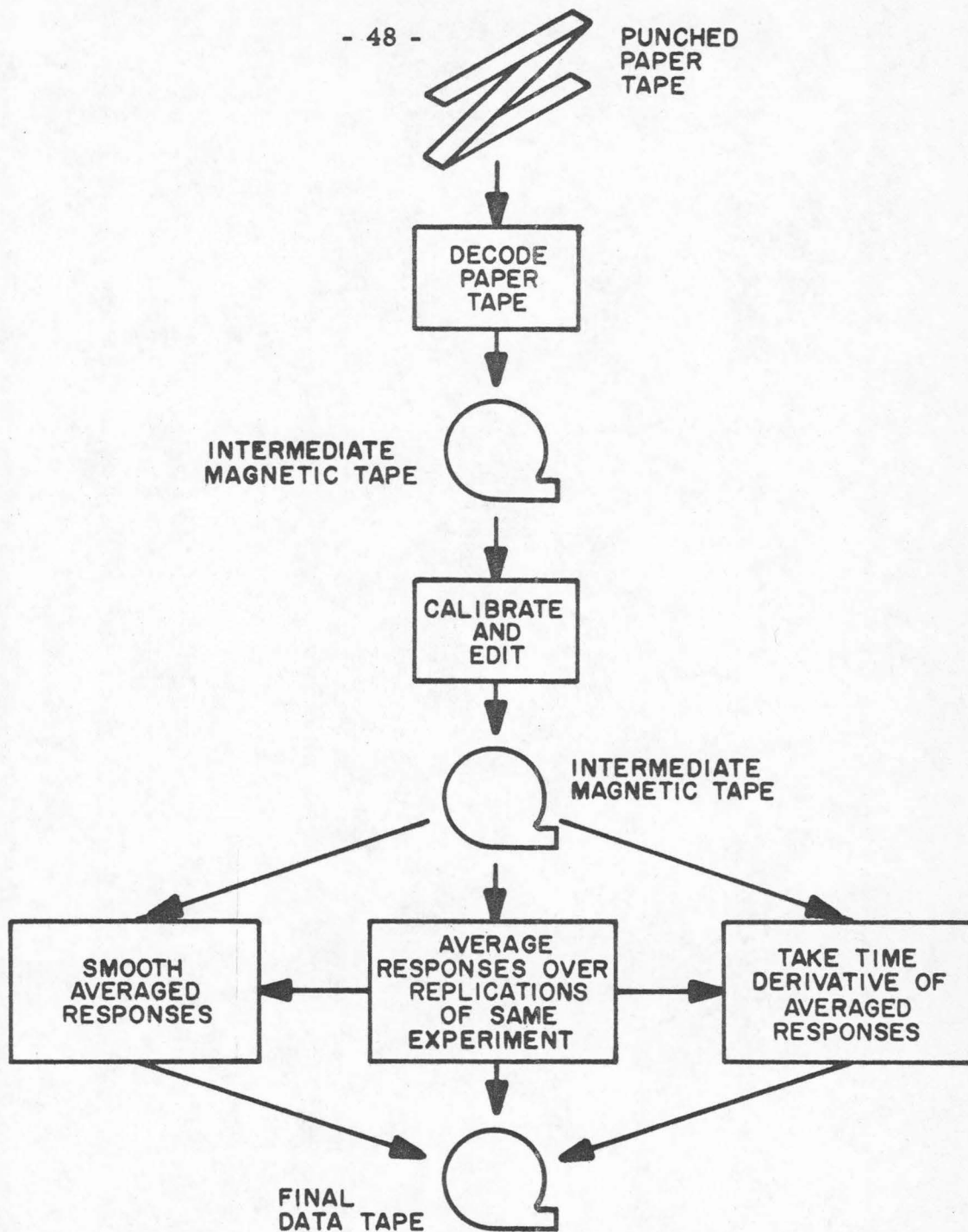


Figure 2-7. Outline of preliminary data reformatting from paper tape records of each replication of each condition to digital magnetic tape of averaged, smoothed responses.

only as numbers on computer tape. Consider only the response to one condition: there are as many as fifty channels and 256 samples per channel, giving approximately 12,500 data points to confuse the observer.

It seems obvious that even plotting out each channel for each condition for each subject still falls short of allowing some reasonable visualization of the data, since that process would yield in this case some 300 responses. Even if one could arrange these plots on the walls of his room it is doubtful any real insight could yet be achieved. What is necessary is a visual summarization of the data which affords discovery of the salient similarities or differences from experiment to experiment. This visual "aid" can be very valuable in quickly examining the large amount of data recorded.

Figure 2-8 shows a sequence of tracings of evoked responses for each subject and each experimental condition. Only a small number of the actual 40-odd channels are shown for illustrative purposes. The only facts really apparent from these records are that the responses to all three stimuli are quite similar, that there appears to be a polarity reversal between the two subjects, and that there is for each subject a polarity reversal from anterior to posterior regions of the skull. The reader will probably concur that this graphical technique is not adequate to show the complete behavior of the evoked responses.

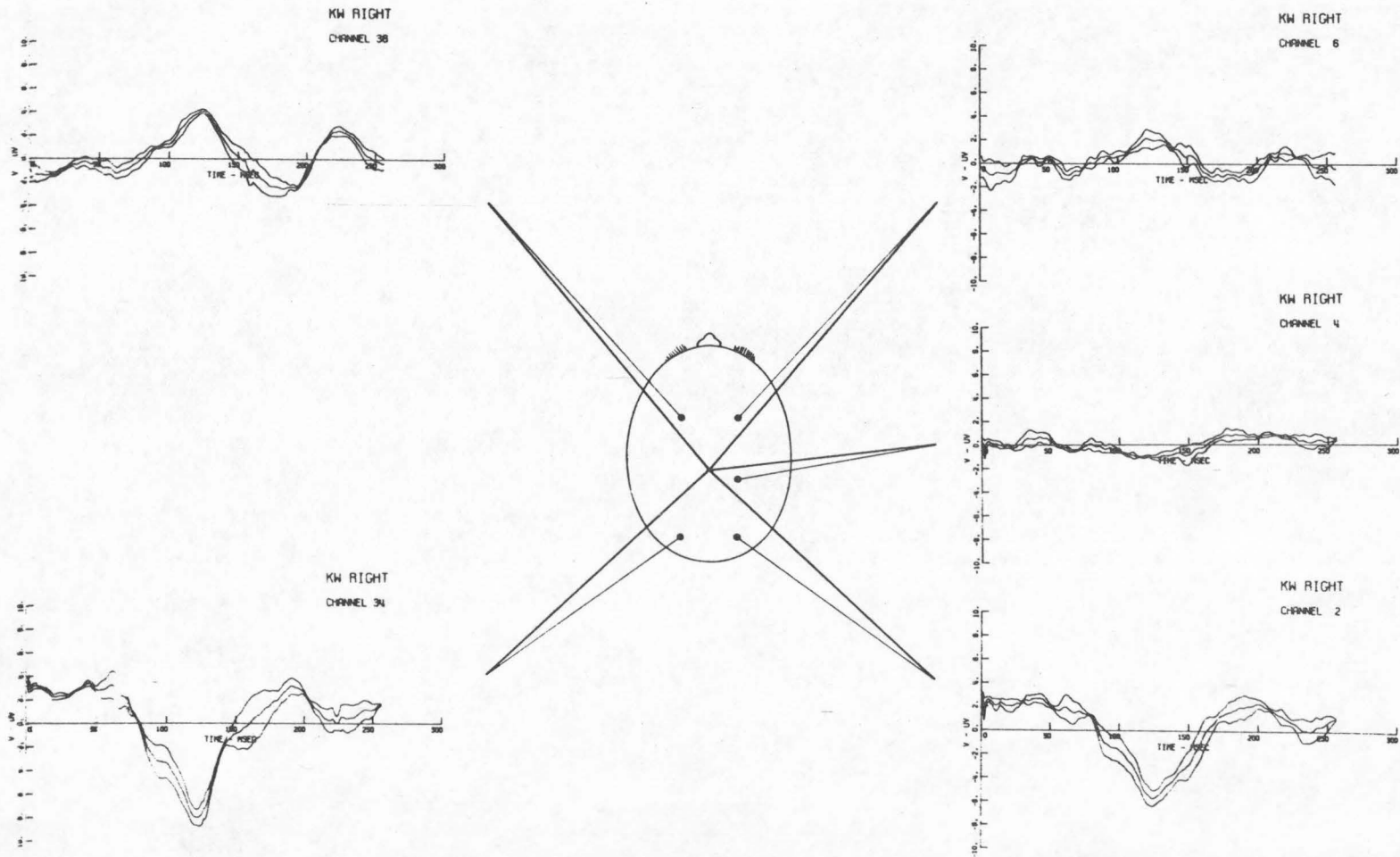


Figure 2-8 (a). Typical evoked responses for flash to right eye, subject KW. Traces shown are mean of 3 replications of experiment and mean plus and minus one standard deviation.

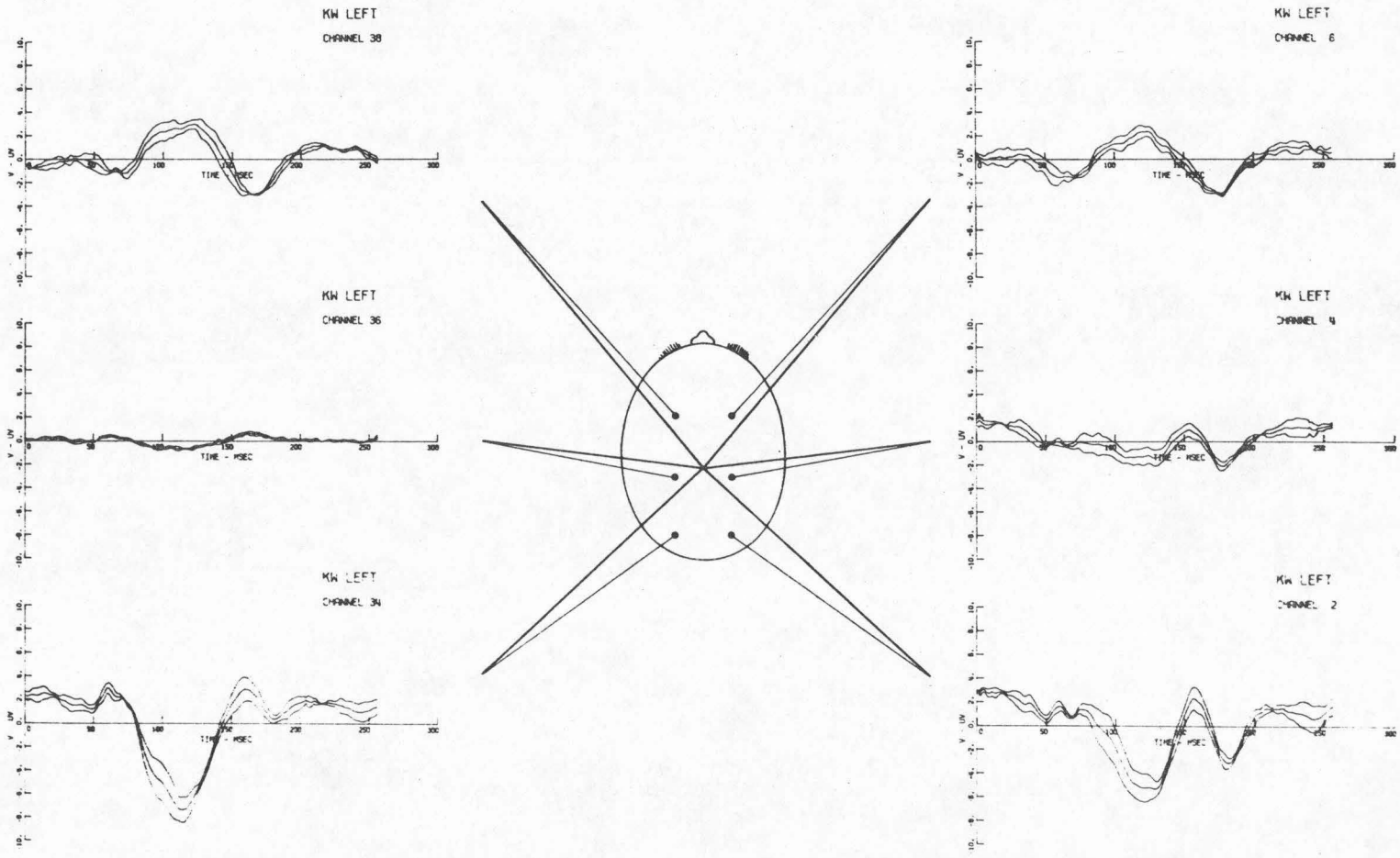


Figure 2-8 (b). Same as for (a) but stimulus is flash to left eye.

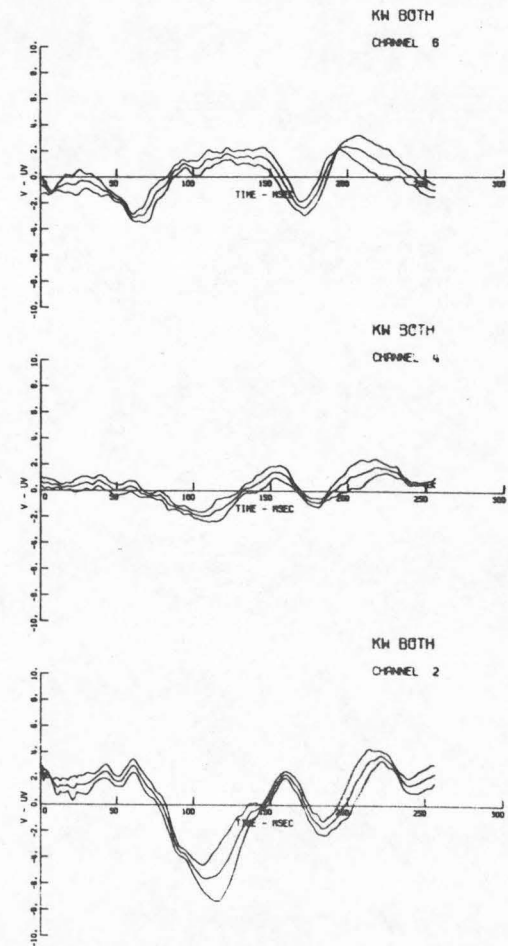
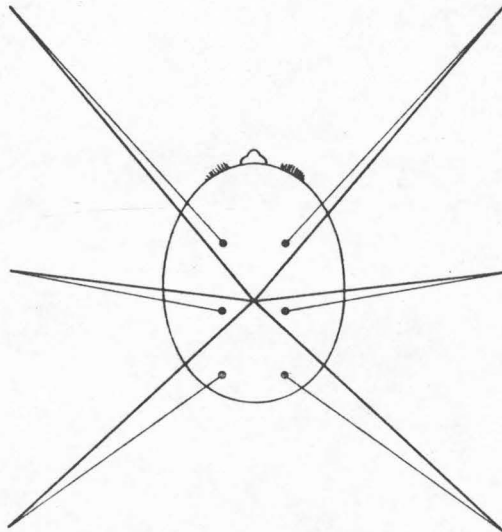
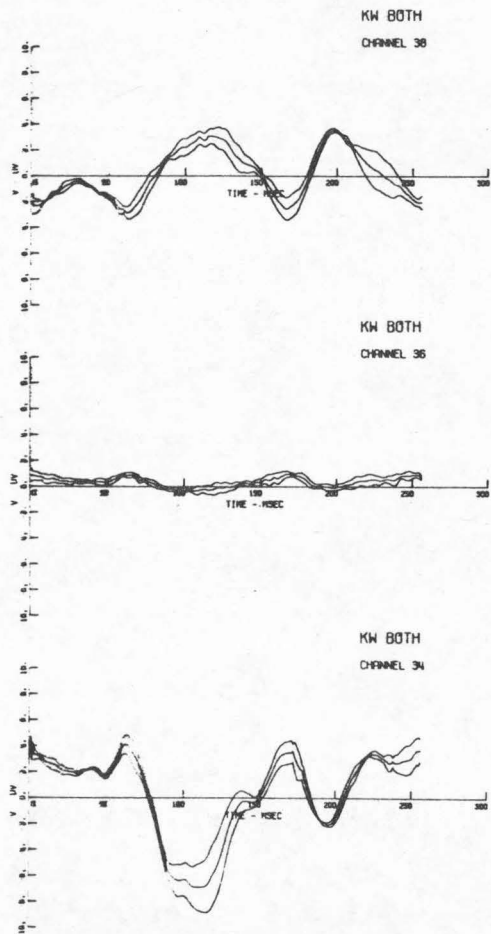


Figure 2-8 (c). Same as for (a) but stimulus is flash to both eyes.

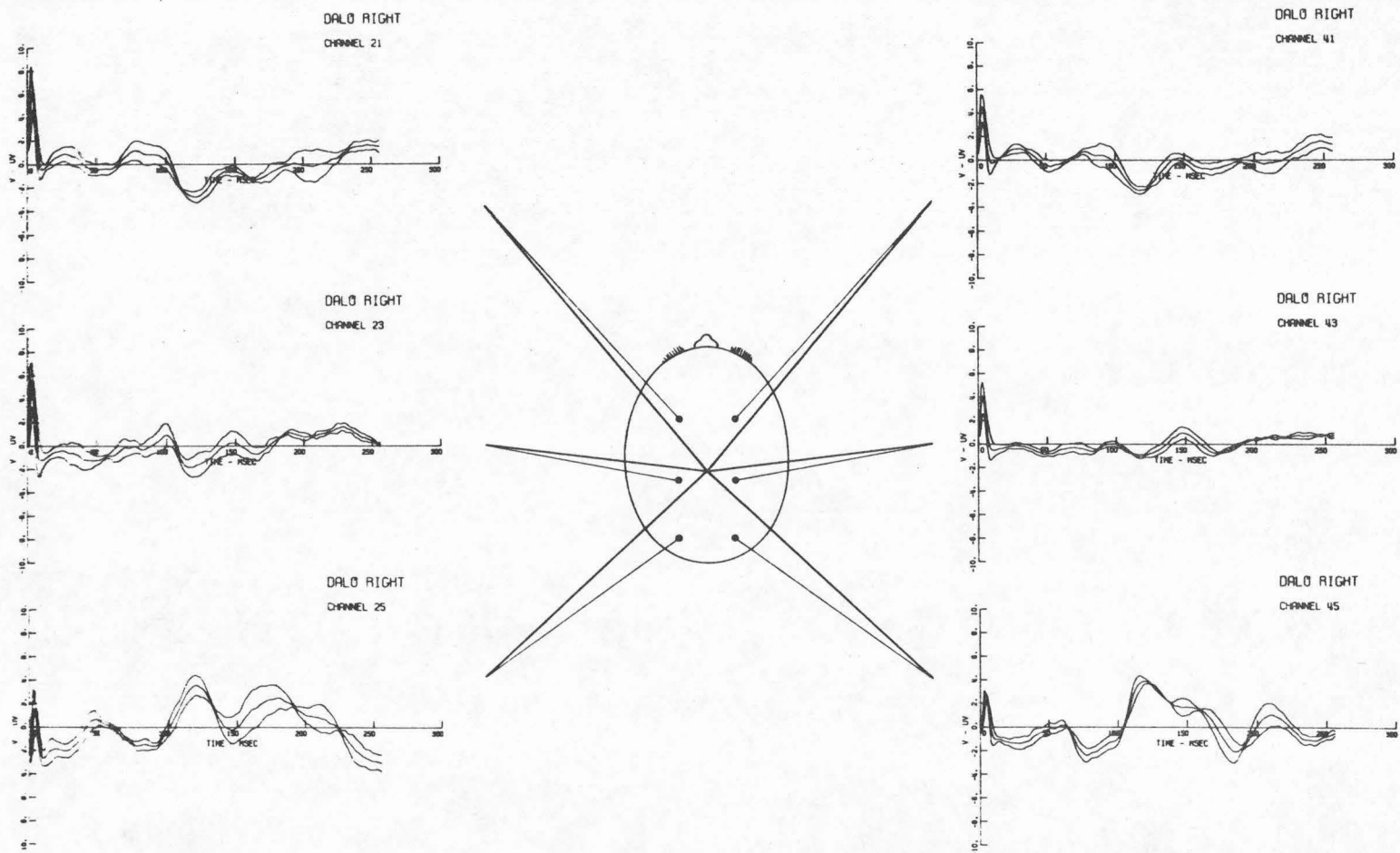


Figure 2-8 (d). Same as for (a) but subject is DALO, stimulus is flash to right eye.

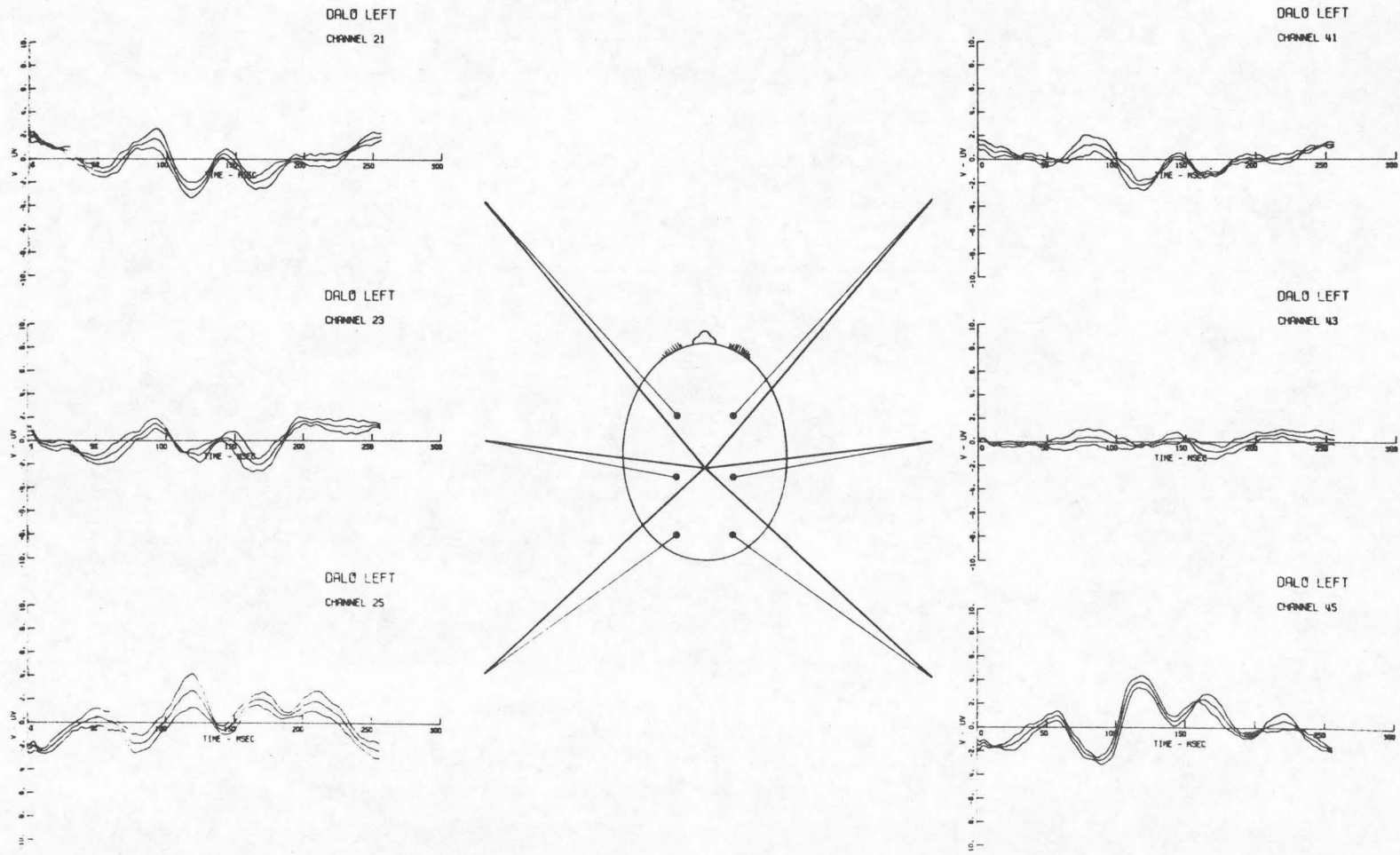


Figure 2-8 (e). Same as for (d) but stimulus is flash to left eye.

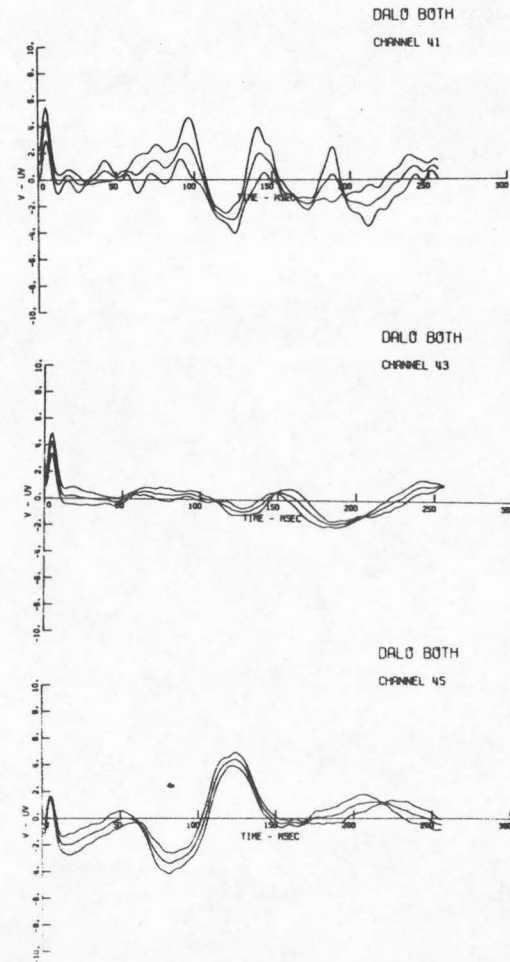
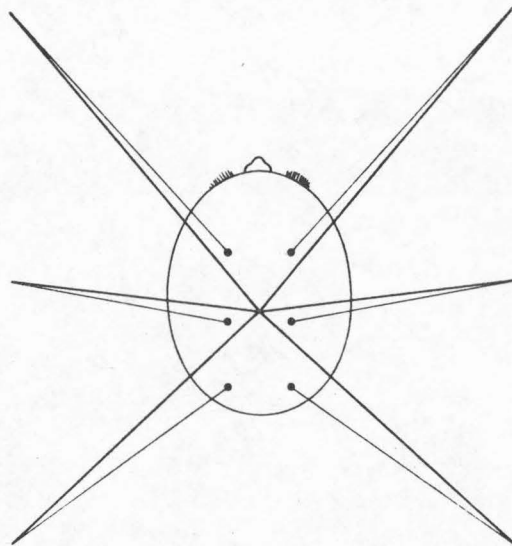
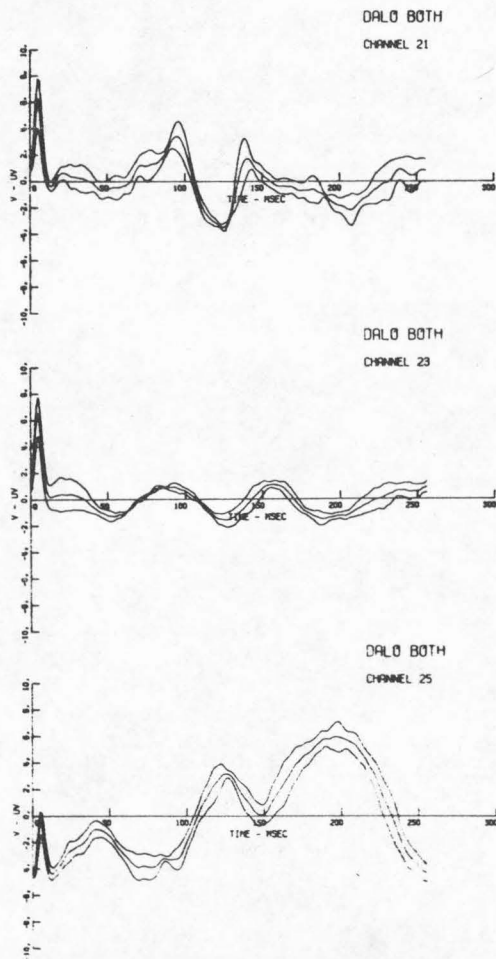


Figure 2-8 (f). Same as for (d) but stimulus is flash to both eyes.

The solution offered here largely springs from the original motivation for the large electrode array in order to define a potential surface on the head. It seemed reasonable to show the data in exactly that form, as equipotential lines sketched on an animation of the head. At each of the 256 sample times a picture was made of the head. In order to compare the responses to different conditions, the results for each are shown simultaneously as in Figure 2-9.

In order to orient the viewer to the drawing, some artwork has been added to the outline of the head. Ears and a neck have been appended, and the elliptical shape is intended to be an imaginary circle which circumscribes the vertex --- this to determine the line of sight the viewer has. The contour lines which of course actually lie on a three-dimensional surface, the head, are shown in orthographic projection. This is not only easy to implement in a computer algorithm but affords a very natural way of viewing a hemispherical shape projected to a plane. Other authors using a smaller number of electrodes, not spread over more than a small portion of a hemisphere (1) have used other projection schemes but a consideration of various methods of displaying a complete hemisphere (9) led to the orthographic view. The eye is imagined to be at infinity and points on the hemisphere are simply dropped perpendicularly to the plane. If the viewer recalls looking at maps of the earth shown this way, and thinks

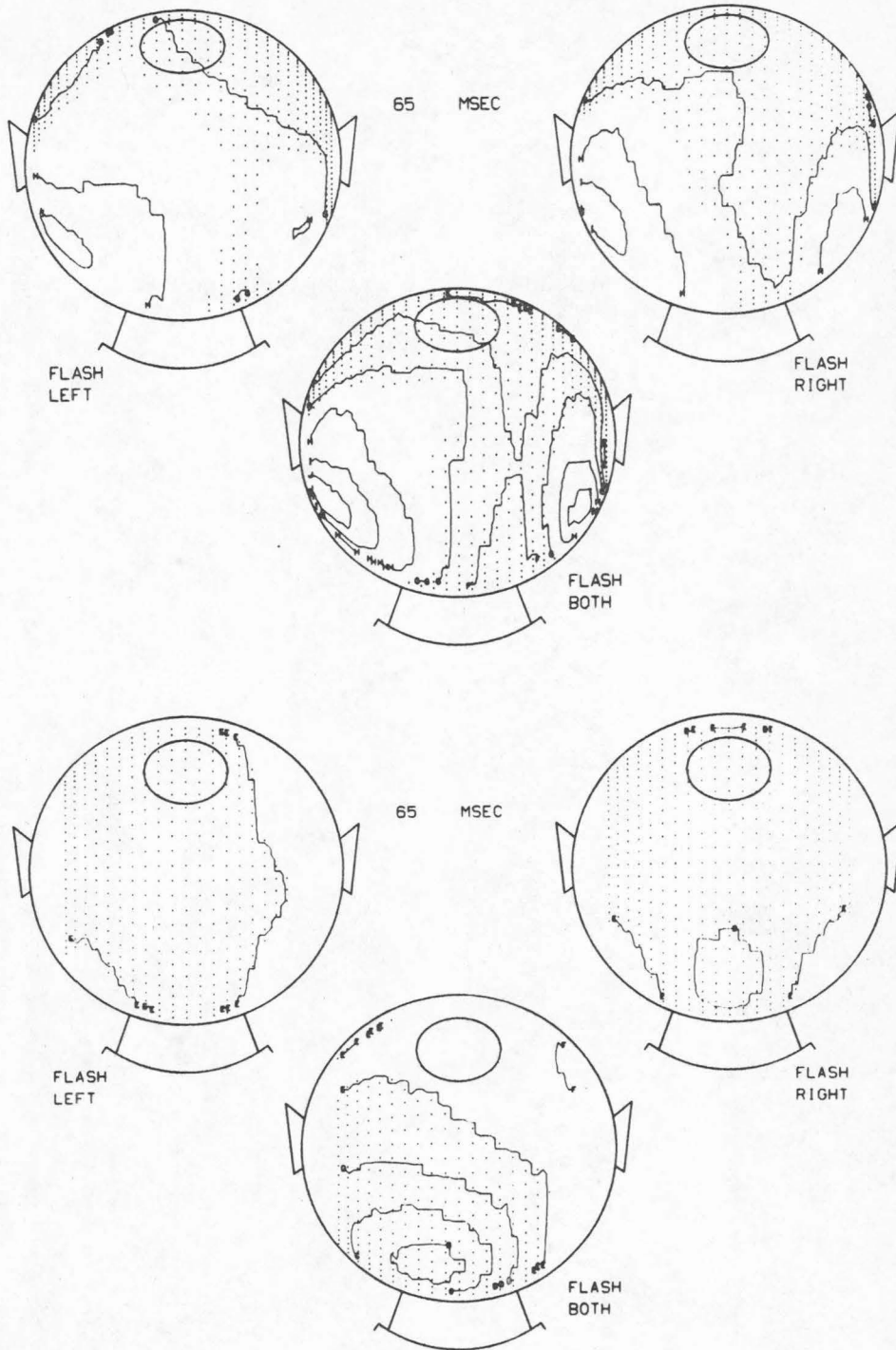


Figure 2-9. Equipotential maps of evoked response activity at 65 ms after stimulus for KW (top) and DALO (bottom).

of the circle around the vertex as the "north pole of the head" there should be few problems.

The contour lines themselves are labeled A through K. The actual "value" of A is the smallest (most negative) potential from all channels from all three conditions for a given subject. Similarly "K" corresponds to the largest (most positive) potential ever attained in one subject. For the subjects KW and DALO, the values of "A" and "K" are:

	KW	DALO
A	-8.04	-5.14
K	4.79	7.58

The reader will realize that in making the drawings for consecutive sample times the extreme potential values denoted by "A" and "K" are attained only once each, hence most pictures do not show the full range of contour lines. This does however permit a more general comparison of the data.

A final observation on the format of the display is that those areas which are electro-negative at any time are shown as dotted.

The actual power of this graphical technique is fully realized when the consecutive "snapshots" are made into a contiguous film and displayed as a movie. Initially a 35 mm film showing 256 frames is produced on a computer microfilm device, an FR-80. In order to slow down the actual viewing time, as well

as to circumvent the fact that most facilities have a 16 mm projector but few have a 35 mm machine, the 35 mm original is reduced to a 16 mm print, and in the process each original frame is printed four times in the 16 mm copy. The end result is a movie 1024 frames in length, which, when shown at SILENT speed (18 frames per second) of a typical projector, lasts about one minute. Since the actual response lasted but 256 msec, the time axis is stretched approximately 250 times in viewing the movie. At this speed an alert viewer can almost keep up to the activity, but will probably want to view the movie several times.

The reader will notice that his copy of this thesis does not come with a special corner-flipping section on which is displayed the movie views of the KW and DALO data. Though this was suggested to the author by a colleague in one of his more facetious moods, the delight of actually viewing this presentation of the data is reserved for those who have access to the film! To partially compensate for this, various frames of one or both movies are reproduced throughout the text.

This problem of adequately viewing enormous data structures is a frequent and fair criticism of those experimenters who use computers to fill their shelves with numbers. Since it will be seen that the analytical portion of this study required large amounts of data, it is a valuable fringe benefit to have discovered a way of

simply looking at the data and deriving qualitative information from it. It will be shown, in fact, in Chapter IV that even quantitative inferences are drawn from the movie format.

REFERENCES FOR CHAPTER II

1. Estrin, T. and Uzgalis, R., "Computerized Display of Spatio-Temporal EEG Patterns," IEEE Trans. Bio-Med. Engrg. BME-16 (1969), pp. 192-196.
2. Jaspard, H. H., "Report of the Committee on Methods of Clinical Examination in Electroencephalography," Electroenceph. clin. Neurophysiol. 10 (1958), pp. 371-375.
3. Lehmann, D. and Fender, D. H., "Component Analysis of Human Averaged Evoked Potentials: Dichoptic Stimuli Using Different Target Structure," Electroenceph. clin. Neurophysiol. 24 (1968), pp. 542-553.
4. Lehmann, D., Kavanagh, R.N. and Fender D.H., "Field Studies of Averaged Visually Evoked EEG Potentials in a Patient with a Split Chiasm," Electroenceph. clin. Neurophysiol. 29 (1969), pp. 193-199.
5. Madey, J.M.J., personal communication
6. McFee, R. and Johnston, F.D., "Electrocardiographic Leads II. Analysis," Circulation 9 (1954), pp. 255-266.
7. Offner, F.F. "The EEG as Potential Mapping: the Value of the Average Monopolar Reference," Electroenceph. clin. Neurophysiol. 2 (1950), pp. 213-214.
8. Plonsey, R., Bioelectric Phenomena, McGraw-Hill, New York (1969).
9. Raisz, E., Principles of Cartography, McGraw-Hill, New York (1962).
10. Rush, S. and Driscoll, D.A., "Current Distribution in the Brain from Surface Electrodes," Anesthesia and Analgesia - Current Researches 47 (1968), pp. 717-723.
11. Walter, W.G., in Hill, D. and Parr, G., (eds.) "Electroencephalography -- A symposium on its Various Aspects," Macmillan Co., New York (1963).

III. THE DIMENSIONALITY OF THE HUMAN VISUAL EVOKED RESPONSE

1. What is the Dimensionality of an Evoked Response?

After placing many electrodes on the head of a subject and eliciting evoked responses from him, the experimenter is quickly impressed by a new analytical difficulty beyond the mere bulk of data referred to in Chapter Two. This problem concerns the inability on the part of most experimenters to objectively contrast the activity in one recording channel with that of another. In other words, given an array of tracings of say fifty evoked responses recorded during a single experiment, how can one objectively study the responses for modes of activity common or unique to various channels. Are all channels independent of one another, or are many recording channels redundant?

The EEG literature is disappointing in this subject area. Some electroencephalographers tenaciously insist that N electrodes can be combined in pairs a total of $N! / (2(n-2)!)$ ways, and hence in order to "exploit" this number of "channels," the recording system must be enlarged accordingly! It is hoped this section will show that very often N recording electrodes measure fewer than N independent variables, let alone any large number of variables arising from combining electrode pairs in all possible ways.

A recent example from studies of the human electrocardiogram illustrates the power of the technique to be described in this section. Inspired by the work of Einthoven and his

"triangle" concept of monitoring cardiac activity, it was long popular to record human ECG signals using the classic "limb - lead" recording system of three recording sites on the body -- the two wrists and one leg. Recently, however, the diminishing cost and compaction in size of one ECG recording channel has allowed extension of clinical electrocardiographic recording to many more channels, up to 12. At least one investigator, Cady, (1) has questioned whether there are in fact twelve independent recordings derived from such a system. He used a principal components analysis of the data to show that there was great redundancy in the twelve lead system. Two channels were selected as a basis for all twelve channels and when a regression analysis was performed, it was shown that each of the remaining ten channels could be almost duplicated by a linear combination of the two leads selected as the basis.

Visual inspection of the ECG data did not betray this strong interdependence in the data. Cady's analysis, however, showed quite forcefully that the twelve leads are far from being independent.

Perhaps there may be a comparable situation in multi-channel evoked response recordings, and the principal factor method may be of use in collapsing the dimension of our data to some small number. It is necessary to find the true dimensionality of a multivariate data space as a precursor to estimating the degree to which the data may retain the identities of complex underlying processes. If the evoked response data suggest that each

recording channel is truly independent of activity in other channels then it would appear that no simple equivalent source could be found to explain the data. On the other hand if it appears that many channels measure activity also present to a greater or lesser degree in other channels then perhaps the data can be used to characterize a simple equivalent generator.

In order to illustrate the analytical difficulty, consider the series of equipotential maps shown in Figure 3-1(a) through Figure 3-1(m). This series of contour maps for the two subjects (KW on top, DALO on the bottom) have been selected as being a reasonably complete summary of the data in this form. (These maps will be referred to frequently throughout the text, so they are included at this relatively central location rather than in an Appendix.) It is apparent that there is considerable similarity in the responses of either subject to all three stimuli, but there is not much similarity between the responses of the two subjects, except in the range 175 ms to 195 ms.

Also, it seems that certain "simple" patterns in the equipotential maps are quite stable. In the case of the KW data for instance, two well demarcated potential "troughs" are prevalent from about 90 ms to 130 ms; and over this same range a stable but apparently different pattern prevails in the DALO data.

It would seem that neighboring channels clearly are interdependent. It also seems that over several intervals in the responses the equipotential maps suggest a simple, stable

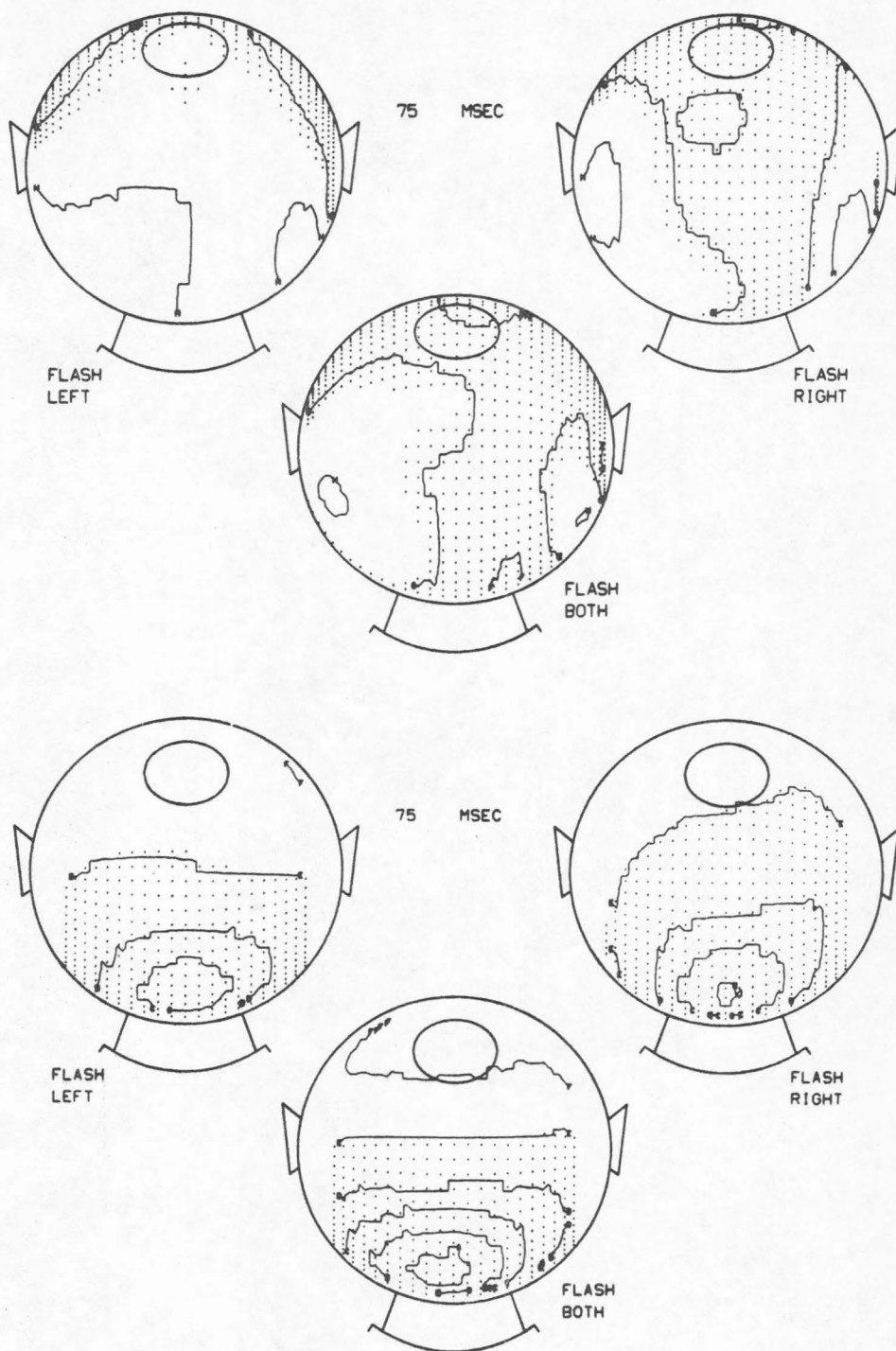


Figure 3-1 (a). Equipotential maps of evoked response activity at 75 ms after stimulus; subject KW on top, DALO on bottom. Following pages show similar plots at other selected sample times during response.

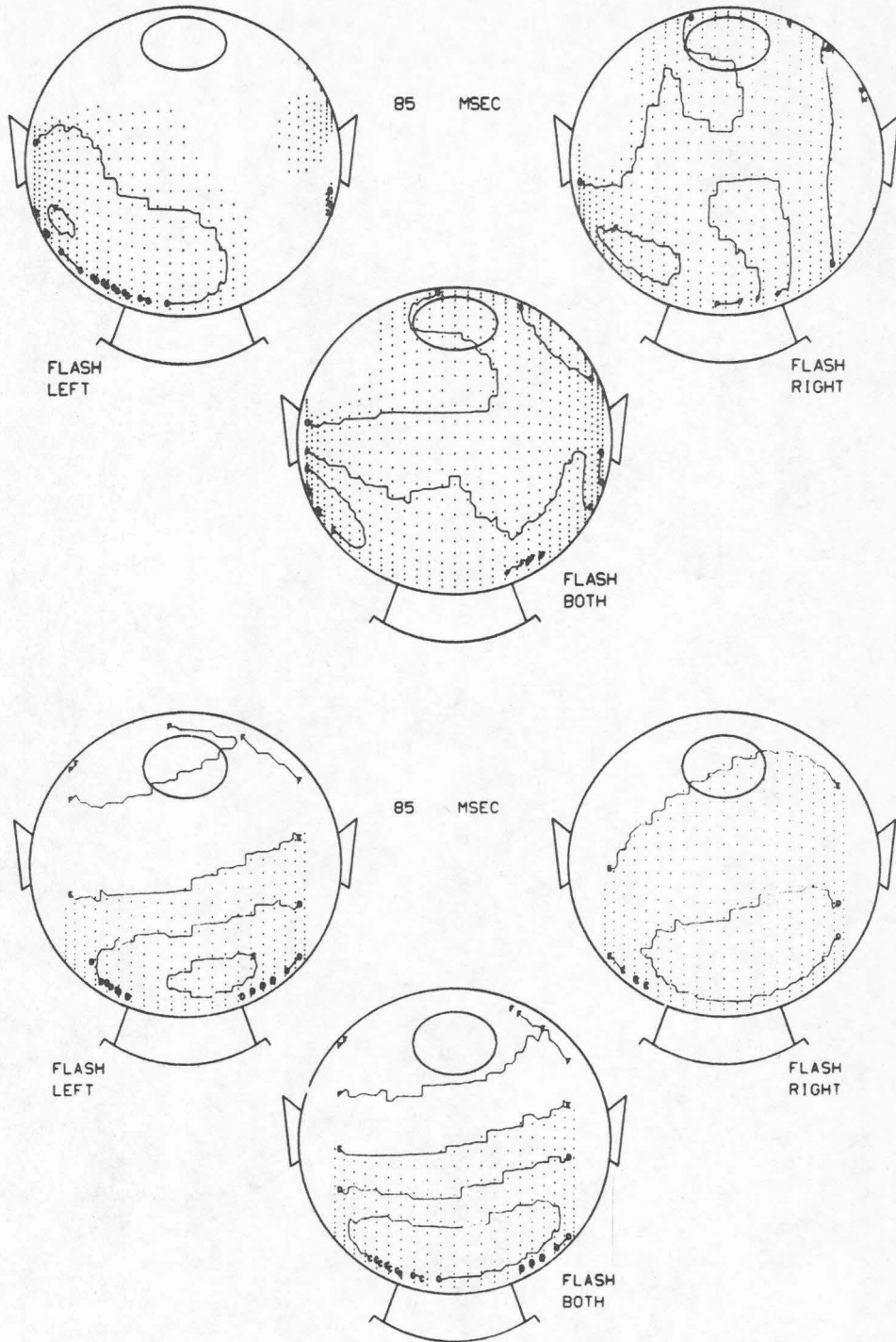


Figure 3-1 (b).

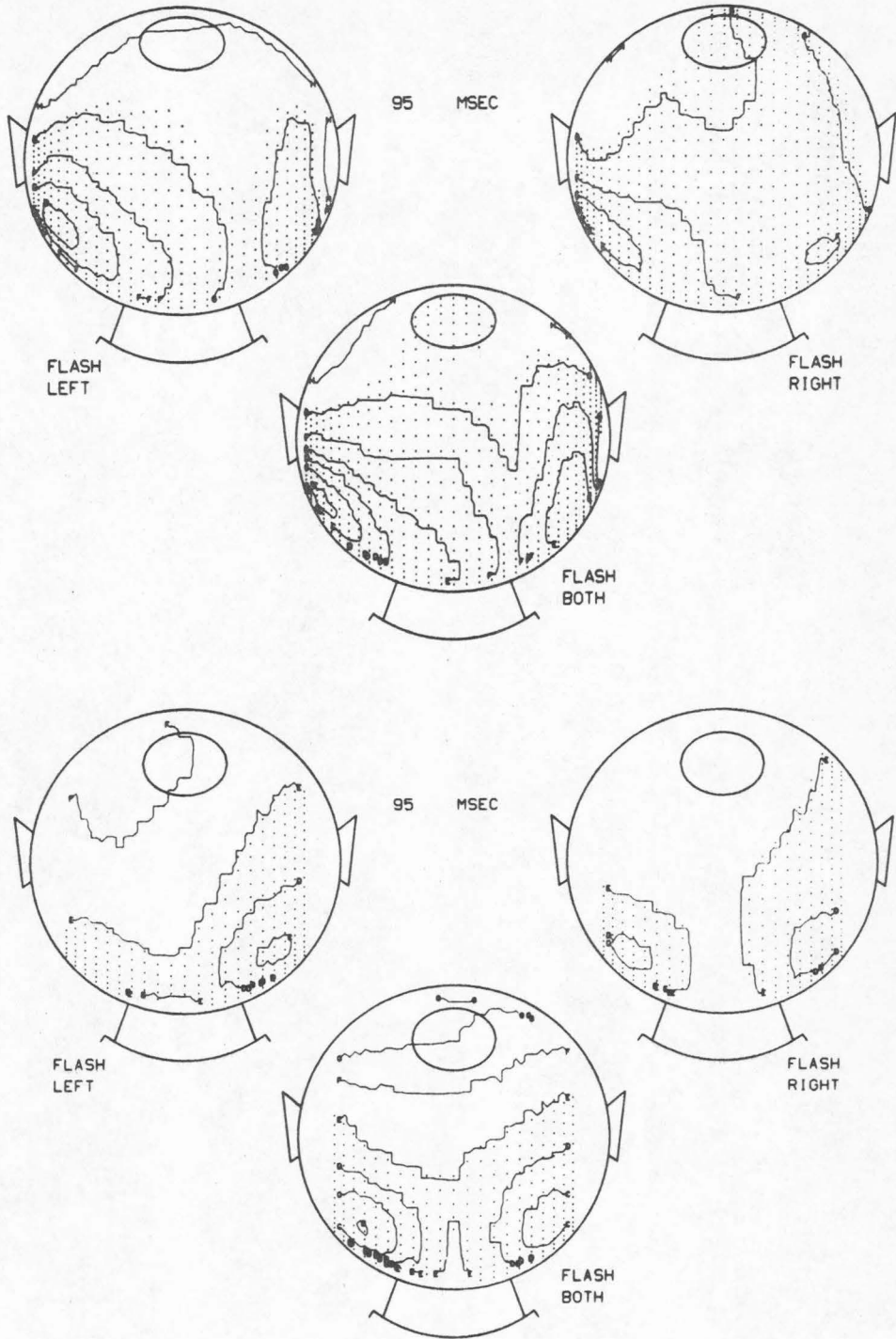


Figure 3-1 (c).

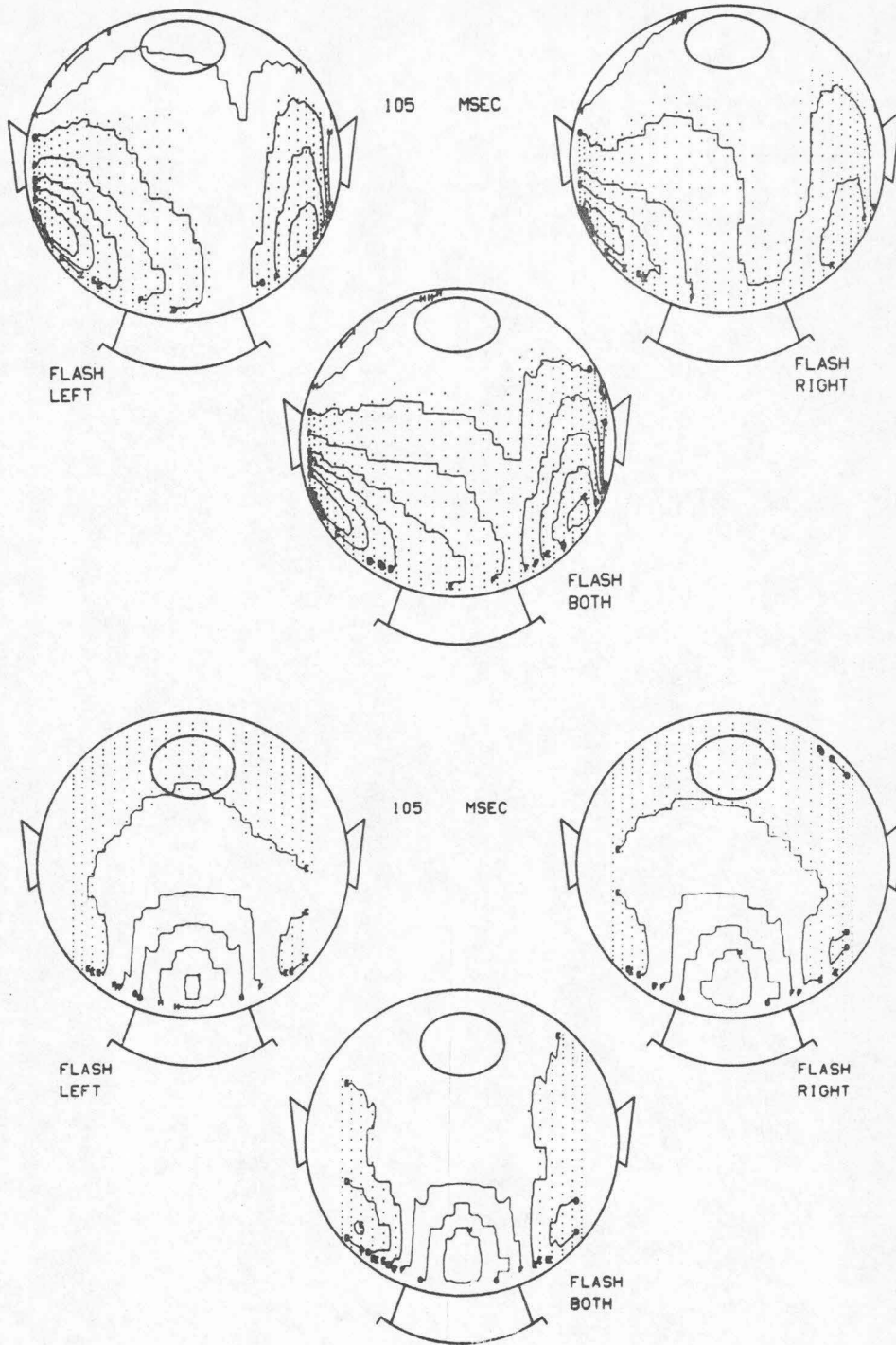


Figure 3-1 (d).

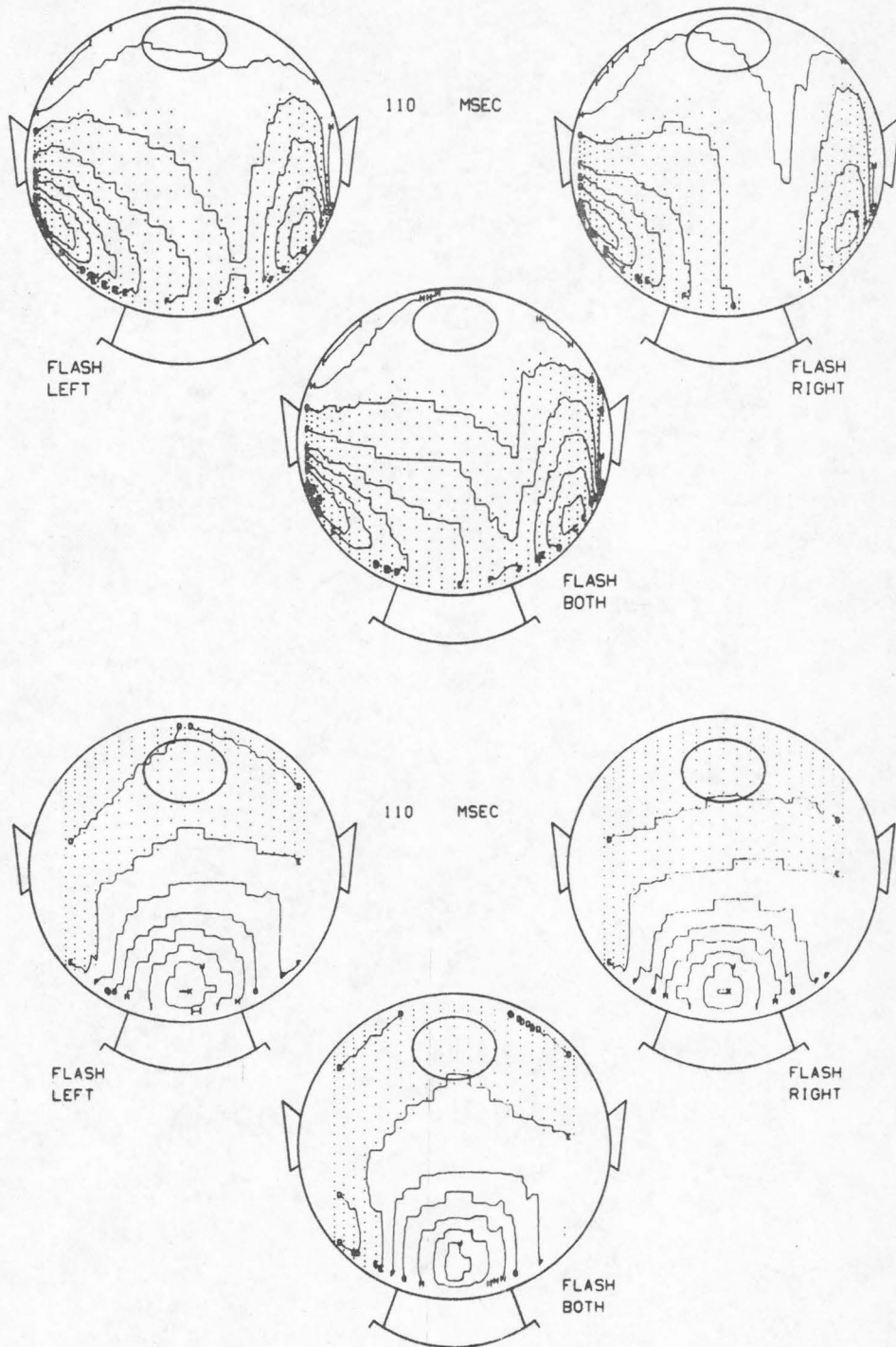


Figure 3-1 (e).

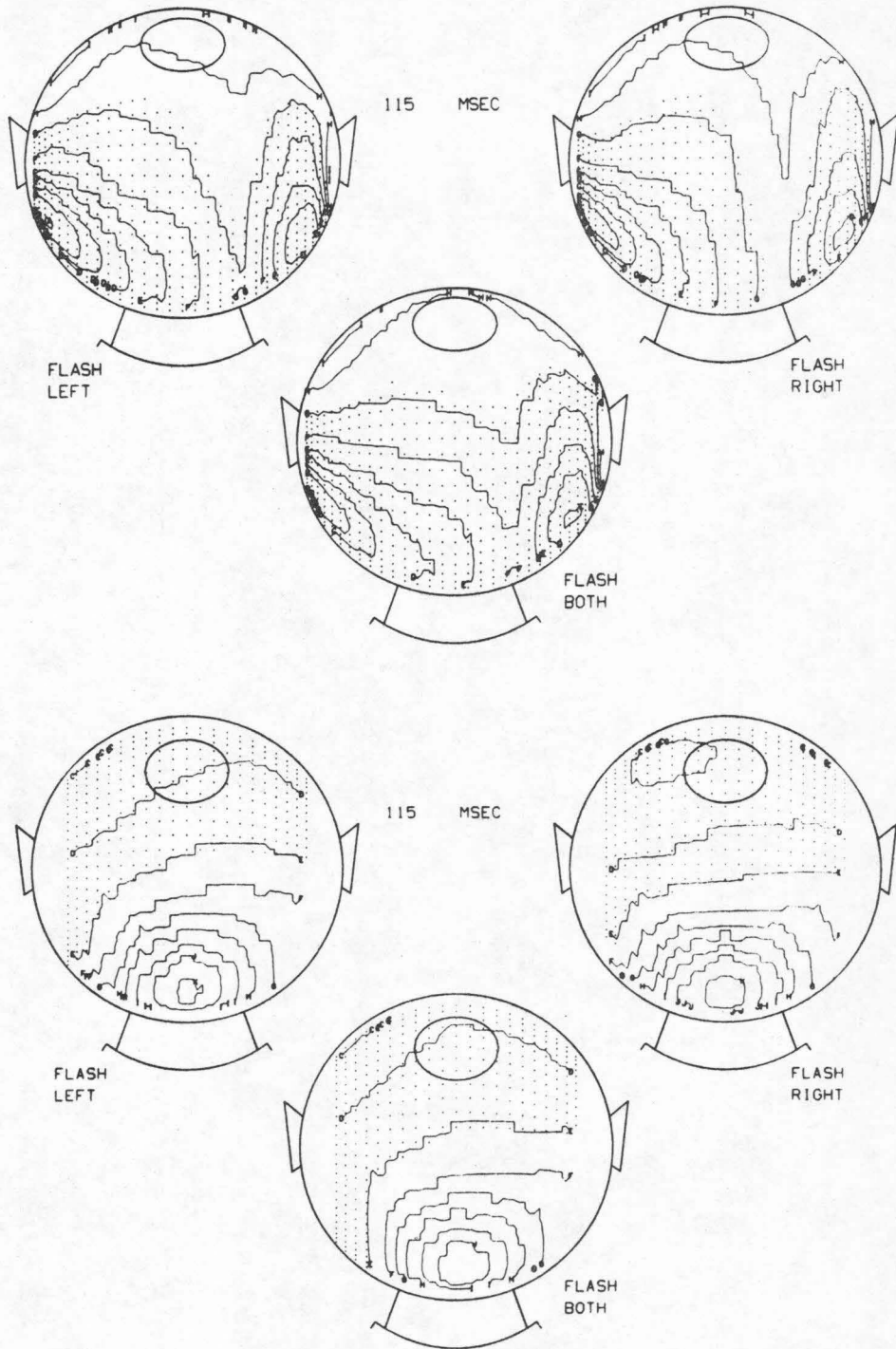


Figure 3-1 (f).

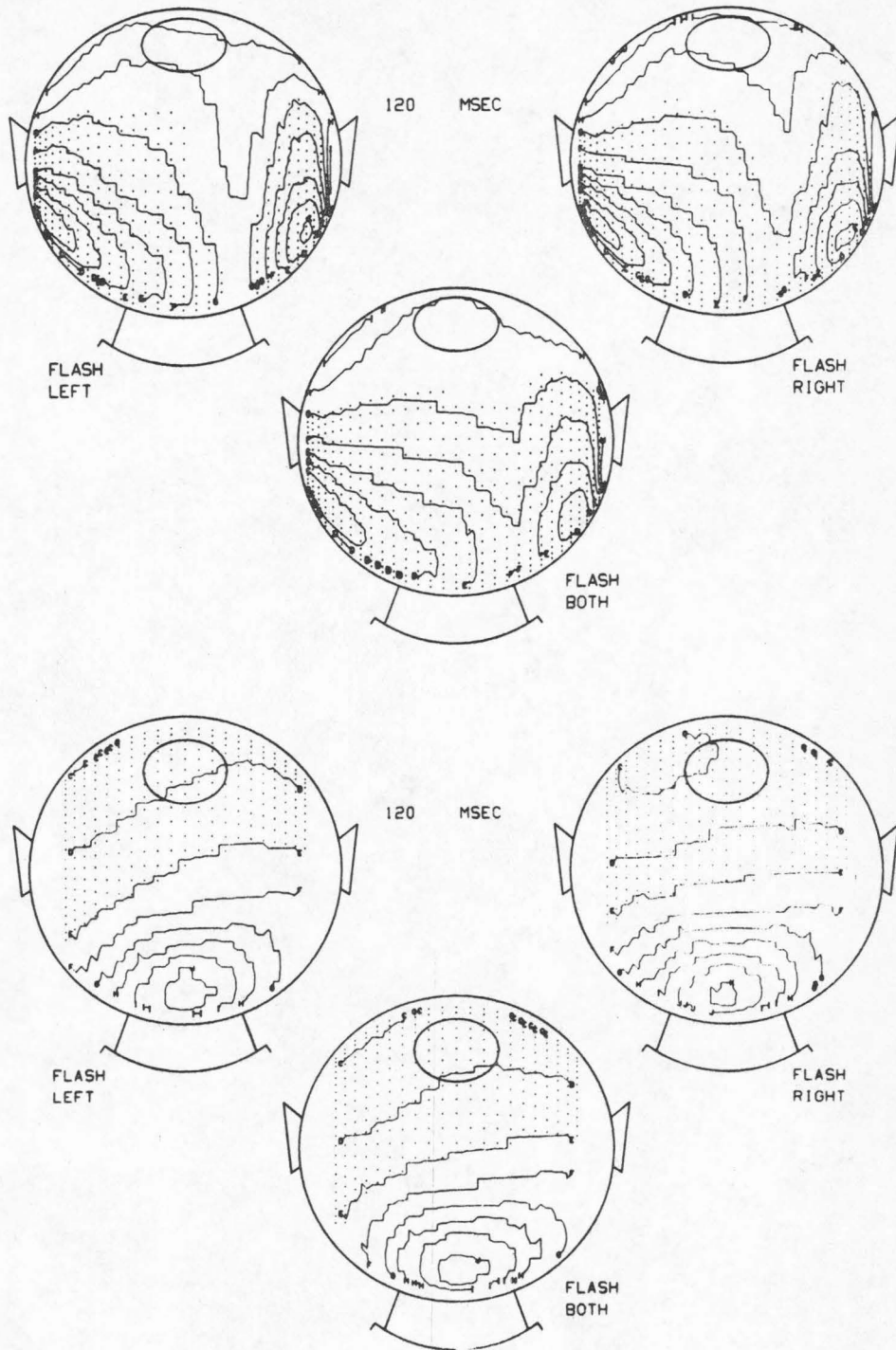


Figure 3-1 (g).

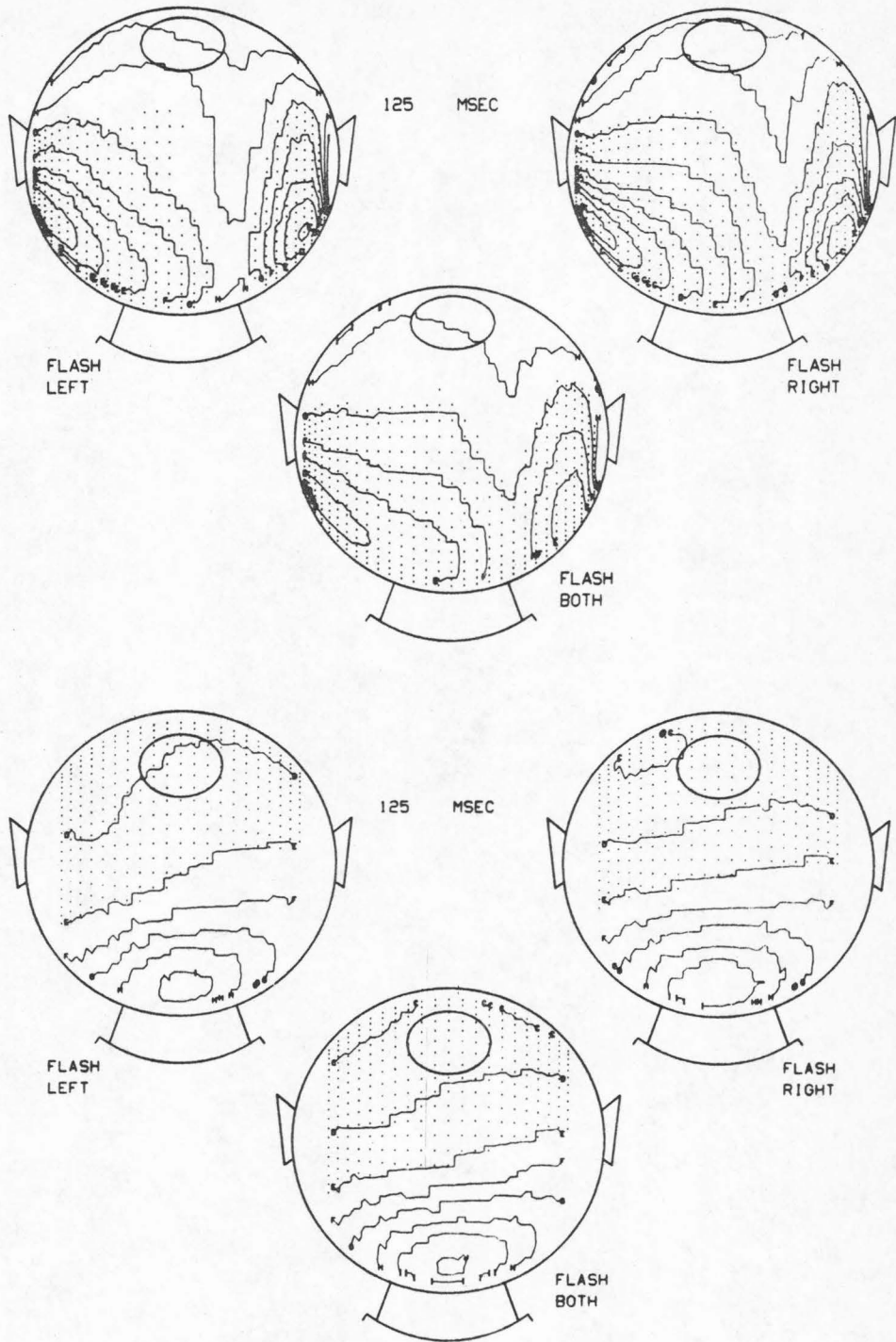


Figure 3-1 (h).

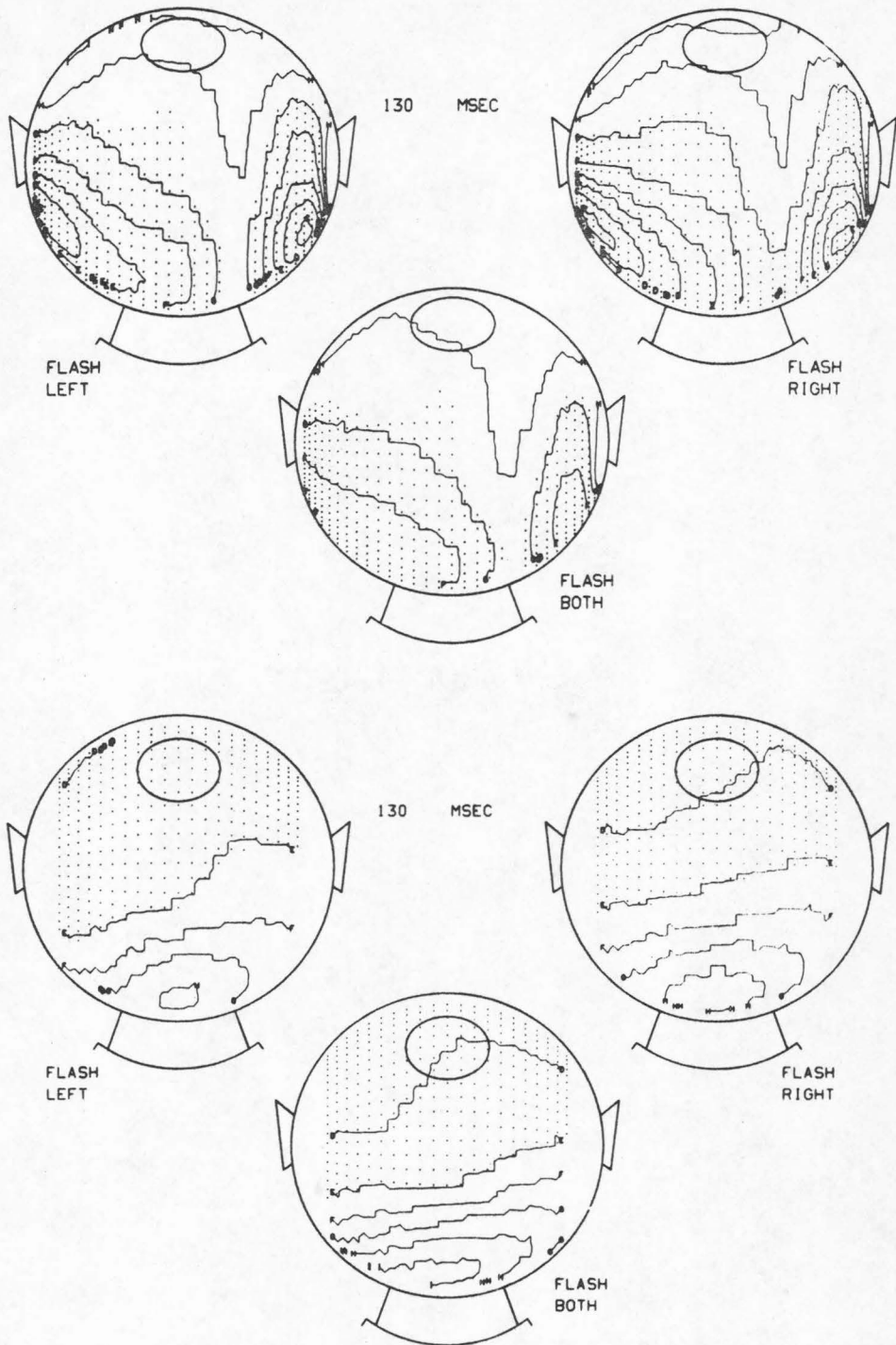


Figure 3-1 (i).

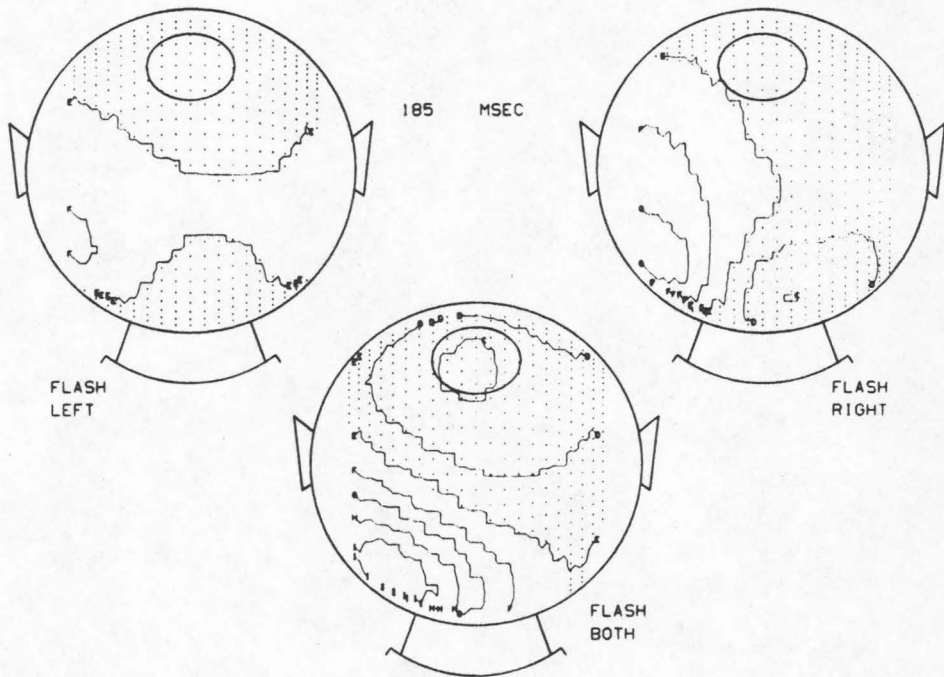
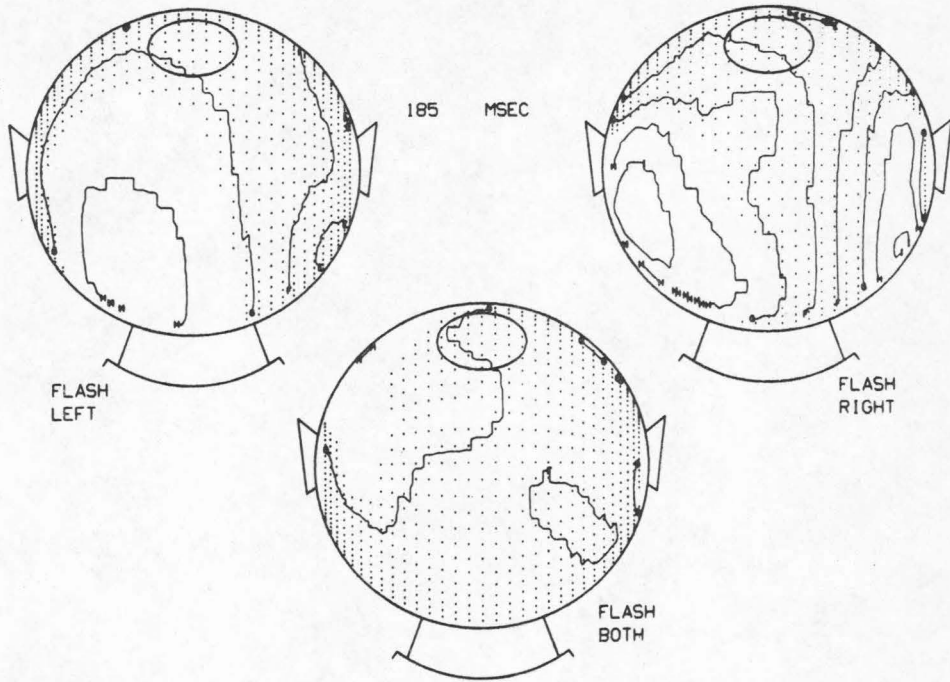


Figure 3-1 (j).

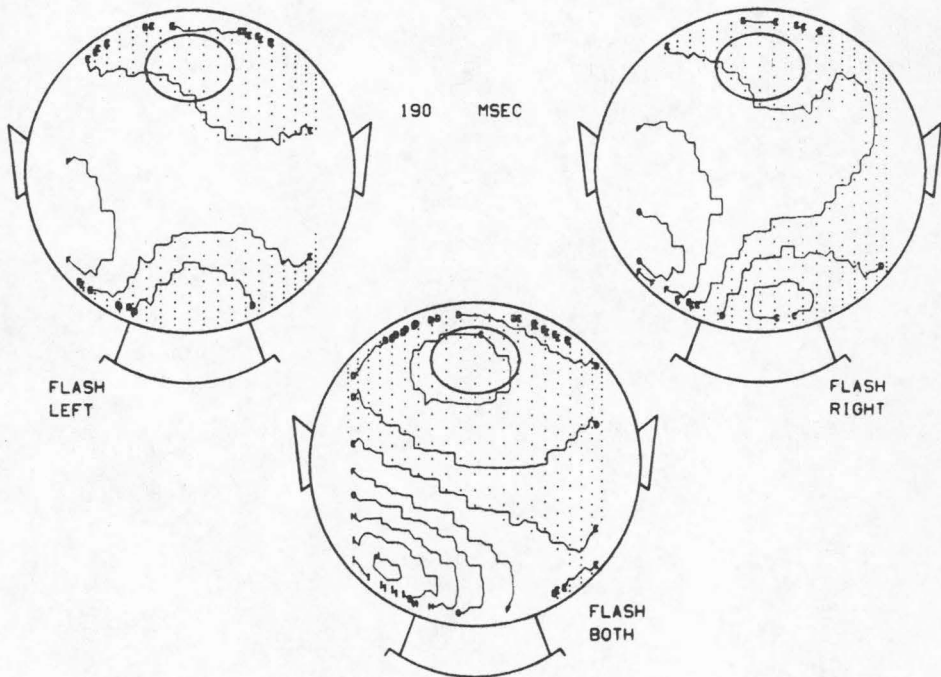
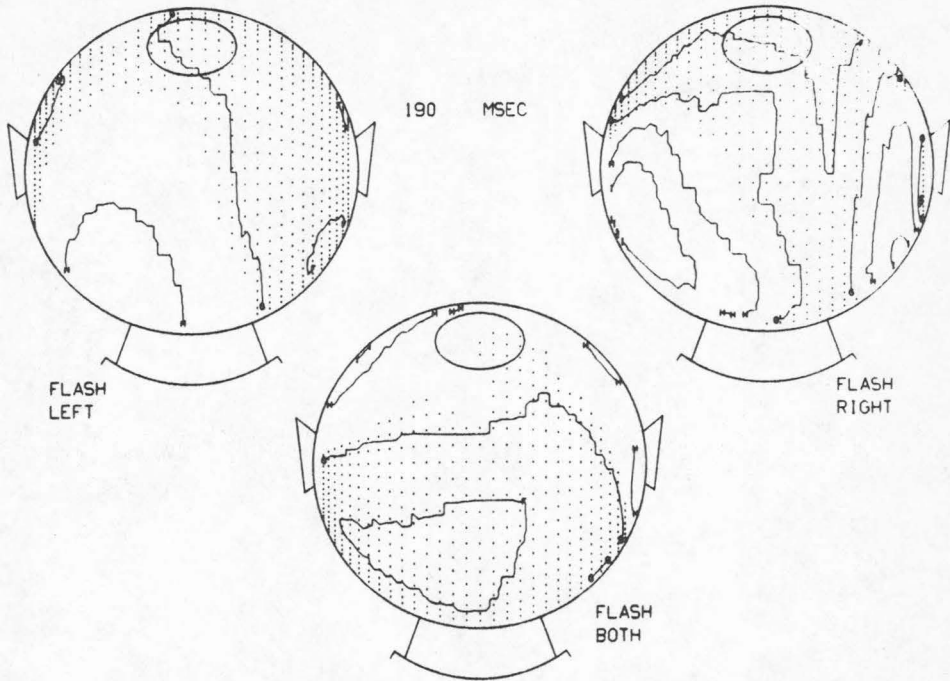


Figure 3-1 (k).

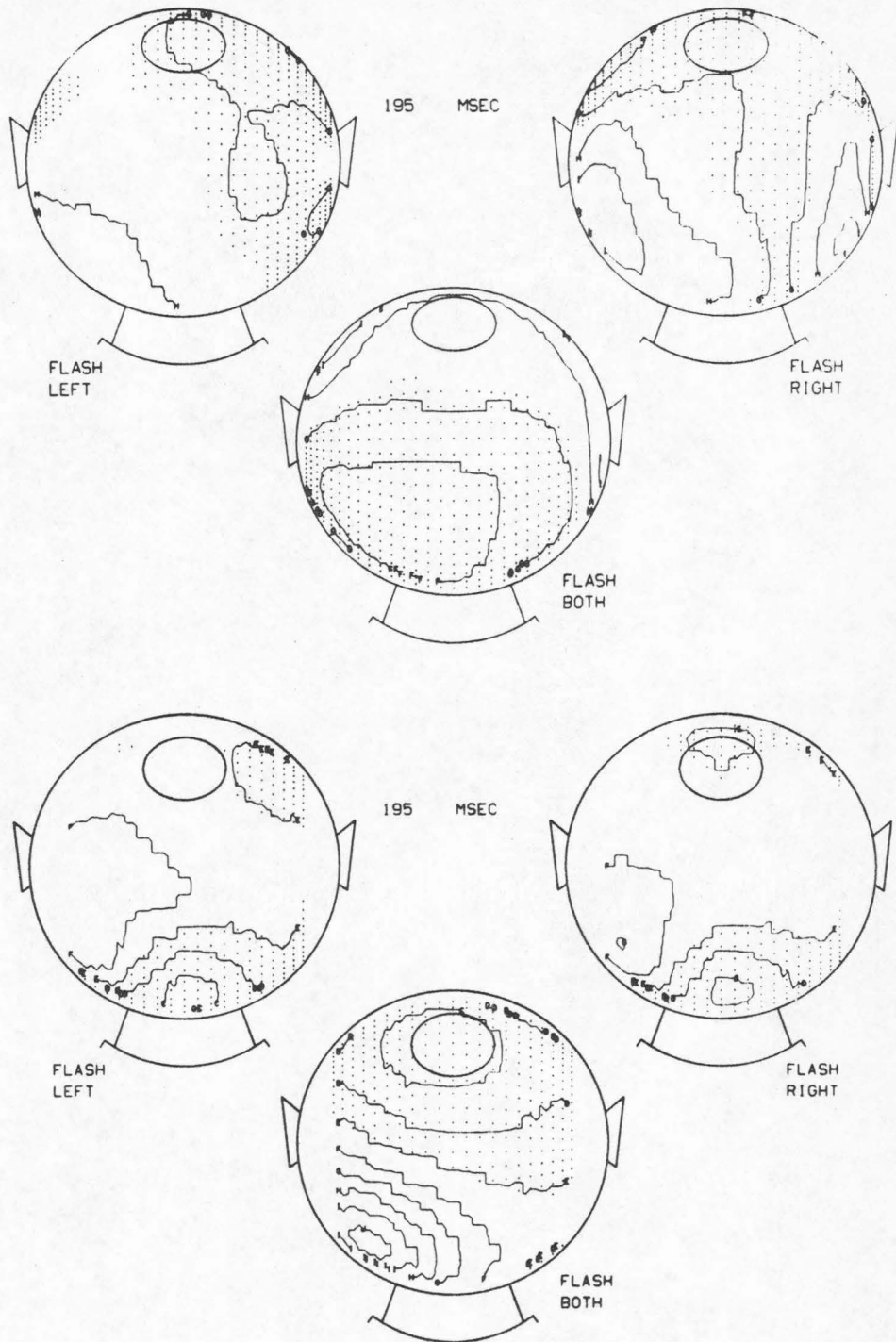


Figure 3-1 (1).

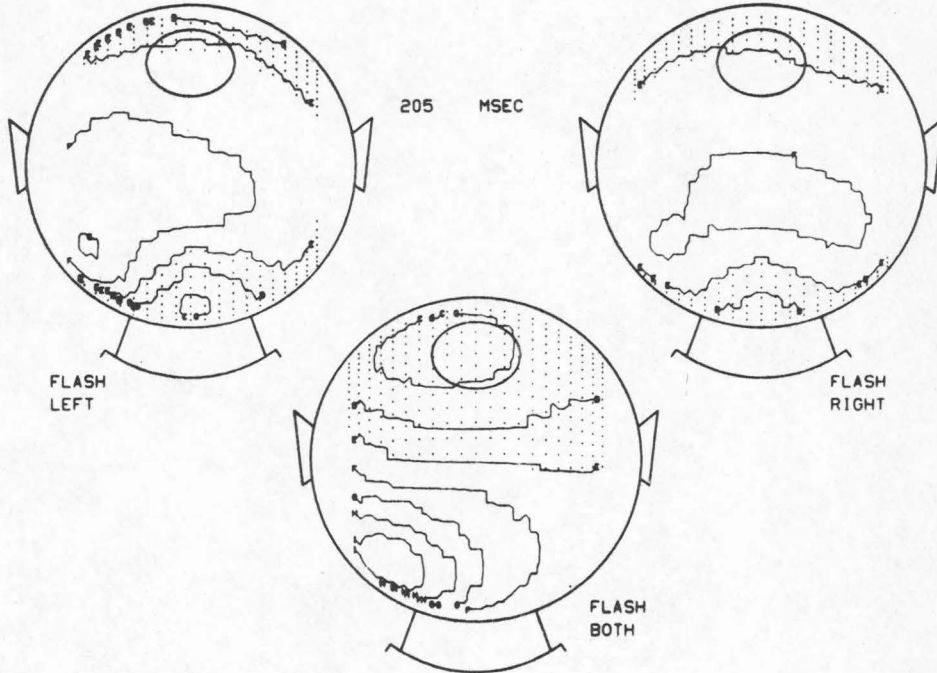
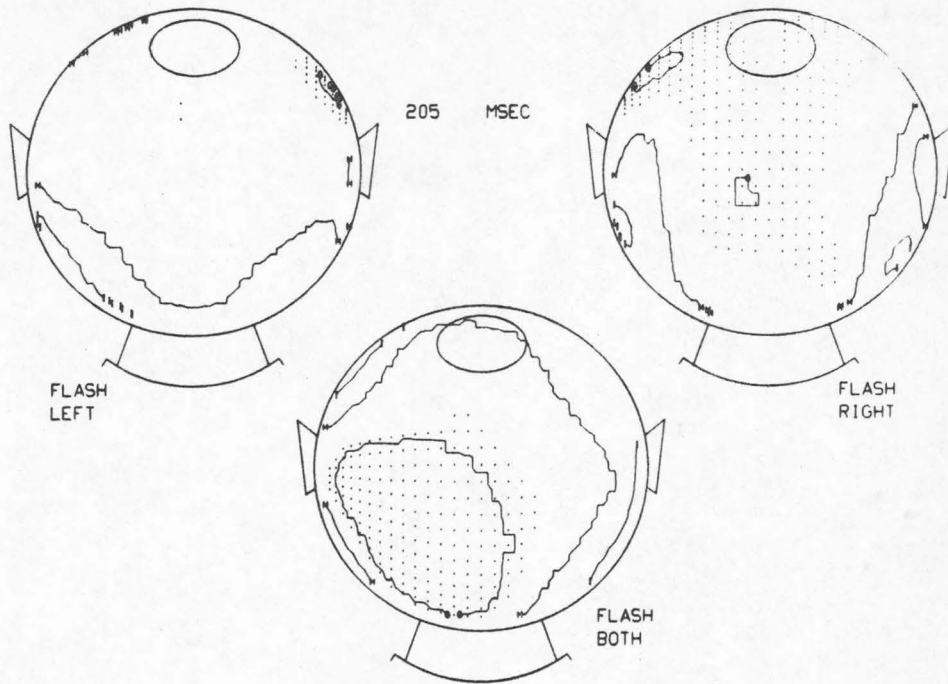


Figure 3-1 (m).

configuration of generators. Without any objective analytical procedures, however, it would be almost impossible to prove that in fact there is strong dependence from channel to channel. It is this objective analysis of the "simplicity" of the data that is to be developed and used in this chapter.

2. The Dipole Hypothesis and its Relationship to Factor Analysis

One motivation for discussing the human visual evoked response in terms of the dimensionality of the data lies in the hypothesis underlying the work of Chapters IV and V. A more detailed description of the "dipole hypothesis" is given later (Chapter IV) and in other sources (5), but in this chapter I will show how one can ask some preliminary questions about the appropriateness of such a model of the evoked response.

If we assume that the potentials on the surface of the head can be explained by an equivalent dipole located somewhere in the brain, then at any point on the surface of the head

$$V_i(t_j) = a_{ix}P_x(t_j) + a_{iy}P_y(t_j) + a_{iz}P_z(t_j) \quad (1)$$

where $V_i(t_j)$ is the voltage which appears at electrode i at time t_j . The three components of the dipole, $P_x(t_j)$, $P_y(t_j)$ and $P_z(t_j)$ are combined in a linear manner at any electrode site, and the constants a_{ix} , a_{iy} and a_{iz} are dependent upon only the dipole location, the reference potential location and the location of the recording electrode. Note that the dipole components may be a function of time but the dipole location is assumed constant (the a_i 's are not functions of time).

In Chapter IV it will be shown that a single dipole is characterized by six parameters: three position coordinates and three orthogonal components of the dipole strength. Equation(1) is apparently a function of only three parameters because the dipole is assumed to be fixed in space and hence the dependence upon the actual position of the dipole is included in the coefficients a_{ix} , a_{iy} and a_{iz} .

During a typical experiment we record from many electrode sites at successive instants of time. The data recorded from the two subjects used yield a collection of potentials $V_i(t_j)$ where $i = 1, 2, \dots, N$ where N is the number of electrodes (41 and 38 for subjects KW and DALO respectively) and $t_j = 1, 2, 3, \dots, 256$ ms.

The data from an evoked response experiment thus consist of V , an $N \times 256$ matrix of potential values. If a relation of the form (1) exists, then two more matrices are imagined. The three dipole components P_x , P_y and P_z have each 256 values, defining P , a 3×256 matrix. The coefficients a_{ix} , a_{iy} and a_{iz} have values for each of $i = 1, 2, \dots, N$ electrodes, constituting A , and $N \times 3$ matrix. Equation (1) is then, in matrix form

$$V = AP \tag{2}$$

Let us leave this hypothetical relationship for the moment and consider only that matrix which thus far actually exists; the matrix of potentials values, V .

The suspicion is that the various channels of the evoked response data are not mutually independent. If this is so, then it

may be possible that some other $N \times 256$ matrix, say W , exists such that the N dependent rows of V can be derived from mapping from N independent rows of W , i. e.

$$V = BW \tag{3}$$

The demonstration of the existence of W is constructive, for we will find out how in fact to find W .

First solve for W in (3);

$$W = B^{-1} V, = CV \tag{4}$$

Now if W is to be an $N \times 256$ matrix whose rows are independent, then its variance - covariance matrix must be diagonal, i. e.

$$\text{Cov} [W W^T] = \Lambda = \text{diag} (\lambda_1, \lambda_2 \dots \lambda_N) \tag{5}$$

But from (4) we can substitute for W ;

$$\begin{aligned} \text{Cov} [W W^T] &= \text{Cov} [C V (C V)^T] \\ &= \text{Cov} [C V V^T C^T] \\ &= C \text{Cov} [V V^T] C^T \\ &= C \Sigma C^T \end{aligned}$$

where Σ is the variance - covariance matrix of the original data, V .

$$\Sigma = \begin{bmatrix} \sigma_{11}^2 & \sigma_{12}^2 & \dots & \sigma_{1N}^2 \\ \sigma_{21}^2 & & & \cdot \\ \cdot & & & \cdot \\ \cdot & & & \cdot \\ \sigma_{N1}^2 & \dots & \dots & \sigma_{NN}^2 \end{bmatrix}$$

Since Σ is a real symmetric matrix we know that some matrix C exists which will diagonalize it, i. e.

$$\Lambda = C\Sigma C^T \quad (6)$$

can be produced, and $W = CV$ is the desired matrix of independent variates.

The diagonal elements of Λ are $\lambda_1, \lambda_2, \dots, \lambda_N$, the N eigenvalues of Σ . Furthermore, since the trace of Λ remains the same as the trace of Σ , i. e.

$$\lambda_1 + \lambda_2 + \dots + \lambda_N = \sigma_{11}^2 + \sigma_{22}^2 + \dots + \sigma_{NN}^2 \quad (7)$$

the total variance of the original data is preserved by the new orthogonal system W .

Each λ_i corresponds to an axis in the basis system W , and the value of λ_i indicates the contribution to the total variance of the corresponding axis. When the λ_i are arranged in descending order, it is often found that a certain $n \ll N$ of them sum to "most" of the total variance in the data. This suggests that the "dimensionality" of the data matrix V is only n and that all of the remaining variance expressed by the sum of the $(N-n)$ smallest eigenvalues of Σ is due to experimental error or noise. This summarization of the variability of V by a small number of the axes of W is the essence of principal factor analysis or principal components analysis.

The relationship between the data and the "factors" is contained in C , the $N \times N$ matrix of the eigenvectors of Σ . Since from (4)

$$V = C^{-1} W \quad (8)$$

the matrix C^{-1} is called the "factor pattern" and gives the coefficients for each data point of V in terms of the orthogonal system W . C is an orthogonal matrix and hence $C^{-1} = C^T$; therefore once the characteristic equation $(\Sigma - \Lambda) C = 0$ is solved for C , the factor pattern easily follows.

Now let us reconsider equation (2) in light of (8). In developing the principal factor solution, suppose that $n = 3$ eigenvalues had dominated the summarization of the variance, (for example, suppose the three largest λ_i 's summarized 99% of the variance in Σ). The first three columns of C^{-1} and the first three rows of W express each data point of V to within some small error, thus the $N \times 3$ matrix A and the 3×256 matrix P can be identified with these sub-matrices of C^{-1} and W respectively!

This then is an application of principal factor analysis to the evoked response data. If indeed $n = 3$ eigenvalues summarize most of the variability of the data, then one might say that a relation of the form (1) could be a reasonable hypothesis. If it developed that it required six principal factors, then one could say that two dipoles were plausible explanations of the evoked responses. (For n dipoles, the right-hand side of (1) has $3 \times n$ terms.) The uncertainty of the applicability of (2) even if n is 3 or an integral multiple of 3 is that the principal factor analysis suggests only the true dimensionality of the data. There are many possible "sources" of the data matrix V which would be expressed in the form (2). The dipole hypothesis cannot be accepted simply by achieving a principal

factor solution having say three or six dominant factors. If such a solution does occur, however, then there is a certain credibility in pursuing dipole sources as the generators of the evoked response.

One further process may be performed on the orthogonal system W . Carrying out this next step is known as factor analysis and is again only briefly described here. The essence of the procedure is to perform a rigid rotation on the orthogonal system W so that any given variable has now large coefficients for some axes (factors) and small coefficients for others. The principal components solution typically has at least one factor for which all variables have large coefficients. This would mean for the evoked responses that one factor would apparently be most significant throughout the entire response, and the remaining $(n-1)$ factors have large coefficients for some variables and small ones for other variables. The factor analysis solution thus eliminates the common factor, developing an equivalent system where all of the n principal factors have large influence on some variables and small influence on others. This often permits grouping of variables by their factor coefficients and hence gives another indication of which variables in the raw data are mutually affected by the same underlying process (factor).

The details of principal components analysis and principal factor analysis can be found in several sources, such as Seal (6), Cooley and Lohnes (2) and Harman (4). What has been described in

the foregoing was intended to illustrate a relationship of this statistical tool to the evoked response problem.

3. Results of Applying Factor Analysis Methods to the Evoked Response Data.

Not all of the assumptions leading to equation (2) are equally valid. Most conspicuous is the fact that the matrix of coefficients A is unlikely to be time-invariant, since in the case of evoked responses one would expect to have either different dipole sources active at different times during the response or, equally in violation of the assumptions, moving sources.

A single dipole, fixed throughout the duration of the evoked response and fitting the data to within some small error would seem to be a most unlikely situation. The immediate question, however, does not include any analysis so sophisticated as to partition the data into intervals when (2) is a reasonable hypothesis. For the moment, it is intended merely to ask how complex is the data on the average, over the entire response?

Note there are two ways of analyzing the data. In the first case the N channels of the evoked response recordings can be considered as the "variables" and the 256 potentials for each channel are then the "observations" of each variable. The principal components analysis can then be used to ask how many independent channels are present in the data. This is directly comparable to the analysis of the ECG data by Cady. If the principal components solution finds $n \ll N$ principal factors one could seek an

n - channel "basis" for the evoked response data. The remaining $(N - n)$ channels could then be derived from the basis channels by a regression analysis.

Treating the data as 256 observations of N variables is also consistent with the discussion of the evoked response data in terms of equivalent dipoles. Instead of using the principal factor solution to simply find how many independent channels are present, one could seek to determine the applicability of equation (1) to the data. This means that not only is it desirable that n be small, but it should be an integer multiple of three. As described in the previous section, a principal factor solution which does in fact yield such a value of n produces matrices which could be identified as the matrices A and P in the dipole formulation.

Alternatively, one could consider the 256 sample times as the variables and N potentials at each sample time as the observations. With this interpretation it is then possible to ask if the sample times are independent of one another, i. e. during successive intervals of the response is the data dependent upon the data in preceding or following intervals. This could be used to partition the response into times during which some source or sources become activated, dominate the data over a certain interval and then yield to some other source.

For both of the above possibilities the data were analyzed using the principal factor method to determine the number of factors necessary to account for most of the variability of the data.

This factor structure was then rotated, using the Varimax criterion to attain a "simplified" factor structure. All of this analysis was done using the factor analysis subroutines available in the IBM Scientific Subroutine Library.

(a) Factor Analysis of Data Using Channels as Variables

There are six sets of data to be analyzed; three conditions for each of the two subjects. Table 3-1 shows the cumulative percentage of the variance summarized by the first six eigenvalues of the correlation matrices of the data.

Table 3-1. Cumulative Percentage of Variance Summarized by Eigenvalues of Correlation Matrices with Recording Channels Considered as Variables.

<u>Eigenvalue</u>	<u>Data Set Analyzed</u>					
	<u>Dalo Flash Right</u>	<u>Dalo Flash Left</u>	<u>Dalo Flash Both</u>	<u>KW Flash Right</u>	<u>KW Flash Left</u>	<u>KW Flash Both</u>
1	47.5	56.6	52.1	56.8	56.2	51.3
2	65.7	79.0	69.9	83.0	84.9	90.6
3	79.7	90.3	84.3	95.3	94.6	96.1
4	93.3	95.9	91.4	96.4	96.6	97.2
5	97.5	97.7	94.9	97.3	97.6	98.0
6	98.4	98.3	96.7	97.9	98.5	98.5

Note that these are the eigenvalues of the correlation matrices, not the variance-covariance matrices. This is quite

consistent with the principal components procedure, since the correlation matrix is simply the variance-covariance matrix of the original data expressed as standard scores. This assigns equal weight to the original data in determining the orientation of the eigenvectors (7).

This table shows that most of the experimental variance can be accounted for by only six eigenvalues - in fact a great deal is summarized by only three eigenvalues. As suggested earlier in section three, this suggests that the channels are not independent of one another. The results also show that perhaps equation (1) does have some justification in terms of the evoked response data. It would appear that three factors are not sufficient to summarize the data, hence it is not possible to think of the evoked response data in terms of a single dipole fixed in space throughout the response --- not a surprising result. If one used six factors, however, it is clear the data are well accounted for, and perhaps one could use this result to argue that over the duration of the response one or perhaps two dipoles could suffice: if necessary these one or two dipoles could be allowed to be relatively fixed for some interval and then move to another relatively fixed site over another interval of the response (in other words equation (1) applies piece-wise over the complete response).

When the factor coefficients (loadings) for the six principal factors for each of the six data sets are submitted to a rotation scheme the factor structures shown in Tables 3-2 through 3-7

Table 3-2. Rotated Factor Loadings for each Channel of DALO data from Flash Right Condition.

Channel	Principal Factors					
	1	2	3	4	5	6
11	.676	-.406	.592	.062	-.053	.072
12	.667	-.480	.501	.194	-.149	.082
13	.411	-.471	.312	.641	-.295	.063
14	.225	-.144	.207	.870	-.345	.036
15	-.185	.049	-.079	.968	-.069	-.053
16	-.414	.207	.124	.833	.206	.061
21	.778	-.323	.500	-.082	-.150	-.001
22	.795	-.350	.389	-.041	-.290	.013
23	.586	-.222	.171	.228	-.714	.043
24	-.065	.096	-.080	.563	-.797	.097
25	-.482	.511	-.242	.625	-.196	.088
26	-.534	.771	.083	.220	-.004	.230
31	.780	-.363	.446	-.116	-.160	-.015
32	.838	-.301	.234	-.200	-.312	.040
33	.593	-.120	-.032	-.156	-.773	-.006
34	-.114	.250	-.325	.086	-.887	-.003
35	-.480	.733	-.186	-.106	-.295	.303
36	-.521	.772	.009	-.094	-.088	.331
41	.882	-.315	.304	-.095	-.023	.001
42	.930	-.207	.119	-.126	-.203	.056

Table 3-2. (continued).

Channel	Principal Factors					
	1	2	3	4	5	6
43	.811	.072	-.030	-.054	-.565	-.054
44	.122	.614	-.332	.053	-.681	-.136
45	-.189	.884	-.332	-.079	-.219	-.050
46	-.340	.911	.081	-.150	.030	.140
51	.951	-.153	.211	-.021	.135	.006
52	.981	-.109	.101	-.029	.065	-.055
53	.890	.281	-.068	.048	-.279	-.174
55	.115	.942	-.123	.099	.052	-.241
56	-.094	.964	.126	.020	.181	-.064
58	.476	.216	.780	-.026	.310	-.041
61	.558	-.303	.705	.232	.048	.129
62	.409	-.466	.604	.461	.064	.110
63	.131	-.183	.649	.707	.107	-.031
64	.904	.048	.367	.079	.081	-.063
65	.889	.095	.140	.095	.340	-.088
66	.356	.546	.492	.093	.483	-.229
68	.205	.051	.941	.074	.221	-.034
54	.399	.760	-.226	.081	-.388	-.219

Table 3-3. Rotated Factor Loadings for each Channel of DALO data from Flash Left Condition.

Channel	Principal Factors					
	1	2	3	4	5	6
11	.681	-.526	-.464	.145	.008	.052
12	.0744	-.410	-.474	.190	.080	.012
13	.626	-.060	-.755	.149	.011	-.037
14	.279	.280	-.900	.057	-.104	-.086
15	-.303	.506	-.766	-.179	-.066	-.075
16	-.842	.035	-.419	-.107	.040	-.034
21	.842	-.404	-.279	.178	.069	-.040
22	.916	-.231	-.204	.203	.126	-.066
23	.862	.342	-.342	.097	-.073	-.054
24	.252	.781	-.409	.071	-.387	-.025
25	-.624	.733	.037	-.139	-.161	-.036
26	-.730	.275	.570	.194	.060	-.023
31	.855	-.392	-.265	.109	.059	-.024
32	.954	-.196	-.068	.172	.098	-.036
33	.878	.450	-.062	.088	-.080	.012
34	.141	.913	-.019	.030	-.369	.036
35	-.497	.578	.611	.174	.038	-.022
36	-.576	.304	.680	.288	.128	-.069
41	.781	-.527	-.299	-.043	-.089	-.015
42	.894	-.425	-.025	-.051	.018	-.058

Table 3-3. (continued).

Channel	Principal Factors					
	1	2	3	4	5	6
43	.890	.254	-.018	-.259	-.130	.123
44	-.238	.882	.211	-.264	-.174	.095
45	-.648	.534	.461	-.215	.146	.066
46	-.707	.194	.653	.111	.126	.043
51	.502	-.814	-.179	-.109	-.068	-.048
52	.375	-.822	-.077	-.376	-.017	-.133
53	-.287	-.039	-.061	-.948	.013	.000
55	-.813	.222	.335	-.372	.161	-.034
56	-.846	.050	.470	-.181	.133	-.015
58	-.075	-.917	.095	.146	-.299	.124
61	.505	-.662	-.513	.137	.067	.082
62	.445	-.531	-.684	.165	.095	-.005
63	.008	-.445	-.853	.025	.179	.108
64	.158	-.890	-.303	-.237	-.101	-.072
65	-.349	-.722	-.239	-.415	-.244	-.140
66	-.832	-.417	.196	-.236	-.095	-.114
68	.095	-.891	-.035	.311	-.089	.283
54	-.620	.521	.272	-.515	.013	.025

Table 3-4. Rotated Factor Loadings for each Channel of DALO data from Flash Both Condition.

Channel	Principal Factors					
	1	2	3	4	5	6
11	.182	-.392	.180	.714	.096	-.082
12	.252	-.357	.231	.838	.167	.073
13	.131	-.247	.848	.382	.047	.135
14	-.062	.016	.982	-.124	-.056	-.073
15	-.240	.098	.774	-.537	-.044	-.160
16	-.221	.46	.661	-.627	.023	-.220
21	.130	-.336	.059	.878	.053	.008
22	.134	-.220	-.080	.949	.120	.063
23	.112	-.025	.265	.901	-.220	.137
24	-.204	.127	.771	-.186	-.456	-.310
25	-.436	.239	.562	-.602	-.113	-.344
26	-.395	.286	.256	-.426	.004	-.622
31	.212	-.331	-.109	.874	.113	.114
32	.111	-.181	-.255	.922	.096	.117
33	.094	.046	-.187	.910	-.254	.213
34	-.150	.351	.208	-.074	-.868	-.197
35	-.325	.394	.026	-.436	-.334	-.649
36	-.300	.450	-.072	-.359	-.197	-.724
41	.169	-.297	-.076	.784	.159	.042
42	.207	-.135	-.237	.901	.123	.197

Table 3-4. (continued).

Channel	Principal Factors					
	1	2	3	4	5	6
43	.239	.181	-.135	.872	-.156	.317
44	-.027	.843	.044	.062	-.527	-.005
45	-.310	.817	-.027	-.342	-.144	-.299
46	-.120	.743	-.236	-.266	-.106	-.534
51	.469	-.076	-.143	.744	.165	.363
52	.422	-.017	-.201	.778	.175	.359
53	.358	.509	.027	.663	-.076	.379
55	-.053	.949	.067	-.270	.011	-.103
56	.060	.921	-.045	-.279	.019	-.240
58	.776	.070	-.210	.542	.143	.161
61	.515	-.268	.400	.594	.069	.242
62	.381	-.385	.697	.404	.107	.173
63	.120	.009	.947	-.151	-.067	.171
64	.568	.085	-.066	.726	.143	.319
65	.601	.291	-.050	.531	.042	.434
66	.555	.748	-.077	-.084	.262	.085
68	.871	-.068	.135	.422	.003	.155
54	.093	.949	.058	.139	-.233	.087

Table 3-5. Rotated Factor Loadings for each Channel of KW Data from Flash Right Condition.

Channel	Principal Factors					
	1	2	3	4	5	6
1	.985	-.081	.060	-.012	.021	.118
2	.956	-.224	.108	-.007	.071	.067
3	.956	-.199	.127	-.089	.054	.055
4	.825	-.051	.065	-.547	.033	-.000
5	.434	.625	-.213	-.023	.599	.004
6	-.617	.684	-.275	.023	.044	-.123
7	.918	.300	.033	-.034	.121	.162
9	.319	.491	-.781	.094	-.043	-.040
10	.249	.230	-.928	.066	.042	.036
11	-.054	.416	-.895	.002	.011	-.031
12	-.231	.467	.845	-.031	-.018	-.043
13	-.307	.505	-.792	-.039	-.017	-.024
14	-.341	.608	-.696	-.054	-.044	-.021
15	-.311	.896	-.293	-.030	-.012	.011
17	.713	-.148	-.660	.034	.021	.158
18	.623	-.445	-.606	-.036	.053	.185
19	.315	-.340	-.894	-.057	.014	.076
21	-.405	.424	-.784	-.026	-.011	-.015
22	-.452	.557	-.678	-.037	-.059	-.016
23	-.230	.941	-.225	-.026	.006	-.038

Table 3-5. (continued).

Channel	Principal Factors					
	1	2	3	4	5	6
25	.935	-.219	-.250	.045	-.013	.037
26	.745	-.612	-.238	-.046	.016	.042
27	.651	-.676	-.311	-.081	.012	-.053
28	.212	-.307	-.894	.052	.096	-.052
29	-.518	.480	-.678	.027	.065	.049
30	-.600	.657	-.435	-.039	-.086	.034
31	-.083	.967	-.196	-.094	.013	-.005
33	.975	-.112	-.161	.040	-.015	-.029
34	.890	-.435	-.052	.012	.002	-.096
35	.985	-.602	.049	-.071	.006	-.095
36	.771	-.534	.057	-.151	-.010	-.156
37	-.620	.702	-.287	.110	.010	.099
38	-.586	.734	-.304	.016	-.065	.068
39	.356	.905	-.073	-.128	.083	.020
41	.986	-.128	-.051	.059	-.004	-.032
42	.930	-.337	.026	.029	.011	-.086
43	.888	-.390	.107	-.017	.019	-.108
44	.958	-.138	.020	-.008	.074	-.108
45	-.087	.930	-.106	.184	.092	-.006
46	-.516	.803	-.222	.107	.012	.016
47	.876	.424	.036	.020	.092	.124

Table 3-6. Rotated Factor Loadings for Each Channel of KW Data from Flash Left Condition.

Channel	Principal Factors					
	1	2	3	4	5	6
1	.013	.955	.195	-.054	.184	-.091
2	.181	.959	.146	-.082	.080	-.083
3	.063	.969	.141	-.171	-.015	-.030
4	-.265	.895	.212	-.231	-.047	.138
5	-.886	.239	-.191	-.310	-.008	.110
6	-.957	-.101	-.183	-.128	.001	.138
7	-.568	.741	.018	-.302	.162	-.030
9	-.790	.189	.514	.121	.075	-.080
10	-.627	.094	.749	-.028	.041	-.116
11	-.869	-.040	.362	.022	-.003	-.314
12	-.930	-.224	.139	.040	-.037	-.228
13	-.915	-.341	-.006	.053	-.034	-.192
14	-.889	-.404	-.122	.086	-.001	-.136
15	-.966	-.010	-.139	-.148	-.053	-.121
17	.100	.426	.823	.133	.212	.103
18	.355	.382	.834	.002	.145	.082
19	.137	.167	.956	-.067	.079	-.071
21	-.872	-.436	-.015	.041	.028	-.186
22	-.851	-.453	-.178	.103	.054	-.132
23	-.962	.065	-.141	-.172	-.059	.100

Table 3-6. (continued).

Channel	Principal Factors					
	1	2	3	4	5	6
25	.276	.760	.494	.268	.104	.103
26	.539	.554	.612	.072	-.034	.108
27	.582	.468	.639	-.011	-.142	.072
28	.205	.287	.850	-.002	-.227	-.083
29	-.863	-.392	-.171	.144	.112	-.061
30	-.843	-.435	-.234	.158	.078	.010
31	-.934	.169	-.139	-.234	-.076	.102
33	.179	.878	.343	.252	.051	.063
34	.480	.771	.344	.142	-.174	.052
35	.628	.626	.404	.039	-.199	.075
36	.680	.474	.435	.001	-.297	-.002
37	-.828	-.342	-.371	.101	.170	.017
38	-.864	-.344	-.267	.166	.150	.075
39	-.827	.408	-.160	-.334	-.052	.062
41	.203	.927	.248	.160	.018	-.027
42	.392	.878	.199	.083	-.153	-.007
43	.356	.893	.201	-.041	-.161	.036
44	-.083	.936	.121	-.089	-.202	.142
45	-.916	.226	-.238	-.150	.032	.051
46	-.948	.153	.228	.030	.086	.090
47	-.614	.715	-.039	-.312	.069	-.009

Table 3-7. Rotated Factor Loadings for Each Channel of KW Data from Flash Both Condition.

Channel	Principal Factors					
	1	2	3	4	5	6
1	.992	.029	.062	.054	-.028	-.015
2	.976	-.148	.068	.095	.056	.025
3	.981	-.045	.127	.081	.095	.029
4	.917	.322	.139	.016	.161	.022
5	.143	.972	-.073	.059	.095	.010
6	-.238	.956	-.118	-.093	-.005	-.031
7	.891	.426	.056	.016	.015	-.059
9	.564	.640	.474	.085	-.145	-.071
10	.587	.536	.578	.141	-.030	-.054
11	.359	.570	.423	.596	.002	.025
12	.195	.852	.388	.280	-.018	.013
13	.056	.927	.242	.242	-.043	.027
14	-.161	.968	.064	.082	-.023	-.002
15	-.094	.977	-.028	-.078	.101	-.028
17	.798	.122	.567	-.003	-.104	-.079
18	.763	-.060	.632	.005	-.022	-.070
19	.668	.102	.703	.122	.079	-.037
21	.015	.934	.219	.214	-.051	.063
22	-.248	.957	.005	.031	-.016	-.000
23	.011	.989	.041	-.090	.049	-.053

Table 3-7. (continued).

Channel	Principal Factors					
	1	2	3	4	5	6
25	.914	-.097	.353	-.021	-.153	-.035
26	.759	-.374	.528	-.009	-.031	-.028
27	.705	-.348	.606	.078	.018	-.005
28	.573	.157	.671	.080	-.002	.413
29	-.220	.933	-.019	.098	-.219	.048
30	-.445	.832	-.263	-.128	-.066	.005
31	.183	.967	.044	-.031	.140	-.020
33	.956	-.017	.253	.014	-.119	-.008
34	.889	-.348	.260	.031	-.025	.050
35	.755	-.484	.422	.011	.043	.022
36	.705	-.505	.418	-.018	.018	.031
37	-.406	.741	-.464	-.045	-.234	-.007
38	-.498	.751	-.355	-.202	-.094	-.019
39	.450	.875	.062	-.017	.143	-.027
41	.980	-.069	.156	.029	-.063	.013
42	.941	-.283	.106	.060	.016	.063
43	.928	-.292	.196	.050	.056	.038
44	.974	.024	.027	.016	.134	.046
45	.031	.898	-.400	-.035	-.038	.030
46	-.385	.811	-.420	-.050	-.036	.042
47	.807	.553	.070	.012	.150	-.042

are obtained. One could select from these tables, if it was desired to find a set of basis channels, six apparently independent recording channels. The first task is to select six independent groups of channels on the basis of their coefficients in the tables. For example, in Table 3-2, there is one group (11, 12, 13, 21, 22, 23, 31, 32, 33) of channels whose coefficients for the first three factors are similar in magnitude and sign. Reference to Figure 2-2(b) shows that these electrodes are all on the left temporal area. One of these nine channels can then be picked as the "most typical" of the group and used as the first basis channel. Other groups in the table are channels 14, 15, 16, 24, 25, 26, 34, 35, 36 (left and midline occipital area); 41, 42, 43, 51, 52, 53 (right temporal); 44, 45, 46, 59, 55, 56 (right occipital); 61, 62, 63, 68 (left ear group) and 64, 65, 66, 58 (right ear group). The tables clearly show that electrodes adjacent to one another record similar evoked responses, hence the dependence from channel to channel.

This grouping process can be continued for all sets of data and then regression analyses performed to find how well some set of basis channels can predict the remaining ($N - 6$) channels. The object of this present analysis, however, was simply to show the strong dependence from channel to channel.

As far as the dipole hypothesis is concerned it is perhaps best to limit the interpretation of the results of the principal

components analysis since many formulations all have the same form (2). The important conclusion is, however, that a small number of independent processes are apparently present, probably six or fewer. The result does suggest that it is appropriate to attempt models which are characterized by a small number of parameters. The dipole models are such, and this in part justifies the analysis of the next chapter.

(b) Factor Analysis of Data Using Sample Times as Variables

The six sets of data were analyzed again by principal factor and factor analysis procedures, but in this case the sample times were treated as the variables. Each of the N electrode potentials were considered as observations. The subroutines in the Scientific Subroutine package dictate that the number of variables must be less than or equal to the number of observations. For this reason the $256 \times N$ matrices of data were compressed to $32 \times N$ matrices by using every 8th sample time during the response.

Table 3-8 shows the cumulative percentage of the variance summarized by the first six eigenvalues of the correlation matrices of the above data. Again, most of the experimental variance is accounted for by three eigenvalues, and over 95% is summarized by six.

A factor rotation was performed on each set of six principal factors. Since the variables here are the sample times, one can show graphically the results of the factor rotation. The traces in

Table 3-8. Cumulative Percentage of Variance Summarized by Eigenvalues of Correlation Matrices with Sample Times Considered as Variables.

Data Set Analyzed

<u>Eigenvalue</u>	<u>Dalo Flash Right</u>	<u>Dalo Flash Left</u>	<u>Dalo Flash Both</u>	<u>KW Flash Right</u>	<u>KW Flash Left</u>	<u>KW Flash Both</u>
1	46.0	51.9	61.5	62.5	56.2	68.1
2	71.8	76.9	77.1	79.6	72.8	83.1
3	86.5	90.3	86.2	91.7	85.2	91.7
4	95.5	95.3	92.3	94.7	90.7	94.3
5	97.7	97.6	95.8	96.1	95.3	96.2
6	98.3	98.3	97.6	97.1	97.2	97.7

Figures 3-2 and 3-3 show the factor coefficients for the six rotated factors over the duration of the evoked responses.

In the first analysis of the data, it was the dependence between channels that was being investigated. In this case, however, it is the dependence between sample times which is under study. The mean of each variable (sample time) in this latter analysis is a measure of the average potential at all electrodes at that sample time, and the correlations between variables are the correlations of the average activity at one sample time with that at another.

Thus in Figures 3-2 and 3-3 are plotted the coefficients of this "average activity" at each sample time with each of the six underlying factors.

These factor coefficient curves show that for each subject there are roughly three intervals of importance during the responses. If we consider factors one and two for each subject we see that between say 50 ms and 90 ms there are generally positive coefficients for these factors, between say 100 ms and 140 ms the coefficients are negative, and between say 150 ms and 180 ms the coefficients are again positive. Remember that the factors are arranged in decreasing order of summarization of the data variability, so these first two factors are the most important to consider. In each of the remaining factors there are various peaks or troughs which generally occur in one or more of the three intervals singled out above. This results in good accord with the appearance of the equipotential maps of Figure 3-1, where for each

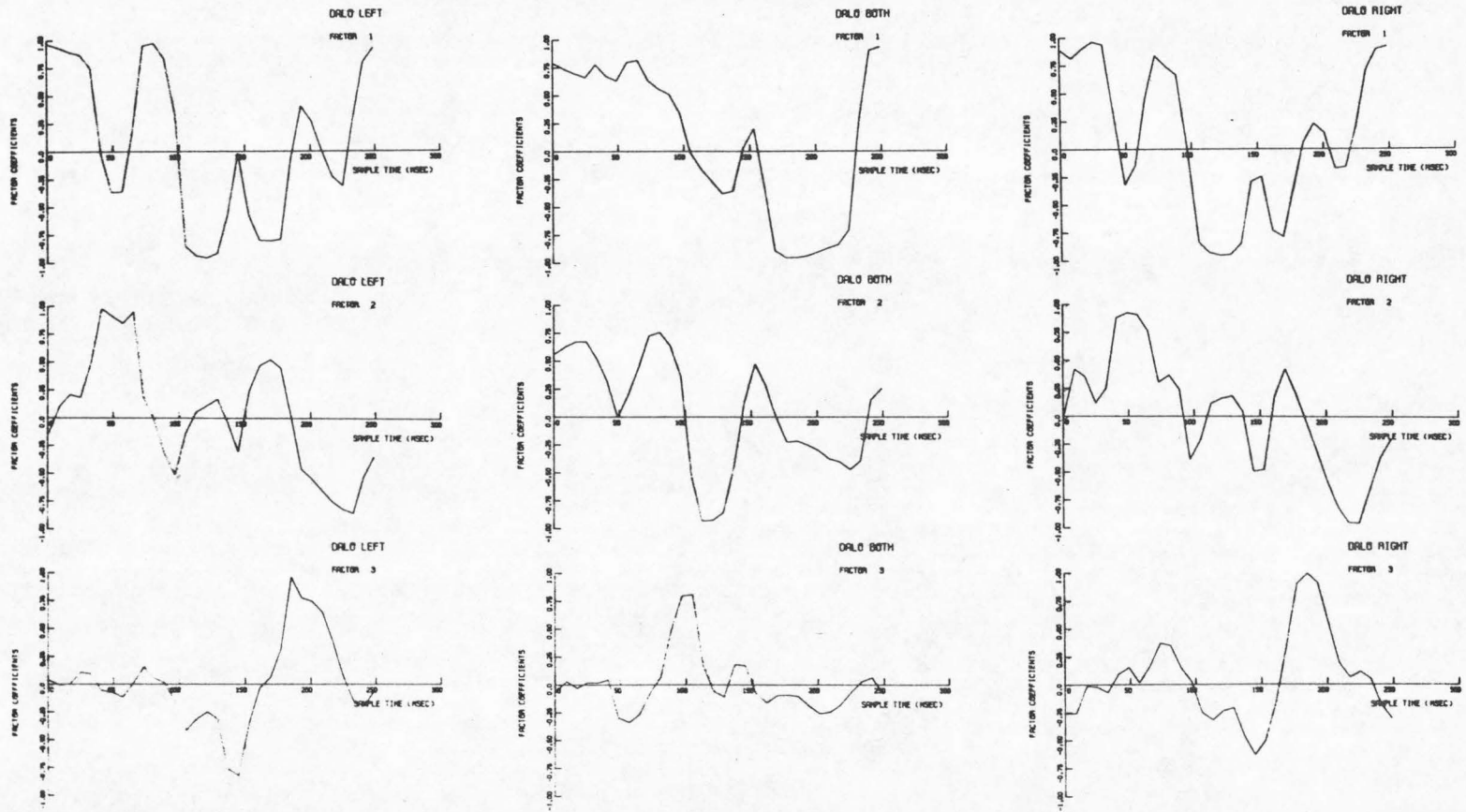


Figure 3-2 (a). Factor coefficients at successive sample times for three most significant factors in DALO data analyzed with sample times as variables.

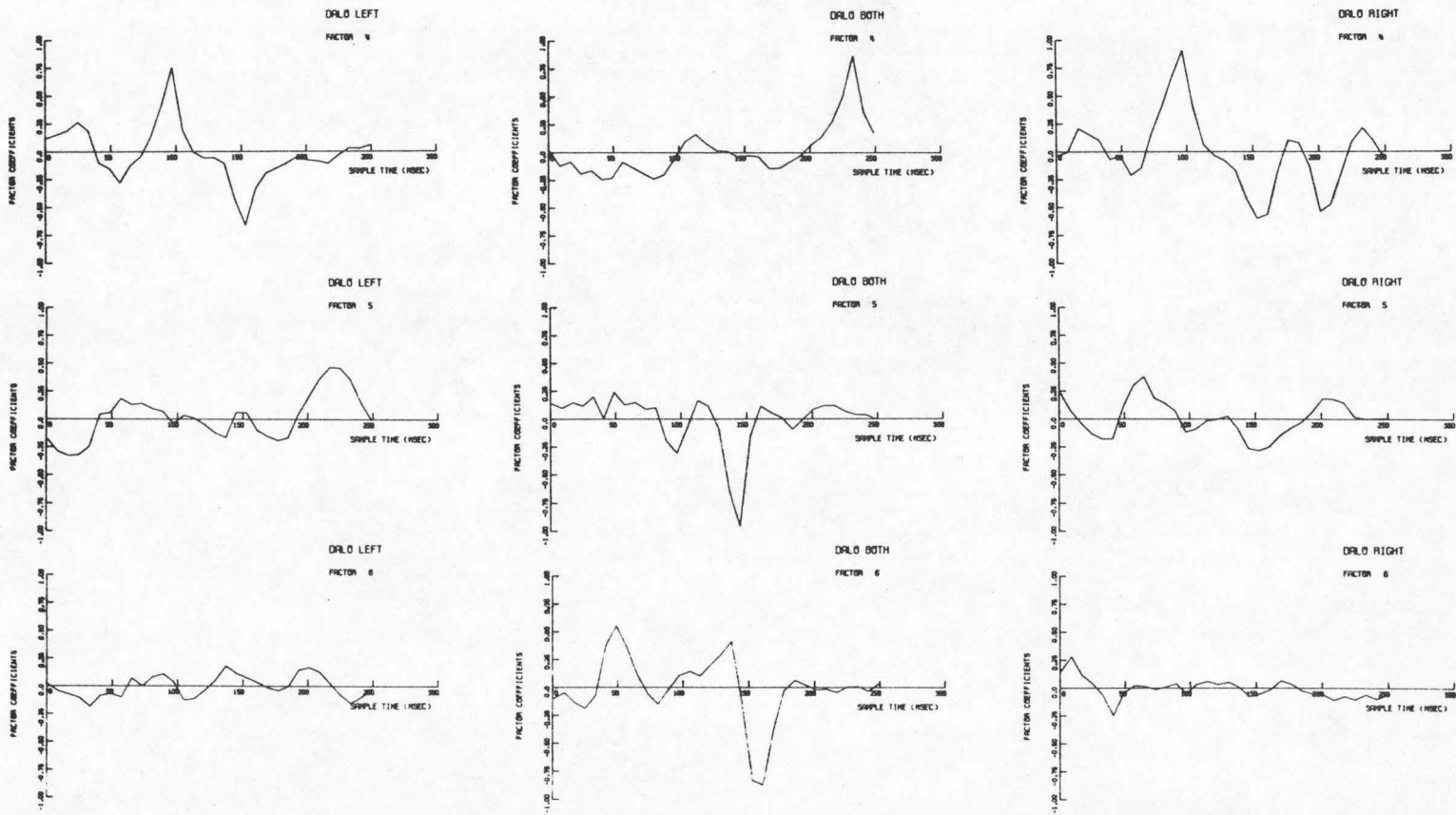


Figure 3-2 (b). Continuation of (a), showing coefficients of three least significant factors.

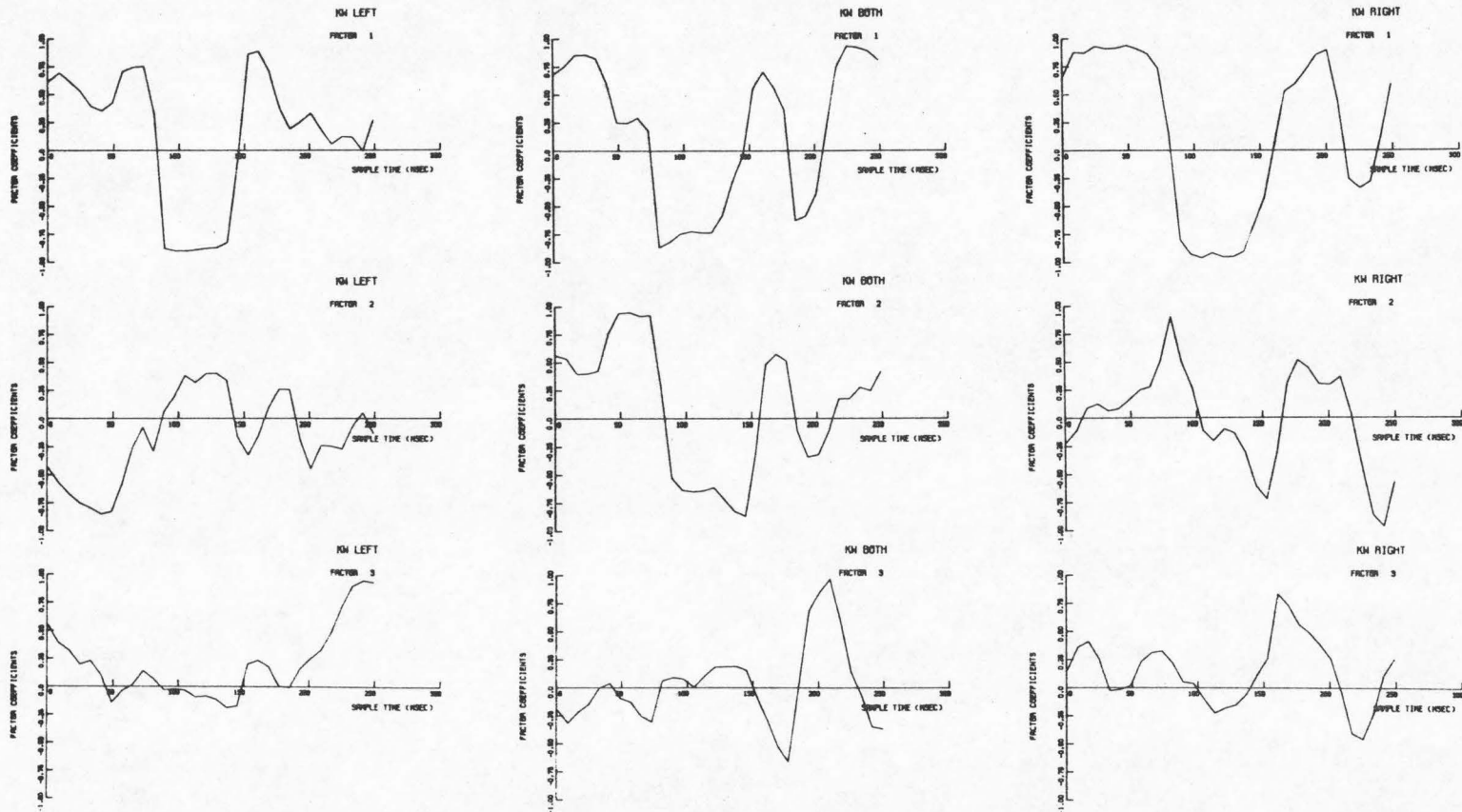


Figure 3-3 (a). Factor coefficients at successive sample times for three most significant factors in KW data analyzed with sample times as variables.

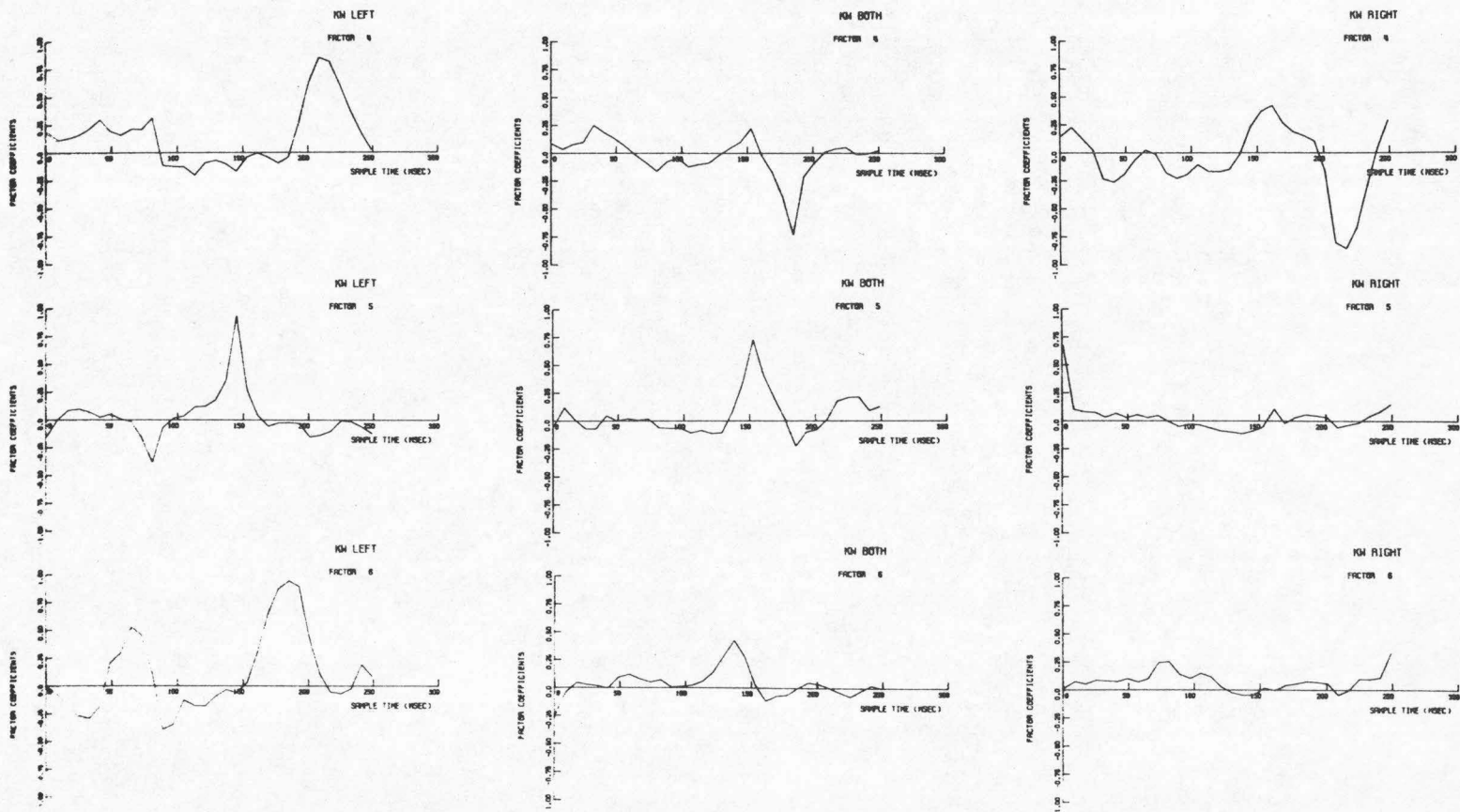


Figure 3-3 (b). Continuation of (a), showing coefficients of three least significant factors.

of these intervals there is a stable pattern in the contour lines. The polarity difference between the responses of the two subjects does not manifest itself generally in the factor coefficients until the last three factors.

The results shown in Figures 3-2 and 3-3 suggest something of the temporal sequence of generators of the evoked responses. We see that over quite long segments of the responses the activity at some sample time is related to the activity at times preceding and following.

4. Inferences Which Can be Drawn from the Factor Analysis of the Evoked Response Data.

Any detailed conclusions drawn from the shapes of the factor coefficient curves would of course be more conjecture than verifiable fact. The really significant result of the factor analysis is rather simple --- a small number of processes can apparently account for most of the evoked response activity in these two subjects. Donchin (3) has shown a similar result, where, instead of analyzing many channels of responses for one condition he has analyzed a single channel over thirty different stimuli. His results are similar; ten factors summarize approximately 95% of the variance in the data from each of two subjects. Analogous treatment of the spontaneous EEG has not yet been brought to my attention, but Walter and Adey (8) have used some factor analytic methods on spectral analyses of the EEG. Their results show that the energy in certain spectral bands of the spontaneous activity is

common to several channels, hence they were able to show some factor structure of small dimension for this aspect of the data. It is, however, difficult to compare their results with those on the evoked responses.

To re-state the question which motivated analyzing the data in this manner: are the many channels of evoked response data highly inter-dependent? The principal components analysis gives an affirmative answer to that question; -- apparently six independent processes can account for approximately 98% of the variability in the data. Moreover, the factor analysis and plots of the factor coefficients yield indications that the times during which these principal factors are "active" agree quite well with the times at which the equipotential maps show some organized activity.

The question of dipoles being the underlying cause of the observed activity is not answered by the factor analysis. The principal factors are not unique --- there is an infinite set of six independent factors whose summarization of the data would be the same. With the results of this chapter, however, models which do have a small number of parameters can be justified, and it is hoped that Chapter IV will demonstrate that, among these models, those based on equivalent dipoles are quite reasonable.

REFERENCES FOR CHAPTER III

1. Cady, L. D. , "Computed Relationship of Standard Electrocardiographic Leads, " Medical Research Engrg. May-June, (1969) pp. 37-42.
2. Cooley, W. W. and Lohnes, P. R. , Multivariate Procedures for the Behavioral Sciences , John Wiley & Sons, New York (1962).
3. Donchin, E. , "A Multivariate Approach to the Analysis of Average Evoked Potentials, " IEEE Trans. Bio-Med. Engrg. , BME-13, (1966) pp. 131-139.
4. Harman, H. H. , Modern Factor Analysis 2nd Ed. , Univ. of Chicago Press, Chicago (1967).
5. Plonsey, R. , Bioelectric Phenomena , McGraw-Hill, New York (1969).
6. Seal, H. L. , Multivariate Statistical Analysis for Biologists , Methuen and Co. Ltd. , London (1964).
7. Suter, C. M. , Computer Analysis of Evoked Potential Correlates of the Critical Band , Univ. of Maryland Computer Science Center, Technical Report 69-98, (1969).
8. Walter, D. O. and Adey, W. R. , "Analysis of Brain-Wave Generators as Multiple Statistical Time Series, " IEEE Trans. Bio-Med. Engrg. , BME-12, (1965) pp. 8-13.

IV. MODELS OF EVOKED RESPONSE GENERATORS AS DIPOLES IN HOMOGENEOUS AND NON-HOMOGENEOUS SPHERES

The preceding chapters suggested that one of the great challenges of EEG research is to locate in the brain the site or sites of the activity manifested as surface potentials. Mappings of cortical functions have to some extent been done on exposed brain during various surgical procedures, but the location of active sites from external recordings is as yet an unrealized tool.

Other workers have studied various schemes for localizing EEG generators. Brazier (3) considered dipoles in homogeneous spheres as comparable generators to certain pathological EEG signals and also to alpha rhythm. No actual foci of measured activity were calculated but qualitative conclusions concerning the similarity between the real data and dipole potentials were drawn. In a similar manner Geisler and Gerstein (9) compared acoustic evoked responses in monkeys with dipole fields but again did not actually compute the locations of equivalent dipoles. Fourment et al (5), Vaughn et al (28, 29) and Shaw and Roth (26) have also merely discussed dipole fields and the apparent similarity of certain evoked response fields, but Schneider and Gerin (25) have actually used certain features of the electric field in order to quantitatively locate equivalent dipoles.

In most of the above work no general theories have been developed for actually determining equivalent generators and their

locations. As indicated, only qualitative comparisons with dipole models have been made, except for the article by Schneider and Gerin. It would seem that one critical area then is that of formulating theoretical models of the evoked response potentials such that surface measurements can be used to quantify some equivalent generators. Perhaps many investigators will be surprised that much of the theory for evoked response models can be "borrowed" from investigations of another signal frequently measured in humans -- the electrocardiogram.

Clearly, the study of electrocardiography has profitted from recent applications of basic physics to the observed electrical phenomena. In particular the electromagnetic properties of the pacemaker tissue, cardiac muscle and surrounding structures are being systematically organized into a rigorous and descriptive theory of the ECG. Many good publications treat this problem, ranging from the general theory of electric fields in biological structures (10, 11, 19, 21, 22), to models of simple electric generators in various geometrical approximations to the body, (1, 2, 7, 13, 20) to considerations of electrode systems for electrocardiography (16, 17, 18).

The essential element in these advances in ECG research is that rigorous physical models have been shown to be invaluable and that very simple (in terms of the structures involved) models have been shown to be acceptably accurate. Thus we see that Einthoven's concept of an equivalent cardiac dipole or "heart

vector" was a prophetic one --- we now know that over the QRS portion of one electrocardiographic cycle a single dipole located in the heart does characterize quite well the activity measured on the surface of the body.

Thus there exists a conceptual framework which can, for the most part, be carried over to the study of evoked responses. It seems reasonable to try to exploit some simple physical models of the brain, its activity and the surrounding structures in an effort to sift through the evoked response activity. Recall that in chapter III, the conclusion was that a process with a small number of parameters could tolerably account for the host of voltages recorded from the scalp. That study did not of course prove that in fact some particular source like a dipole was a good equivalent model, but there are other clues which suggest that a dipole model may be a reasonable one. These clues spring from the appearance of the maps of potential activity during the evoked response. Consider Figure 4-1.

The contour maps "look" very much like dipole-type fields. In the figure we show the activity of the two subjects at 175 ms after the stimulus. The equipotential pattern for the condition of flashing the stimulus to both eyes is similar in the two subjects and indeed, looks very much like the field due to a single dipole located somewhere in the left occipital region.

In this chapter then, we want to consider the implications of modeling the human evoked response as due to dipole-like

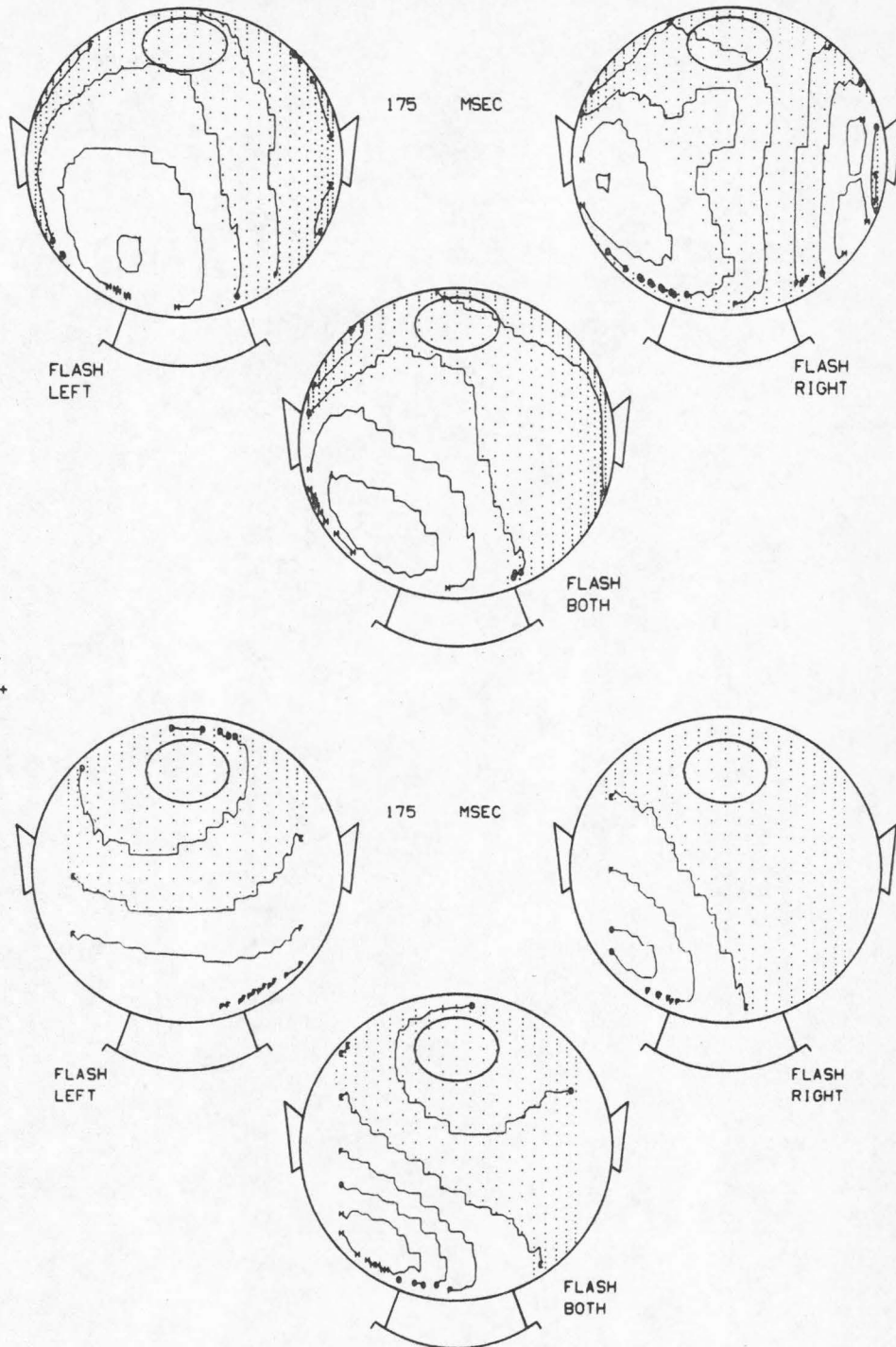


Figure 4-1. Equipotential maps at 175 ms after stimulus. Subject KW on top, DALO on bottom.

generators in the brain. First, what does it mean to cast diffuse neuronal activity into a single equivalent source? Secondly, what kinds of models can be developed in this way? Finally we will discuss how these models can be used to locate foci of cortical activity.

1. The Dipole Approximation

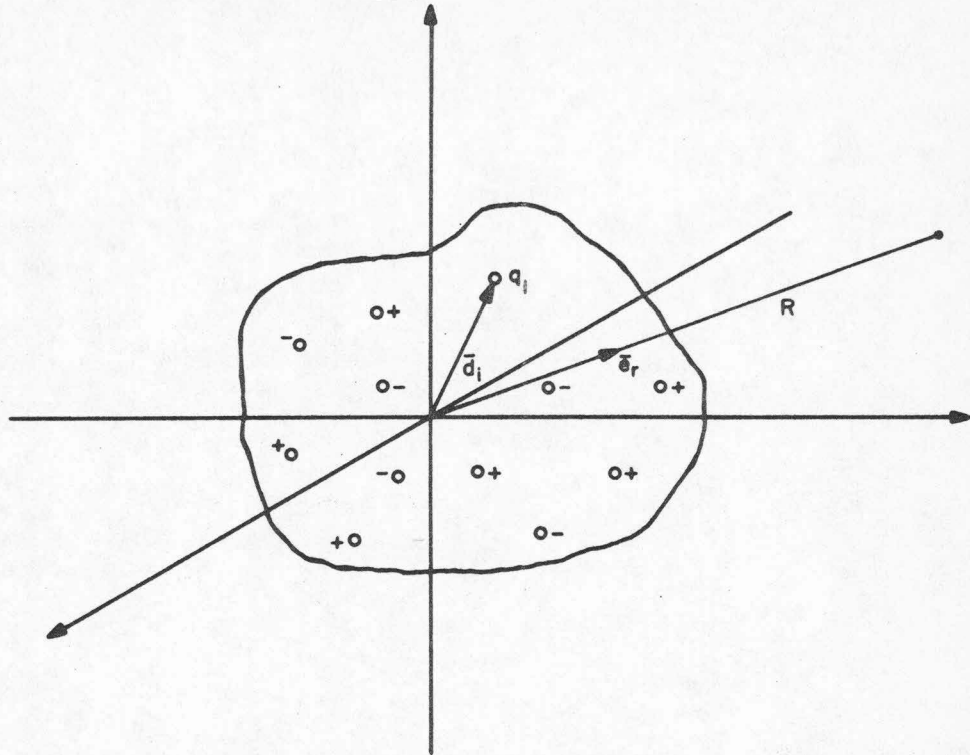
One of the first characteristics of electrostatic fields that the student of physics learns is that any diffuse cloud of charges that is as a whole neutral has a potential field that is a dipole potential at points far from the charges. A clear description of why this is so is given by Feynman et al (4), but the essential feature is that the exact expression for the potential due to such a cloud of charges is an infinite series whose successively higher terms decrease rapidly for points distant from the charges. Thus, to a good approximation, the first term, the dipole term, suffices to determine the potential field. This potential field is given by:

$$\phi = \frac{1}{4\pi\epsilon_0} \frac{\overline{P} \cdot \overline{e}_r}{R^2} \quad (1)$$

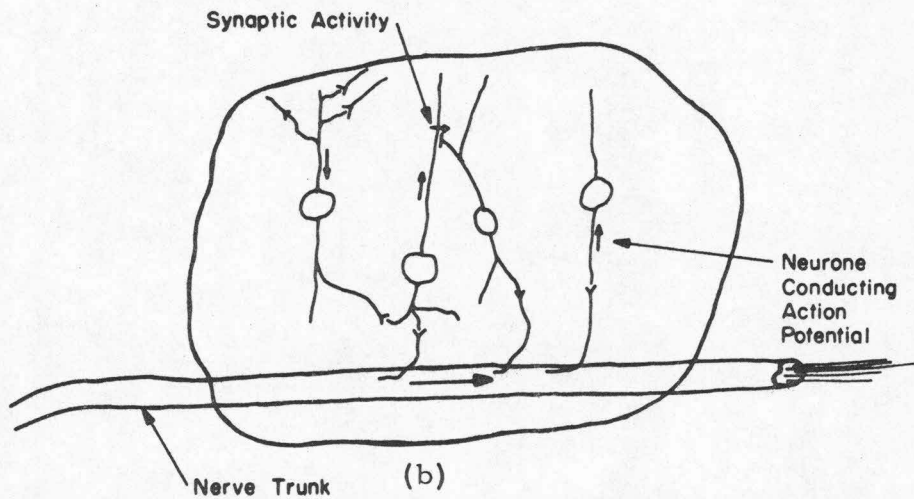
where the net dipole moment term \overline{P} is determined by the vector sum of the individual dipole moments,

$$P = \sum q_i \overline{d}_i \quad (2)$$

as shown in Figure 4-2(a); \overline{e}_r is a unit vector in the direction of R and R is the distance from the field point to some origin in the middle of the cloud of charges.



(a)



(b)

Figure 4-2. (a) A diffuse cloud of charges whose electric field at a point sufficiently far away is approximately a dipole field. (b) Some region in the cortex where a diffuse distribution of current dipoles can also be approximated by a dipole.

In order to associate this dipole concept with cortical activity, consider Figure 4-2(b). In this figure is shown a region of the cortex wherein some action potentials are being propagated and some post-synaptic potentials are also present. Plonsey (19) has described the field due to an action potential in a single neurone as a dipole field where the dipole is colinear with the axon of the neurone and centered within the ring of active membrane which propagates along the axon. Moreover an active nerve trunk has a field due to the superposition of the fields arising from the dipole elements appropriately located in each of the active fibers. Finally, at synaptic sites in this region there are other dipole-like fields produced by local membrane depolarizations or hyperpolarizations. Thus in this small volume of the cortex there is a distribution of dipole moments of varying magnitudes and directions. We can, by arguments following the case of a cloud of charges, say that there is some single equivalent dipole which is a vector function of all the individual dipoles. At distances large compared with the dimensions of the volume of material the field due to this equivalent dipole is indistinguishable from the superposition of the contributions from the individual dipole elements.

Let us assume then that at some instant in time there is one small cortical volume whose activity is spatially organized in such a fashion as to produce a single equivalent dipole field. Turn again to Plonsey (19) for a discussion of volume conduction in biological media. First note that the rise time of a typical action

potential is roughly 1 ms, hence the highest frequency of interest is about 1KHz. This means that we can exclude capacitive, propagation and inductive effects and treat the problem as an electrostatic one at any time during the evoked response. Secondly, note that we can use the principles of volume conduction --- the current due to a neural event does spread everywhere throughout the surrounding medium. While ion currents generated by synaptic transmission or action potentials are most dense near the active tissue, the fact remains that current must flow throughout all surrounding tissue which is non-insulating. Admittedly the current density is low at sites distant from the source, but it does not abruptly become zero at any point within the bounding media. Thus at any point in time the scalp potential distribution is related to some electrostatic dipole located within the skull. Of course this approximation is less useful when many cortical sites are active. In the case of the spontaneous activity there are many regions simultaneously active, hence even with a large number of electrodes it becomes very difficult to resolve the activity into individual generators. As already stated in Chapters I and III, however, during an evoked response there are presumably fewer generators active and hence it becomes more likely that one can map out the field into resolvable dipole patterns. On this basis then, some models of dipoles as equivalent evoked response generators can now be developed.

2. The Dipole in a Homogeneous Sphere

The first model to be tried is a relatively simple one conceptually (but less so in its implementation!). Consider the head to be a homogeneous sphere of radius R and conductivity σ , as shown in Figure 4-3. Other authors (6, 12) have derived equations for the potential on the surface of a conducting sphere surrounded by an insulating medium, when a dipole is somewhere within the sphere. The particular form of the equation used here is due to Geselowitz and Ishiwatari (12), but I have made some modifications to it to suit more general coordinate systems (Appendix A of this thesis).

For a dipole located at (x, y, z) in the sphere, with dipole components P_x , P_y , and P_z , the potential on the surface is shown in the Appendix to be:

$$V(R, \theta, \phi) = \frac{1}{4\pi\sigma R^2} [V_1 V_2 + V_3 V_4] \quad (3)$$

$$\text{where: } V_1 = \frac{P_x \sin\beta + (P_y \sin\alpha + P_z \cos\alpha)\cos\beta}{f} \quad (4)$$

$$V_2 = \frac{1 - f^2}{(1 + f^2 - 2f\mu)^{3/2}} - 1 \quad (5)$$

$$V_3 = \frac{\{P_x \cos\beta - (P_y \sin\alpha + P_z \cos\alpha)\sin\beta\}C + \{P_y \cos\alpha - P_z \sin\alpha\}E}{fA} \quad (6)$$

$$V_4 = \frac{3f - 3f^2\mu + f^3 - \mu}{(1 + f^2 - 2f\mu)^{3/2}} + \mu \quad (7)$$

The original dipole parameters (x, y, z, P_x, P_y, P_z) have been transformed into an equivalent set $(\alpha, \beta, f, P_x, P_y, P_z)$ in a

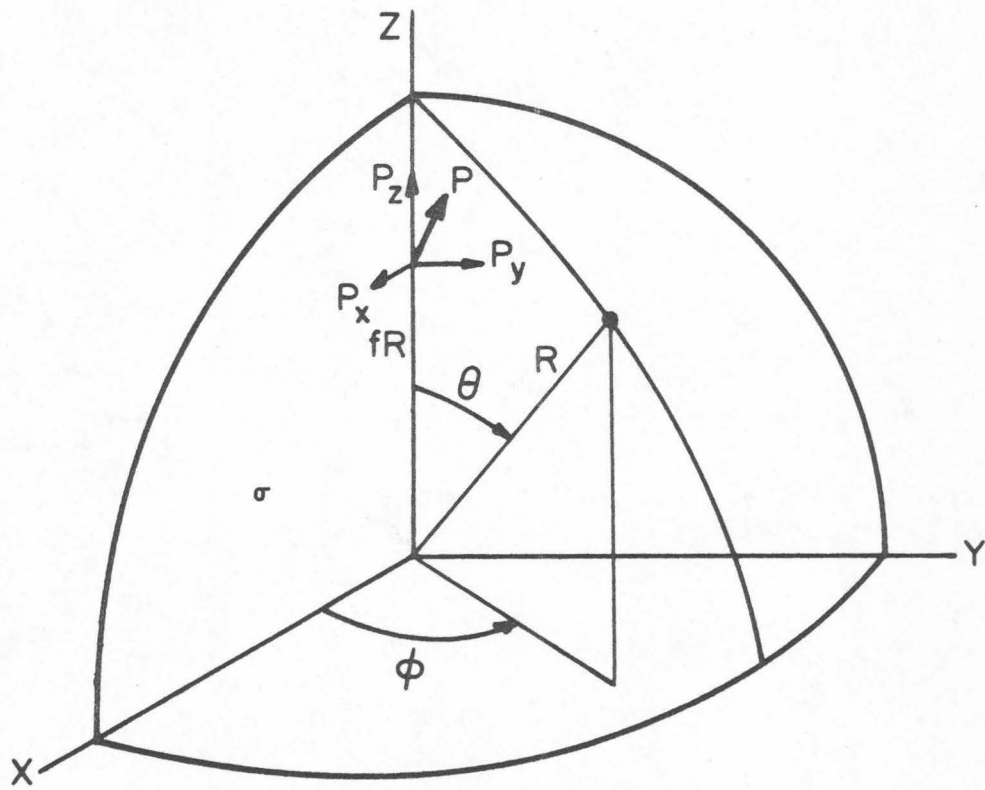


Figure 4-3. A dipole of components P_x , P_y and P_z located at $r = fR$ along the z-axis, in a sphere of radius R and conductivity σ .

manner outlined in the Appendix, where also one can find explanations of all other terms in equations (3) - (7).

One can now calculate the surface potential distribution for various dipoles. In Figure 4-4 is shown the effect of increasing eccentricity (distance from the center of the sphere) of a radially oriented dipole. Note that in all calculations the potential is normalized to the multiplicative factor $\frac{1}{4\pi\sigma R^2}$. This factor merely scales the potential values up or down at all surface points. The actual shape of the curve is due only to the dipole location and relative component strengths.

Of perhaps more comparative value are the illustrations in Figure 4-5 through 4-7. Here I have used the dipole equation (1) to generate equipotential contour maps in the same format as the movie frames of the experimental data. Figure 4-5(a) shows a dipole oriented radially (along the line of sight) at a high eccentricity and Figure 4-5(b) shows the field pattern for a lower eccentricity. Note that all rectangular coordinates are referred to the system shown in Figure 4-3, that is, the (+) x-direction passes out of the left ear, the (+) y-direction passes posteriorly out through the occipital region and the (+) z-direction passes out the top of the head, along the line of sight.

In Figure 4-6 is shown the field that results when two dipoles are placed in a sphere and the potential at any point is thus simply the sum of the potentials that would occur from each source separately. In Figure 4-6(a) there is no question of there being

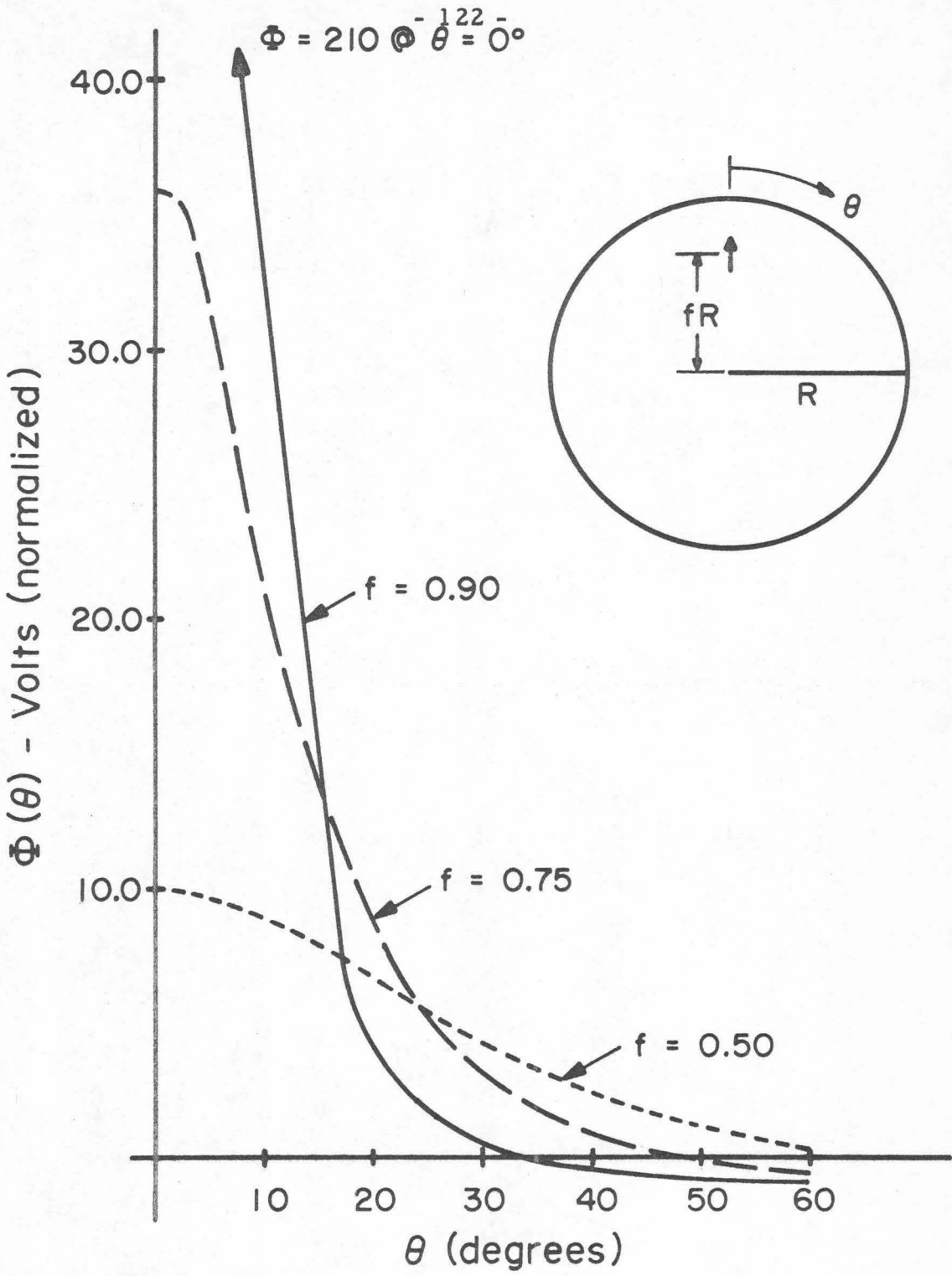


Figure 4-4. Effect of increasing eccentricity for radial dipole in homogeneous sphere.

CONTOUR RANGE :

K = 209.9927

A = -1.0244

MODEL : HOMOGENEOUS

DIPOLE PARAMETERS :

X = 0.000

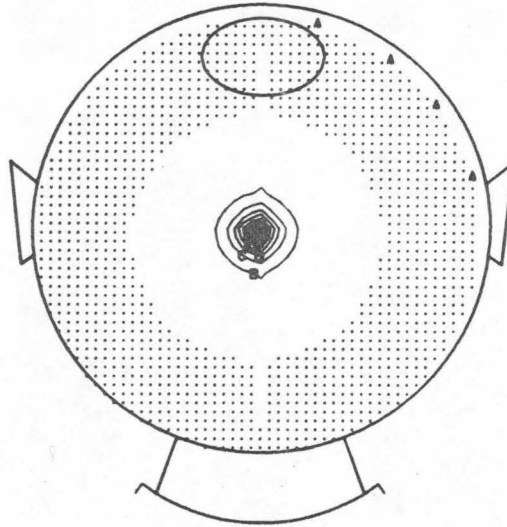
Y = 0.000

Z = 0.900

PX = 0.000

PY = 0.000

PZ = 1.000



(a)

CONTOUR RANGE :

K = 25.5555

A = -1.0280

MODEL : HOMOGENEOUS

DIPOLE PARAMETERS :

X = 0.000

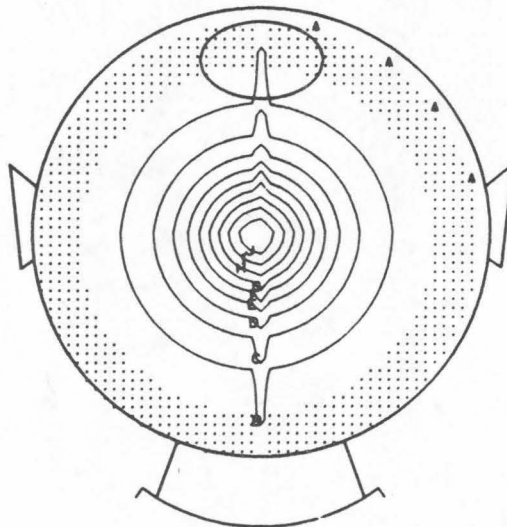
Y = 0.000

Z = 0.700

PX = 0.000

PY = 0.000

PZ = 1.000



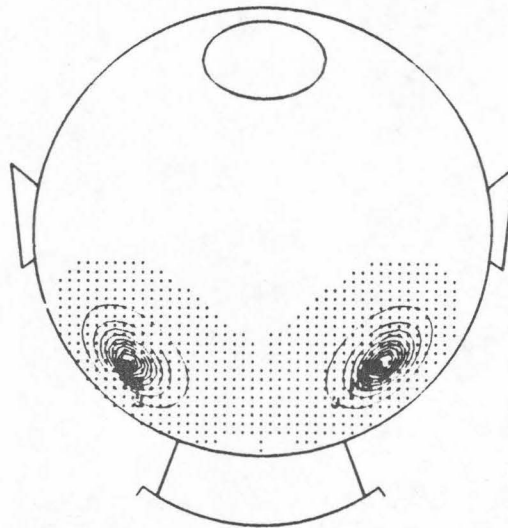
(b)

Figure 4-5. Radially oriented dipoles in a homogeneous sphere (a) $f = 0.90$ (b) $f = 0.70$. Bumps along mid-line are plotting artifact.

CONTOUR RANGE :

K = 2.1772
A = -110.9343

MODEL : HOMOGENEOUS



(a)

DIPOLE PARAMETERS :

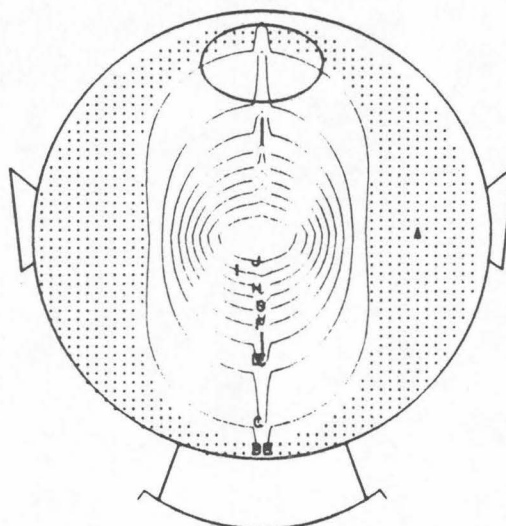
X = 0.500
Y = 0.500
Z = 0.500
PX = -0.577
PY = -0.577
PZ = -0.577

X = -0.500
Y = 0.500
Z = 0.500
PX = 0.577
PY = -0.577
PZ = -0.577

CONTOUR RANGE :

K = 35.2760
A = -3.3748

MODEL : HOMOGENEOUS



(b)

DIPOLE PARAMETERS :

X = 0.200
Y = 0.000
Z = 0.700
PX = -0.707
PY = 0.000
PZ = 0.707

X = -0.200
Y = 0.000
Z = 0.700
PX = 0.707
PY = 0.000
PZ = 0.707

Figure 4-6. Fields from two dipole sources in a homogeneous sphere. (a) Sources easily separable by sight. (b) Combined fields not easily ascribed to one source.

two sources that are easily differentiable. Figure 4-6(b), however, is not easily distinguished from the case of a single radially oriented source. It requires study of this figure and those shown in Figure 4-5 to reveal that there are some differences in the two dipole case which can be detected by eye.

Finally, Figure 4-7 shows a contour map derived from equation (1) in (a), and a frame from the KW data in (b). It seems apparent that at this particular sample time (175ms) the experimental data for the flash in both eyes and flash in the left eye look very much like that due to a single dipole in a homogeneous sphere. I will in fact go on to show the degree to which the evoked response data can be fitted to a dipole model in a homogeneous sphere. In anticipation of both conceptual and analytical difficulties, however, it is perhaps desirable to reflect on some inconsistencies inherent with this modeling scheme.

First, of course, is the fact that human heads are not homogeneous spheres -- not any kind of spheres in fact. This non-sphericity must introduce analytical errors, but one should bear in mind that geometrical models could at least have a point-by-point correspondence with the actual shape. I do not discount the reality that the head is perhaps more elliptical than spherical over the area upon which the electrodes are placed, but for the moment at least I choose to work with spherical coordinates. At worst such errors can be eliminated by some single valued mapping from the sphere to some more satisfying shape.

CONTOUR RANGE :

DIPOLE PARAMETERS :

K = 3.2167
A = -1.4696

X = 0.210
Y = 0.020
Z = 0.330
PX = 0.250
PY = 0.450
PZ = 0.200

MODEL : HOMOGENEOUS

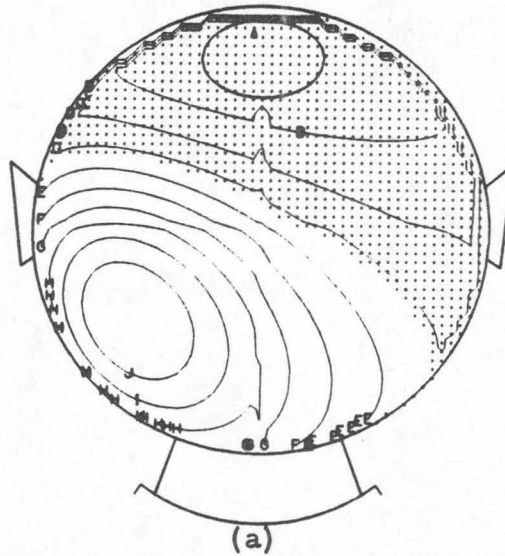
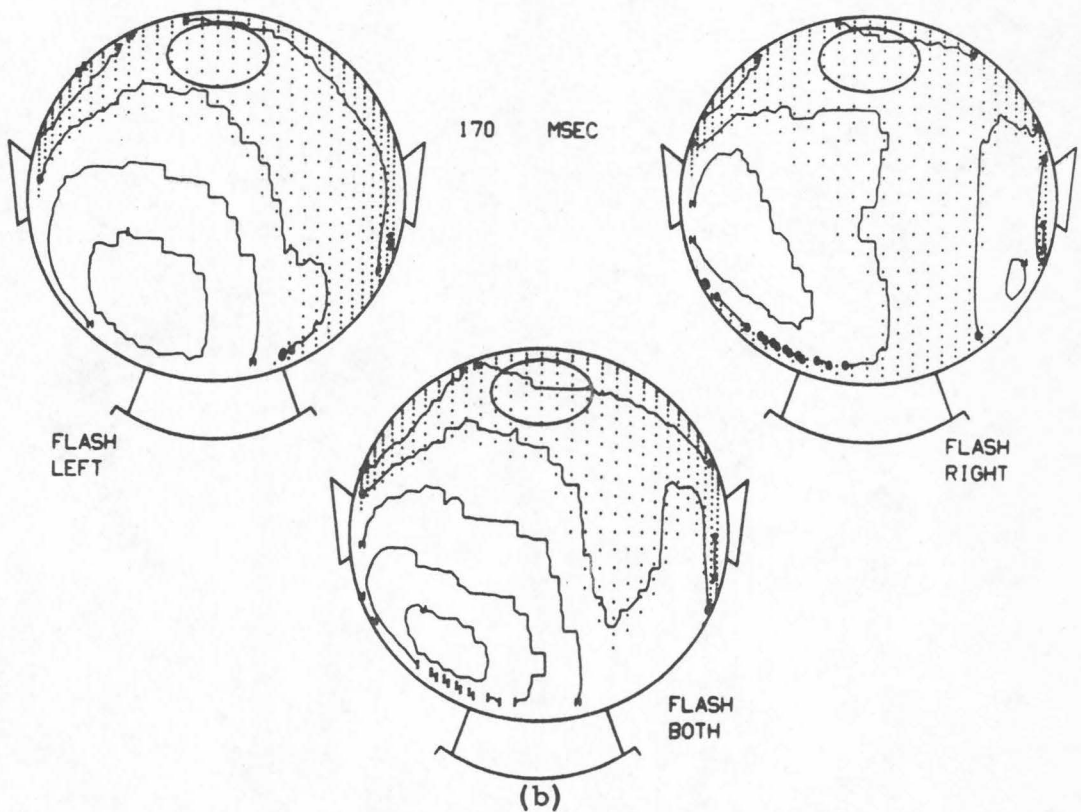


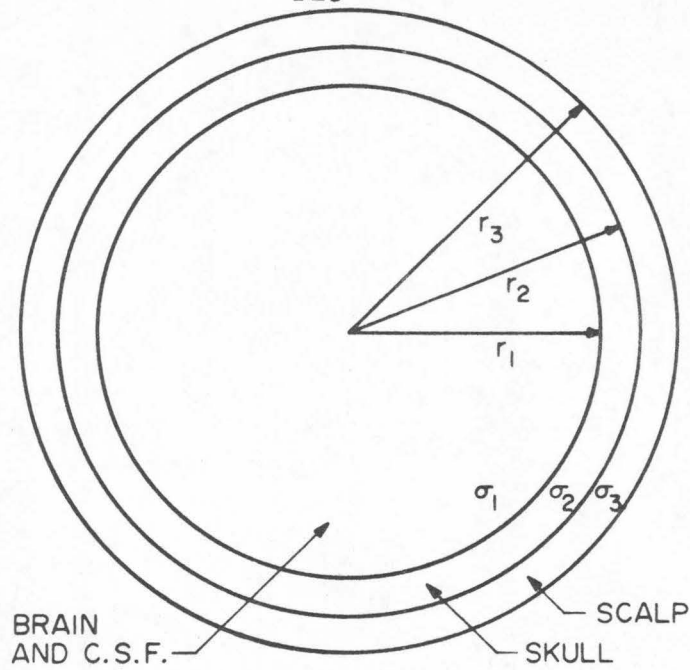
Figure 4-7. Equipotential map calculated from hypothetical dipole in (a) is comparable to maps of evoked response data in (b).



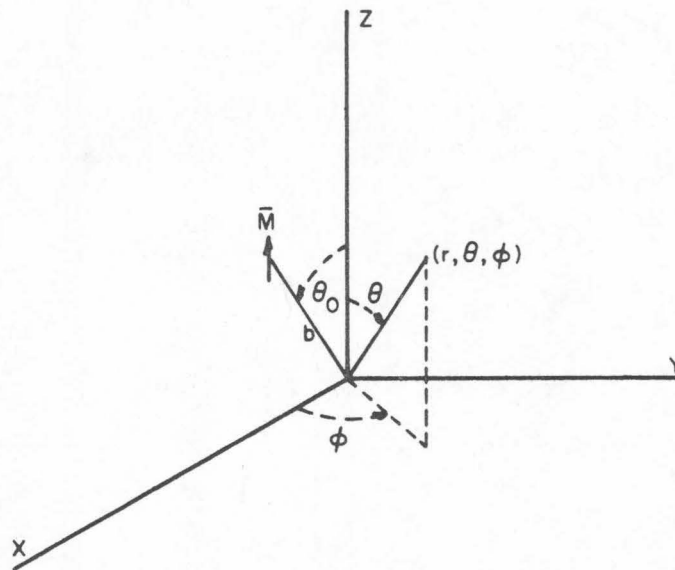
The inhomogeneities are potentially a more disastrous problem. The brain, cerebro-spinal fluid, skull and scalp have quite different conductivities, particularly noticeable when you compare the relative conductivities of brain to skull (approximately 100:1). Earlier it was mentioned that the scalp has an appreciable shunting effect on the EEG signals, and now we must also note a similar effect due to the relatively high conductivity of the C.S.F. -- effectively a shield placed around the brain. One could also note for completeness that the brain itself is likely not isotropic as far as the conductivity is concerned --- the conductivity in a radial direction is not the same as that parallel to the surface. This last factor is not as frequently noticed as the other problems, but in the aggregate one may rightly shelter certain discomfoting thoughts about modeling the head as a homogeneous sphere. Some more quantitative assessments of the validity of this model will be presented later in this chapter.

3. The Dipole in a Non-Homogeneous Sphere

In an effort to accommodate some of the more noticeable shortcomings of the homogeneous model of the head I have developed another model based on Figure 4-8. The brain and C.S.F. are now approximated by a spherical volume of radius r_1 and conductivity σ_1 ; the skull is now a separate region of conductivity σ_2 and thickness $r_2 - r_1$ and the scalp is modeled as a final layer of conductivity σ_3 and outer radius r_3 . The surface potential now is the potential at the boundary r_3 .



(a)



(b)

Figure 4-8. (a) Concentric shell model of the head. (b) Orientation of dipole for equation (8).

This type of model has been suggested earlier in a study by Rush and Driscoll (23, 24) on applications of the reciprocity theorem to EEG electrode sensitivity. This solution for the potential on the surface is not as straightforward as that for the homogeneous case; I have derived (in Appendix B) the equation, and it is shown to be:

$$V(r_3, \theta, \phi) = \sum_{n=0}^{\infty} \sum_{m=0}^n M_0 K_{mn} P_n^m(\mu) \cos m\phi \quad (8)$$

where:

$$M_0 = \frac{M}{4\pi\sigma_1} \frac{(2 - \delta_m^0)(n-m)!}{(n+m-1)!} b^{n-1} P_{n-1}^m(\mu_0) \quad (9)$$

$$K_{mn} = \frac{K_1}{K_2 + K_3 K_4} \quad (10)$$

$$K_1 = (2n+1)^2 (r_2/r_1)^{2n+1} r_3^{-(n+1)} \quad (11)$$

$$K_2 = \{1 - \sigma_2/\sigma_1\} \{n^2 + n(n+1)(r_2/r_3)^{2n+1}\} \quad (12)$$

$$K_3 = \{n/2n+1\} \{\sigma_3(n+1)/\sigma_2 + n\} + n\{(n+1)/(2n+1)\} (1 - \sigma_3/\sigma_2) (r_2/r_3)^{2n+1} \quad (13)$$

$$K_4 = (r_2/r_1)^{2n+1} \{(n+1)\sigma_2/\sigma_1 + n\} + n(\sigma_2/\sigma_1 - 1) \quad (14)$$

$$\mu = \cos\theta \quad (15)$$

$$\mu_0 = \cos\theta_0 \quad (16)$$

This solution is for a dipole located as shown in Figure 4-8(b), i. e. a dipole of moment M located in region 1 at $r=b$, $\theta=\theta_0$, $\phi=0$ and parallel to the z axis. In the appendix is shown how to transform any arbitrary dipole into the desired orientation for Figure 4-8(b) to hold.

With this model it is now possible to study the effects of conductivity discontinuities in the basic spherical model of the head. Geddes and Baker (8) have made measurements on many physiological materials, and from this source I have taken the conductivities to be in the ratios $\sigma_1:\sigma_2:\sigma_3 = 160:1:60$. The first ratio $\sigma_1:\sigma_2$ is also confirmed by Van Harreveld (27). Note the conductivities are stated in this manner because, as is shown by equations (8) - (14), only the ratios of the three conductivities enter into the solution. As was the case in the homogeneous model the potentials are normalized to the multiplicative factor $\frac{1}{4\pi\sigma_1}$; all other terms involving conductivities are ratios. Also as in the homogeneous case the sphere is normalized geometrically by setting $r_3=1$. The inner radii r_1 and r_2 are taken to be 0.90 and 0.98, simply by estimating these relative dimensions from anatomical diagrams.

One can now investigate the effect of including the step changes in conductivities in the head. Simply stated, the surface potential derived from equation (8) (hereinafter referred to as the "shell" model) is "smoother" for any given dipole. That is to say the surface distribution in the shell model exhibits less variation

in potential than does the field from the same dipole located in the homogeneous model. Consider Figure 4-9. The field which shows the greatest surface variation is that arising from an eccentric, radial dipole. For such sources note in Figure 4-9 that the homogeneous model exhibits a considerable peak along the dipole axis while the shell model gives a potential field which is generally more flat. This characteristic is perhaps shown more graphically by Figures 4-10 and 4-11, where the differences between the two models are shown in the equipotential map format.

The differences thus shown by the two models have the following effect as far as locating equivalent dipoles. It seems obvious from considering Figure 4-9 that a relatively deep dipole in the homogeneous model produces a field which is similar to a more eccentric source in the shell model. Presumably the shell model is a more realistic model of the actual characteristics of the head. One can conclude then that the homogeneous model is biased in favor of locating equivalent sources deeper than should be the case. This is an important difficulty that should be recognized by all who choose to accept the less complicated model.

The motivation for constructing these two models was to be able to locate equivalent sources for the visual evoked response data. As mentioned earlier in this chapter, some authors have "compared" evoked response potentials with fields due to a dipole. This is, of course, a viable tool, but less desirable than actually quantitatively defining an equivalent source from the surface

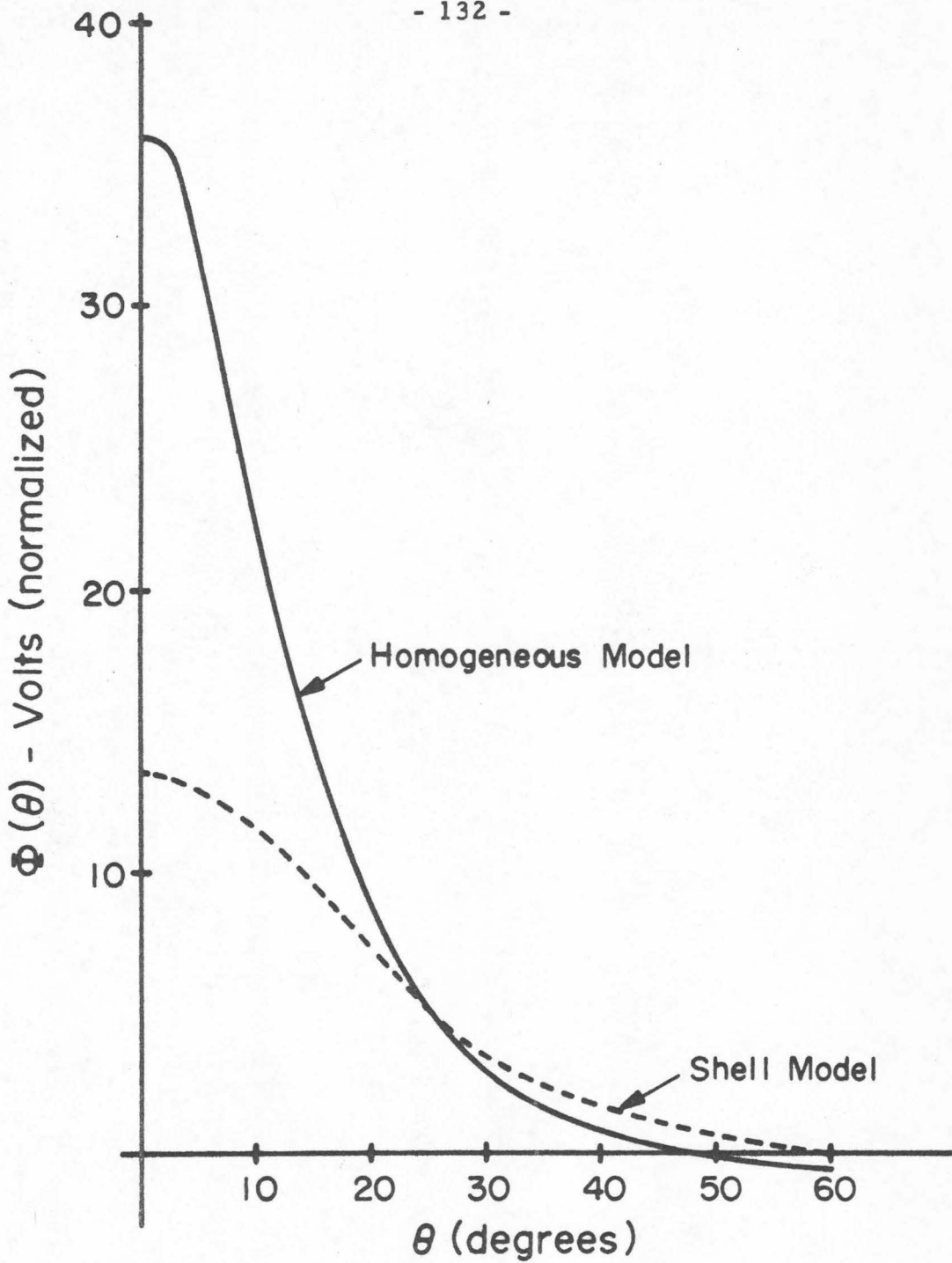


Figure 4-9. Comparison of surface potential fields for radial dipole of eccentricity $f = 0.75$ in homogeneous and shell models.

CONTOUR RANGE :

- 133 -

DIPOLE PARAMETERS :

K = 35.4463

A = -0.9972

X = 0.000

Y = 0.000

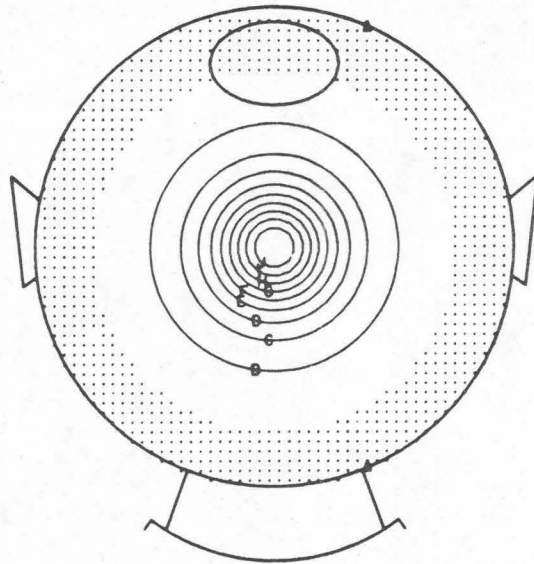
Z = 0.750

PX = 0.000

PY = 0.000

PZ = 1.000

MODEL : HOMOGENEOUS



(a)

CONTOUR RANGE :

DIPOLE PARAMETERS :

K = 13.5106

A = -0.7558

X = 0.000

Y = 0.000

Z = 0.750

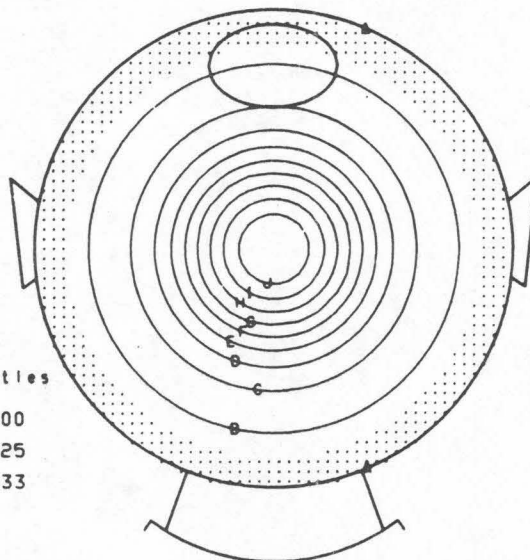
PX = 0.000

PY = 0.000

PZ = 1.000

MODEL : SHELL

radii	conductivities
0.90	1.00000
0.98	0.00625
1.00	0.33333



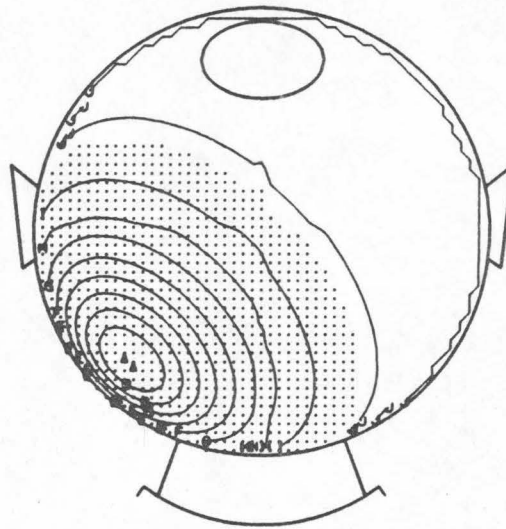
(b)

Figure 4-10. Equipotential maps for identical radial dipole sources of eccentricity 0.75. (a) Homogeneous model. (b) Shell model.

CONTOUR RANGE :

K = 1.4661
A = -10.7113

MODEL : HOMOGENEOUS



DIPOLE PARAMETERS :

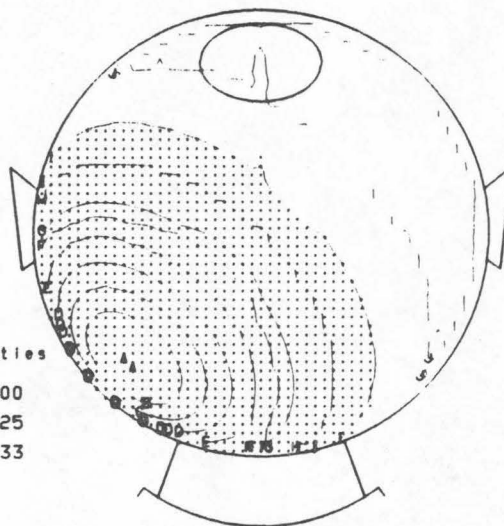
X = 0.300
Y = 0.300
Z = 0.300
PX = -0.577
PY = -0.577
PZ = -0.577

CONTOUR RANGE :

K = 1.5350
A = -6.4870

MODEL : SHELL

radii	conductivities
0.90	1.00000
0.98	0.00625
1.00	0.33333



DIPOLE PARAMETERS :

X = 0.300
Y = 0.300
Z = 0.300
PX = -0.577
PY = -0.577
PZ = -0.577

Figure 4-11. Equipotential maps for identical dipole sources in (a) the homogeneous model, and (b) the shell model. Note greater range of voltages in (a).

potential measurements. The development of these models proceeds now to a technique for making this final analytical leap.

4. The Inverse Problem

The two models have thus far shown how one can generate from some hypothesized dipole source (or sources) a potential surface on the scalp. That is not, of course, the state in which the real problem exists, i. e. we already have, at each sampling time, a map of the surface potentials. How can one calculate an equivalent source for such a voltage distribution?

This so-called "inverse problem" is not a trivial one. It has been discussed as it applies to the location of ECG generators by Plonsey (20, 21) and Geselowitz (13) and the cautions developed in those articles are equally applicable here.

First, we must observe that any solution is not a unique one. Any harmonic function (solution of Laplace's Equation) can be added to some particular solution as long as the boundary conditions are met. There are thus many equivalent source distributions whose surface potential fields are identical. The solution of this first problem is to restrict the models and inverse calculations thereon only to unique generator schemes. In other words, only equivalent dipole sources will be sought, since for the present no significance is attached to any additive harmonic functions.

One must next recognize that it is impossible to determine an arbitrarily complex source distribution from a finite number of

surface measurements. No more than n parameters can be estimated by measuring the potential at n electrodes. In fact, it is in some sense more desirable to estimate a small number of parameters from a large number of surface measurements i. e. an "over-determined" problem. Given an array of n electrode readings, some arbitrary model of n parameters can of course exactly fit the data, but no summarization of the data has taken place, and such a model may have no physical relationship to the processes under study. The theoretically equivalent models in this discussion will thus in all cases be characterized by no more than 12 parameters.

The intensity of the electric field falls off inversely with the distance from the source. At some stage experimental noise becomes comparable to the field strength from some postulated source. Equation (1) shows that the dipole field decreases with $1/R^2$, but the successively higher "poles" in the series which was truncated to (1) decrease even faster. The next higher term is the quadrupole and it decreases as $1/R^3$. Determining these higher order terms then becomes more problematic than finding the parameters which characterize only the dipole term, another reason why the present models are restricted only to dipoles.

The technique by which dipole sources are determined from the surface potentials is a probabilistic one. For each of the homogeneous and shell models there are equations which compute the potential at a given point on the head arising from some dipole

inside the skull. In each model a single dipole is characterized by six parameters. The inverse problem is solved by computing an "optimum" set of these parameters for a given sample time of the evoked response. This optimum set is determined in the least-squares sense, that is, the sum of the squared deviations of the actual surface potentials from surface potentials computed from a dipole source are to be minimized.

The theory of least-squares fitting is well developed for models which are linear in the parameters to be optimized. Equations (3) and (8) however, are nonlinear in the dipole parameters, and nonlinear estimation techniques are more difficult to derive. Fortunately an IBM SHARE program (14) exists, called LSQENP (Least Squares Estimation of Nonlinear Parameters), based on an algorithm due to Marquardt (15). From a set of initial "guesses" of the dipole parameters the program iteratively produces more optimal parameters until the sum of the squared errors attains some minimum. In order to change the parameters at each iteration, the program is supplied with equations such as (3) or (8) to compute the potential at any point, as well as equations for the partial derivatives of (3) and (8) with respect to each of the dipole parameters (see Appendices A and B for complete derivations for each model).

Before applying this procedure to the real evoked response data, I felt it useful to gain some experience with the process in order to have a basis for interpreting the results on the

experimental data. A test program was written as follows. Starting with either the homogeneous or shell models, it generates with either equations (3) or (8) some distribution of potentials at 50 points over a surface comparable to the area covered by electrodes in the actual experiments. Some arbitrarily chosen dipole is used as the source. This potential surface then is presented to the next stage of the program, which invokes the LSQENP subroutine in order to "solve" for the dipole parameters of this contrived set of data. Optional features of the program include perturbations of the calculated potentials in order to simulate "noise" in the potential readings, and/or perturbing the postulated positions of the electrodes in order to simulate errors in placement of the recording electrodes.

Consider Figure 4-12. The abscissa value is the amount of "noise" in the test data and the ordinate is the error in determining the dipole parameters by the least squares procedure. The noise is added by first determining S^2 , the variance of the calculated potential distributions, then adding to the potential at each electrode, samples from a Gaussian distribution of zero mean and variance equal to some fraction of S^2 . Values of 0.1, 0.2, 0.5 and 1.0 times S^2 were taken, in addition of course to the case of adding zero noise to the test data.

Figure 4-12 thus shows the error in determining the six dipole parameters as a function of perturbation of the surface potential, in the homogeneous model. By error here is meant the

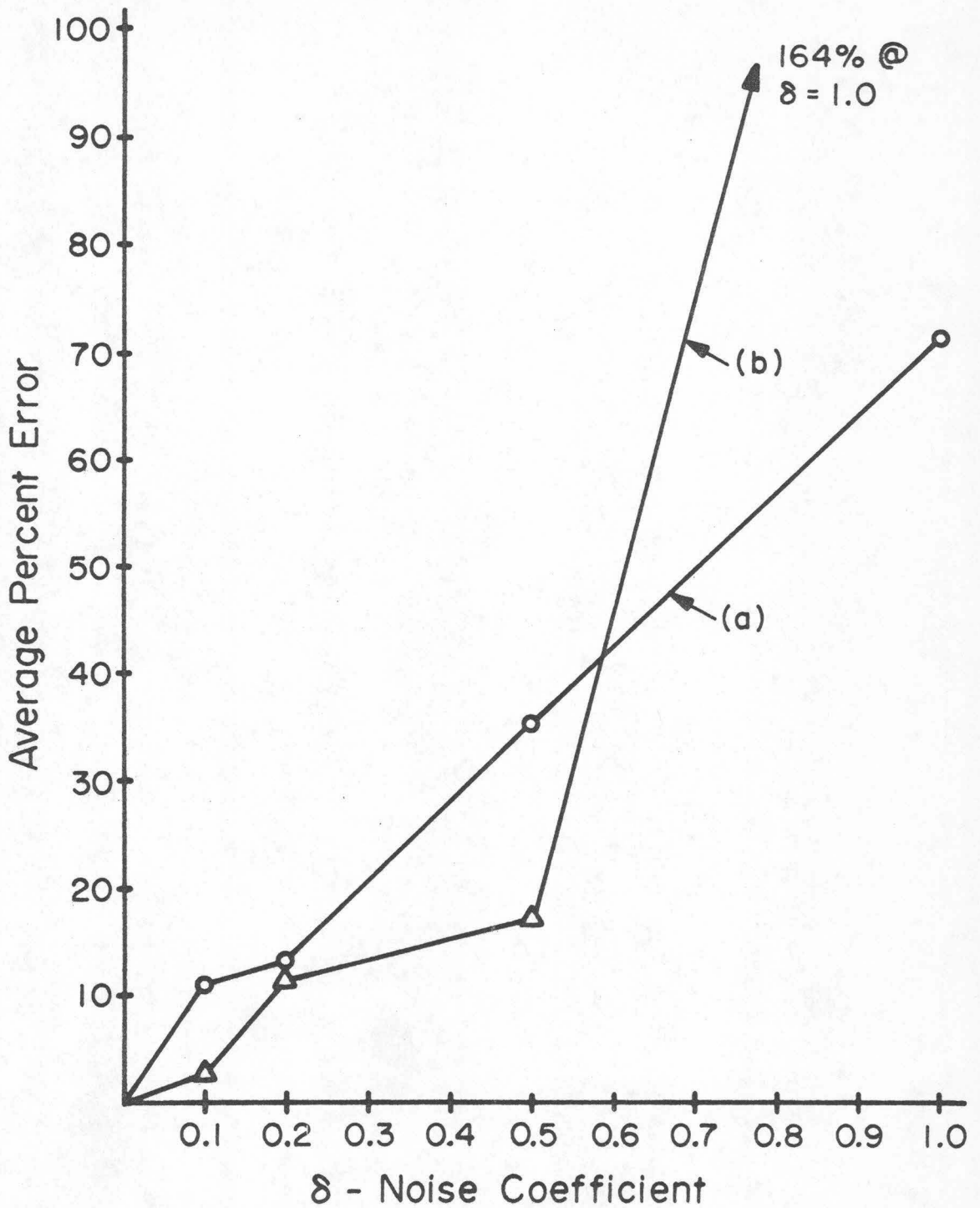


Figure 4-12. Sensitivity of inverse solutions in homogeneous model to noise in potential measurements. Dipole (a): (.70, .35, .25, -.40, -.60, -.30), average error in initial guesses 15.7%. Dipole (b): (.15, .20, .32, -.50, -.20, -.30), average error in initial guesses 18.8%.

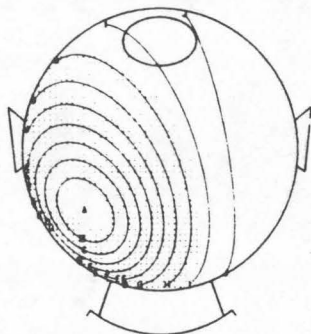
average percentage error in each of the six dipole parameters. Two different cases are shown, picking one arbitrary dipole of relatively low eccentricity in case (a) and some other one of higher eccentricity in (b). Before drawing any conclusions about the acceptability of this error increase with perturbation of the data it is important to have some feeling for the degree of "noisiness" actually represented by these figures. Again our contour maps come to service. In Figures 4-13 and 4-14 are shown maps of the data used to determine the error analysis of Figure 4-12. Here the effect of adding successively larger amounts of noise becomes obvious. When the multiplicative noise factor exceeds approximately 0.2 the equipotential plots degenerate quite drastically. The equipotential maps of the evoked response data seem to be as well defined as these test plots would be at noise factor values of 0.1 to 0.2.

Similar accuracy tests can be conducted for the shell model. A typical dipole determination in this model, and the effect of adding noise to each electrode is shown in Figure 4-15. Again, the corresponding contour maps are shown in Figure 4-16, illustrating the effects of the perturbations in the appearance of the data. The equipotential maps of the shell model data seem to degenerate slightly faster with increasing levels of noise added to the data than in corresponding cases of the homogeneous model. Again it appears that a noise factor level of 0.1 to 0.2 is comparable to the evoked response contour maps.

CONTOUR RANGE :

K * = 1.2755
A * = -4.2166

MODEL : HOMOGENEOUS



(a)

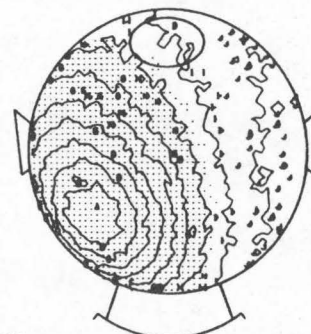
DIPOLE PARAMETERS :

X * = 0.150
Y * = 0.200
Z * = 0.320
PX * = -0.500
PY * = -0.200
PZ * = -0.300

CONTOUR RANGE :

K * = 1.6294
A * = -4.3064

MODEL : HOMOGENEOUS



(b)

NOISE FACTOR : 0.10000

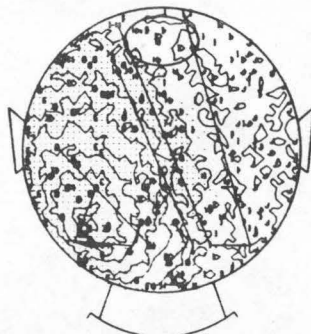
DIPOLE PARAMETERS :

X * = 0.150
Y * = 0.200
Z * = 0.320
PX * = -0.500
PY * = -0.200
PZ * = -0.300

CONTOUR RANGE :

K * = 1.9635
A * = -4.8228

MODEL : HOMOGENEOUS



(c)

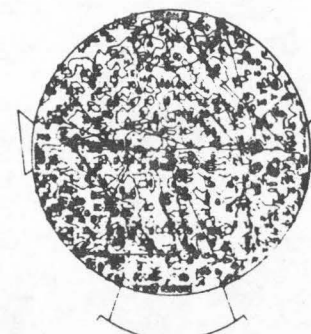
DIPOLE PARAMETERS :

X * = 0.150
Y * = 0.200
Z * = 0.320
PX * = -0.500
PY * = -0.200
PZ * = -0.300

CONTOUR RANGE :

K * = 3.2019
A * = -5.3607

MODEL : HOMOGENEOUS



(d)

NOISE FACTOR : 0.50000

DIPOLE PARAMETERS :

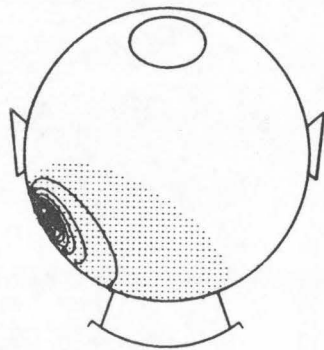
X * = 0.150
Y * = 0.200
Z * = 0.320
PX * = -0.500
PY * = -0.200
PZ * = -0.300

Figure 4-13. Degradation of equipotential maps in homogeneous model with increasing noise added to potentials. Dipole: (.15, .20, .32, -.50, -.20, -.30). Noise factors: (a) no noise; (b) 0.5; (c) 0.2; (d) 0.5.

CONTOUR RANGE :

K = 2.2182
A = -47.3835

MODEL : HOMOGENEOUS



(a)

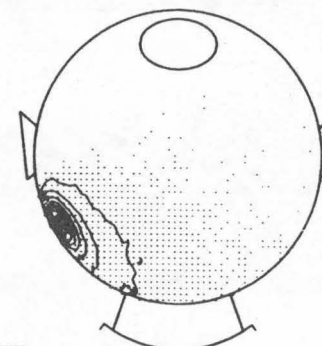
DIPOLE PARAMETERS :

X = 0.700
Y = 0.350
Z = 0.250
PX = -0.400
PY = -0.600
PZ = -0.300

CONTOUR RANGE :

K = 2.5650
A = -47.4135

MODEL : HOMOGENEOUS



(b)

NOISE FACTOR : 0.10000

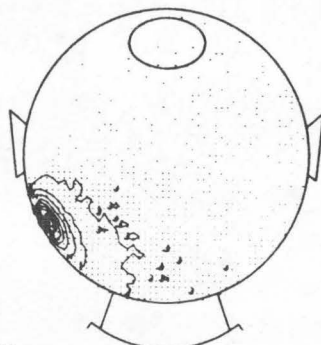
DIPOLE PARAMETERS :

X = 0.700
Y = 0.350
Z = 0.250
PX = -0.400
PY = -0.600
PZ = -0.300

CONTOUR RANGE :

K = 3.2541
A = -47.7170

MODEL : HOMOGENEOUS



(c)

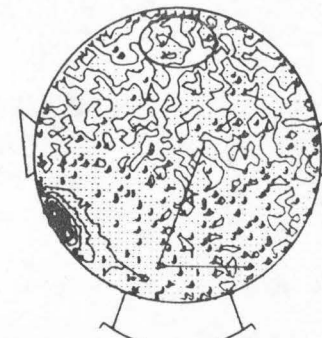
DIPOLE PARAMETERS :

X = 0.700
Y = 0.350
Z = 0.250
PX = -0.400
PY = -0.600
PZ = -0.300

CONTOUR RANGE :

K = 6.3873
A = -46.6044

MODEL : HOMOGENEOUS



(d)

NOISE FACTOR : 0.50000

DIPOLE PARAMETERS :

X = 0.700
Y = 0.350
Z = 0.250
PX = -0.400
PY = -0.600
PZ = -0.300

Figure 4-14. Degradation of equipotential maps in homogeneous model with increasing noise added to potentials. Dipole: (0.70, 0.35, 0.25, -0.40, -0.60, -0.30). Noise factors: (a) no noise; (b) 0.10; (c) 0.20; (d) 0.50.

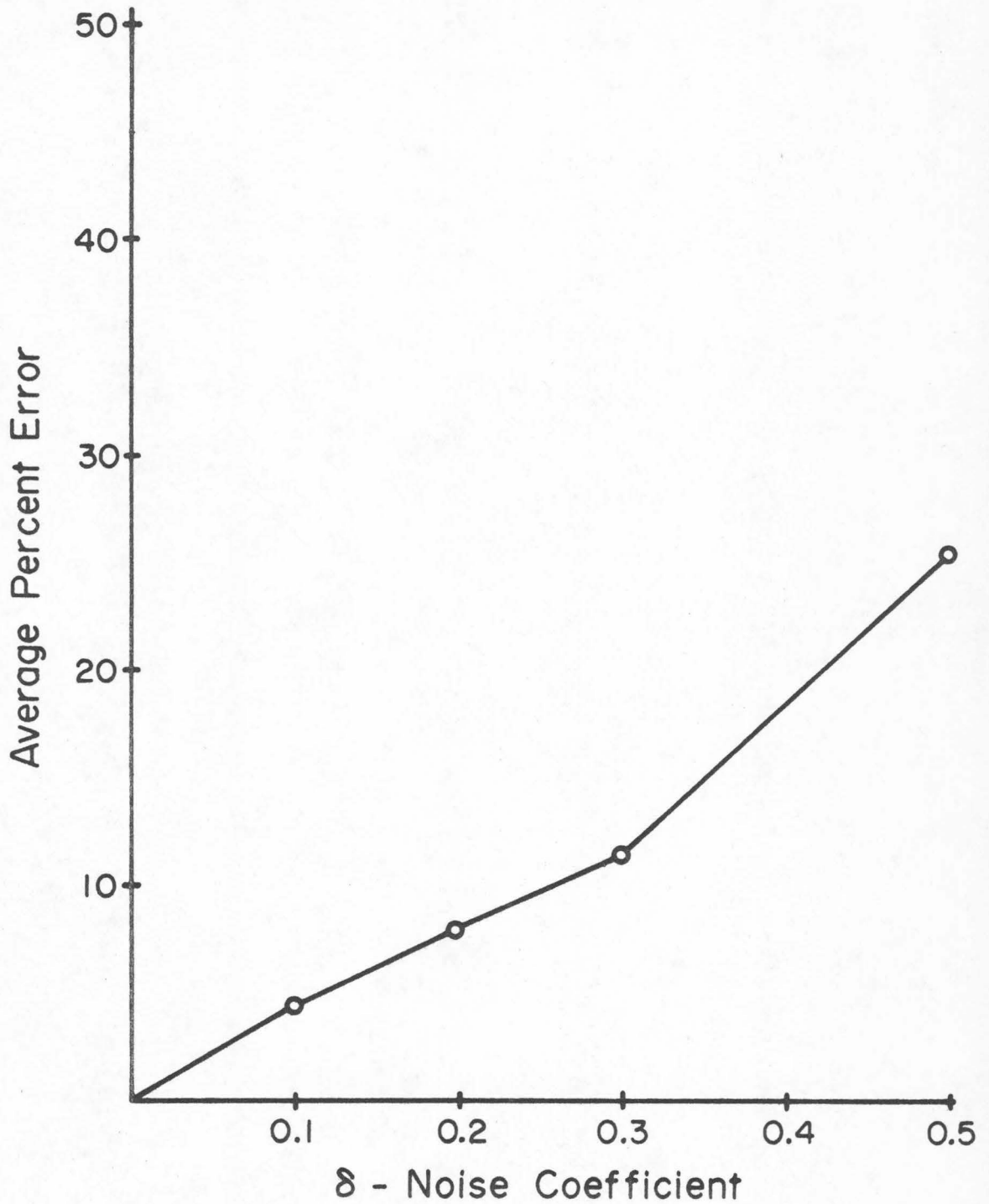


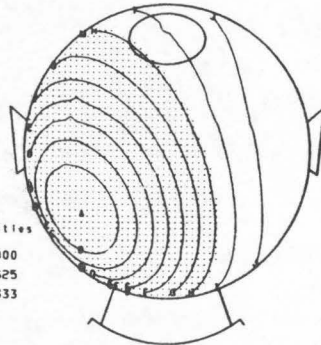
Figure 4-15. Sensitivity of inverse solutions in shell model to noise in potential measurements. Dipole: (.15, .20, .32, -.50, -.20, -.30), average error in initial guesses 18.8%.

CONTOUR RANGE :

K = 1.1410
A = -2.9434

MODEL : SHELL

radii	conductivities
0.90	1.00000
0.98	0.00625
1.00	0.33333



(a)

DIPOLE PARAMETERS :

X = 0.150
Y = 0.200
Z = 0.320
PX = -0.500
PY = -0.200
PZ = -0.300

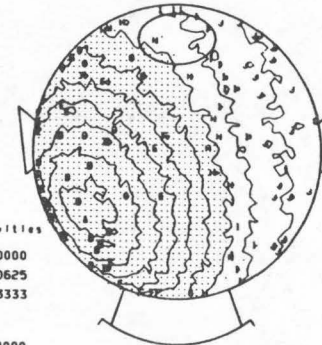
CONTOUR RANGE :

K = 1.3433
A = -3.2249

MODEL : SHELL

radii	conductivities
0.90	1.00000
0.98	0.00625
1.00	0.33333

NOISE FACTOR : 0.10000



(b)

DIPOLE PARAMETERS :

X = 0.150
Y = 0.200
Z = 0.320
PX = -0.500
PY = -0.200
PZ = -0.300

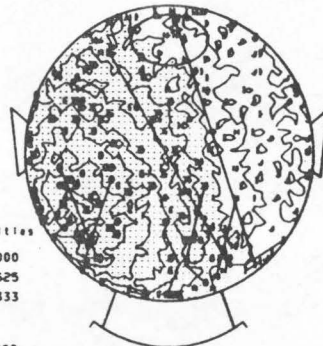
CONTOUR RANGE :

K = 1.5411
A = -3.4598

MODEL : SHELL

radii	conductivities
0.90	1.00000
0.98	0.00625
1.00	0.33333

NOISE FACTOR : 0.20000



(c)

DIPOLE PARAMETERS :

X = 0.150
Y = 0.200
Z = 0.320
PX = -0.500
PY = -0.200
PZ = -0.300

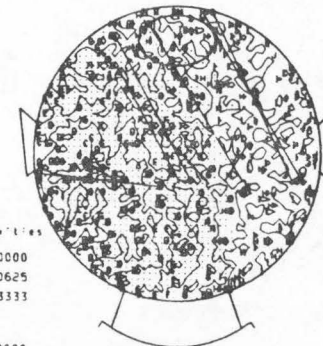
CONTOUR RANGE :

K = 1.8439
A = -3.5032

MODEL : SHELL

radii	conductivities
0.90	1.00000
0.98	0.00625
1.00	0.33333

NOISE FACTOR : 0.30000



(d)

DIPOLE PARAMETERS :

X = 0.150
Y = 0.200
Z = 0.320
PX = -0.500
PY = -0.200
PZ = -0.300

Figure 4-16. Degradation of equipotential maps in shell model with increasing noise added to potentials. Dipole: (0.15, 0.20, 0.32, -0.50, -0.20, -0.30). Noise factors: (a) no noise; (b) 0.10; (c) 0.20; (d) 0.30.

These tests of the sensitivity of the solutions to noise in the potential measurements indicate that the probable error in any inverse determinations using the evoked response data can be expected to be in the order of 10%. Besides the noise in the evoked response potentials, there is another source of error in locating the equivalent generators --- the errors in locating the recording electrodes on the surface of the head. The electrode arrangements shown in Figure 2-2(a) and 2-2(b) are only approximations to the actual pattern used in the sense that Dr. Lehmann attempted to follow those schemes, but with unknown error. In order to simulate this error, one can again generate a potential surface for some arbitrary dipole, but instead of perturbing the potential values one can add "noise" to the electrode positions. This noise is simply Gaussian noise of zero mean and variance \times degrees. As a rough estimate, an error in location of the electrodes of one cm. corresponds to about five degrees. Figure 4-17 shows the error in the determinations of equivalent dipoles in both models for this type of experimental inaccuracy.

One final test was made in order to further understand the differences between the two models. Some arbitrary source dipole was used to generate the surface potentials with the shell model. These surface potentials were then used to compute an optimum dipole in the homogeneous case. In other words, what dipole in the homogeneous model generates a surface distribution which is identical to that calculated from another dipole in the shell model?

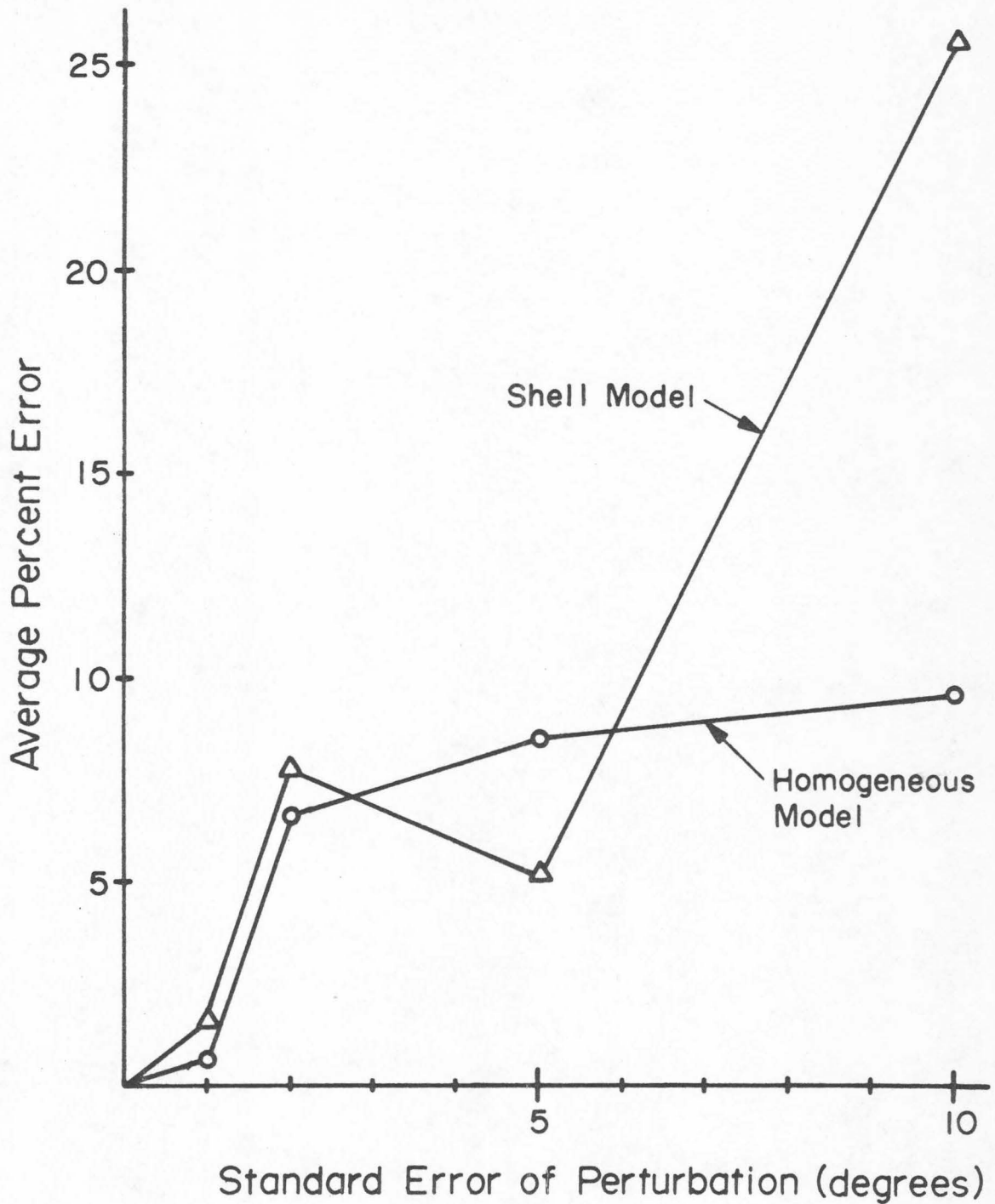


Figure 4-17. Sensitivity of inverse solutions to errors in electrode location in homogeneous and shell models. Dipole: (.15, .20, .32, -.50, -.20, -.30), average error in initial guesses 18.8%.

This was done for five different cases and the results are shown in Table 4-1. The "source" dipole is the one used to generate the voltages using the shell model; the "calculated" parameters are those of the equivalent homogeneous case. Most of these determinations were carried out with relatively tight estimates of the optimum parameters, indicated by the standard deviations (S. D.) of the calculated parameters.

The last column of the table, labeled "E", is either the eccentricity of the dipoles in the table or the standard error of the calculated eccentricity. This characteristic of the dipoles is included because it is the clue to the systematic disparity between the two models. In all cases the equivalent homogeneous dipoles are less eccentric and less strong than the source dipole in the shell model. As the eccentricity of the source dipole becomes less and less, however, note there is a diminishing difference in the location of the dipole in the homogeneous model. For example, the fourth case taken shows that the two dipoles are very close to being in the same locations, but the dipole parameters have been decreased in the homogeneous model. Thus it appears that as the eccentricity of the source dipole decreases, there is less difference in the location of the equivalent dipole in the homogeneous model. At all eccentricities, however, the dipole moments are less strong for the homogeneous model.

This test confirms the earlier suggestion that a homogeneous model of the head produces equivalent dipoles which are generally

Table 4-1. Calculation of Dipoles in the Homogeneous Model which fit Surface Potential Distributions arising from Source Dipoles in the Shell Model.

CASE	DIPOLE PARAMETERS							
	X	Y	Z	P _x	P _y	P _z	E	
1	Source	0.70	0.35	0.25	-0.40	-0.60	-0.30	0.82
	Calc.	0.55	0.27	0.29	-0.35	-0.49	-0.26	0.67
	S.D.	0.06	0.02	0.01	0.02	0.03	0.04	0.05
2	Source	0.60	0.40	0.30	-0.45	-0.50	-0.35	0.78
	Calc.	0.45	0.31	0.27	-0.39	-0.43	-0.29	0.61
	S.D.	0.03	0.01	0.01	0.02	0.02	0.01	0.02
3	Source	0.20	0.23	0.36	-0.45	-0.25	-0.25	0.47
	Calc.	0.18	0.17	0.32	-0.37	-0.21	-0.21	0.40
	S.D.	0.01	0.01	0.00	0.01	0.01	0.00	0.01
4	Source	0.15	0.20	0.32	-0.50	-0.20	-0.30	0.41
	Calc.	0.15	0.17	0.33	-0.38	-0.15	-0.25	0.40
	S.D.	0.02	0.01	0.00	0.01	0.01	0.01	0.01
5	Source	0.0	0.0	0.75	0.0	0.0	1.0	0.75
	Calc.	0.00	0.00	0.61	0.00	0.00	0.88	0.61
	S.D.	0.00	0.00	0.00	0.01	0.01	0.01	0.00

deeper than would be the case when the conductivity discontinuities are considered. Table 4-1 shows that this discrepancy is not a large one in some cases, but there is a systematic tendency for the homogeneous model to underestimate the proximity of the dipole to the surface of the head. The same conclusion has previously been stated for electrocardiogram models (1).

Before analyzing any experimental data then, it is possible by the processes indicated above to study many basic properties of the models proposed. At this stage the analysis of the evoked response data can proceed with reasonable awareness of what can be expected in the results.

5. Caveat Emptor

Before analyzing the evoked response experiments in terms of equivalent dipoles, some comments are appropriate concerning the implementation of the foregoing theory in the form of a computer program. Lest anyone rush to apply equations (3) through (17) and the endless relations for the partial derivatives of these to his own evoked response data, be now forewarned! A reasonable estimate of the effort required to program all of the equations used to bring about the results of this chapter is probably between 500 and 1000 man-hours. The Fortran program which achieved the tests of simulated dipoles and their inverse determinations is approximately 3000 cards in length. In addition to these comments on the travails involved, I would like to point out some other details of the computer implementation.

When coding the computer programs it is quite advisable to incorporate a system for precisely checking the implementation of equations (3) through (17) and their partial derivatives. In this case the method of achieving this was to utilize program variable names which could easily be identified with the factors in all equations. By checking and re-checking during the coding process the implementation of the numerous equations, it was found that when finally the testing of some dipoles was started, only a single sign mistake was incurred.

In parallel with these problems in programming the algorithms once they are derived, there are some difficulties in achieving the correct algorithms as well. This is especially true in the case of the shell model, since none of the important equations therein exist in closed form. One has thus to study carefully the convergence criteria used to terminate calculations of higher and higher terms of the infinite series solutions. The scheme used here was to be satisfied with the convergence of the series when three successive terms are all smaller than some fraction, δ , of the current value of the series. Also in this regard, note that even if one starts with a convergent series for the potential at any point on the surface of the shell model, differentiation of that series may not yield another convergent series. The computer tests indicate that for most cases the various partial derivatives in the shell model are relatively stable, but some extra programming

precautions were necessary in order to detect and avoid any evaluations which became unstable.

Lastly I wish to point out the speed with which one can compute equivalent dipoles in the two models. The homogeneous model can solve the inverse problem for a typical dipole in approximately ten seconds. Because of the need to evaluate the series solutions for the shell model, however, the computing time to characterize a dipole in this more complicated model is about 400 seconds on an IBM 360/75. This sort of programming and subsequent computing is thus not for the person with a small, slow computing facility --- nor for one with a small budget. At the Caltech computing center it costs about a dollar to solve the problem in the homogeneous case, but close to \$50.00 to locate one dipole with the shell model.

Implementation of the techniques discussed here is thus a problem. The most meticulous of programming procedures are recommended and one will quickly find the calculations to be costly. The title of this section thus stands as a well intended precaution -- CAVEAT EMPTOR -- Buyer Beware!

REFERENCES FOR CHAPTER IV

1. Arthur, R.M. and Geselowitz, D.B., "Effect of Inhomogeneities on the Apparent Location and Magnitude of a Cardiac Current Dipole Source," IEEE Trans. Bio-Med. Engrg. BME-17 (1970), pp. 141-146.
2. Barr, R.C., Pilkington, T.C., Boineau, J.P. and Spach, M.S., "Determining Surface Potentials from Current Dipoles, with Application to Electrocardiography," IEEE Trans. Bio-Med. Engrg. BME-13 (1966), pp. 88-92.
3. Brazier, M.A.B., "A Study of the Electrical Fields at the Surface of the Head," Second International Congress on Electroencephalography, Electroenceph. clin. Neurophysiol. Suppl. 2 (1949), pp. 38-52.
4. Feynman, R.P., Leighton, R.B. and Sands, M., The Feynman Lectures on Physics II. Electromagnetism and Matter, Addison-Wesley Pub. Co., Reading, Mass. (1964).
5. Fourment, A., Jami, A., Carter, J. and Sheiner, J., "Comparaison de L'EEG Recueilli sur le Scalp avec l'Activite Elementaire des Dipoles Corticaux Radiates," Electroenceph. clin. Neurophysiol. 19 (1965), pp. 217-229.
6. Frank, E., "Electric Potential Produced by Two Point Current Sources in a Homogeneous Conducting Sphere," J. Appl. Physics 23 (1952), pp. 1225-1228.
7. Gabor, D. and Nelson, C.B., "Determination of the Resultant Dipole of the Heart from Measurements on the Body Surface," J. Appl. Physics 25 (1954), pp. 413-416.
8. Geddes, L.A. and Baker, L.E., "The Specific Resistance of Biological Material --- A Compendium of Data for the Biomedical Engineer and Physiologist," Med. & Biol. Engrg. (1967), pp. 217-293.
9. Geisler, C.D. and Gerstein, G.L., "The Surface EEG in Relation to its Sources," Electroenceph. clin. Neurophysiol. 13 (1961), pp. 927-934.
10. Gelernter, H.L. and Swihart, J.C., "A Mathematical-Physical Model of the Genesis of the Electrocardiogram," Biophysical Journal 4 (1964), pp. 285-301.

11. Geselowitz, D.B., "On Bioelectric Potentials in an Inhomogeneous Volume Conductor," Biophysical Journal 7 (1967), pp. 1-11.
12. Geselowitz, D.B. and Ishiwatari, H., "A Theoretic Study of the Effect of the Intracavitary Blood Mass on the Dipolarity of an Equivalent Heart Generator," Proc. Long Island Jewish Hosp. Symposium Vectorcardiography, North Holland Pub. Co. (1966), pp. 393-402.
13. Geselowitz, D.B., "Multipole Representation for an Equivalent Cardiac Generator," Proc. IRE 48 (1960), pp. 75-79.
14. Marquardt, D.W., "Least-Squares Estimation of Nonlinear Parameters," IBM Share Program Catalog No. 3094 (1964).
15. Marquardt, D.W., "An Algorithm for Least-Squares Estimation of Nonlinear Parameters," J. Soc. Industrial and Appl. Math. 11 (1963), pp. 431-441.
16. McFee, R. and Johnston, G. D., "Electrocardiographic Leads I. Introduction," Circulation 8 (1953), pp. 554-568.
17. _____, "Electrocardiographic Leads II. Analysis," Circulation 9 (1954), pp. 255-266.
18. _____, "Electrocardiographic Leads III. Synthesis," Circulation 9 (1954), pp. 868-880.
19. Plonsey, R., Bioelectric Phenomena, McGraw-Hill, New York (1969).
20. Plonsey, R., "Limitations on the Equivalent Cardiac Generator," Biophysical Journal 6 (1966), pp. 163-173.
21. Plonsey, R., "Reciprocity Applied to Volume Conductors and the ECG," IRE Trans. Bio-Med. Engrg. BME-10 (1963), pp. 9-12.
22. Plonsey, R., "Volume Conduction Fields of Action Currents," Biophysical Journal 4 (1964), pp. 317-328.
23. Rush, S. and Driscoll, D.A., "EEG Electrode Sensitivity - an Application of Reciprocity," IEEE Trans. Bio-Med. Engrg. BME-16 (1969), pp. 14-22.

24. Rush, S. and Driscoll, D.A., "Current Distribution in the Brain from Surface Electrodes," Anesth. and Analgesia -- Current Researches 47 (1968), pp. 717-723.
25. Schneider, M. and Gerin, P., "Une Methode de Localization des Dipoles Cerebraux," Electroenceph. clin. Neurophysiol. 28 (1970), pp. 69-78.
26. Shaw, J.C. and Roth, M., "Potential Distribution Analysis II. A Theoretical Consideration of its Significance in terms of Electric Field Theory," Electroenceph. clin. Neurophysiol. 28 (1970), pp. 360-367.
27. Van Harreveld, A., personal communication.
28. Vaughn, H.G. and Ritter, W., "The Sources of Auditory Evoked Responses Recorded from the Human Scalp," Electroenceph. clin. Neurophysiol. 28 (1970), pp. 360-367.
29. Vaughn, H.G., Costa, L.D. and Ritter, W., "Topography of the Human Motor Potential," Electroenceph. clin. Neurophysiol. 25 (1968), pp. 1-10.

V. EQUIVALENT DIPOLES FOR HUMAN
VISUALLY EVOKED RESPONSES

1. Preparation of Evoked Response Data for Dipole Analysis.

In Chapter IV there were shown various equipotential maps of data generated by dipoles in either the homogeneous or shell models. Preceding these were the maps of the experimental data, in Chapter III. By comparing pictures of the evoked response data with pictures of typical dipole fields, the value of the experience gained in Chapter IV becomes apparent. This "catalogue" of typical dipole fields allows one to select patterns which most closely resemble the data taken from subjects KW and DALO. The parameters used to generate the matching dipole patterns can then be used as the initial guesses for analyzing the evoked response data.

The procedure then was as follows. The movie for each of the two subjects was studied in order to pick out intervals during which the fields showed relatively stable, dipole-like patterns. Following this initial screening individual frames of the movie were studied in greater detail, comparing them with the catalogue of typical dipole fields. This process was carried out for all three conditions for each subject.

Not every sample time for the responses was analyzed with the equivalent dipole procedure. In Chapter III, the conclusion

was that there were basically three intervals during which the responses seem to best be attributed to a small number of processes, and generally both subjects showed dipole-like patterns during each of the three intervals. These three periods occur roughly at the same times as the major amplitude peaks of the evoked responses (Figure 2-8); from say 60ms to 90ms, 90ms to 135ms, and 165ms to 185ms. Furthermore, within each such period the responses are quite stable over small time increments, and it thus seemed redundant to analyze the responses more frequently than at every 5ms within each of the three segments.

In looking for dipole-like patterns in the responses it became evident that many aspects of the responses were similar in the two subjects while others were quite different. During the last interval of interest for example (165ms - 185ms) the responses appear quite similar in the two subjects --- the data suggest a single source located in the left posterior region of the head. Earlier, however, there is not a similarity in either shape or polarity of the responses. The DALO data from 60ms to 90ms and from 90ms to 130ms indicate a single source located in the occipital region, close to the midline, while the KW data from 90 to 130ms suggest two sources, somewhat laterally located in the head. There are some further comparisons which can be made, and they will be mentioned later. For the moment I have mentioned only those features which are central to the process of hypothesizing equivalent dipole sources.

Note there is not an analytical problem in seeking two independent dipole sources for the 90ms to 130ms interval of the KW data. Since the laws of superposition hold, the potential at any point on the surface of a sphere containing two sources is simply the sum of the potentials from each individual source. The program used to fit equivalent dipoles to the data was thus written to seek either one or two dipoles, i. e. to find optimum values for either six or twelve parameters. This does not mean that the program also decided which solution to attempt. The decision to use either one or two sources for a particular pattern was made in the initial screening and fed into the analysis program.

During the normal analysis of the evoked response data there was only one segment (the above mentioned interval in the KW data) of the responses wherein two sources were suggested by the equipotential maps and subsequently found by the dipole analysis program. Eventually some test analyses were conducted where two sources were sought for potential distributions which seemed to arise from only one source, and the results of these attempts to locate two equivalent sources for potentials which were originally well explained by one source will be discussed later in this Chapter.

The foregoing summarizes the preliminary data screening and formulation of equivalent dipole hypotheses. The computer analysis which followed is briefly described in Figure 5-1.

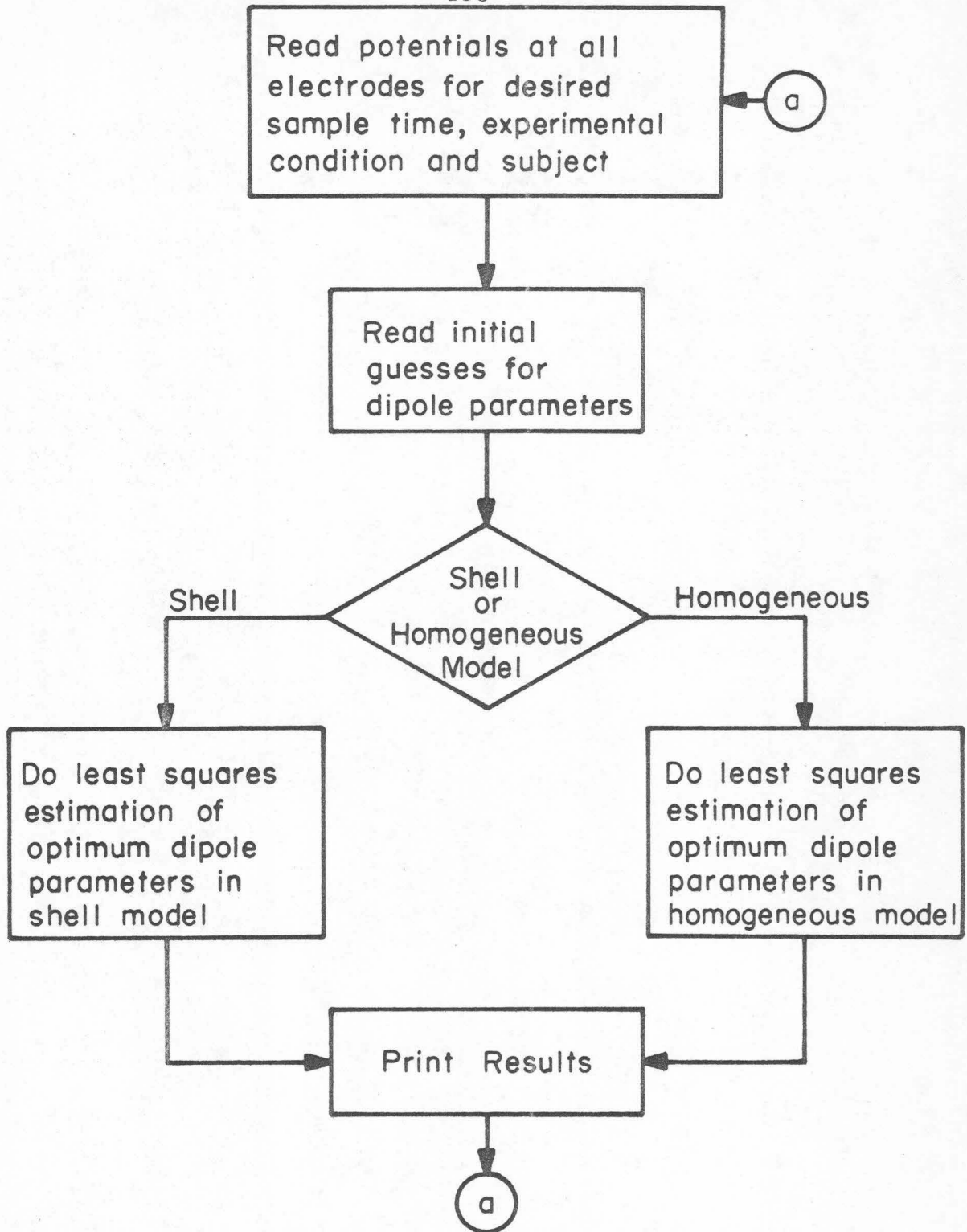


Figure 5-1. Outline of computer analysis of evoked response data in terms of equivalent dipoles.

2. Some Comments on Non-linear Confidence Region Calculations.

The Marquardt program produces three different sets of confidence regions as well as the correlation matrix for the parameter estimates. Since in the region of convergence to the minimum squared error the model may become linear in the parameter space to a good approximation, it is possible to apply conventional linear confidence region theory. The standard one-parameter confidence interval assumes no correlation between parameters, and may be the narrowest of the three regions calculated. For a parameter estimate b_j with standard error s_j , the one-parameter confidence interval is calculated from:

$$b_j - [t_{1-\alpha}(n-k)] s_j \leq \beta_j \leq b_j + [t_{1-\alpha}(n-k)] s_j \quad (1)$$

where $t_{1-\alpha}(n-k)$ is the two-tailed $(1-\alpha)$ value of the t-distribution with $(n-k)$ degrees of freedom (n is the number of observations or electrodes and k is the number of estimated parameters). β_j is the true parameter value, lying in the region above with probability $(1-\alpha)$. When correlations do exist between the parameters the above region tends to underestimate the confidence interval, and an upper bound can be found from the so-called support-plane confidence limits. Marquardt states (1) that the latter is the "most conservatively wide," but within the applicability of linear theory, it is the most realistic estimate of the confidence limits when significant correlations exist.

This confidence region is defined by

$$b_j - \sqrt{kF_{1-\alpha}(k, n-k)} s_j \leq \beta_j \leq b_j + \sqrt{kF_{1-\alpha}(k, n-k)} s_j \quad (2)$$

where $F_{1-\alpha}(k, n-k)$ is the upper $(1-\alpha)$ point of the F distribution with k and $(n-k)$ degrees of freedom.

It is perhaps important to realize just how "conservatively wide" the support plane regions are. In equation (1) the critical value of the t - statistic is typically near 2.0 for the evoked response experiments. Thus the one-parameter confidence region is roughly two standard deviations on either side of the parameter estimate b_j . In equation (2), however, the typical value of the term $kF_{1-\alpha}(k, n-k)$ is in the order of 5. The support plane confidence region is thus approximately two and a half times as wide as the one-parameter region.

Finally, non-linear confidence limits are found by calculating a critical value of the squared error and then finding the upper and lower values of each parameter which cause the sum of squared deviations to just exceed the critical value. The details of this are as follows. At the point in the parameter space where the minimum in the sum of the squared deviations occurs, call this minimum value ϕ . The program then computes

$$\phi_c = \phi \left[1 + \frac{k}{n-k} F_{1-\alpha}(k, n-k) \right] \quad (3)$$

as the "critical value" of the sum of squared deviations.

This springs from Marquardt's statement that

$$\frac{(\phi_c - \phi)/k}{\phi/(n-k)} \leq F_{1-\alpha}(k, n-k)$$

In other words he has apparently partitioned the total sum of squares ϕ into an "error" variance, $\phi/(n-k)$, and a variance due to deviations of the parameter estimates from their true values, $(\phi_c - \phi)/k$, and the ratio of these two sums of squares follows an F distribution. Equation (3) gives this critical value of ϕ , and the parameters are then varied, one at a time, in both directions from their estimated values, until ϕ_c is attained. The corresponding upper and lower values of the parameters are what Marquardt refers to as the non-linear confidence limits. If the deviations from linearity are negligible the non-linear and the one-parameter confidence regions are substantially the same.

The motivation here is not to completely describe the LSQENP algorithm, but rather to properly interpret the various statistics and confidence regions produced by that program. From the above we see that the first question is whether or not linear confidence limits apply. To decide this we must compare the one-parameter confidence limits with the non-linear confidence limits. A typical case is shown in Table 5-1. This table shows that the two confidence regions are similar --- sometimes the non-linear region is slightly wider than the one-parameter and other times the reverse is true. This is the general case in the

Table 5-1. Comparison of One-Parameter versus Nonlinear confidence regions for Analysis of DALO data, flash to right eye, at 70ms after stimulus. Parameters are in form of Homogeneous Model.

Parameter	Estimated Value	Lower One-Parameter	Lower Nonlinear	Upper One-Parameter	Upper Nonlinear
P_x	0.084	-0.016	-0.012	0.153	0.180
P_y	-0.112	-0.194	-0.120	-0.049	-0.043
P_z	-0.161	-0.235	-0.255	-0.087	-0.066
α	0.849	0.574	0.416	1.123	1.092
β	0.145	-0.053	-0.099	0.343	0.421
f	0.609	0.489	0.424	0.730	0.712

analyses, and the conclusion is that since the non-linear confidence intervals are so close to the one-parameter regions, the dipole models are approximately linear in the parameter space near the minimum of the sum of the squared deviations. Hence linear confidence regions can be used, as suggested by Marquardt.

Next there is the question of which of the linear confidence regions to use, the one-parameter or the support plane. The former is indicated when, as discussed above, zero or insignificant correlations among the parameters exist, and the evoked response analyses suggest this to be the case. A typical correlation matrix is shown in Table 5-2. Marquardt unfortunately does not indicate any criteria by which the correlations may be tested for significance. A statistic based on a simple t-test with $n-2$ degrees of freedom where n is the number of observations would indicate that for this DALO case the critical value of the correlations would be approximately 0.325 at the 5% level. This means that only two of the 15 cross correlations would be significant at that level.

Perhaps the best criterion is a consideration of the various test cases of Chapter IV. In all of the trials of inverse determinations for various hypothetical dipoles, the original dipole parameters used to generate the potentials were contained in the one-parameter confidence regions, even in the "noisiest" of test cases. It seems reasonable to expect that the "true" parameter values for the evoked response analyses can be ably estimated by the one-parameter confidence regions.

Table 5-2. Parameter correlation matrix for analysis of subject DALO, flash to right eye, at 75ms after the stimulus. Parameters one through six are those for the homogeneous model, i. e. P_x , P_y , P_z , α , β , and f respectively.

1.000	-0.036	-0.021	-0.030	-0.316	-0.078
-0.036	1.000	-0.062	-0.124	-0.021	-0.599
-0.021	-0.062	1.000	0.436	-0.021	-0.028
-0.030	-0.124	0.436	1.000	0.029	-0.231
-0.316	-0.021	-0.021	0.029	1.000	0.003
0.078	-0.599	-0.208	-0.231	0.003	1.000

3. Analysis of Evoked Responses with the Homogeneous Model.

As suggested earlier there are, for each subject, three principal intervals in the evoked response during which the surface potentials seem to be comparable to those generated by simple dipole sources. Not every condition for each subject produced responses which could be attributed to equivalent dipoles in each of these intervals; each subject showed responses to some stimuli that were less dipole-like than the responses to the other stimuli. Generally, however, each subject showed some very good dipole fields during each of these intervals and the inverse dipole determinations were attempted.

There is a problem again in display of information. The dipole analyses were performed at 5ms increments during each of the above intervals, generating some forty or so equivalent dipole solutions for each subject. Each solution is characterized by either six or twelve dipole parameters, six or twelve standard deviations, eighteen or thirty-six confidence regions (three confidence regions for each parameter), and a correlation matrix for the parameter estimates. To present all of these numbers would obscure the results! In order to compact the analyses the dipole solutions will first be presented simply as the optimal parameter values and their standard errors, then following will be given some diagrams which illustrate both the dipole locations and the confidence regions.

The optimal parameter estimates and their associated standard errors for dipoles in a homogeneous sphere for the various stimuli and subjects are shown in Tables 5-3 through 5-5. In all these tables, and those for the shell analysis later, the entry "P" is the absolute magnitude of the dipole of components P_x , P_y and P_z .

From these analyses I have extracted a number of illustrative solutions for each subject and have presented the results in the diagrams shown in Figure 5-2 through 5-14. In these diagrams the dipole locations as determined by the parameter estimates and the one-parameter confidence regions (at the 95% level) are shown along with the orientation of the dipoles as determined by the estimates of the dipole components. One should imagine confidence "ellipsoids" to be drawn within the rectangular volumes shown.

Before mentioning some of the more obvious features of the results, I wish to point out that no attempt has been made to relate any absolute neurophysiological characteristics with the magnitudes of the dipole strengths. The dipole magnitudes from one analysis to another give indications only of the relative strengths of the activity at these times. Since the derivation of the dipole approximation has "lumped" all of the contributions of the millions of miniature current dipoles into one dipole near the center of the region containing the activity, only the location of

Table 5-3. Parameter Estimates and Standard Deviations for interval 60ms to 90ms, in homogeneous models. (a) Subject DALO, flash to right eye.

Parameters and Standard Deviations	Analysis Time (ms)			
	65	70	75	80
x	-.142	.088	.084	.155
Δx	.045	.067	.062	.075
y	.426	.423	.323	.213
Δy	.111	.092	.079	.075
z	.548	.399	.431	.392
Δz	.038	.028	.008	.006
P_x	-.052	.084	.143	.096
ΔP_x	.022	.034	.040	.040
P_y	-.005	-.122	-.224	-.228
ΔP_y	.019	.036	.041	.040
P_z	-.109	-.161	-.202	-.215
ΔP_z	.023	.036	.044	.043
P	.120	.219	.334	.370

Table 5-3. (b) Subject DALO, flash to left eye.

Parameters and Standard Deviations	Analysis Time (ms)			
	75	80	85	90
x	-.015	-.035	-.052	-.082
Δx	.048	.040	.038	.031
y	.272	.217	.145	.115
Δy	.069	.057	.051	.047
z	.444	.438	.437	.431
Δz	.014	.026	.040	.044
P_x	-.001	.032	.083	.176
ΔP_x	.028	.026	.025	.025
P_y	-.276	-.333	-.356	-.358
ΔP_y	.030	.029	.029	.027
P_z	-.109	-.103	-.054	.015
ΔP_z	.032	.029	.028	.026
P	.297	.350	.369	.399

Table 5-3. (c) Subject DALO, flash to both eyes.

Parameters and Standard Deviations	Analysis Time (ms)				
	60	65	70	75	80
x	-.020	.011	.053	.055	.068
Δx	.043	.051	.054	.054	.053
y	.334	.325	.258	.239	.213
Δy	.072	.074	.064	.061	.056
z	.376	.398	.402	.403	.413
Δz	.003	.003	.008	.012	.017
P_x	-.280	-.236	-.093	.002	.078
ΔP_x	.036	.045	.050	.050	.096
P_y	-.155	-.288	-.494	-.551	-.563
ΔP_y	.033	.045	.053	.055	.052
P_z	-.197	-.221	-.239	-.235	-.193
ΔP_z	.037	.049	.056	.057	.053
P	.376	.433	.556	.600	.600

Table 5-4. Parameter estimates and Standard Deviations for interval 90ms to 135ms, in Homogeneous model. (a) Subject DALO, flash to right eye.

Parameters and Standard Deviations	Analysis Time (ms)					
	105	110	115	120	125	130
x	.028	.022	.012	.020	.016	.016
Δx	.048	.056	.044	.040	.039	.041
y	.808	.357	.278	.244	.206	.213
Δy	.023	.077	.059	.050	.048	.051
z	.476	.461	.438	.418	.401	.374
Δz	.015	.006	.010	.014	.020	.019
P_x	.011	-.092	-.107	-.098	-.086	-.075
ΔP_x	.013	.063	.061	.053	.043	.034
P_y	.411	.472	.739	.791	.717	.560
ΔP_y	.080	.066	.068	.060	.051	.041
P_z	.359	.150	.127	.120	.088	.059
ΔP_z	.063	.068	.069	.060	.049	.039
P	.546	.504	.757	.806	.727	.568

Table 5-4. (b) Subject DALO, flash to left eye.

Parameters and Standard Deviations	Analysis Time (ms)					
	105	110	115	120	125	130
x	.082	.080	.031	.031	.025	.040
Δx	.027	.052	.045	.043	.042	.045
y	.798	.509	.310	.277	.274	.397
Δy	.017	.061	.060	.055	.054	.057
z	.474	.427	.433	.411	.391	.366
Δz	.012	.008	.002	.008	.009	.004
P_x	-.015	-.193	-.205	-.193	-.165	-.126
ΔP_x	.016	.058	.059	.051	.041	.033
P_y	.398	.334	.590	.625	.545	.365
ΔP_y	.069	.054	.062	.056	.046	.038
P_z	.365	.233	.224	.188	.114	.070
ΔP_z	.054	.061	.065	.057	.046	.035
P	.540	.451	.664	.681	.581	.392

Table 5-4. (c) Subject DALO, flash to both eyes.

Parameters and Standard Deviations	Analysis Time (ms)					
	105	110	115	120	125	130
x	.157	.074	.017	.006	.012	.056
Δx	.053	.031	.052	.043	.039	.045
y	.774	.805	.313	.240	.206	.263
Δy	.022	.013	.075	.058	.051	.053
z	.525	.487	.484	.438	.368	.331
Δz	.021	.012	.004	.018	.020	.007
P_x	-.061	-.046	-.216	-.242	-.237	-.214
ΔP_x	.030	.021	.061	.054	.049	.047
P_y	.334	.615	.462	.639	.789	.698
ΔP_y	.112	.096	.062	.059	.058	.057
P_z	.266	.532	.207	.146	.097	.065
ΔP_z	.081	.071	.068	.060	.055	.052
P	.431	.814	.550	.699	.830	.733

Table 5-4. (d) Subject KW, flash to right eye. i) Dipole one.

Parameters and Standard Deviations	Analysis Time (ms)				
	110	115	120	125	130
x	.487	.484	.452	.456	.429
Δx	.078	.076	.075	.084	.091
y	.149	.129	.116	.117	.111
Δy	.038	.034	.033	.030	.038
z	.241	.205	.184	.145	.180
Δz	.061	.075	.077	.102	.088
P_x	-.257	-.291	-.333	-.294	-.297
ΔP_x	.079	.110	.134	.171	.128
P_y	-.432	-.605	-.805	-.861	-.752
ΔP_y	.076	.101	.116	.147	.117
P_z	-.212	-.320	-.427	-.504	-.300
ΔP_z	.125	.173	.220	.279	.210
P	.546	.744	.970	1.040	.862

Table 5-4. (d) (ii) Dipole two.

Parameters and Standard Deviations	Analysis Time (ms)				
	110	115	120	125	130
x	-.758	-.778	-.774	-.804	-.775
Δx	.143	.056	.203	.074	.288
y	.312	.321	.330	.342	.343
Δy	.405	.371	.410	.302	.409
z	.456	.412	.344	.352	.323
Δz	.114	.026	.073	.015	.088
P_x	.112	.135	.047	.145	.017
ΔP_x	.223	.310	.360	.480	.322
P_y	-.070	-.107	-.105	-.167	-.098
ΔP_y	.102	.150	.170	.240	.150
P_z	-.150	-.202	-.237	-.285	-.238
ΔP_z	.210	.302	.403	.434	.368
P	.200	.265	.263	.856	.255

Table 5-4. (e) Subject KW, flash to left eye. (i) Dipole one.

Parameters and Standard Deviations	Analysis Time (ms)					
	105	110	115	120	125	130
x	.499	.497	.479	.449	.443	.450
Δx	.072	.069	.072	.086	.097	.107
y	.165	.159	.154	.134	.128	.110
Δy	.038	.031	.029	.039	.045	.043
z	.275	.226	.199	.223	.230	.196
Δz	.051	.064	.073	.071	.075	.100
P_x	-.293	-.305	-.327	-.405	-.407	-.311
ΔP_x	.075	.097	.121	.127	.128	.121
P_y	-.390	-.511	-.609	-.630	-.558	-.518
ΔP_y	.068	.083	.097	.105	.104	.106
P_z	-.229	-.329	-.406	-.321	-.248	-.177
ΔP_z	.123	.156	.192	.196	.187	.176
P	.534	.680	.802	.815	.728	.630

Table 5-4. (e) (ii) Dipole two.

Parameters and Standard Deviations	Analysis Time (ms)					
	105	110	115	120	125	130
x	-.811	-.806	-.797	-.774	-.789	-.770
Δx	.021	.060	.055	.075	.085	.054
y	.311	.321	.315	.305	.304	.309
Δy	.265	.296	.314	.297	.272	.363
z	.387	.359	.366	.433	.438	.381
Δz	.033	.027	.031	.050	.038	.056
P_x	.178	.126	.126	.208	.292	.102
ΔP_x	.210	.265	.321	.316	.315	.314
P_y	-.116	-.122	-.136	-.150	-.194	-.126
ΔP_y	.095	.132	.152	.137	.135	.145
P_z	-.246	-.274	-.272	-.277	-.334	-.248
ΔP_z	.245	.346	.375	.304	.283	.393
P	.325	.325	.329	.377	.484	.296

Table 5-4. (f) Subject KW, flash to both eyes. (i) Dipole one.

Parameters and Standard Deviations	Analysis Time (ms)					
	100	105	110	115	120	125
x	.496	.507	.496	.463	.424	.359
Δx	.081	.087	.083	.079	.081	.106
y	.117	.120	.105	.091	.061	.057
Δy	.038	.042	.038	.037	.039	.053
z	.275	.285	.258	.233	.188	.193
Δz	.044	.046	.052	.053	.063	.065
P_x	-.237	-.259	-.281	-.274	-.238	-.241
ΔP_x	.062	.072	.075	.075	.078	.077
P_y	-.527	-.543	-.615	-.688	-.726	-.612
ΔP_y	.097	.111	.116	.114	.112	.098
P_z	-.033	-.025	-.053	-.103	-.160	-.100
ΔP_z	.094	.104	.116	.125	.139	.141
P	.579	.602	.678	.748	.781	.665

Table 5-4. (f) (ii) Dipole two.

Parameters and Standard Deviations	Analysis Time					
	100	105	110	115	120	125
x	-.828	-.820	-.826	-.829	-.836	-.799
Δx	.073	.059	.087	.107	.163	.202
y	.400	.426	.396	.386	.364	.343
Δy	.231	.242	.221	.219	.233	.246
z	.167	.180	.186	.197	.212	.216
Δz	.097	.086	.077	.073	.070	.004
P_x	-.865	-.882	-.851	-.731	-.536	-.259
ΔP_x	.315	.364	.343	.318	.303	.217
P_y	.288	.301	.247	.191	.105	.013
ΔP_y	.175	.207	.179	.157	.135	.095
P_z	-.254	-.273	-.296	-.276	-.233	-.209
ΔP_z	.473	.503	.475	.438	.402	.176
P	.946	.971	.934	.804	.594	.333

Table 5-5. Parameter estimates and Standard Deviations for interval 165 ms to 200 ms. (a) Subject DALO, flash to right eye.

Parameters and Standard Deviations	Analysis Time (ms)			
	175	180	185	190
x	.219	.173	.161	.151
Δx	.042	.030	.029	.036
y	.261	.397	.454	.491
Δy	.043	.035	.032	.036
z	.471	.413	.415	.416
Δz	.002	.011	.010	.010
P_x	.218	.325	.333	.299
ΔP_x	.021	.023	.024	.028
P_y	.156	.052	-.034	-.083
ΔP_y	.019	.016	.017	.021
P_z	.011	.029	.021	.027
ΔP_z	.020	.020	.019	.021
P	.268	.330	.335	.311

Table 5-5 (continued). (b) Subject DALO, flash to both eyes.

Parameters and Standard Deviations	Analysis Time (ms)						
	170	175	180	185	190	195	200
x	.178	.163	.157	.170	.202	.215	.222
Δx	.054	.048	.046	.053	.049	.049	.056
y	.278	.224	.225	.241	.228	.198	.152
Δy	.056	.045	.094	.050	.043	.039	.040
z	.440	.451	.444	.434	.465	.436	.418
Δz	.004	.007	.006	.002	.004	.004	.007
P_x	.303	.301	.323	.346	.304	.302	.271
ΔP_x	.037	.036	.039	.050	.095	.044	.096
P_y	.220	.382	.971	.540	.537	.612	.641
ΔP_y	.032	.035	.041	.053	.047	.049	.053
P_z	.065	.015	-.006	-.004	.009	.032	.058
ΔP_z	.037	.037	.041	.053	.048	.048	.052
P	.380	.487	1.023	.641	.617	.683	.698

Table 5-5. (c) Subject KW, flash to left eye.

Parameters and Standard Deviations	Analysis Time (ms)		
	165	170	175
x	.186	.005	-.157
Δx	.092	.089	.023
y	-.035	.041	.049
Δy	.048	.095	.146
z	.329	.420	.304
Δz	.032	.093	.178
P_x	.178	.317	.421
ΔP_x	.051	.075	.120
P_y	.431	.353	.230
ΔP_y	.051	.070	.097
P_z	.221	.153	-.030
ΔP_z	.057	.080	.118
P	.516	.499	.481

Table 5-5. (d) Subject KW, flash to both eyes.

Parameters and Standard Deviations	Analysis Time (ms)		
	165	170	175
x	.063	.202	.089
Δx	.047	.092	.096
y	.000	.017	.078
Δy	.009	.055	.088
z	.053	.341	.409
Δz	.024	.021	.059
P_x	.115	.258	.326
ΔP_x	.048	.056	.063
P_y	.506	.466	.316
ΔP_y	.049	.056	.058
P_z	.286	.193	.084
ΔP_z	.052	.062	.067
P	.593	.567	.462

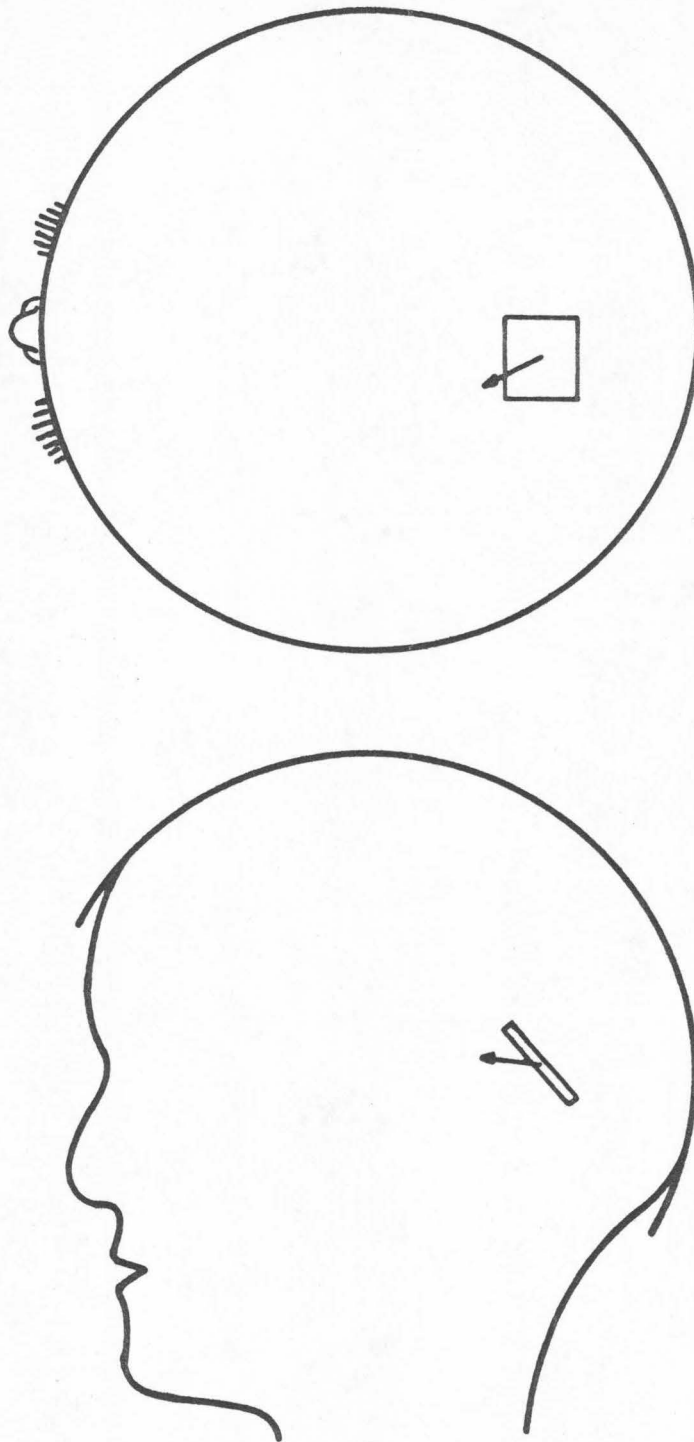


Figure 5-2. Equivalent dipole solution for DALO data, flash to right eye, at 75 ms after stimulus, homogeneous model. Dipole location enclosed by 95% confidence region.

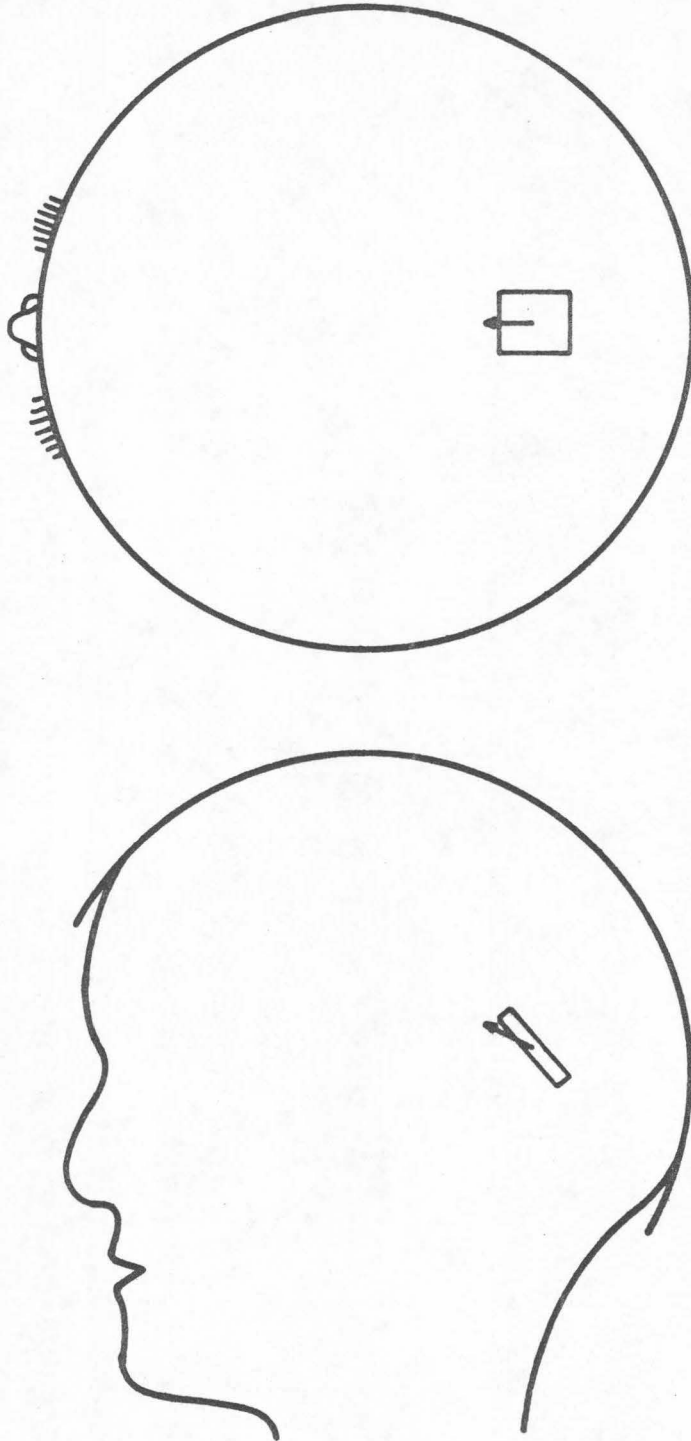


Figure 5-3. Equivalent dipole for DALO data, flash to left eye, at 75 ms after stimulus, homogeneous model.

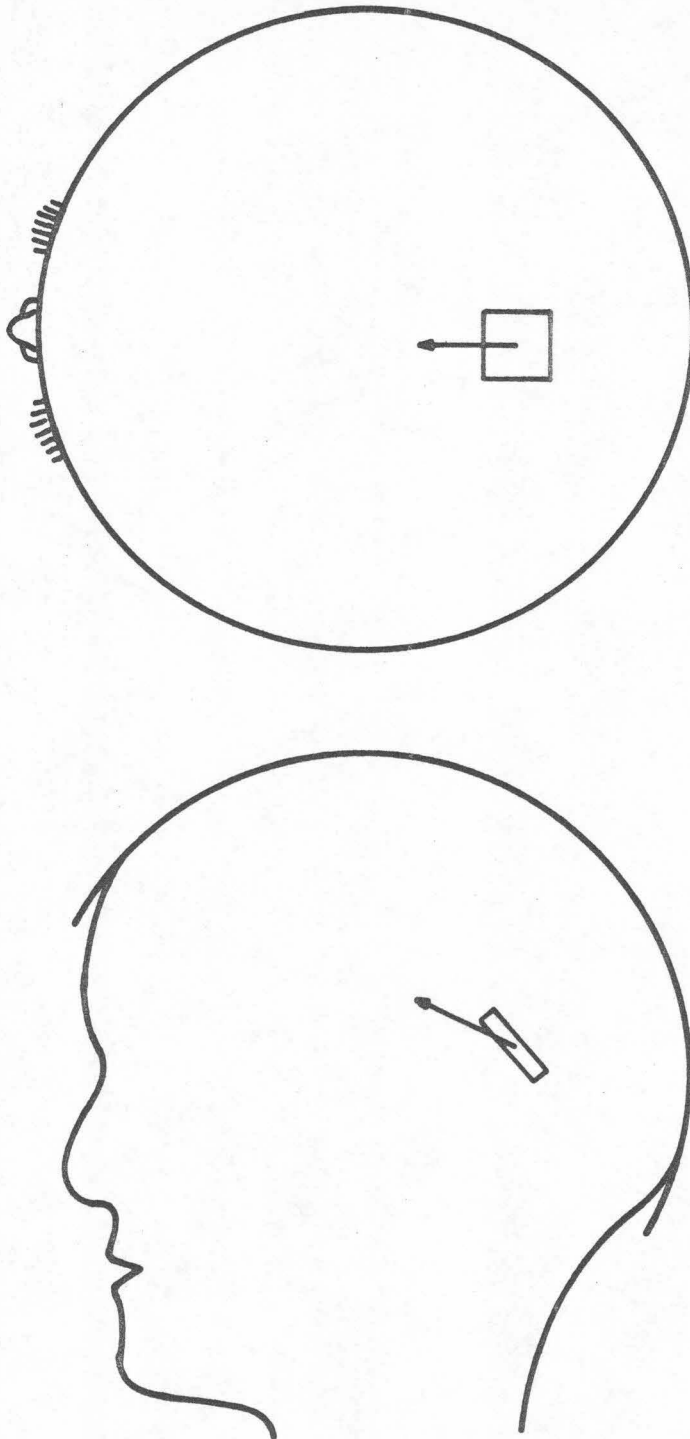


Figure 5-4. Equivalent dipole for DALO data, flash to both eyes, at 75 ms after stimulus, homogeneous model.

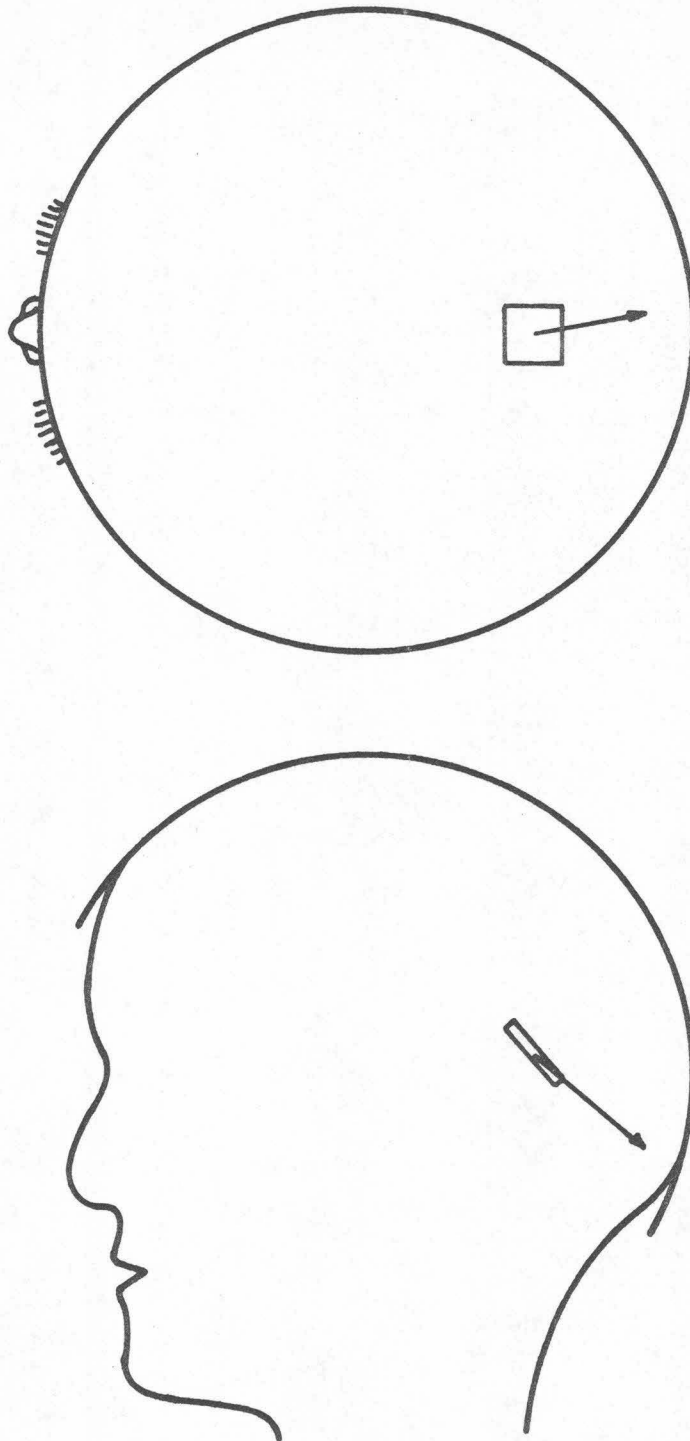


Figure 5-5. Equivalent dipole for DALO data, flash to right eye, at 115 ms after stimulus, homogeneous model.

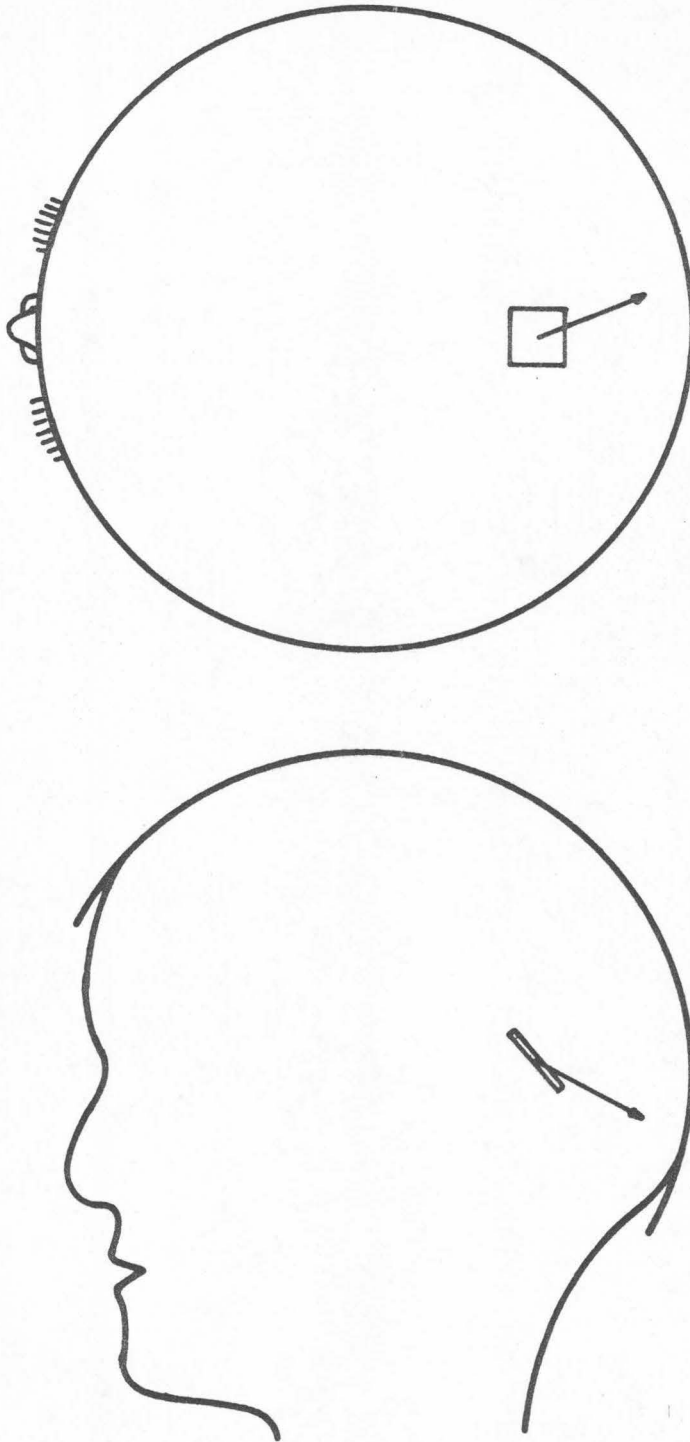


Figure 5-6. Equivalent dipole for DALO data, flash to left eye, at 115 ms after stimulus, homogeneous model.

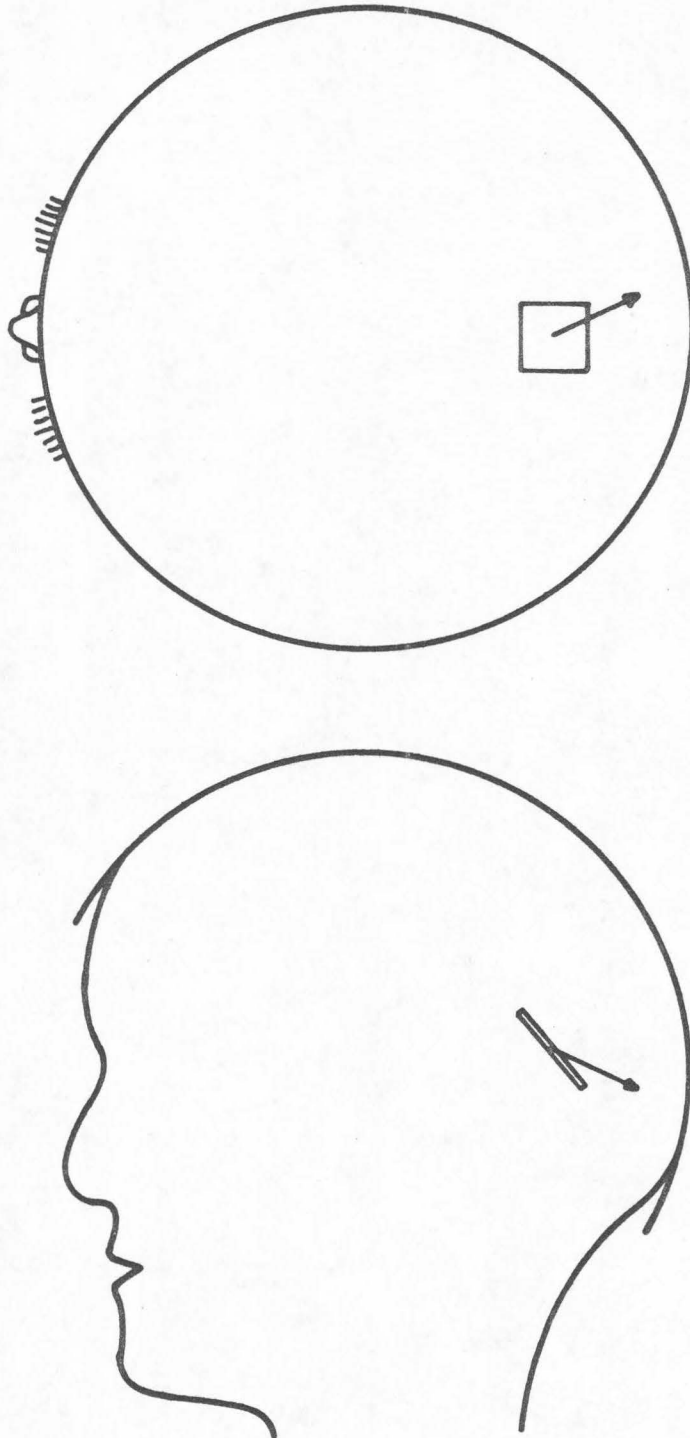


Figure 5-7. Equivalent dipole for DALO data, flash to both eyes, at 115 ms after stimulus, homogeneous model.

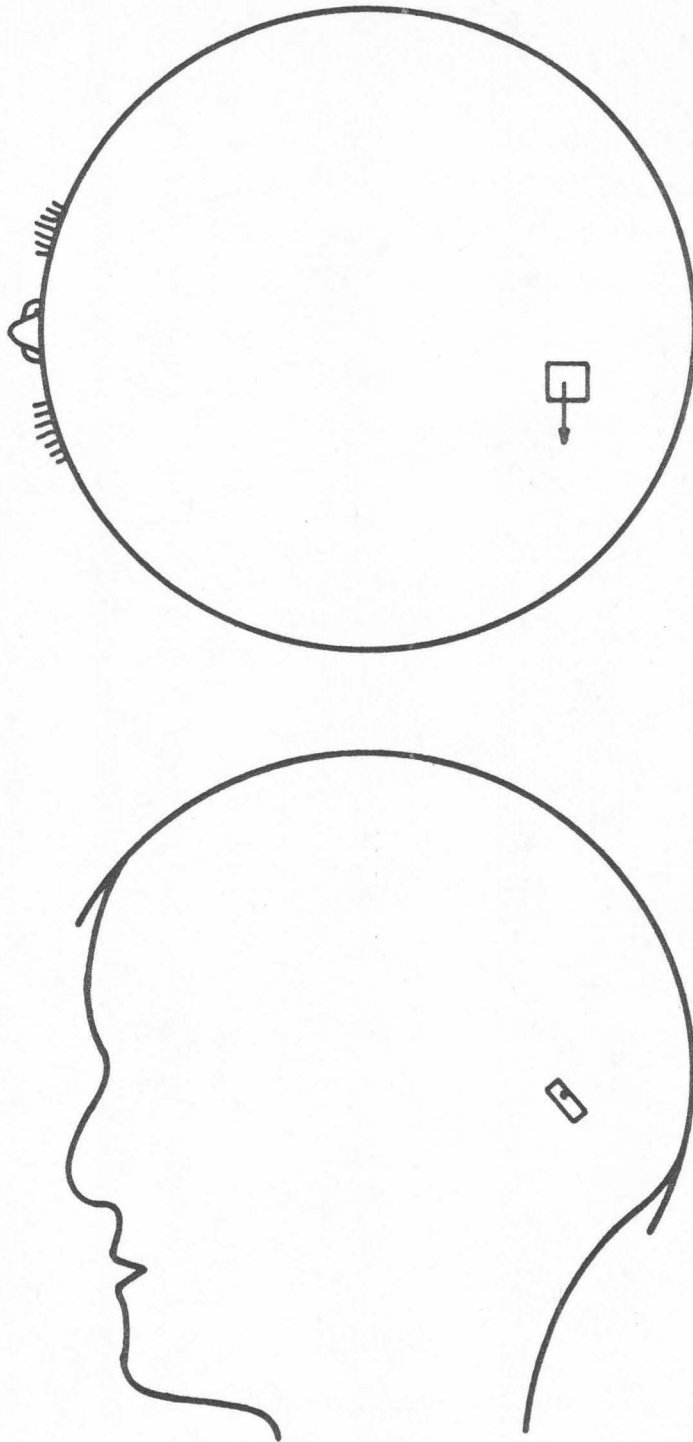


Figure 5-8. Equivalent dipole for DALO data, flash to right eye, at 185 ms after stimulus, homogeneous model.

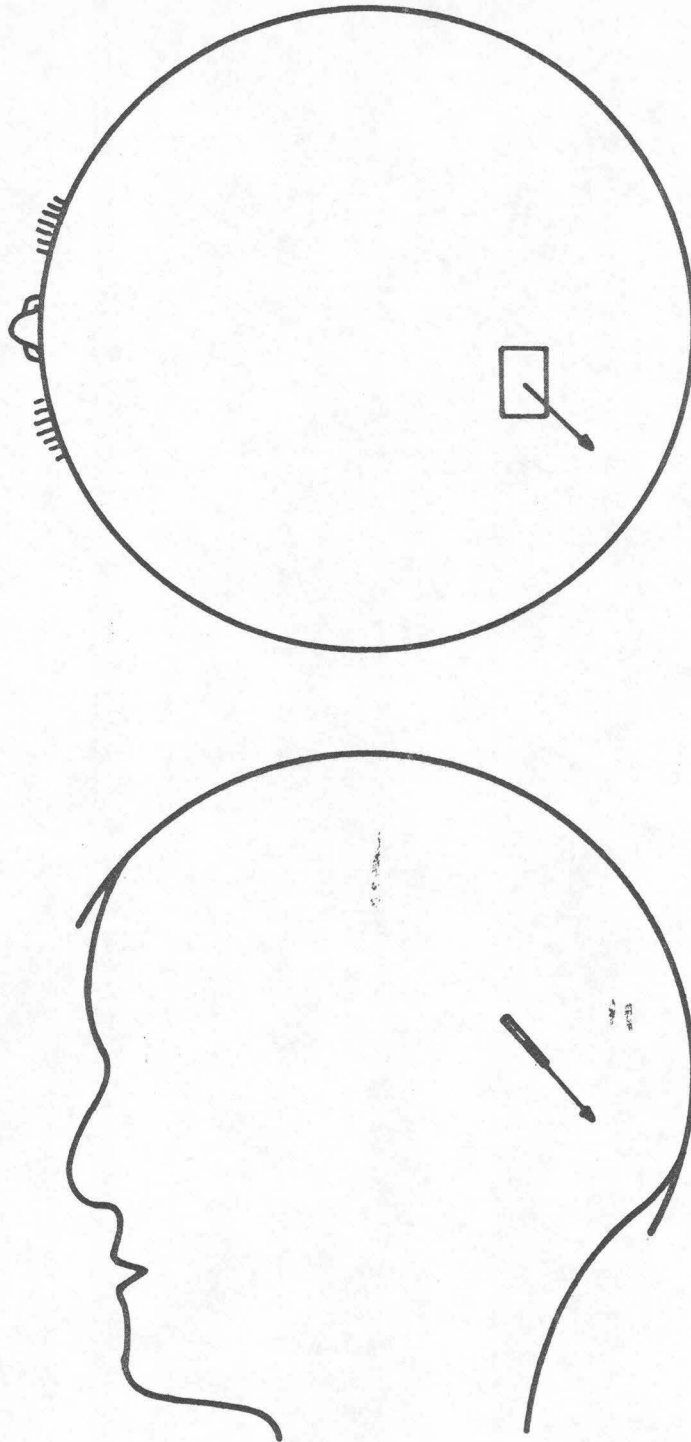


Figure 5-9. Equivalent dipole for DALO data, flash to both eyes, at 185 ms after stimulus, homogeneous model.

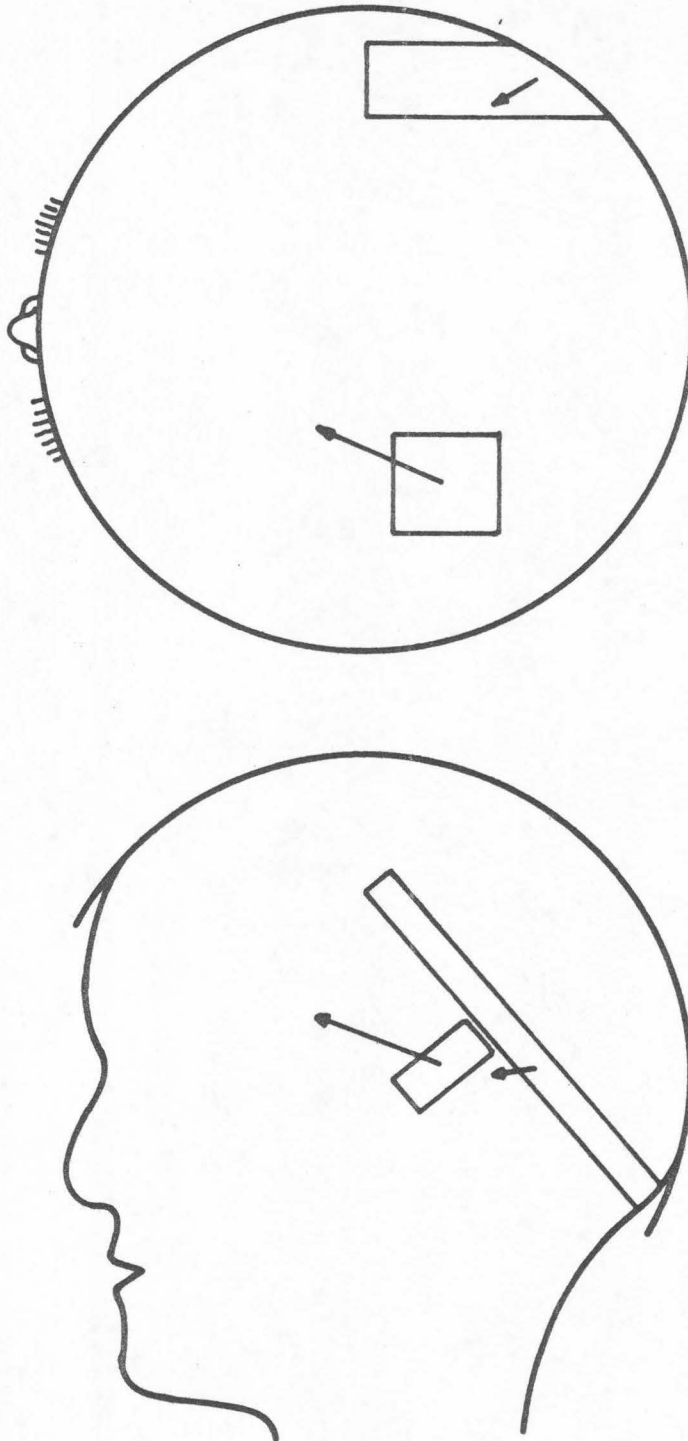


Figure 5-10. Equivalent dipoles for KW data, flash to right eye, at 115 ms after stimulus, homogeneous model.

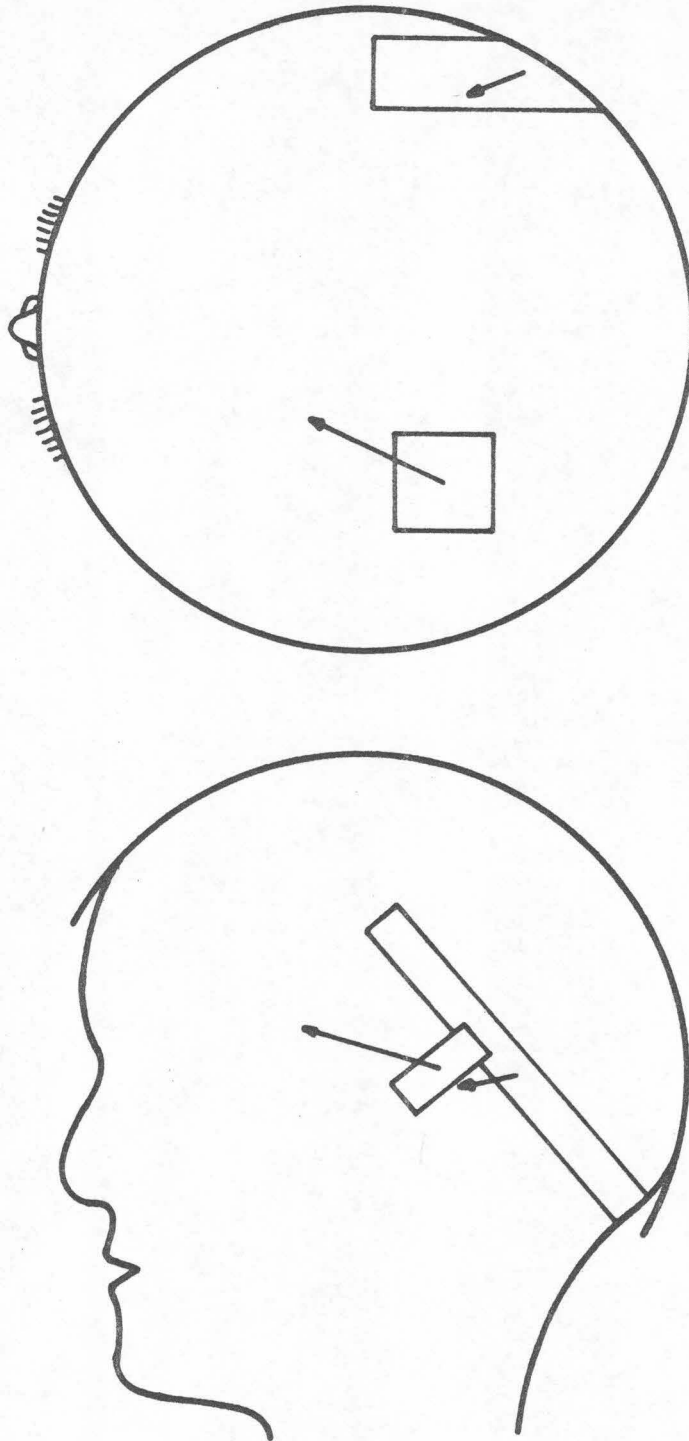


Figure 5-11. Equivalent dipoles for KW data, flash to left eye, at 115 ms after stimulus, homogeneous model.

- 193 -

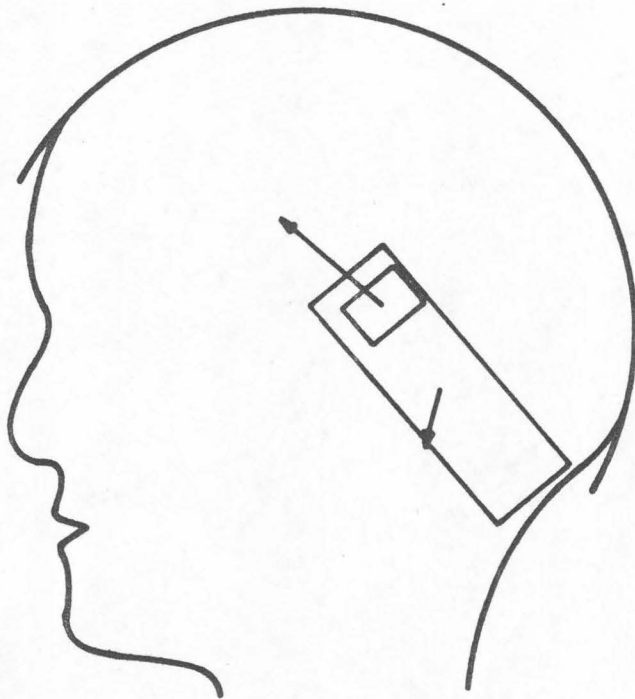
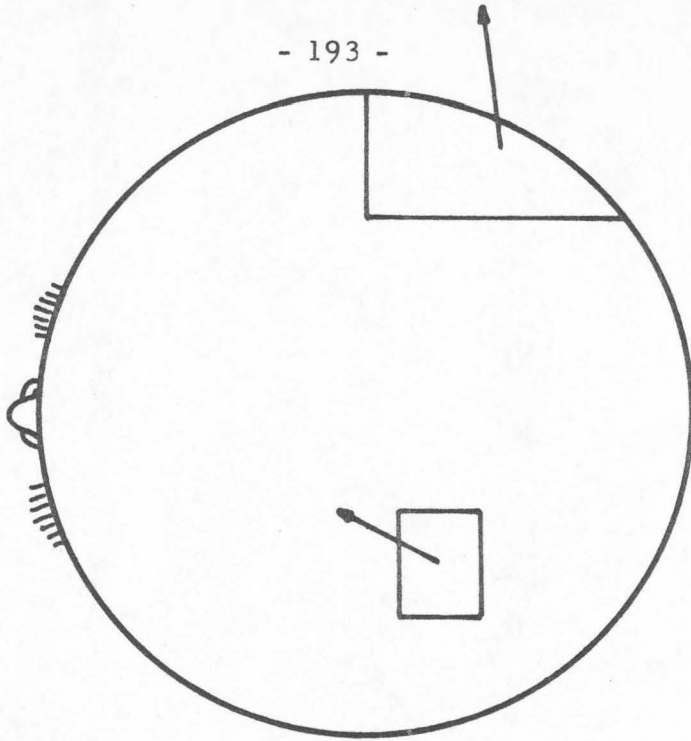


Figure 5-12. Equivalent dipoles for KW data, flash to both eyes, at 115 ms after stimulus, homogeneous model.

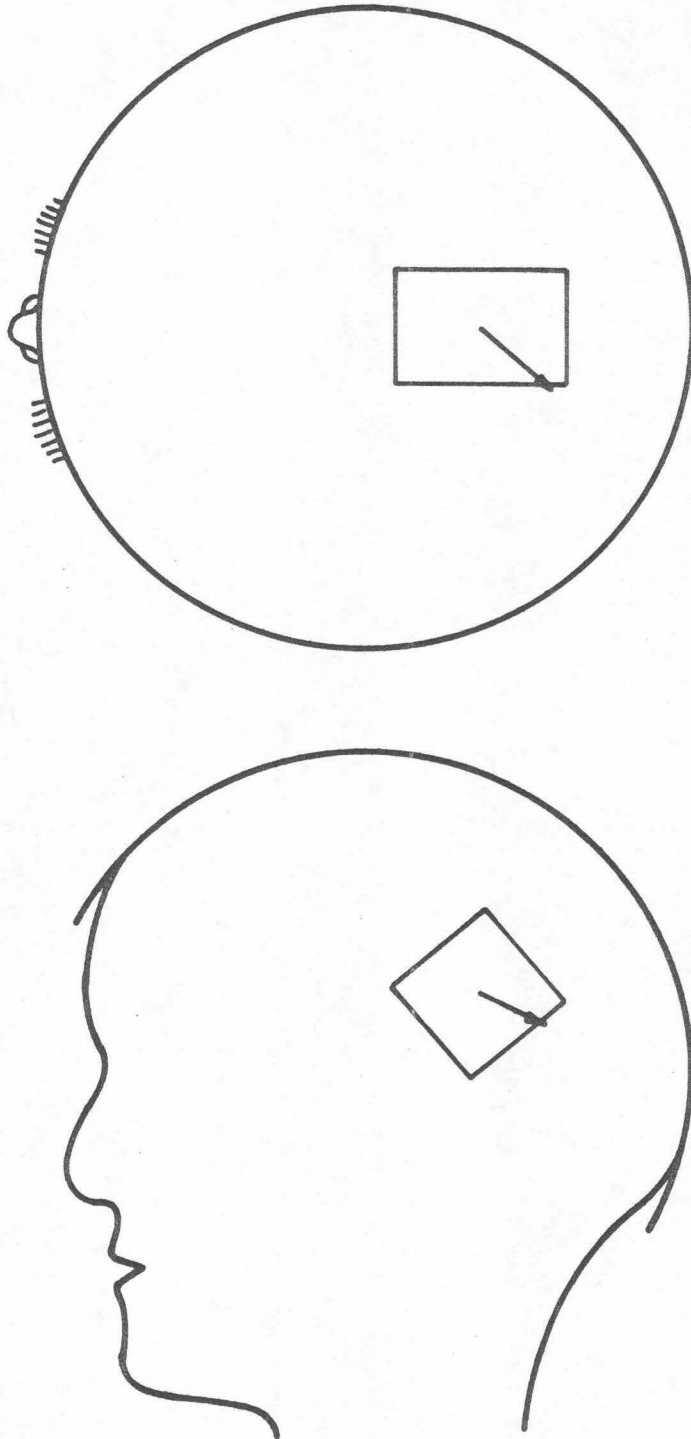


Figure 5-13. Equivalent dipole for KW data, flash to left eye, at 170 ms after stimulus, homogeneous model.

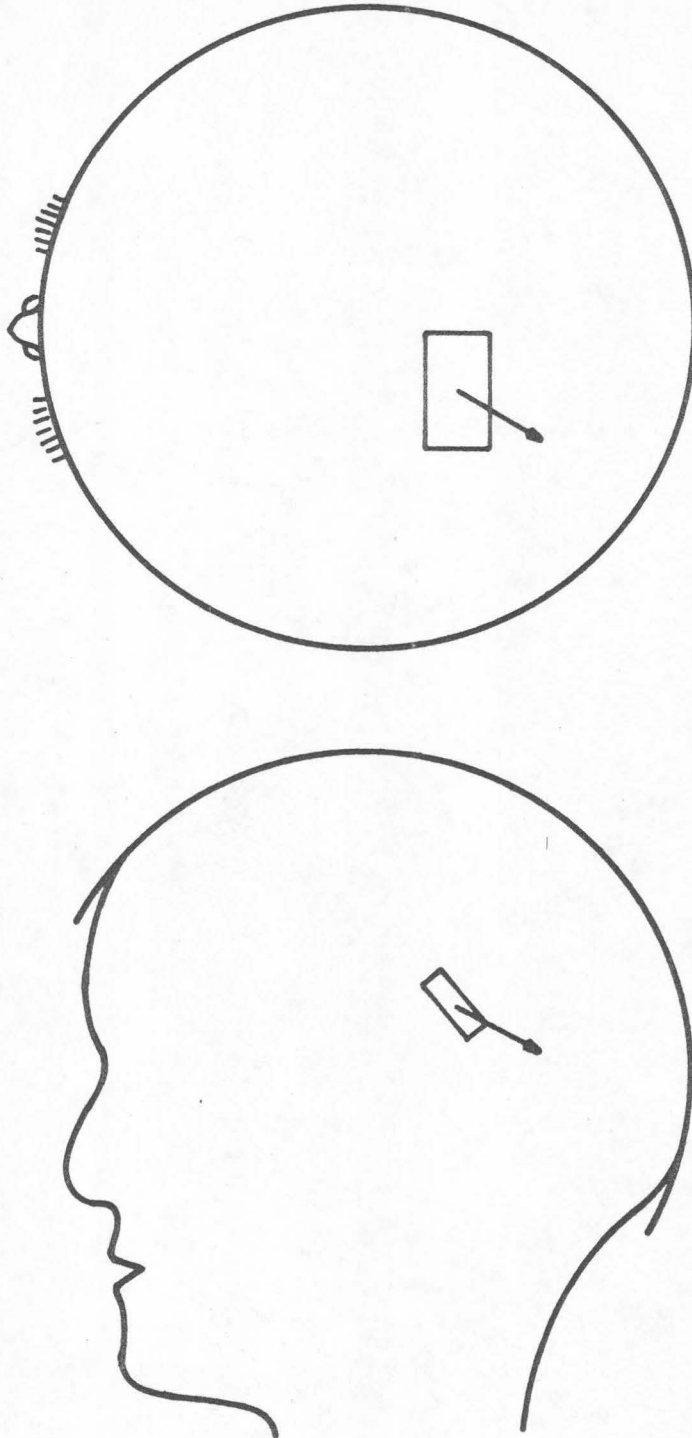


Figure 5-14. Equivalent dipole for KW data, flash to both eyes, at 170 ms after stimulus, homogeneous model.

the equivalent dipole is interpreted as having any absolute significance. Thus for the moment the dipole magnitudes show only when sources are "stronger" or "weaker"; it is not possible to determine the inverse mapping of the three components of dipole strength into any meaningful description of the individual neural dipole generators.

The results of the analysis, from a technical point of view are very promising. First we see that it is possible to find equivalent dipoles for the evoked response data, with reasonable resolution. Particularly with the DALO data, the standard deviations of the parameter estimates afford localization of the sources within rather small volumes of the cortex. For the case of the KW data, the analyses in the interval 90ms to 130ms produced solutions with larger standard errors than were obtained for the DALO data over the same interval, but in the KW case the analysis was intended to produce two sources, and hence twice as many parameter estimates as for the single source in the DALO data. Even though the two sources appear to be quite easily separated by eye in the equipotential maps, the dipole analysis procedure must deal with the interaction of the two sources, and this interaction may cause the parameter estimates to be somewhat "blurred."

The other principal result, and one which will be discussed more completely in the context of its neurophysiological

implications, in the final chapter, is that the dipole locations are relatively constant within each of the three major intervals. This result was not intuitively expected from considerations of the equipotential maps, since there are slow changes in the appearance of the maps. Typically a dipole pattern slowly builds to some peak over the first half of the selected interval, and then again slowly subsides during the second half. One possible explanation is that a source of constant strength slowly moves toward the surface during the first half of the response and then retreats during the latter half. It would appear, however, that the evoked response data analyzed here suggests rather that a source fixed in location grows alternately stronger and weaker during some given interval, thus explaining the waxing and waning of the equipotential lines. This result is evident from the tabulated dipole parameters and the number of pictorial presentations necessary to show the equivalent dipoles was thus much decreased.

It was not possible to produce inverse determinations for the KW data over the interval 60ms to 90ms. The equipotential maps at this time give weak indications of two sources at roughly the same locations as the sources in the interval 90ms to 130ms. The surface potential distribution during this time for this subject was, however, too tranquil to produce reliable inverse solutions.

Even in the absence of inverse determinations at this time, however, there is an interesting observation to be made. Note

that in both subjects the equipotential maps during the earliest interval and during the second interval are quite similar. The difference between the two periods is that a polarity change occurs from one to the other. In the DALO data the dipole calculations produced sources in the second interval which were in the same locations as in the first, but showing the difference in polarity by a reversal of the orientation of the dipole. Hence the lack of inverse determinations in the early stages of the KW responses is not such a loss, since we can infer that if the fields had permitted equivalent sources to be found, they would have been in the same locations as those between 100ms and 135ms.

4. Analysis of the Evoked Responses with the Shell Model.

The evoked response data were also analyzed using the shell model, though less exhaustively than with the homogeneous model. In Chapter IV we saw that for any given surface distribution the shell model produced inverse dipole solutions which were both more eccentric and stronger than equivalent sources in the homogeneous case. It was also evident, however, that there was not a great deal of difference between the two inverse solutions. The homogeneous model could most quickly and inexpensively be used to study the responses over the full spans of the three intervals selected, and when this was done we saw that there was not an appreciable change in the inverse solutions within any one interval and any one set of data. Hence it seemed unnecessary to repeat all

of the analyses with the shell model. The application of the shell analysis would serve to confirm the supposed slight differences between the models when analyzing the experimental data at sample times which previously yield "typical" solutions in the homogeneous analysis.

The results of the analysis with the more complicated model are shown in Tables 5-6 through 5-8, and the illustrations of these solutions are given in Figures 5-15 through 5-24. When these results are compared with the corresponding analyses of the homogeneous model, it becomes evident that the prediction of Chapter IV has been borne out --- the shell solutions are generally slightly more eccentric and stronger than the homogeneous determinations.

One other feature is also clear. The standard deviations in the shell model are usually larger than in the homogeneous case. This is not surprising, since the thrust of the shell model was to more realistically portray the shielding effects of the intervening layers between brain and scalp. The inclusion of these effects is thus a mixed blessing, for the increased insensitivity of the scalp potentials to changes in source dipoles results in less accurate determinations of the dipole parameters. Further discussion of this point will be found in Chapter VI where the two models are critically compared.

Table 5-6. Parameter Estimates and Standard Deviations for DALO data at 75ms in Shell Model.

Parameters and Standard Deviations	Flash Right	Flash Left	Flash Both
x	.147	.059	.123
Δx	.214	.189	.142
y	.345	.365	.295
Δy	.062	.066	.057
z	.560	.562	.521
Δz	.185	.068	.075
P_x	.163	.025	.029
ΔP_x	.062	.035	.057
P_y	-.267	-.282	-.577
ΔP_y	.005	.015	.025
P_z	-.231	-.146	-.295
ΔP_z	.051	.058	.092
P	.389	.319	.649

Table 5-7. Parameter Estimates and Standard Deviations for DALO and KW data at 115 ms, in Shell Model.

Parameters and Standard Deviations	DALO Flash Right	DALO Flash Left	DALO Flash Both	KW Flash Left Dipole One	KW Flash Left Dipole Two
x	.071	.061	.040	.530	-.401
Δx	.138	.212	.274	.174	.309
y	.344	.413	.414	.260	.366
Δy	.053	.002	.048	.124	.348
z	.576	.578	.650	.352	.525
Δz	.062	.102	.132	.048	.107
P_x	-.169	-.236	-.247	-.504	.133
ΔP_x	.052	.035	.024	.242	.171
P_y	.801	.610	.479	-.562	-.175
ΔP_y	.112	.117	.120	.190	.048
P_z	.156	.263	.229	-.380	-.178
ΔP_z	.064	.043	.035	.005	.184
P	.833	.705	.586	.845	.283

Table 5-8. Parameter Estimates and Standard Deviations for DALO data at 185ms and KW data at 170ms, in Shell Model.

Parameters and Standard Deviations	DALO Flash Both	KW Flash Left	K Flash Both
x	.226	-.010	.200
Δx	.012	.056	.054
y	.297	.071	.029
Δy	.134	.318	.185
z	.598	.540	.484
Δz	.127	.161	.077
P_x	.370	.346	.320
ΔP_x	.008	.001	.012
P_y	.594	.393	.492
ΔP_y	.080	.069	.059
P_z	.019	.178	.220
ΔP_z	.064	.132	.103
P	.700	.553	.627

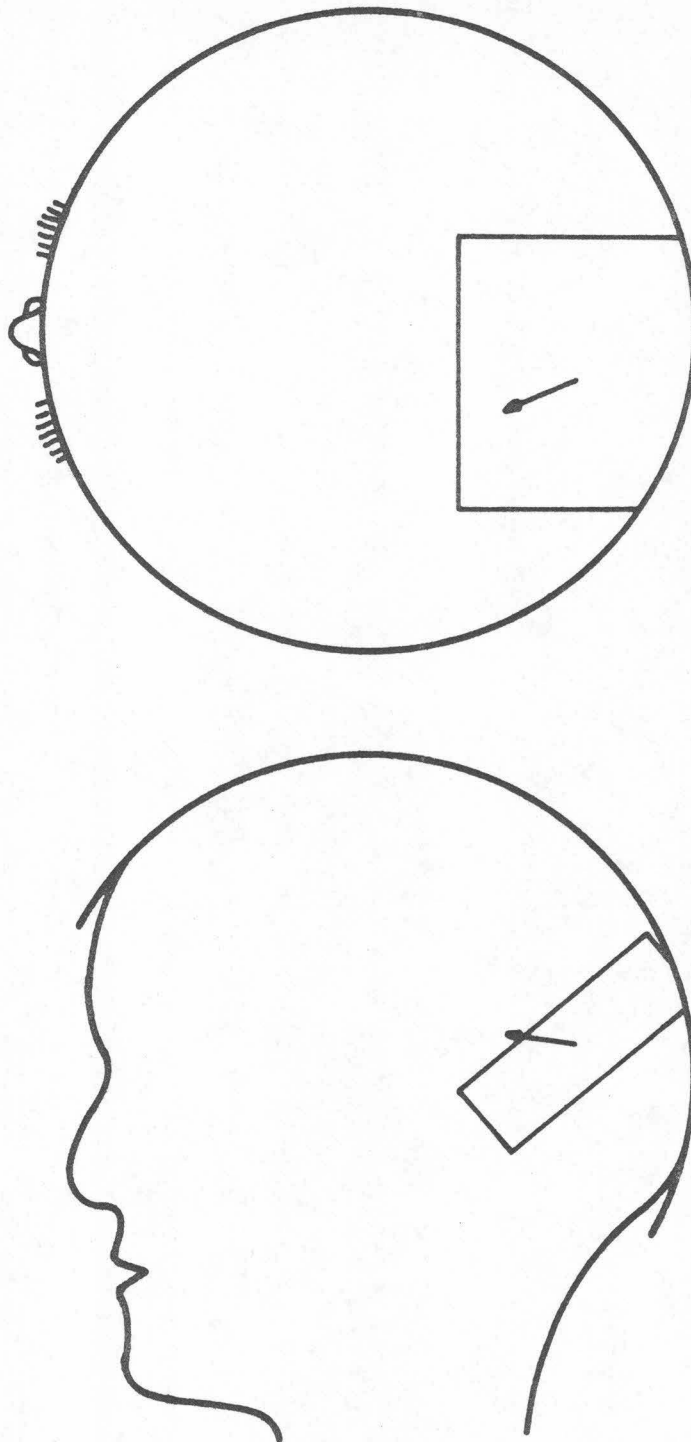


Figure 5-15. Equivalent dipole for DALO data, flash to right eye, at 75 ms after stimulus, shell model.

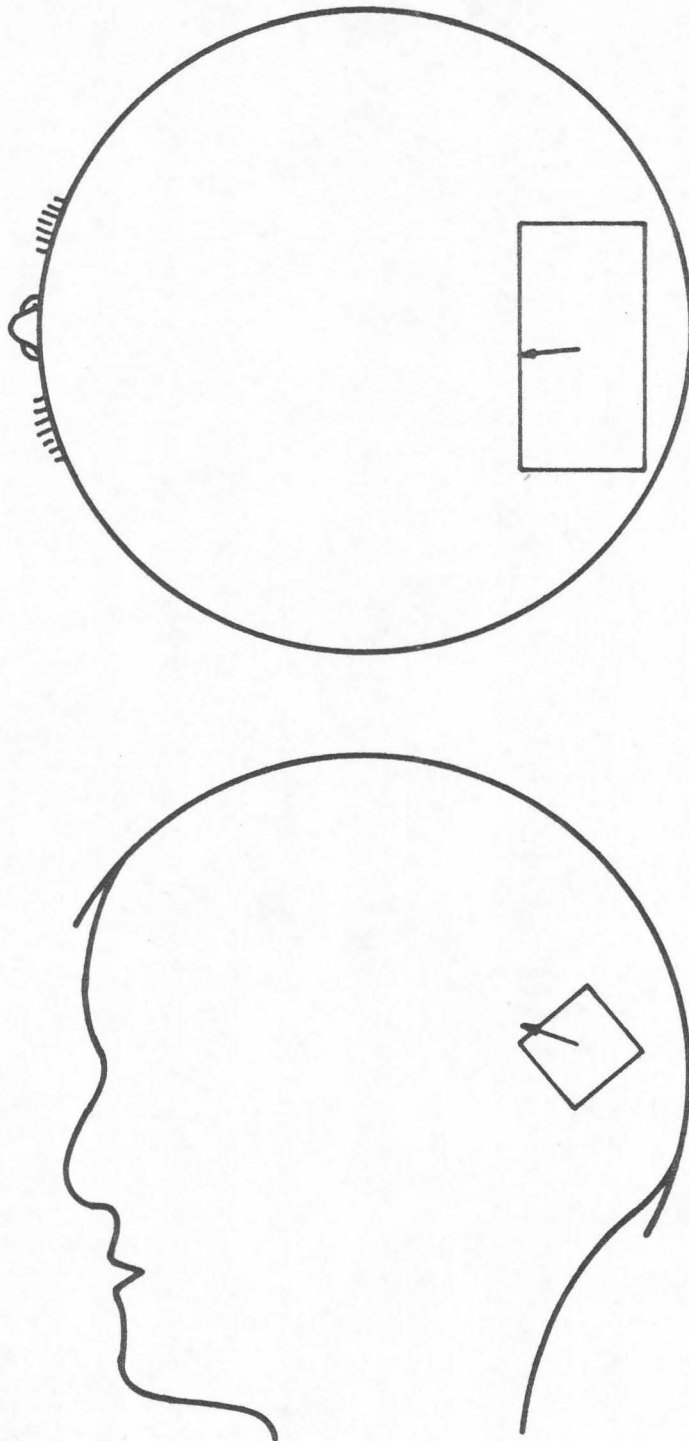


Figure 5-16. Equivalent dipole for DALO data, flash to left eye, at 75 ms after stimulus, shell model.

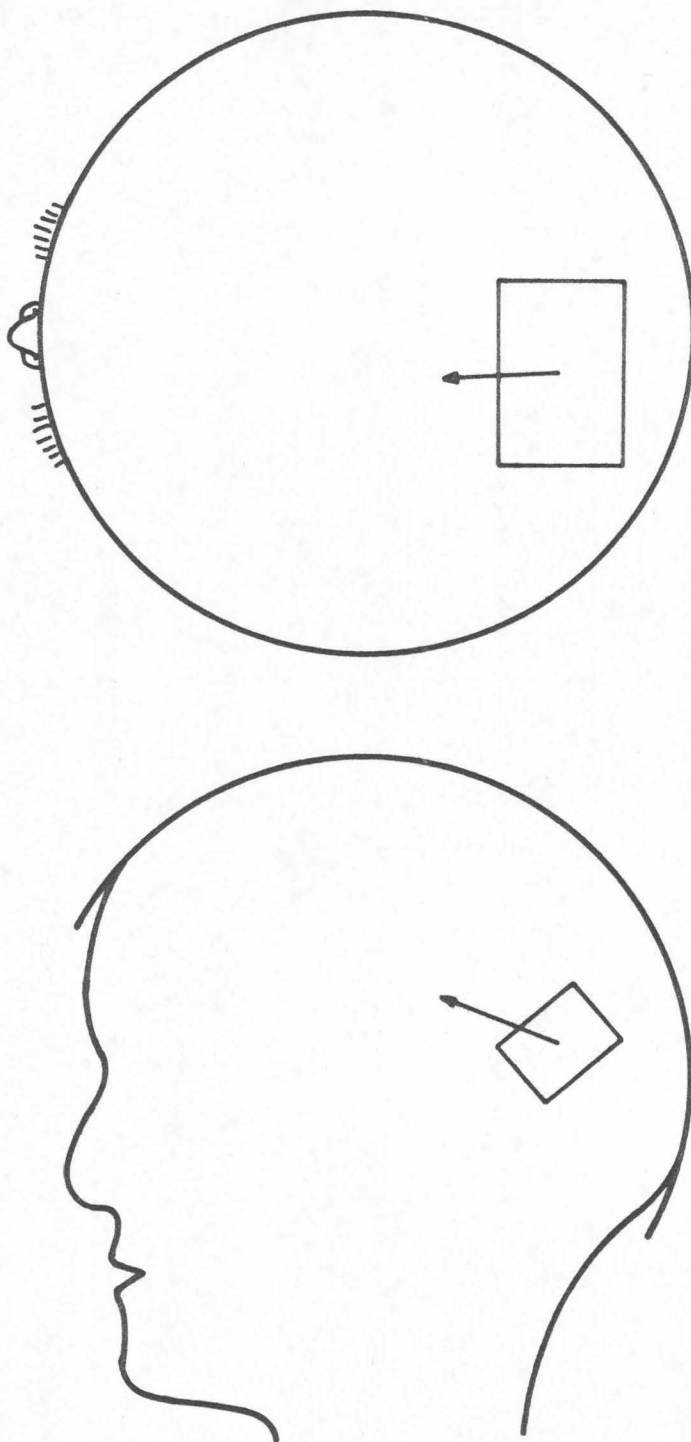


Figure 5-17. Equivalent dipole for DALO data, flash to both eyes, at 75 ms after stimulus shell model.

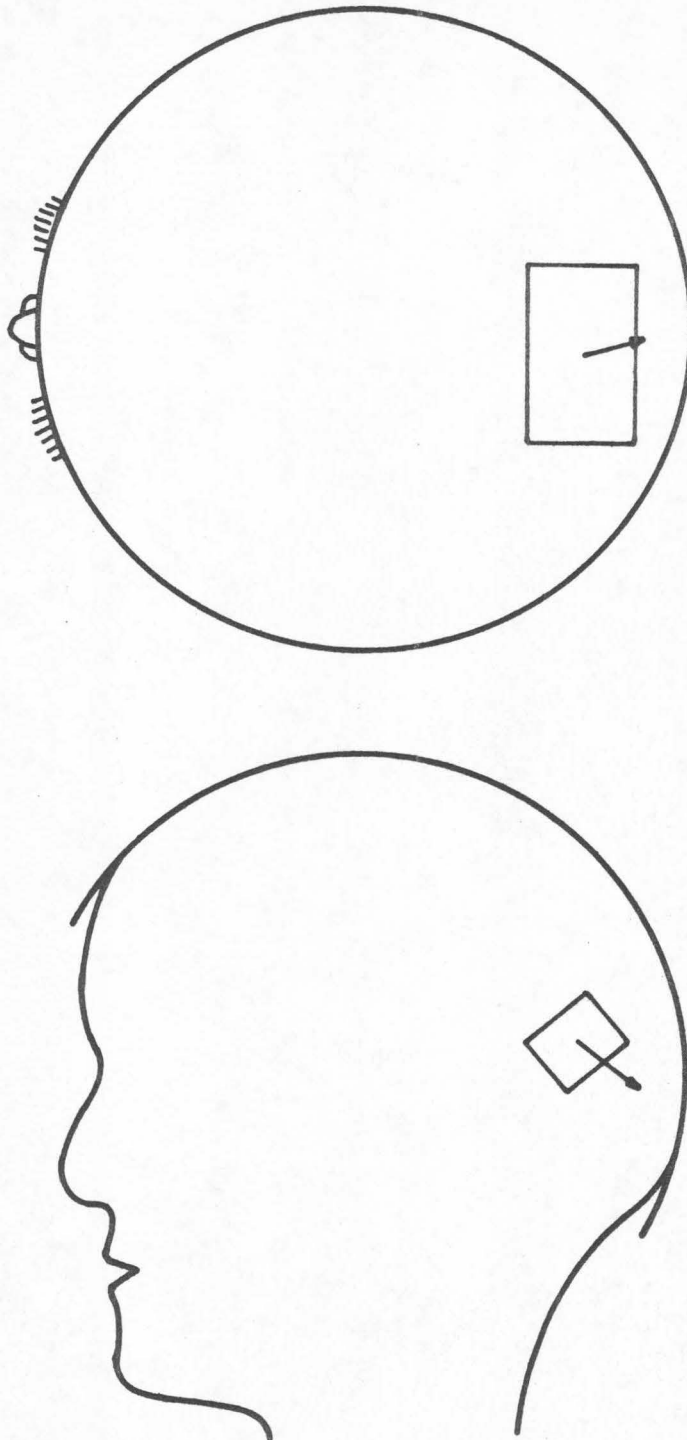


Figure 5-18. Equivalent dipole for DALO data, flash to right eye, at 115 ms after stimulus, shell model. Dipole magnitude drawn 1/2 scale used in previous drawings.

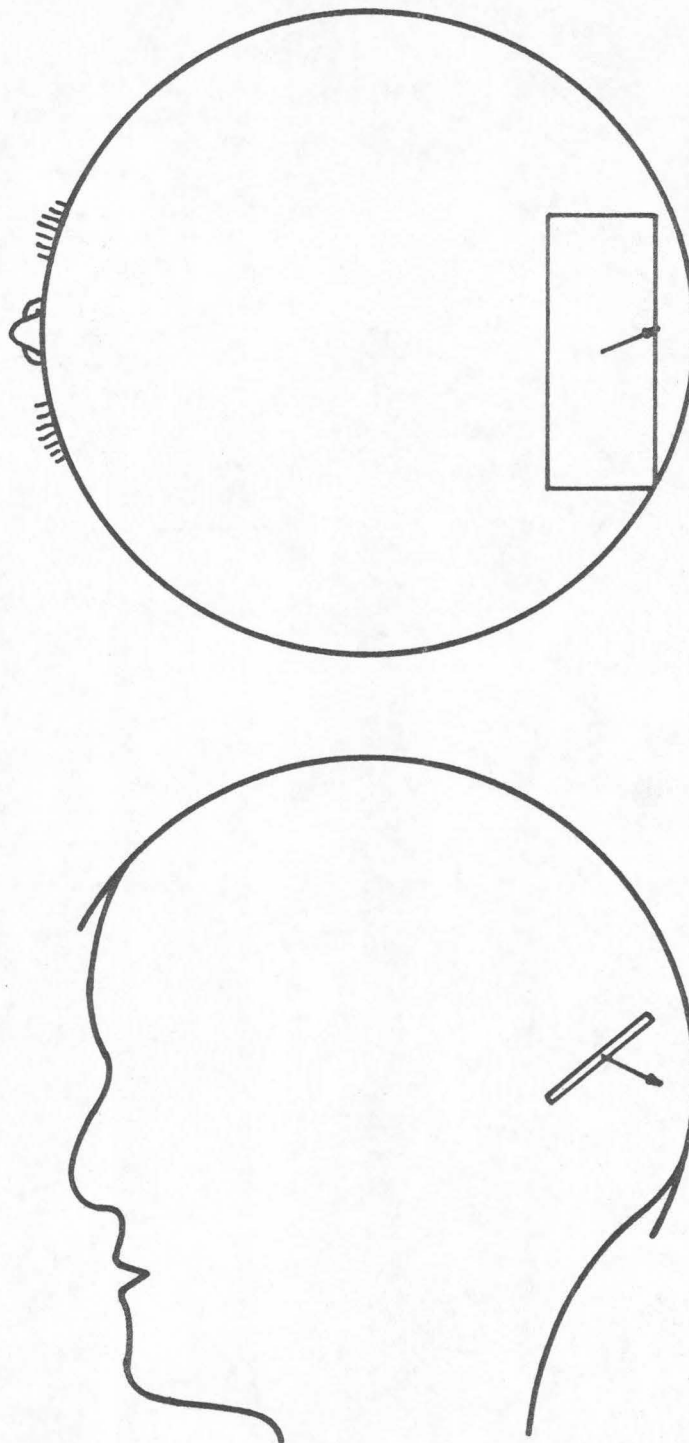


Figure 5-19. Equivalent dipole for DALO data, flash to left eye, at 115 ms after stimulus, shell model. Dipole magnitude drawn 1/2 scale.

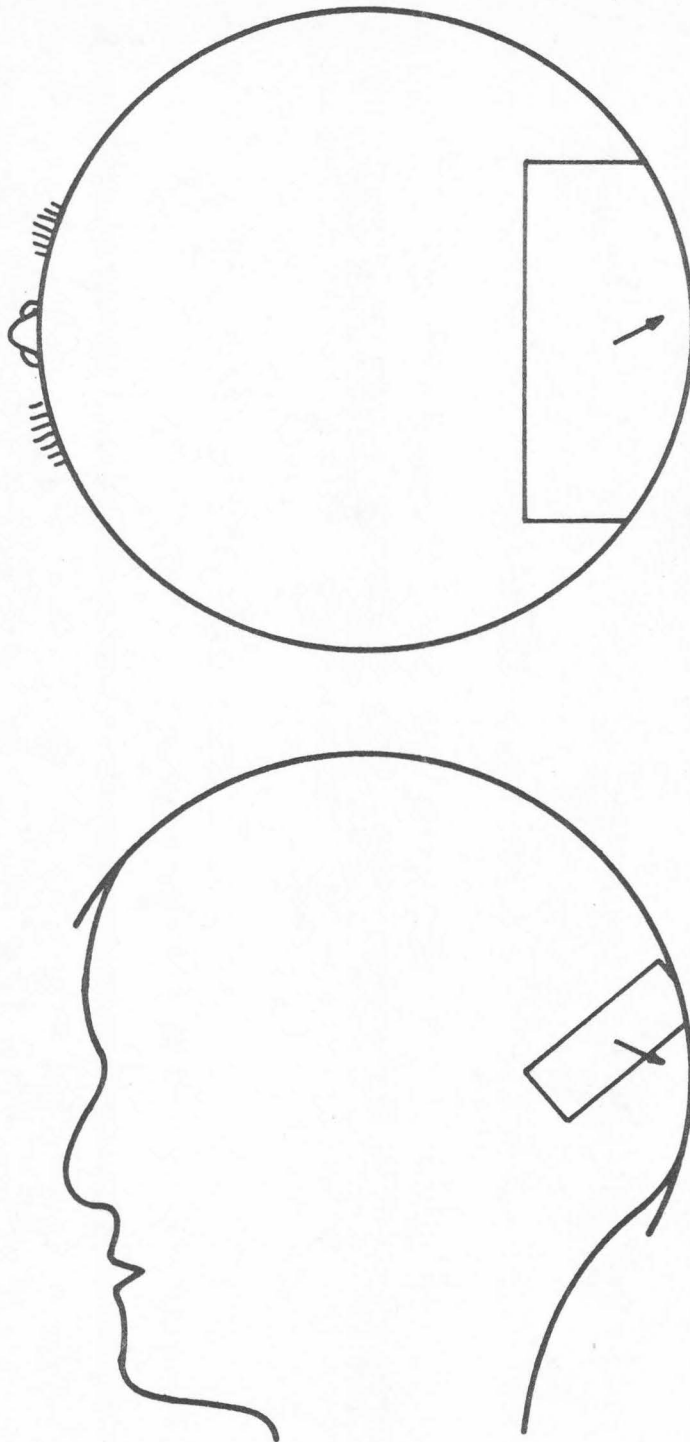


Figure 5-20. Equivalent dipole for DALO data, flash to both eyes, at 115 ms after stimulus, shell model. Dipole magnitude drawn 1/2 scale.

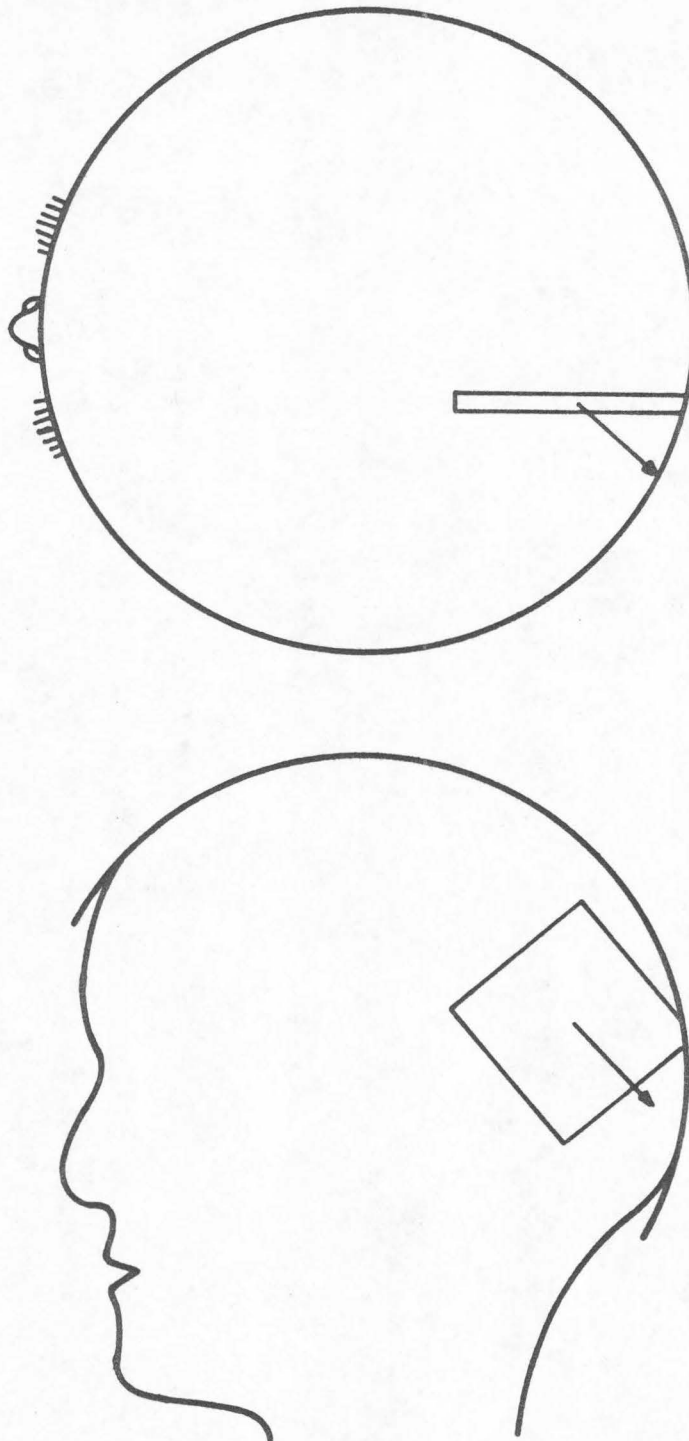


Figure 5-21. Equivalent dipole for DALO data, flash to both eyes, at 185 ms after stimulus, shell model.

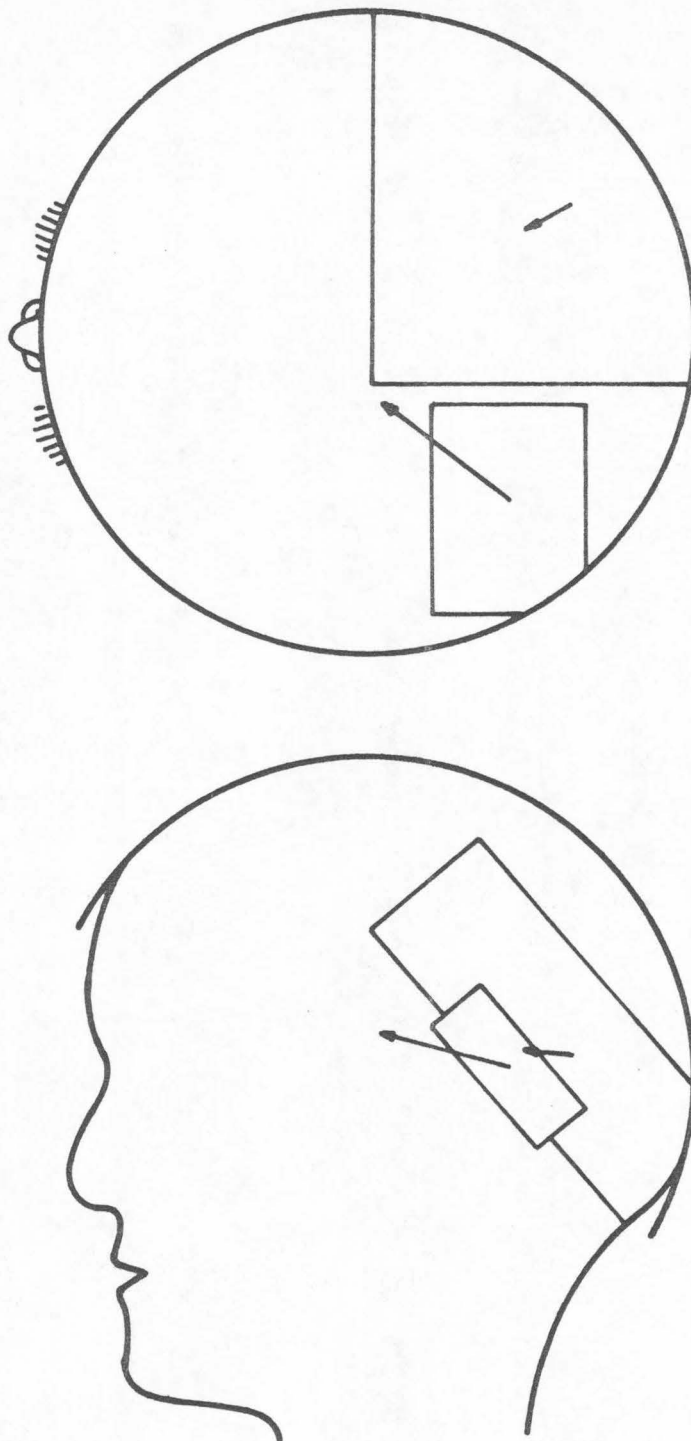


Figure 5-22. Equivalent dipoles for KW data, flash to left eye, at 115 ms after stimulus, shell model.

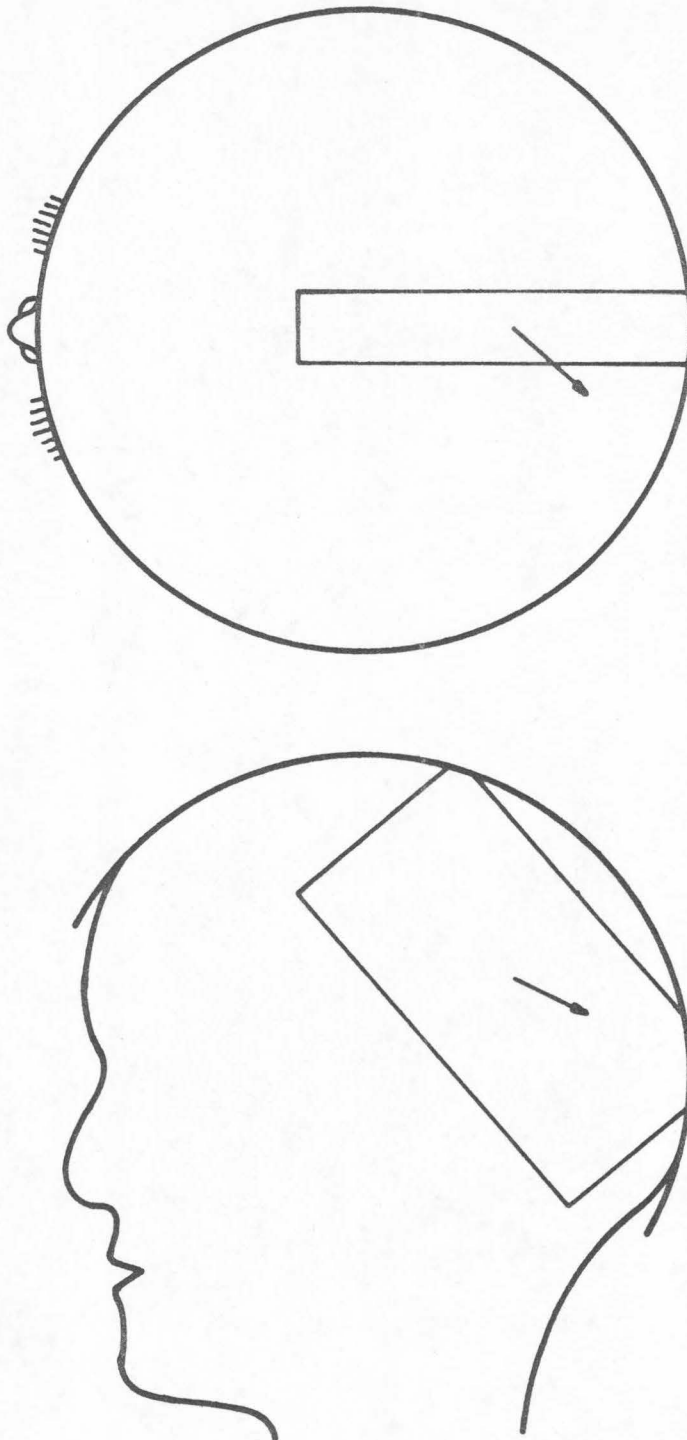


Figure 5-23. Equivalent dipole for KW data, flash to left eye, at 170 ms after stimulus, shell model.

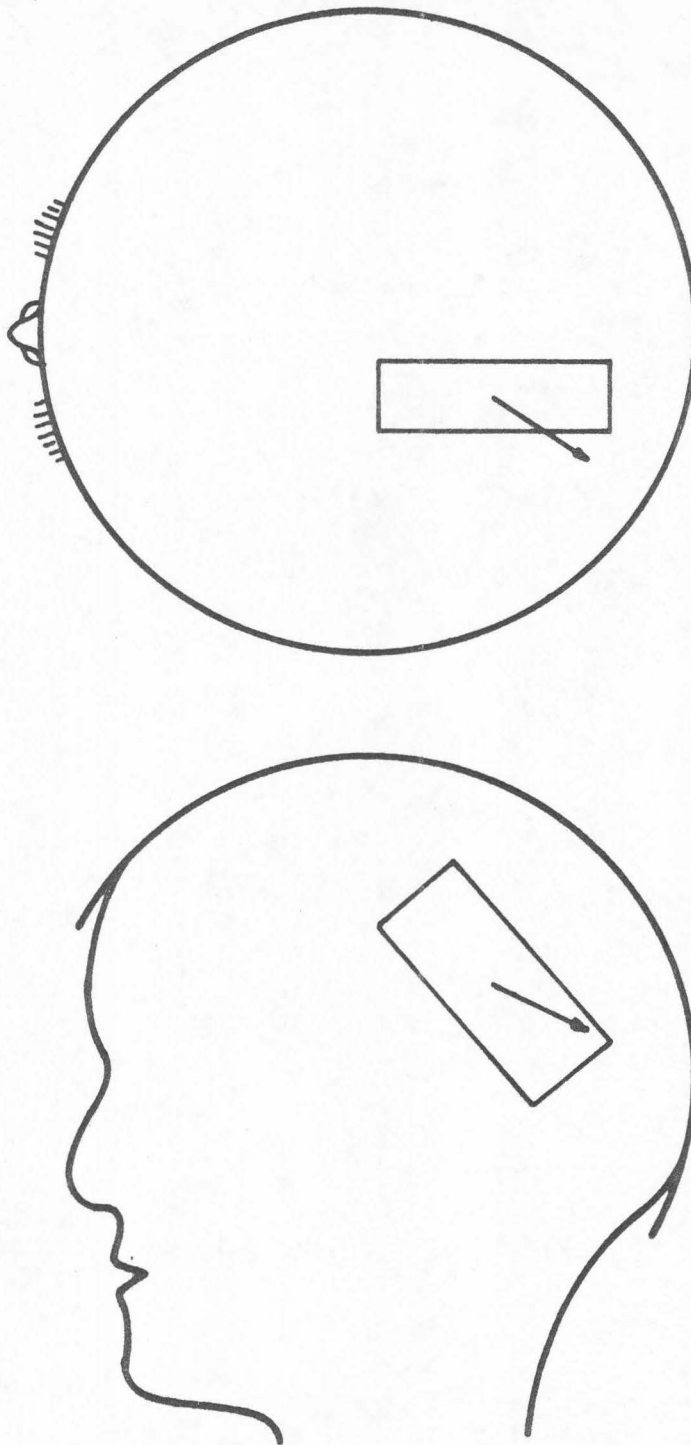


Figure 5-24. Equivalent dipole for KW data, flash to both eyes, at 170 ms after stimulus, shell model.

5. Some Technical Aspects of the Analysis of the Evoked Response Data.

In attempting to analyze the evoked response data in terms of equivalent dipole sources one of the criteria by which the technique is assessed is the stability of the solutions. One may well wonder if a deep but strong source could just as easily fit a given surface distribution as a more eccentric but weaker one. This situation was never successfully provoked with the evoked response analysis. For many of the analyses I attempted to force a different solution by supplying initial guesses which were quite different to the given solution but possibly equivalent, or perhaps guesses which were simply quite different from the solution. These efforts failed to produce any different equivalent sources --- the solutions always returned to whatever point in the parameter space was first produced, with two exceptions. The first exception to the stability of the results involved attempting to guess two dipole sources when only one was suggested. For example, in both the KW and DALO data there appears to be a single source on the left side around 170ms, and the analyses produced estimates of that source. When I repeated the analysis with guesses for two sources (such as the computed one and its mirror image, or one similar to the computed one and a weak one on the other side, etc.), the program failed to return the original result. In other words it was not able to depress the second dipole to one having zero effect on the surface while returning the first one as essentially the solution initially

achieved. It would thus seem that the subjective decision regarding the number of dipole sources is a necessary process preceding any computer analysis.

It is not perhaps too surprising that the analysis would stumble in this case, since the data are probably not capable of estimating twelve parameters when the field is essentially due to a single source, characterized by six parameters. Remember that the principal components analysis suggested that on the average the dimension of the data was close to that which could be filled by a single dipole source. The dipole analysis program has no rules for optimizing the interaction of the two sources, and thus has no "intelligent" way of deciding that if it were to eliminate one source altogether the fit for the potentials would be a better one.

The second exception to the solution stability involves the KW data when apparently two sources were present. In this case the solution is slightly more sensitive to the accuracy of the initial guesses than when a single source seems warranted. If the analyses were repeated with guesses which were in error by more than approximately ± 50% the program usually failed to produce plausible results (the solutions would fall outside of the head, on the underside of the head, near the center of the head with zero dipole moments, etc.). Here again the need to initially view the equipotential maps is shown, since an experienced observer can usually guess the solutions within an average error of 20 to 30 percent.

This same caution is present in the shell analysis, for the reasons already mentioned in section four of this chapter. Since the model is more insensitive to changes in the dipole parameters, the analyses are more sensitive to errors in the initial guesses than their homogeneous counterparts. There was never an example when the shell model failed to produce a solution because of grossly incorrect initial guesses, simply because I already had the homogeneous solutions. Since the two results were expected to be similar it was simple to supply initial parameters for the shell analysis by using the corresponding homogeneous results.

In a sense the results of this and in part the preceding chapter can be considered as a feasibility study. Before attempting to analyze the evoked response data in terms of some simple electrostatic models there were few indications that it was indeed possible to locate equivalent sources for this neuroelectric event. Certainly the qualitative studies mentioned in Chapter IV did not indicate at all the precision which could be expected of such analyses. The present results, although obtained from a restricted subject space, seem to clearly indicate that it is indeed feasible to extract equivalent dipole parameters from such experiments. Such a result has great significance in the analysis of evoked responses. This technique provides a means for comparing evoked responses in a way which is perhaps more appropriate to the nature of the signals than any other analytical method used to date. Now that the

results of this chapter demonstrate the existence of a new tool for analyzing evoked responses, I shall now discuss in the final chapter the significance of the present analyses from a neurophysiological point of view.

References for Chapter V

1. Marquardt, D. W., "Least-Squares Estimation of Nonlinear Parameters," IBM Share Program Catalog No. 3094 (1964).

VI. DISCUSSION

1. The Results of this Research

In the beginning stages of our study of human visual responses some very broad analytical questions were asked. What is the dimensionality of an evoked response? What set of parameters completely specifies the response and can changes in this set of general parameters be correlated with stimulus characteristics? What relationship exists between the surface potentials during a response and underlying cortical activity? As might perhaps be expected, the results to date do not completely answer these questions, particularly the last one. Rather, our analytical horizons spiralled inward somewhat and we selected some more specific subsets of the above queries for detailed study.

One of the first decisions was to attempt to study the evoked responses for what they rightfully are --- electromagnetic fields. This choice led to recordings of evoked responses with far greater spatial resolution of the potential fields than previously attempted and with it, our first problem. We were faced with the need to have some qualitative technique for reviewing data arrays which were almost overwhelming in size and dimension. I chose to meet this need with a graphical display of the evoked responses as equipotential lines on the head. As eventually expressed as an animated movie, this technique proved to be quite lucrative.

After developing this facility for rapid viewing and comparison of the data, the pursuit of simple physical models of the evoked response continued by seeking to find some bound on the complexity of the data space. The factor analytic methods of Chapter III extracted from the data the facts that firstly, the evoked responses, as suspected from the appearance of the movies of equipotential lines, showed great dependence from channel to channel, and secondly, that apparently the activity during three intervals of the responses was highly correlated within each such interval. The number of independent processes required to summarize the data variability suggested in fact that even electromagnetic models as simple as dipole sources could be used.

It thus seemed reasonable, in light of these results and recent advances in the fields of electrocardiography in particular and theoretical studies of bioelectric phenomena in general, to formulate some relationships between evoked responses and electrostatic dipoles. Equivalent sources for the activity during various phases of the evoked response were postulated, sought and eventually found. The result is that through this "painless" technique for analyzing this type of signal, the information flow through various regions in the brain can now in part be followed.

Certain features of these results deserve considerable expansion and even critical review, and I shall now attempt to evaluate more fully those aspects of this research that seem pivotal to what has already been done and to what should logically follow.

2. What is the Relevance of Equivalent Dipoles to Human Visual Evoked Responses?

No one pretends that the normal brain activity, even when performing whatever (alleged) simple processing accrues watching a light flash, is likely to be completely represented by one or two dipoles appearing and disappearing at various times following the light flash. These dipoles must be recognized as very gross approximation to the myriad neuroelectric events which are actually taking place. Yet the equivalent dipoles are not simply abstractions of the data consistent with the observed number of independent processes present.

The physical models of Chapter IV are after all, well steeped in the electromagnetic properties of neuroelectric phenomena. While the dipole model cannot differentiate between action potential fields and post-synaptic potential fields, it does represent the first order effect of the diffuse ionic currents that give rise to the measured scalp potentials. The key assumptions are first, that the stimulus - correlated activity following the light flash is confined to a relatively small region of the entire brain and second, that the potential measurement points are far from the source compared with the dimensions of the cortical volume containing the activity. One of the very founding premises concerning the evoked response activity is that a specific sense modality is stimulated and hence a limited population of neurones is involved at any given time during the response. This is a crucial point and should perhaps be reinforced.

The assumption of confinement of activity does not mean that the activity must be confined to a given volume over the entire response --- only that at each instant a certain small region can be identified as containing most of the processing appropriate to the stimulus. Hence, it seems that the first assumption is quite a reasonable one. As for the idea that the potential fields are measured at distances large compared with the distances between active neurones, it seems obvious that any single source is always quite far from most of the recording electrodes and is close to those electrodes directly over it only when it is highly eccentric. Most of the analyses of the evoked response potentials did not produce sources whose eccentricity challenged this assumption. Consider a case where the eccentricity was, say, 0.7. If the radius of the head is 10 cm, then the distance from the source to the surface is roughly 3 cm. Remembering that the dipole term in the potential field decreases as $1/R^2$ and the next term, the quadrupole term, falls off as $1/R^3$, the ratio of the contributions of the dipole field to the quadrupole field is roughly 3:1. Thus, even at this relatively high eccentricity, the non-dipolar terms are becoming small compared with the first order term, and the dipole approximation seems well justified.

Those intervals in the responses when the activity does not appear to be dipolar may in fact be the times when the neural processing is so diffuse that the higher order poles (quadrupole, octapole, etc.) should be included in postulating any equivalent

sources. Alternatively, they may simply be the times when information from one cortical area is being relayed to another area, hence no stable patterns emerge for long durations. In any event, the analyses in this thesis were confined to those periods in the response when the surface potentials seemed to be highly dipole-like.

Note that there is a precaution here in attempting to relate surface potentials attributable to equivalent dipoles and potential recordings in depth. The depth recordings can be derived from sites very close to the neural activity, and the fields at these close ranges are likely to be more complex than simple dipole fields.

There is no question of their being certain errors in locating the sources, caused by the non-sphericity of the head and errors in electrode placement. Adjustments could be made, however, to account for the actual shape of the head and to precisely locate each electrode on this true geometry of the head. In the meantime, the solutions derived prove the feasibility of the technique, and the geometric stretchings necessary to account for the above errors are simply refinements of the principle. I predict that when the analysis is extended to a larger number of subjects, we will find that the equivalent dipole will offer a new device for realistically studying the evoked response and related electroencephalographic signals. By recording the surface potentials during activation of an epileptic focus, for example, and subsequently locating the focus by surgical techniques, one will be

able to test the accuracy of the source location as predicted by the dipole analysis.

In summary, considering the strong physical basis from which the analysis follows and the already good agreement of the results with known neuroanatomical features, the dipole analysis seems both relevant and fertile.

3. What Neurological Insights Have Been Gained?

It is not surprising that the responses to all three stimuli were so similar for any one subject. The light flashes did not selectively stimulate temporal or nasal halves of either retina, hence both cortical hemispheres were excited in all three conditions. A full field flash to one eye is not grossly different stimulus from such a flash to the other eye, or to both eyes. When we look at a scene with only one eye, we see almost exactly that which is viewed with both eyes. Hence, the stimuli used in these experiments were not at all subtle, and by and large, the same cortical areas were probably active for all three conditions.

In this regard one might, however, hypothesize that while the stimulus presented to one eye triggers much the same cortical response as the stimulus to the other eye, there should perhaps be some summation effect when stimulating both eyes. In other words, should not some aspects of the equipotential maps and/or the dipole determinations suggest a superposition of the same aspects in the monocular cases? This appears not to be the case for the two

subjects here. One would have to conclude from looking at the equipotential maps that the flash to both eyes never seems to elicit any patterns which seem to be anything like the sum of the patterns arising from the monocular stimuli. Moreover, the dipole determinations of Chapter V show that the sources in the flash to both eyes condition are not significantly different from the sources in the other two conditions. The dipole magnitude and locations are generally identical for all three conditions. Neuroanatomically, this suggests that as far as these stimuli are concerned, the optic pathways at some point lose the ability to differentiate between "left eye origins" and "right eye origins" of the activation of a particular point in the mapping of overlapping visual areas. In other words, when light from a particular point in the visual field illuminates both retinae, the neural pathways from the eyes eventually seem to innervate in parallel the cortical area corresponding to the point, hence excitation arising from the stimulus to both eyes is redundant, and the responses to all three conditions are similar.

These experiments thus did not offer contrasts among evoked responses arising from various subdivisions of the primary visual cortex. Instead, the present analyses are more pertinent to understanding something of the time course of activity within the given responses.

I mentioned in Chapter I that the conduction time from retina to cortex has been estimated at approximately 40ms. Over this early portion of the evoked response one would not expect to see

patterns in the equipotential maps which were suggestive of any activity in the outer cortical layers. The excitation of the lateral geniculate and other relay centers along the route to the cortex presumably occurs at this time, but not with any accompanying manifestation of this activity in the surface potentials. It is in fact unlikely that activity at that depth has strong influence upon EEG signals. In Figure 4-4 I showed that as sources became less eccentric in the homogeneous model, the effect on the surface potentials is much attenuated. If we recall that the equations for the potential fields in both models (Equations 4-3 and 4-8) are linear in dipole magnitude but behave approximately as the inverse square of eccentricity, it is obvious that the location of the source has much more influence on the eventual surface potentials than does the magnitude of the source. Thus, even comparatively weak sources close to the surface can obscure the effect of stronger but deeper sources. To be precise about this, let us consider some calculations in the shell model, as a realistic measure of the trade-off between strength and location. A radial dipole of unit strength at an eccentricity of 0.85 produces a peak potential on the surface of $19.6 \mu\text{v}$, while such a dipole at an eccentricity of 0.2 produces a peak of only $3.6 \mu\text{v}$. The lateral geniculate structures are at approximately this latter eccentricity, hence in order to generate surface potentials of the same magnitude, any activity at this level would have to generate a dipole moment almost six times as strong as moments due to activity in the outer cortical layers. In the

homogeneous model the ratio is even higher, approximately 22:1. Thus, at times when processing is taking place at deeper sites in the brain, it becomes difficult for this activity to produce surface potentials that can be distinguished from those due to activity in more eccentric locations. This can occur at any time when information may be flowing from one cortical site to another, say, across the cerebral commissures (also relatively deep structures), or in particular during the first 50 ms of the response when the retinal afference is on its way to the visual cortex.

This alleged reticence of the evoked response during the first 40-50 ms seems to have been substantiated by our recordings --- the equipotential maps show no sign of any activity which seems to emanate from some cortical site for a significantly long period. In other words, the activity taking place at first seems to be largely the conduction of afferent information to the processing centers; at no time during this interval does the activity apparently remain in any one cortical site for any appreciable time.

Following this initial spread of the visual afference, however, some quite different events take place, and now our dipole analyses come into play. We saw that in both subjects there was a suggestion that some particular pattern of activity remained relatively stable for, say, 30ms (from about 60ms to 90ms), then this pattern abruptly yielded to a different one lasting from about 100ms to 130ms, then after a delay of some 25 or 30ms, a third stable configuration gained precedence. There is nothing sacred about this

division of the response into an initial conduction time followed by three intervals during which the activity is apparently confined to some region of the cortex. Each subject showed some violations of these general rules, and perhaps experimentation on a larger group of subjects will modify these generalizations. For now, however, let us consider what apparently takes place during these three active times.

The first conclusion one can draw from the results from both subjects (though more weakly for the KW data than for that from subject DALO) is that the activity taking place during the first and second active intervals is apparently in the same location for a given subject. Notice that during these two intervals, the equivalent dipoles are roughly perpendicular to the surface of the cortex, suggesting perhaps that many adjacent columns of cells are simultaneously active. The conduction of excitation up or down these columns would, as suggested in Chapter IV, generate many component dipoles all pointing in the same direction, and the net equivalent dipole would be oriented perpendicular to the cortical surface. (Note for the moment I am assuming that the cortical surface is parallel with the skull surface.)

Furthermore, whatever direction of flow exists during the interval from 60 to 90 ms seems to have been reversed in the second interval. This is particularly evident in the DALO data, for the equivalent dipoles seem to be in the same locations during both

intervals, but the orientation of the dipoles reverse direction by 180 degrees.

The equivalent dipoles for the DALO data in these intervals seem to be in the occipital region. As we know, however, the two occipital poles lie on opposite sides of the central fissure, and in fact, a considerable portion of the retinal representation is located along the medial aspects of the hemispheres, along the walls of the fissure. Assuming that both halves of the visual cortex are active, why are there not two symmetric equivalent dipoles for the activity at this time?

As we saw in Figure 4-6, it is not always easy to differentiate by eye the equipotential maps arising from two sources, when those sources are close to one another. And, as discussed in Chapter V, inverse determinations which attempt to fit two sources to data which seem best to arise from one source are not possible. The dipole technique as formulated here does not have the ability to resolve two such closely spaced sources.

But are there truly two symmetric sources for the DALO data in these first two active intervals? It would seem at least that if there are two, they are not symmetric, since there is generally a non-zero x-component of the dipole location, placing the dipole slightly left of center. Also, if there are two sources, they are so close together as to be well expressed as one, judging from the small standard deviation of the parameter estimates.

Thus for the DALO data, it would seem that during the time from about 60 ms to 130 ms, activity takes place in the primary visual cortex. There is activity predominantly in one direction along columns perpendicular to the scalp surface lasting until about 90 ms, followed by a reversal in this direction from 100 ms to 130 ms. If this activity takes place symmetrically in the occipital poles, then such activity is so close as to coalesce into one apparent source shifted slightly to the left hemisphere as far as equivalent dipoles are concerned.

The KW data over this same span are more difficult to interpret. There is the same suggestion in the appearance of the equipotential maps that whatever activity occurs from 50 to 70 ms is in the same location as the activity from 100 ms to 130 ms, but with reversed polarity. As mentioned in the previous chapter, however, there is not sufficient variation in the surface potentials to characterize these two sources in the earlier of the two periods. Beyond this problem, however, is the question of significance of the locations of the two sources found for the data from 100 ms to 130 ms.

In considering this question, let us consider that one of the features of this particular experiment which could quite possibly be in error is the electrode placement. If the assumed electrode positions represents a systematic stretching of the true locations forward and laterally, then it is not impossible that the true source

locations could be brought posteriorly and medially until they lay nearer the occipital regions than they presently are located. If this conjecture is allowed to run its course, it is also feasible that the two sources as betrayed by the surface distributions would again coalesce into a single source near the midline.

The above exercise is not intended to force the two subjects to be more similar in their responses. There is a strong possibility that the KW experiment suffered from lack of a precise location of the electrode array. It was the early realization of this problem that led to many conversations with Dr. Lehman and Mr. Madey concerning a diagrammatic retention of the actual electrode positions in future experiments.

In spite of the apparent disparity in locations of the equivalent dipoles for the two subjects during the first two active periods, however, other features of the analyses are similar. The dipole orientations for the KW data are also perpendicular to the cortical surface, but they have directions opposing those for the DALO data at comparable times.

In the aggregate then, if we allow some latitude with the KW determinations, both subjects seem to indicate that during the first two intervals in the evoked response when activity seems to reside in one location for some time, that location is in the occipital region. Certainly the DALO results indicate this with considerable force. It may be that this time during the response is the

principal period during which the visual event receives the attention of the primary visual cortex.

Following these two intervals, both subjects display another period where the surface potentials do not indicate that the activity is resident in any one site for any length of time. Then, at around 150 ms, there appears the beginning of a period of activity which is again confined to one region. As noted earlier, the equivalent dipoles for the two subjects are more similar here than at any other time, and would not become widely different even if we stretched the KW electrode positions as suggested above. At this third active period, it seems that the equivalent dipoles are again roughly perpendicular to the surface, but the locations are displaced laterally and anteriorly from the earlier determinations. It seems credible to hypothesize that if the earlier two regions contain the activity of the primary visual cortex, then this later period represents the activity of the association cortex in the left hemisphere. Perhaps some higher abstraction, beyond the simple sensation of the light flash, occurs at this time in the association cortex. One can wonder why the activity takes place only on one side, and perhaps there is a clue here which correlates with the dominance of the left hemisphere over the right in right-handed split-brain patients (I believe both subjects were right-handed). Whether, in fact, this activity does take place in the association cortex will have to be confirmed by many more experiments. It

does seem evident, however, that later in the evoked response the activity has shifted to a different focus from that active during early stages of the response.

Evoked responses have for years been conspicuously dissimilar from subject to subject. Perhaps the most remarkable result of this research is that even though the responses of these two subjects as classically displayed (Figure 2-8) are also different from subject to subject, there are many features which are quite similar when considered from an equivalent generator point of view. Continued application of these techniques seems warranted as a new tool in studying the evoked response.

4. The Homogeneous Model versus the Shell Model.

Intuitively, the shell model seems to be the more desirable representation of the brain and its surrounding structures. Beyond the mere qualitative charm of this model compared with the homogeneous model, we saw in Chapter IV that the potentials calculated in the shell model also seemed more reasonable than those in the homogeneous model --- the large peaks and troughs of the latter were quite subdued in the former, as is the case in the evoked response data. Thus, at first it seems that the shell model is the technique most likely to produce physically meaningful inverse solutions.

Also in Chapter IV, however, I found that when equivalent dipoles in the homogeneous model were calculated for potentials

generated from some dipole in the shell model, the disparity between the two sources was surprisingly small. Mostly the case was that for any given surface potential distribution, the homogeneous model produced dipoles which were less eccentric and less strong than in the shell model. In the accounting which really matters then, there is not a great difference in the two models, and this was shown to be true in the evoked response analyses of Chapter V.

In fact, there is a somewhat paradoxical property of the shell model which makes it more difficult to use in locating equivalent dipoles. This model apparently does represent more accurately the shielding effects of the layers of different conductivity surrounding the brain. This means that it more realistically portrays the fact that scalp EEG potentials are quite protected from underlying activity, i. e., moving a source around inside the shell model produces less effect on the surface potentials than changing the source in the homogeneous model. In other words, because the shell model is a more realistic model, it is more difficult to determine inverse dipole solutions with narrow confidence intervals for the parameter estimates, simply because one source in the shell model has much the same surface potential field as does another source in the same general area. This is also borne out by the relative widths of the confidence regions for the shell model analyses of Chapter V.

As a practical matter, one must then consider the cost-effectiveness of using the more sophisticated model.

Computationally, the homogeneous analysis is roughly one-hundredth as costly as the analysis with the shell model. Also, because of the relative insensitivity of the shell model to changes in the dipole parameters, it is less tolerant of sloppiness in the initial guesses of the dipole parameters. And, as we now see, the two models produce solutions which are quite similar. In view of these facts, was the shell model worth the great effort spent in deriving the necessary equations, programming the equations successfully and the cost of subsequent computing?

The answer to this is much more than a qualified yes. What the current shell model provides is not only the result that the homogeneous model is not as inaccurate as first suspected but also a system for improving the results derived from any analysis using the less complicated model. By this I infer that by more exhaustively studying the differences in inverse solutions from the two approaches, a method of "correcting" any result in the homogeneous case to agree more closely with the shell determination may be derived. The results expressed in Table 4-1 suggest that this correction process may not be as simple as a linear scaling from one set of dipole parameters to another, but further analyses such as produced that table should provide the

tools with which the homogeneous model can be adjusted to produce solutions closer to those of the shell model.

If we assume that the shell model is indeed the more realistic of the two, then we now have the ability to achieve the reality of the solutions from this model without having to incur its high computing cost. I propose then that there are two reasonable strategies for doing the analysis. The first is to compute equivalent dipoles using the homogeneous model and adjust them by some correction process to resemble the solution that would have been achieved by the shell analysis. Alternatively, as was done in this thesis, the analyses using the homogeneous model at many times during the response can be followed by a small number of analyses with the shell model, using modified versions of the homogeneous results as initial guesses for the shell calculations. Since the equivalent dipoles are relatively stable over each of the various intervals in the response, one needs comparatively few shell calculations to span most of the interesting cases.

In the aggregate then, one can conclude that the homogeneous model should provide for some time a technique for evaluating evoked response, and the shell model can always be used to provide more realistic determinations for the equivalent dipoles.

5. What Must Be Done Next?

The most obvious extension of the analysis described here is to increase the number of subjects. Given that the limited sampling

presented here offered the suggestion of certain similarities in the evoked response which were unnoticed prior to this time, it is desirable to determine the extent of these common features of the evoked response.

Coincident with enlarging the number of subjects must be a more rigorous study of actual head shapes and especially of electrode placement on the heads of the subject. Probably spherical models are satisfactory, if a "least-squares" sphere is chosen for the actual shape of the head of each subject. Of equal importance is the provision of an accurate mapping of electrode placement onto a spherical approximation to the posterior portion of the skull. The custom-fitted helmet mentioned in Chapter II may be of assistance here, since the electrode positions and the head shape are permanently recorded in the construction of the helmet. Alternatively, but probably more time consuming, is to construct a stereotaxic device for recording head shape and electrode positions.

Assuming that these instrumentation improvements can be realized, there are some modifications to the experimental procedures used in these studies which would produce recordings of more neuroanatomical significance than the results discussed there. More selective stimuli should be used to try to activate smaller sub-populations of the visual nervous system. Assymmetric stimuli, such as illumination of only portions of the retina, should

produce cortical responses which are more specific than those to a gross, full-field light flash. The flexibility in this regard is enormous. Patterns can be introduced into the stimuli, different patterns could be used in different retinal areas, flashes to both eyes can be presented at various latencies (to perhaps elicit some interactive effects); many other experiments, all more specific than those conducted in this study, are desirable.

In this same regard, there may be instances of subjects with known pathologies or who have experienced certain surgical interventions who would represent further ways of restricting the stimulus conditions. Split-brain patients and split optic chiasm patients represent ways of confining the visual afferent information to smaller regions of the cortex.

From an analytical point of view, there are also many procedures which seem to follow logically from what has been accomplished here. There may be an "optimum" physical model of the head from the point of view of locating equivalent sources for evoked response. Continued studies of homogeneous and inhomogeneous models in spherical and other geometries could probably improve the accuracy of the inverse determinations. There may be some useful information to be derived in assessing the contribution to the surface potentials of higher order poles than the dipole term, bearing in mind that this makes more stringent demands upon the accuracy with which the potentials are recorded.

This type of analysis at present requires considerable computing effort. One single procedure which is perhaps impractical for investigators who do not have access to devices which produce graphical output on film is the movie of equipotential maps. The principal use of this display was to allow formulation of dipole hypotheses for various sampling times of the evoked response. It may be possible to implement a pattern recognition scheme which circumvents the making of pictures and subsequent visual study by the experimenter. There may, for instance, be certain criteria based upon the spatial derivatives of the potentials which would allow coarse determinations of the "appearance" of the data. These procedures might be developed to the extent that the number and approximate location of possible sources could be ascertained without actually going through the process of making movies.

As is the case with any new type of analysis, especially analyses of biological phenomena, there is at this early stage of development a certain posture of "not knowing quite what to look for." The models presented here have removed the cloak from certain aspects of the human visual evoked response. I have shown merely the development of a new tool, but hopefully this tool will now be exploited in answering what was described in Chapter I as "the challenge of the evoked response."

The Dipole in a Homogeneous Sphere

1. The Potential Field Due to an Eccentric Dipole

Figure A-1 shows a dipole located in a homogeneous sphere at $r = fR$ along the z -axis. The dipole is of magnitude P , with components P_x, P_y and P_z as shown.

The field due to a dipole in a homogeneous sphere has been described by several authors. Frank⁽¹⁾ has produced a solution for a dipole coplanar with the x - z axes, while Smythe⁽³⁾ has a form of solution for a dipole both coplanar with the x - z axes and parallel with the z -axis. The form of solution used here is due to Geselowitz and Ishiwatari⁽²⁾, for a dipole as oriented in Figure A-1. For a dipole as shown, in a sphere with an insulating boundary, the potential at the surface of the sphere is given by:

$$V = \frac{P_z}{4\pi\sigma fR^2} \left[\frac{1-f^2}{(1+f^2-2f\mu)^{3/2}} - 1 \right] + \frac{P_x \cos\phi + P_y \sin\phi}{4\pi\sigma fR^2 \sin\theta} \left[\frac{3f-3f^2\mu+f^3-\mu}{(1+f^2-2f\mu)^{3/2}} + \mu \right] \quad (\text{A. 1})$$

where $\mu = \cos\theta$,

θ, ϕ are the azimuth and latitude in the coordinate system (r, θ, ϕ) .

In order to use this relation, we first show how to transform a coordinate system with an arbitrary dipole so that the z -axis passes through the center of the dipole.

Consider Figure A-2(a). In this rectangular x, y, z coordinate

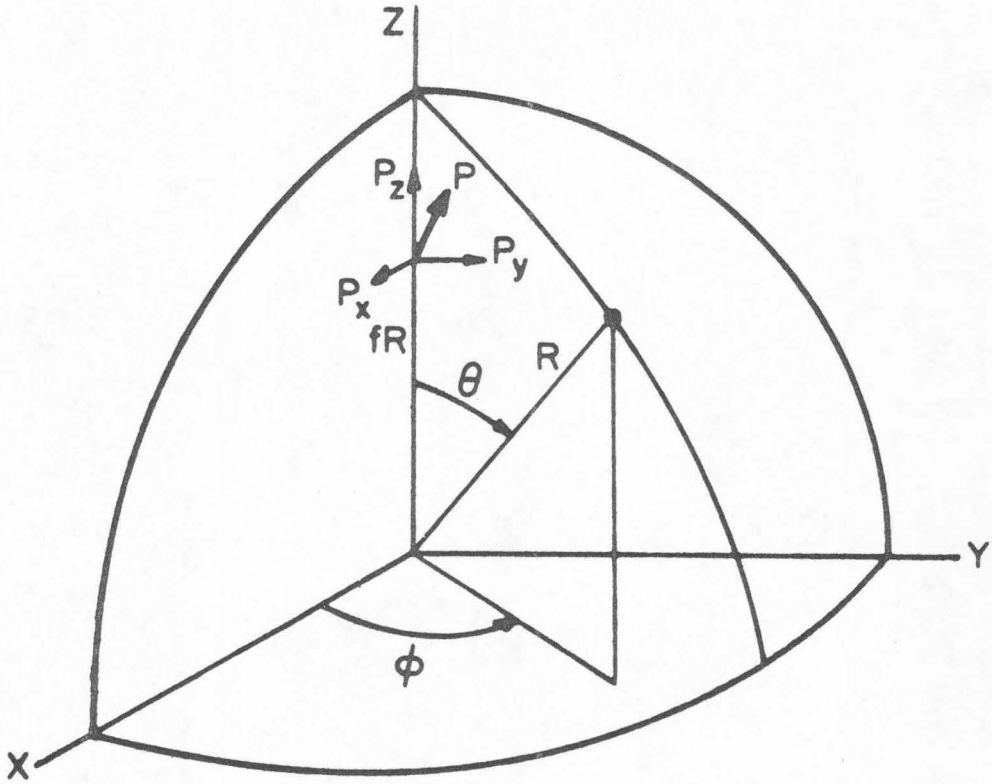


Figure A-1. A dipole of moment P , located at $(fR, 0, 0)$ in a homogeneous sphere of radius R .

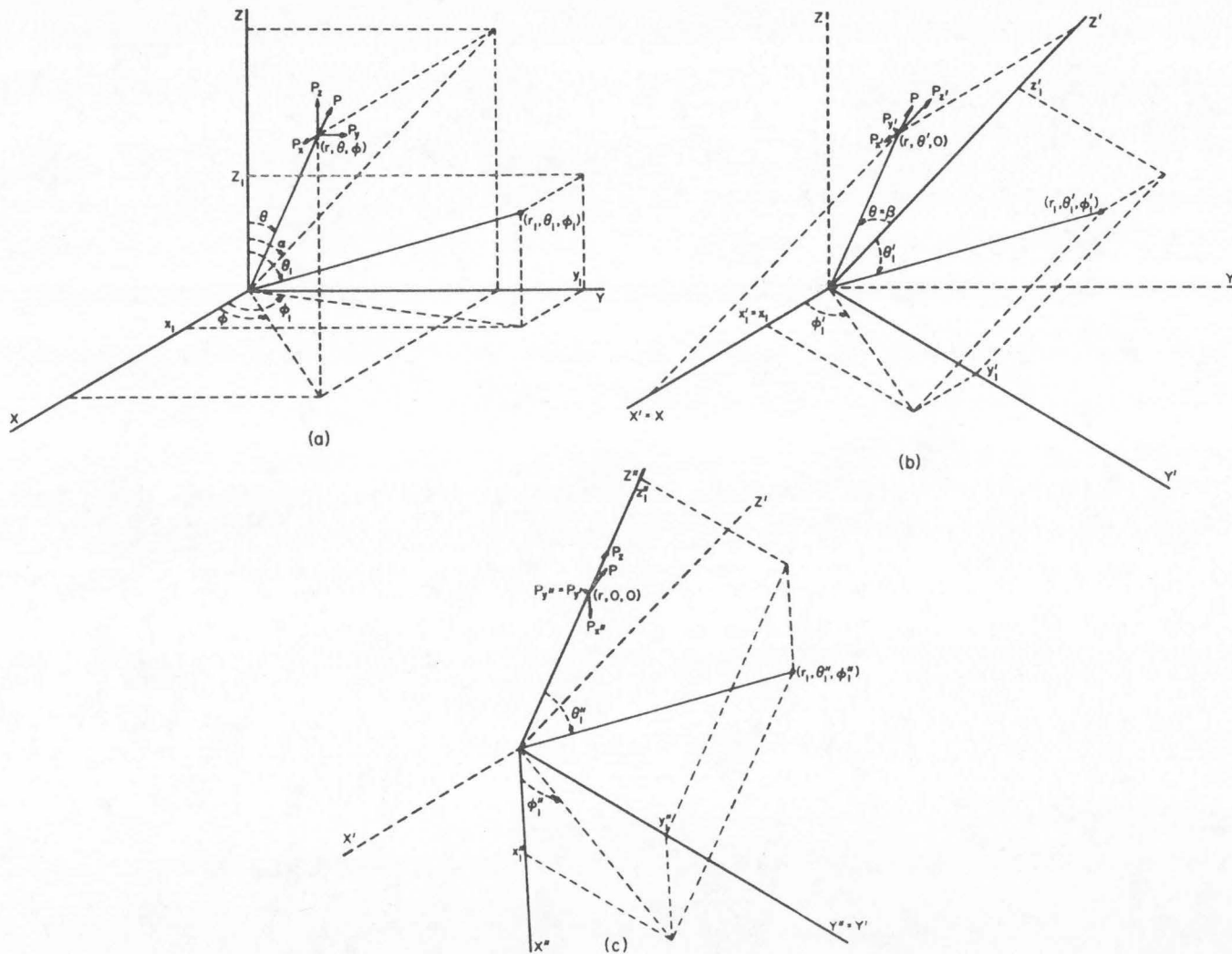


Figure A-2. Rotation of coordinate system. (a) an arbitrary dipole in original coordinate system, (b) resultant system after rotation of angle α about x -axis, (c) final system, after rotation of angle β about y' -axis.

system let the dipole be located at $(x, y, z) = (r, \theta, \phi)$ and let any other point $(x_1, y_1, z_1) = (r_1, \theta_1, \phi_1)$ be included for illustrative purposes.

In this system (a);

$$\begin{aligned}x &= r \sin \theta \cos \phi & x_1 &= r_1 \sin \theta_1 \cos \phi_1 \\y &= r \sin \theta \sin \phi & y_1 &= r_1 \sin \theta_1 \sin \phi_1 \\z &= r \cos \theta & z_1 &= r_1 \cos \theta_1\end{aligned}$$

We first wish to rotate the coordinate system about the x-axis such that the new z-axis is colinear with the projection of r onto the y-z plane. If this angle of rotation is α , then

$$\alpha = \tan^{-1} y/z . \quad (\text{A. 2})$$

Note we have considered α to be positive in the clockwise direction-- this is not necessary but serves to keep the rotation angles within the range 0 to $\pi/2$ for dipoles located in the first quadrant.

After this first rotation, the coordinates of the dipole in the new system (x', y', z') are

$$\begin{aligned}x' &= x \\y' &= 0 \\z' &= y \sin \alpha + z \cos \alpha\end{aligned}$$

At any point (x_1, y_1, z_1) in the original system (a) is now located at:

$$\begin{bmatrix} x'_1 \\ y'_1 \\ z'_1 \end{bmatrix} = \begin{bmatrix} 1 & 0 & 0 \\ 0 & \cos \alpha & -\sin \alpha \\ 0 & \sin \alpha & \cos \alpha \end{bmatrix} \begin{bmatrix} x_1 \\ y_1 \\ z_1 \end{bmatrix}$$

i. e.,

$$X'_1 = T_1 X_1 \quad . \quad (\text{A. 3})$$

Similarly, the dipole components in system (b) are given by:

$$\begin{bmatrix} P_{x'} \\ P_{y'} \\ P_{z'} \end{bmatrix} = T_1 \begin{bmatrix} P_x \\ P_y \\ P_z \end{bmatrix} \quad (\text{A. 4})$$

Finally, in order to pass the z' axis through the dipole location, system (b) must be rotated counterclockwise about the y' axis through an angle

$$\beta = \tan^{-1} \frac{x'_1}{z'_1} \quad . \quad (\text{A. 5})$$

Then in this final system (c) the dipole is located at

$$x'' = 0$$

$$y'' = 0$$

$$z'' = r$$

and any point (x_1'', y_1'', z_1'') in system (c) is related to system (b) by:

$$\begin{bmatrix} x_1'' \\ y_1'' \\ z_1'' \end{bmatrix} = \begin{bmatrix} \cos \beta & 0 & -\sin \beta \\ 0 & 1 & 0 \\ \sin \beta & 0 & \cos \beta \end{bmatrix} \begin{bmatrix} x_1' \\ y_1' \\ z_1' \end{bmatrix}$$

i. e. ,

$$X_1'' = T_2 X_1' = T_2 T_1 X_1 = T X_1 \quad (\text{A. 6})$$

where the final rotation matrix T is given by

$$\begin{bmatrix} \cos \beta & -\sin \alpha \sin \beta & -\cos \alpha \sin \beta \\ 0 & \cos \alpha & -\sin \alpha \\ \sin \beta & \sin \alpha \cos \beta & \cos \alpha \cos \beta \end{bmatrix}$$

and the dipole components in system (c) are given by:

$$\begin{bmatrix} P_{x''} \\ P_{y''} \\ P_{z''} \end{bmatrix} = T \begin{bmatrix} P_x \\ P_y \\ P_z \end{bmatrix} \quad (\text{A. 7})$$

System (c) is the necessary form for equation (A. 1) to apply. By substituting from (A. 7) we obtain the surface potential $V(R, \theta'', \phi'')$:

$$\begin{aligned}
 & V(R, \theta'', \phi'') \\
 &= \frac{1}{4\pi\sigma R^2} \left[\left\{ \frac{P_x \sin\beta + (P_y \sin\alpha + P_z \cos\alpha) \cos\beta}{f} \right\} \left\{ \frac{1-f^2}{(1+f^2-2f\mu'')^{3/2}} - 1 \right\} \right. \\
 &+ \left. \left\{ \frac{(P_x \cos\beta - (P_y \sin\alpha + P_z \cos\alpha) \sin\beta) \cos\phi'' + (P_y \cos\alpha - P_z \sin\alpha) \sin\phi''}{f \sin \theta''} \right\} \right. \\
 &\quad \left. \left\{ \frac{3f-3f^2\mu''+f^3-\mu''}{(1+f^2-2f\mu'')^{3/2}} + \mu'' \right\} \right] \quad (\text{A. 8})
 \end{aligned}$$

where $\mu'' = \cos \theta''$, $f = r/R$.

It remains to substitute into (A. 8) certain further relationships between system (a) and system (c). One can easily derive the following:

$$\cos \theta'' \equiv \mu(\alpha, \beta, \theta, \phi) = \sin\theta \cos\phi \sin\beta + (\sin\theta \sin\phi \sin\alpha + \cos\theta \cos\alpha) \cos\beta \quad (\text{A. 9})$$

$$\begin{aligned}
 \sin \theta'' &\equiv A(\alpha, \beta, \theta, \phi) \\
 &= [1 - \{ \sin\theta \cos\phi \sin\beta + (\sin\theta \sin\phi \sin\alpha + \cos\theta \cos\alpha) \cos\beta \}^2]^{\frac{1}{2}} \\
 &= [1 - \mu^2]^{\frac{1}{2}} \quad (\text{A. 10})
 \end{aligned}$$

$$\begin{aligned}
 \cos \phi'' &\equiv C(\alpha, \beta, \theta, \phi) \\
 &= [\sin\theta \cos\phi \cos\beta - (\sin\theta \sin\phi \sin\alpha + \cos\theta \cos\alpha) \sin\beta] / A \quad (\text{A. 11})
 \end{aligned}$$

$$\sin \phi'' = E(\alpha, \beta, \theta, \phi) = [\sin\theta \sin\phi \cos\alpha - \cos\theta \sin\alpha] / A \quad (\text{A. 12})$$

We can then finally write equation (A. 8) in terms of the original co-ordinate system (a) :

$$V(R, \theta, \phi) = \frac{1}{4\pi\sigma R^2} [V_1 V_2 + V_3 V_4] \quad (\text{A. 13})$$

where:

$$V_1 = [P_x \sin\beta + (P_y \sin\alpha + P_z \cos\alpha) \cos\beta] / f \quad (\text{A. 14})$$

$$V_2 = [(1-f^2)/(1+f^2-2f\mu)^{3/2} - 1] \quad (\text{A. 15})$$

$$V_3 = \frac{\{P_x \cos\beta - (P_y \sin\alpha + P_z \cos\alpha) \sin\beta\} C + \{P_y \cos\alpha - P_z \sin\alpha\} E}{fA} \quad (\text{A. 16})$$

$$V_4 = [(3f-3f^2\mu+f^3-\mu)/(1+f^2-2f\mu)^{3/2} + \mu] \quad (\text{A. 17})$$

2. Partial Derivatives of the Field

In order to use the technique of least squares estimation of non-linear parameters, it is also necessary to compute the partial derivatives of V with respect to the six parameters $P_x, P_y, P_z, \alpha, \beta,$ and f . These equations are somewhat more laborious to derive, but they can be shown to be:

$$\text{a) } \frac{\partial V}{\partial P_x} = V_2 \sin\beta / f + V_4 C \cos\beta / fA \quad (\text{A. 18})$$

$$b) \quad \frac{\partial V}{\partial P_y} = [V_2 \sin \alpha \cos \beta + V_4 \{E \cos \alpha - C \sin \alpha \sin \beta\} / A] / f \quad (A.19)$$

$$c) \quad \frac{\partial V}{\partial P_z} = [V_2 \cos \alpha \cos \beta - V_4 \{C \cos \alpha \sin \beta + E \sin \alpha\} / A] / f \quad (A.20)$$

$$d) \quad \frac{\partial V}{\partial \alpha} = V_2 \frac{\partial V_1}{\partial \alpha} + V_1 \frac{\partial V_2}{\partial \alpha} + V_4 \frac{\partial V_3}{\partial \alpha} + V_3 \frac{\partial V_4}{\partial \alpha} \quad (A.21)$$

where

$$\frac{\partial V_1}{\partial \alpha} = \frac{1}{f} \cos \beta [P_y \cos \alpha - P_z \sin \alpha] \quad (A.21a)$$

$$\frac{\partial V_2}{\partial \alpha} = 3\mu_\alpha f(1-f^2) / (1+f^2-2f\mu)^{5/2} \quad (A.21b)$$

$$\begin{aligned} \frac{\partial V_3}{\partial \alpha} = \frac{1}{fA} [& \{P_x \cos \beta - (P_y \sin \alpha + P_z \cos \alpha) \sin \beta\} C_\alpha \\ & - C \{ \sin \beta (P_y \cos \alpha - P_z \sin \alpha) \} + E_\alpha (P_y \cos \alpha - P_z \sin \alpha) \\ & - E (P_y \sin \alpha + P_z \cos \alpha) - V_3 f A_\alpha] \end{aligned} \quad (A.21c)$$

$$\frac{\partial V_4}{\partial \alpha} = \left[\frac{\{(1+f^2-2f\mu)(-3f^2\mu_\alpha - \mu_\alpha) + 3f\mu_\alpha(3f-3f^2\mu+f^3-\mu)\}}{\{1+f^2-2f\mu\}^{5/2}} + \mu_\alpha \right] \quad (A.21d)$$

$$\mu_\alpha = \cos \beta (\sin \theta \sin \phi \cos \alpha - \cos \theta \sin \alpha) \quad (A.21e)$$

$$A_\alpha = -\mu \mu_\alpha / A \quad (A.21f)$$

$$C_{\alpha} = \frac{1}{A^2} [A\{-\sin\beta(\sin\theta\sin\phi\cos\alpha - \cos\theta\sin\alpha)\} - A_{\alpha}\{\sin\theta\cos\phi\cos\beta - (\sin\theta\sin\phi\sin\alpha + \cos\theta\cos\alpha)\sin\beta\}] \quad (\text{A. 21g})$$

$$E_{\alpha} = \frac{1}{A} [A\{-\sin\theta\sin\phi\sin\alpha - \cos\theta\cos\alpha\} - A_{\alpha}\{\sin\theta\sin\phi\cos\alpha - \cos\theta\sin\alpha\}] \quad (\text{A. 21h})$$

$$e) \quad \frac{\partial V}{\partial \beta} = V_2 \frac{\partial V_1}{\partial \beta} + V_1 \frac{\partial V_2}{\partial \beta} + V_4 \frac{\partial V_3}{\partial \beta} + V_3 \frac{\partial V_4}{\partial \beta} \quad (\text{A. 22})$$

where

$$\frac{\partial V_1}{\partial \beta} = \frac{1}{f} [P_x \cos\beta - \sin\beta(P_y \sin\alpha + P_z \cos\alpha)] \quad (\text{A. 22a})$$

$$\frac{\partial V_2}{\partial \beta} = 3f\mu_{\beta}(1-f^2)/(1+f^2-2f\mu)^{5/2} \quad (\text{A. 22b})$$

$$\begin{aligned} \frac{\partial V_3}{\partial \beta} = & \frac{1}{fA} [C\{-P_x \sin\beta - \cos\beta(P_y \sin\alpha + P_z \cos\alpha)\} \\ & + C_{\beta}\{P_x \cos\beta - \sin\beta(P_y \sin\alpha + P_z \cos\alpha)\} \\ & + E_{\beta}\{P_y \cos\alpha - P_z \sin\alpha\} - fV_3 A_{\beta}] \end{aligned} \quad (\text{A. 22c})$$

$$\frac{\partial V_4}{\partial \beta} = \left[\frac{\{(1+f^2-2f\mu)(-3f^2\mu_{\beta}-\mu_{\beta})+3(3f-3f^2\mu+f^3-\mu)f\mu_{\beta}\}}{\{1+f^2-2f\mu\}^2+\mu_{\beta}} \right] \quad (\text{A. 22d})$$

$$\mu_{\beta} = \sin\theta\cos\phi\cos\beta - \sin\beta(\sin\theta\sin\phi\sin\alpha + \cos\theta\cos\alpha) \quad (\text{A. 22e})$$

$$A_{\beta} = -\mu\mu_{\beta}/A \quad (\text{A. 22f})$$

$$C_{\beta} = \frac{1}{A^2} [A\{-\sin\theta\cos\phi\sin\beta - \cos\beta(\sin\theta\sin\phi\sin\alpha + \cos\theta\cos\alpha)\} \\ - A_{\beta}\{\sin\theta\cos\phi\cos\beta - \sin\beta(\sin\theta\sin\phi\sin\alpha + \cos\theta\cos\alpha)\}] \quad (\text{A. 22g})$$

$$E_{\beta} = -A_{\beta}\{\sin\theta\sin\phi\cos\alpha - \cos\theta\sin\alpha\}/A^2 \quad (\text{A. 22h})$$

$$\text{f) } \frac{\partial V}{\partial f} = V_2 \frac{\partial V_1}{\partial f} + V_1 \frac{\partial V_2}{\partial f} + V_4 \frac{\partial V_3}{\partial f} + V_3 \frac{\partial V_4}{\partial f} \quad (\text{A. 23})$$

where

$$\frac{\partial V_1}{\partial f} = -V_1/f \quad (\text{A. 23a})$$

$$\frac{\partial V_2}{\partial f} = [2f(2f\mu - 1 - f^2) + 3(\mu - f)(1 - f^2)] / (1 + f^2 - 2f\mu)^{5/2} \quad (\text{A. 23b})$$

$$\frac{\partial V_3}{\partial f} = -V_3/f \quad (\text{A. 23c})$$

$$\frac{\partial V_4}{\partial f} = [(1 + f^2 - 2f\mu)(3 - 6f\mu + 3f^2) - 3(f - \mu)(3f - 3f^2\mu + f^3 - \mu)] / (1 + f^2 - 2f\mu)^{5/2} \quad (\text{A. 23d})$$

3. The Location of the Dipole

After the computer program has computed the optimum values for the parameters $P_x, P_y, P_z, \alpha, \beta,$ and $f,$ the parameters can be transformed back to system (a) so that the dipole is characterized by a location expressed as x, y, z coordinates and a magnitude composed

of the components P_x , P_y , and P_z . These latter three parameters are of course identically those returned by the program LSQENP, and the coordinates of the dipole are seen to be

$$x = f \sin \beta \quad (\text{A.24})$$

$$y = f \cos \beta \sin \alpha \quad (\text{A.25})$$

$$z = f \cos \beta \cos \alpha \quad (\text{A.26})$$

The errors in computing each of x , y , and z are seen to be:

$$\Delta x = \frac{\partial x}{\partial f} \Delta f + \frac{\partial x}{\partial \beta} \Delta \beta = \sin \beta \Delta f + f \cos \beta \Delta \beta \quad (\text{A.27})$$

$$\begin{aligned} \Delta y &= \frac{\partial y}{\partial f} \Delta f + \frac{\partial y}{\partial \alpha} \Delta \alpha + \frac{\partial y}{\partial \beta} \Delta \beta \\ &= \cos \beta \sin \alpha \Delta f + f \cos \beta \cos \alpha \Delta \alpha - f \sin \alpha \sin \beta \Delta \beta \end{aligned} \quad (\text{A.28})$$

$$\begin{aligned} \Delta z &= \frac{\partial z}{\partial f} \Delta f + \frac{\partial z}{\partial \alpha} \Delta \alpha + \frac{\partial z}{\partial \beta} \Delta \beta \\ &= \cos \beta \cos \alpha \Delta f - f \cos \beta \sin \alpha \Delta \alpha - f \cos \alpha \sin \beta \Delta \beta \end{aligned} \quad (\text{A.29})$$

4. Programming Notes

Notice that there are several equations in which the factor A appears in the denominator of one or more terms. As a programming consideration it is appropriate to consider what happens as $A \rightarrow 0$. By cataloging all those circumstances under which $A \rightarrow 0$ (or alternatively $\mu \rightarrow 1$) it is seen that for all possible ways in which this occurs, the following terms are also identically zero:

$$A_\alpha, A_\beta, C, C_\alpha, C_\beta, E, E_\alpha, E_\beta, \mu_\alpha, \mu_\beta, V_3, \frac{\partial V_3}{\partial \alpha}, \frac{\partial V_3}{\partial \beta} .$$

Also under these conditions the following are true:

$$\frac{\partial V}{\partial P_x} = V_2 \sin \beta / f ; \quad \frac{\partial V}{\partial P_y} = V_2 \sin \alpha \cos \beta / f ;$$

$$\frac{\partial V}{\partial P_z} = V_2 \cos \alpha \cos \beta / f .$$

References for Appendix A

1. Frank, E., "Electric Potential Produced by Two Point Current Sources in a Homogeneous Conducting Sphere," J. Appl. Physics 23 (1952), pp. 1225-1228.
2. Geselowitz, D. B. and Ishiwatari, H., "A Theoretical Study of the Effect of the Intracavity Blood Mass on the Dipolarity of an Equivalent Heart Generator," Proc. Long Island Jewish Hospital Symposium Vectorcardiography, North Holland Publ. Co. (1966), pp. 393-402.
3. Smythe, W. R., Static and Dynamic Electricity, McGraw-Hill, New York (1968), p. 276.

APPENDIX B

The Dipole in a Homogeneous Sphere Surrounded by
Two Concentric Shells of Different Conductivities

An expression is desired for the surface potential due to a dipole located in the innermost region of the model shown in Figure B-1(a). Region 1 of conductivity σ_1 and radius r_1 is intended to be an approximation to the brain and surrounding cerebro-spinal fluid, while regions 2 and 3 are used to represent the skull and scalp, respectively.

In order to solve this problem, consider a dipole source as shown in Figure B-1(b). Smythe⁽¹⁾ has shown that the potential due to a dipole of moment M , located parallel to the z -axis at $r = b$, $\theta = \theta_0$, $\phi = 0$ in an infinite region of conductivity σ is given by:

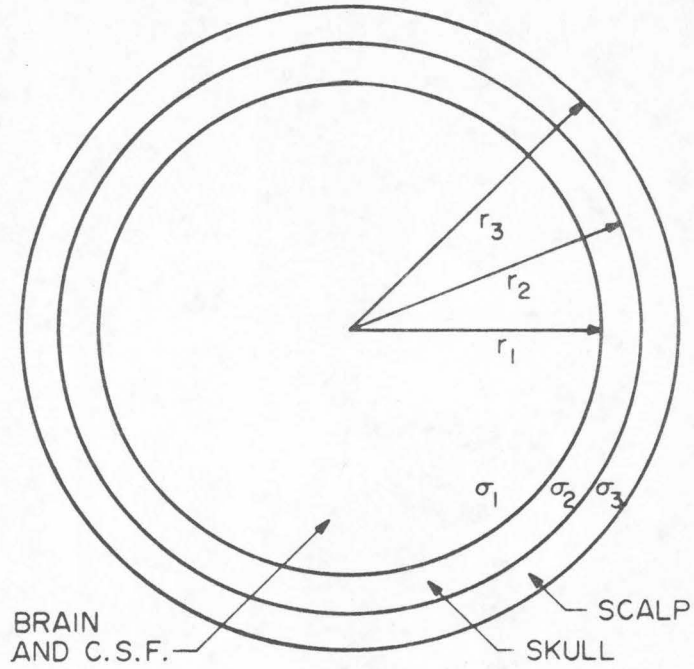
$$\Phi_P(r, \theta, \phi) = \sum_{n=0}^{\infty} \sum_{m=0}^n M_o r^{-(n+1)} P_n^m(\mu) \cos m\phi \quad (B.1)$$

where

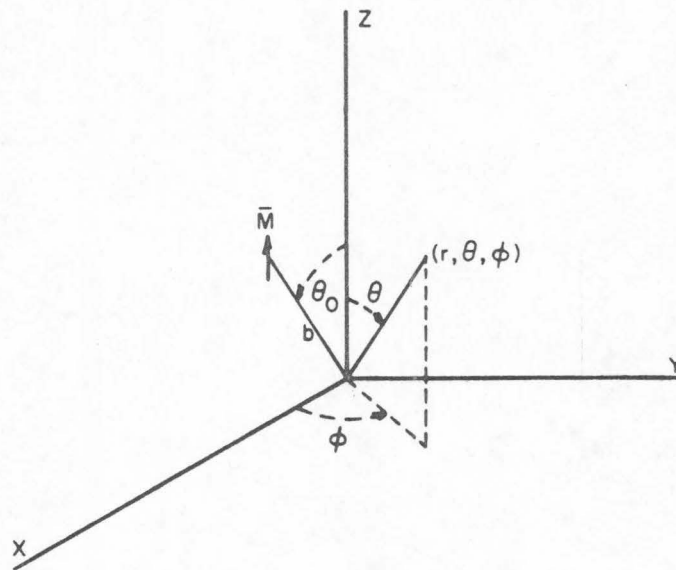
$$\begin{aligned} M_o &\equiv \frac{M}{4\pi\sigma b^2} \frac{(2-\delta_m^0)(n-m)!}{(n+m-1)!} b^{n+1} P_{n-1}^m(\mu_o) \\ &= \frac{M}{4\pi\sigma} \frac{(2-\delta_m^0)(n-m)!}{(n+m-1)!} b^{n-2} P_{n-1}^m(\mu_o) \end{aligned} \quad (B.2)$$

$$\mu_o = \cos \theta_o \quad (B.3)$$

$$\mu = \cos \theta \quad (B.4)$$



(a)



(b)

Figure B-1. (a) Concentric shell model of the head.
(b) Orientation of dipole in equation (B. 1).

$P_n^m(\mu)$ is the associated Legendre function of the first kind. The argument μ is real and in the range $-1 \leq \mu \leq 1$.

As was the case in Appendix A, the first problem is to transform a coordinate system with an arbitrary dipole into the form assumed by the equation for the potential.

1. Coordinate Transformation

Consider Figure B-2. In (a) is shown an arbitrary dipole \bar{M} with components \bar{M}_x , \bar{M}_y , and \bar{M}_z . The first stage of transformation is to rotate system (a) about the x-axis an angle α , where

$$\begin{aligned} \alpha &= \frac{\pi}{2} + \tan^{-1} \frac{M_z}{M_y} \quad , \quad M_y \neq 0 \quad , \\ \alpha &= 0 \quad , \quad M_y = 0 \quad . \end{aligned} \tag{B.5}$$

This rotation (note all positive angles are measured counterclockwise in this section) results in system (b) where

$$\begin{bmatrix} x' \\ y' \\ z' \end{bmatrix} = \begin{bmatrix} 1 & 0 & 0 \\ 0 & \cos\alpha & \sin\alpha \\ 0 & -\sin\alpha & \cos\alpha \end{bmatrix} \begin{bmatrix} x \\ y \\ z \end{bmatrix} \tag{B.6}$$

i. e. ,

$$X' = T_1 X$$

The next step is to rotate system (b) about the y' -axis an angle β , where

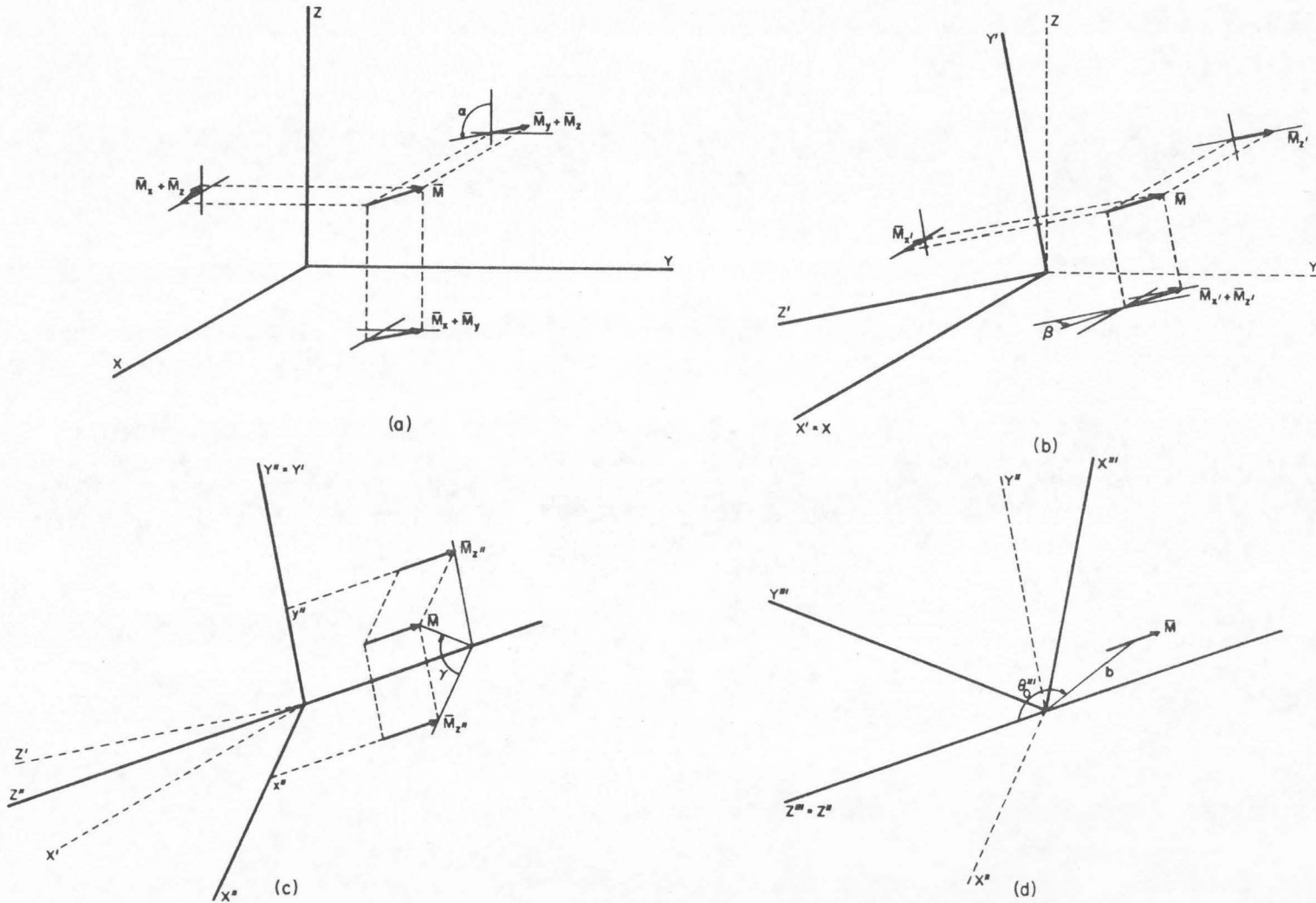


Figure B-2. Rotation of coordinate system. (a) dipole in original system, (b) system after rotation an angle α (C. C. W.) about x -axis, (c) system after rotation an angle β (C. C. W.) about y' -axis, (d) final system, after rotation angle γ (C. C. W.) about z'' -axis.

$$\beta = \tan^{-1} \frac{M_{x'}}{M_{z'}} \quad , \quad M_{z'} \neq 0$$

$$\beta = \pi/2 \quad , \quad M_{z'} = 0 \quad , \quad M_{x'} \neq 0 \quad .$$
(B.7)

System (c) is thus defined, wherein

$$\begin{bmatrix} x'' \\ y'' \\ z'' \end{bmatrix} = \begin{bmatrix} \cos\beta & 0 & -\sin\beta \\ 0 & 1 & 0 \\ \sin\beta & 0 & \cos\beta \end{bmatrix} \begin{bmatrix} x' \\ y' \\ z' \end{bmatrix}$$
(B.8)

i. e. ,

$$X'' = T_2 X' \quad .$$

Finally, system (c) is rotated about the z'' -axis an angle γ , such that in the final system the ϕ -coordinate of the dipole is 0.

$$\gamma = \tan^{-1} y''/x'' \quad , \quad x'' > 0$$

$$\gamma = \pi + \tan^{-1} y''/x'' \quad , \quad x'' < 0$$

$$\gamma = \pi/2 \quad , \quad x'' = 0 \quad , \quad y'' \geq 0$$

$$\gamma = -\pi/2 \quad , \quad x'' = 0 \quad , \quad y'' < 0 \quad .$$
(B.9)

The desired system (d) is thus achieved, wherein

$$\begin{bmatrix} x''' \\ y''' \\ z''' \end{bmatrix} = \begin{bmatrix} \cos\gamma & \sin\gamma & 0 \\ -\sin\gamma & \cos\gamma & 0 \\ 0 & 0 & 1 \end{bmatrix} \begin{bmatrix} x'' \\ y'' \\ z'' \end{bmatrix}$$
(B.10)

i. e. ,

$$X''' = T_3 X'' \quad .$$

And in system (d) note that

$$\begin{aligned}\theta_o &= \pi/2 - \tan^{-1} \frac{z'''}{|x'''}|, & x''' \neq 0 \\ &= 0, & x''' \rightarrow 0, \quad z''' > 0 \\ &= \pi, & x''' \rightarrow 0, \quad z''' < 0\end{aligned}\tag{B. 11}$$

The complete transfer from system (a) to system (d) is

$$\begin{aligned}x''' &= T_3 T_2 T_1 X \\ &= TX\end{aligned}\tag{B. 12}$$

where $T = T_3 T_2 T_1$ is:

$$\begin{bmatrix} \cos\beta\cos\gamma & \sin\alpha\sin\beta\cos\gamma + \cos\alpha\sin\gamma & -\cos\alpha\sin\beta\cos\gamma + \sin\alpha\sin\gamma \\ -\cos\beta\sin\gamma & -\sin\alpha\sin\beta\sin\gamma + \cos\alpha\cos\gamma & \cos\alpha\sin\beta\sin\gamma + \sin\alpha\cos\gamma \\ \sin\beta & -\sin\alpha\cos\beta & \cos\alpha\cos\beta \end{bmatrix}\tag{B. 13}$$

since T is an orthogonal transformation, $T^{-1} = T^T$.

2. The Surface Potential Distribution for the Concentric Shell Model

We now return to the problem of deriving the surface potential for a dipole placed somewhere inside region 1 of B-1(a). Let ϕ_1, ϕ_2, ϕ_3 be the potential in region 1, 2, and 3:

$$\phi_1 = \phi_p + \phi_g\tag{B. 14}$$

where ϕ_p is the dipole term given by (B. 1) and ϕ_g is the general solution of Laplace's Equation in spherical coordinates, i. e.,

$$\phi_g = \sum_{n=0}^{\infty} \sum_{m=0}^n \{A_{m_1} \cos m\phi + B_{m_1} \sin m\phi\} \{C'_{n_1} r^n + D'_{n_1} r^{-(n+1)}\} P_n^m(\cos\theta) \quad (\text{B. 15})$$

$$\phi_2 = \sum_{n=0}^{\infty} \sum_{m=0}^n \{A_{m_2} \cos m\phi + B_{m_2} \sin m\phi\} \{C'_{n_2} r^n + D'_{n_2} r^{-(n+1)}\} P_n^m(\cos\theta) \quad (\text{B. 16})$$

$$\phi_3 = \sum_{n=0}^{\infty} \sum_{m=0}^n \{A_{m_3} \cos m\phi + B_{m_3} \sin m\phi\} \{C'_{n_3} r^n + D'_{n_3} r^{-(n+1)}\} P_n^m(\cos\theta) \quad (\text{B. 17})$$

Note that in all regions there is symmetry with respect to the x-z plane, due to the orientation of the dipole in the coordinate system.

Hence, all $B_{m_i} \equiv 0$, $i = 1, 2$, and 3 . Then let all

$$A_{m_i} C'_{n_i} \equiv C_{mn_i}, \quad i = 1, 2, 3 \quad (\text{B. 18})$$

$$A_{m_i} D'_{n_i} \equiv D_{mn_i}, \quad i = 1, 2, 3 \quad (\text{B. 19})$$

Thus, for region 1,

$$\phi_1 = \sum_{n=0}^{\infty} \sum_{m=0}^n [C_{mn_1} r^n + D_{mn_1} r^{-(n+1)} + M_0 r^{-(n+1)}] P_n^m(\mu) \cos m\phi \quad (\text{B. 20})$$

but since the dipole is the only source in the region $r \leq b$ and there are no sources for $b < r \leq r_1$ $D_{mn_1} \equiv 0$. Hence, the forms of the

solutions in each of the three regions are given by:

$$\Phi_1 = \sum_{n=0}^{\infty} \sum_{m=0}^n [C_{mn_1} r^n + M_o r^{-(n+1)}] P_n^m(\mu) \cos m\phi \quad b < r \leq r_1 \quad (\text{B. 21})$$

$$\Phi_2 = \sum_{n=0}^{\infty} \sum_{m=0}^n [C_{mn_2} r^n + D_{mn_2} r^{-(n+1)}] P_n^m(\mu) \cos m\phi \quad r_1 \leq r \leq r_2 \quad (\text{B. 22})$$

$$\Phi_3 = \sum_{n=0}^{\infty} \sum_{m=0}^n [C_{mn_3} r^n + D_{mn_3} r^{-(n+1)}] P_n^m(\mu) \cos m\phi \quad r_2 \leq r \leq r_3 \quad (\text{B. 23})$$

In order to evaluate the unknown coefficients C_{mn_1} , C_{mn_2} , C_{mn_3} , D_{mn_2} , and D_{mn_3} , note the following boundary conditions. First, the potential must be continuous at the boundaries between regions 1 and 2 and between regions 2 and 3, i. e.,

$$\Phi_1(r_1, \theta, \phi) = \Phi_2(r_1, \theta, \phi) \quad (\text{B. 24})$$

$$\Phi_2(r_2, \theta, \phi) = \Phi_3(r_2, \theta, \phi) \quad (\text{B. 25})$$

Secondly, the normal current must be continuous at these same boundaries, i. e.,

$$\sigma_1 \frac{\partial \Phi_1}{\partial r}(r_1, \theta, \phi) = \sigma_2 \frac{\partial \Phi_2}{\partial r}(r_1, \theta, \phi) \quad (\text{B. 26})$$

$$\sigma_2 \frac{\partial \Phi_2}{\partial r}(r_2, \theta, \phi) = \sigma_3 \frac{\partial \Phi_3}{\partial r}(r_2, \theta, \phi) \quad (\text{B. 27})$$

Finally, the normal current at the outer surface of region 3 must be zero since the surrounding medium is assumed to be an insulator, i. e.,

$$\sigma_3 \frac{\partial \phi_3}{\partial r} (r_3, \theta, \phi) = 0 . \quad (\text{B. 28})$$

Evaluating these boundary conditions in terms of equations (B. 21), (B. 22), and (B. 23) yields:

$$r_1^n C_{mn_1} - r_1^n C_{mn_2} - r_1^{-(n+1)} D_{mn_2} = -r_1^{-(n+1)} M_o \quad (\text{B. 29})$$

$$r_2^n C_{mn_2} - r_2^n C_{mn_3} + r_2^{-(n+1)} D_{mn_2} - r_2^{-(n+1)} D_{mn_3} = 0 \quad (\text{B. 30})$$

$$\begin{aligned} \sigma_1 n r_1^{n-1} C_{mn_1} - \sigma_2 n r_1^{n-1} C_{mn_2} + (n+1) r_1^{-(n+2)} \sigma_2 D_{mn_2} = \\ (n+1) \sigma_1 M_o r_1^{-(n+2)} \end{aligned} \quad (\text{B. 31})$$

$$\begin{aligned} \sigma_2 n r_2^{n-1} C_{mn_2} - \sigma_3 n r_2^{n-1} C_{mn_3} - \sigma_2 (n+1) r_2^{-(n+2)} D_{mn_2} + \sigma_3 (n+1) r_2^{-(n+2)} D_{mn_3} = 0 \\ (\text{B. 32}) \end{aligned}$$

$$n r_3^{n-1} C_{mn_3} - (n+1) r_3^{-(n+2)} D_{mn_3} = 0 \quad (\text{B. 33})$$

or, combining the equation into matrix form:

$$A X = B \quad (\text{B. 34})$$

where

$$A = \begin{bmatrix} r_1^n & -r_1^n & 0 & -r_1^{-(n+1)} & 0 \\ 0 & r_2^n & -r_2^n & r_2^{-(n+1)} & -r_2^{-(n+1)} \\ \sigma_1 nr_1^{n-1} & -\sigma_2 nr_1^{n-1} & 0 & (n+1)\sigma_2 r_1^{-(n+2)} & 0 \\ 0 & \sigma_2 nr_2^{n-1} & -\sigma_3 nr_2^{n-1} & -\sigma_2 (n+1)r_2^{-(n+2)} & \sigma_3 (n+1)r_2^{-(n+2)} \\ 0 & 0 & nr_3^{n-1} & 0 & -(n+1)r_3^{-(n+2)} \end{bmatrix} \quad (B.35)$$

$$X = \begin{bmatrix} C_{mn_1} \\ C_{mn_2} \\ C_{mn_3} \\ D_{mn_2} \\ D_{mn_3} \end{bmatrix} \quad (B.36)$$

$$B = \begin{bmatrix} -r_1^{-(n+1)} M_o \\ 0 \\ (n+1)\sigma_1 r_1^{-(n+2)} M_o \\ 0 \\ 0 \end{bmatrix} \quad (B.37)$$

This system can be solved by the method of elimination to produce an equation of the form

$$\begin{bmatrix} 1 & - & - & - & - \\ 0 & 1 & - & - & - \\ 0 & 0 & 1 & - & - \\ 0 & 0 & 0 & 1 & - \\ 0 & 0 & 0 & 0 & 1 \end{bmatrix} X = B' \quad (B.38)$$

where the vector B' is the transformation of the vector B realized by carrying out the elimination procedure on the matrix composed of B adjoined to A . Now the unknowns can be found by recursion.

When this operation is carried out, the triangular matrix above is given by:

$$\begin{bmatrix} 1 & -1 & 0 & -r_1^{-(2n+1)} & 0 \\ 0 & 1 & -1 & r_2^{-(2n+1)} & -r_2^{-(2n+1)} \\ 0 & 0 & 1 & 0 & -\frac{(n+1)}{n} r_3^{-(2n+1)} \\ 0 & 0 & 0 & 1 & -K_1 \\ 0 & 0 & 0 & 0 & 1 \end{bmatrix} \quad (B.39)$$

where

$$K_1 = \left[\left(\frac{n}{2n+1} \right) \left(\frac{\sigma_3}{\sigma_2} \frac{(n+1)}{n} + 1 \right) + \left(1 - \frac{\sigma_3}{\sigma_2} \right) \left(\frac{n+1}{2n+1} \right) \left(\frac{r_3}{r_2} \right)^{-(2n+1)} \right] \quad (B.40)$$

The vector of constants, B', becomes

$$\begin{bmatrix} -r_1^{-(2n+1)} M_o \\ 0 \\ 0 \\ 0 \\ \frac{\sigma_1 r_1^{-(2n+1)} \frac{(2n+1)}{n} M_o}{K_3 + K_1 K_2} \end{bmatrix} \quad (\text{B. 41})$$

where

$$K_2 = \sigma_1 r_2^{-(2n+1)} \left[\left(\frac{r_1}{r_2} \right)^{-(2n+1)} \left\{ \left(\frac{n+1}{n} \right) \left(\frac{\sigma_2}{\sigma_1} \right) + 1 \right\} + \frac{\sigma_2}{\sigma_1} - 1 \right] \quad (\text{B. 42})$$

$$K_3 = \sigma_1 \left(1 - \frac{\sigma_2}{\sigma_1} \right) r_2^{-(2n+1)} \left\{ 1 + \frac{n+1}{n} \left(\frac{r_3}{r_2} \right)^{-(2n+1)} \right\} \quad (\text{B. 43})$$

Hence, since only the solution at the surface is desired, one need only solve for C_{mn_3} and D_{mn_3} and substitute into (B. 23).

Let $\bar{\phi}_s = \bar{\phi}_3 \Big|_{r=r_3}$ be the surface potential:

$$\bar{\phi}_s(r_3, \theta''', \phi''') = \sum_{n=0}^{\infty} \sum_{m=0}^n M_o K_{mn} P_n^m(\mu) \cos m\phi''' \quad (\text{B. 44})$$

where

$$M_o = \frac{M}{4\pi\sigma_1} \frac{(2-\delta_m^o)(n-m)!}{(n+m-1)!} b^{n-1} P_{n-1}^m(\mu_o) \quad (\text{B. 45})$$

$$\mu = \cos \theta'''$$

$$\mu_o = \cos \theta_o'''$$

$$K_{mn} = \frac{CK_1}{CK_2 + (CK_3)(CK_4)} \quad (\text{B. 46})$$

where

$$CK_1 = (2n+1)^2 \left(\frac{r_2}{r_1}\right)^{2n+1} r_3^{-(n+1)} \quad (\text{B. 47})$$

$$CK_2 = \left\{1 - \frac{\sigma_2}{\sigma_1}\right\} \left\{n^2 + n(n+1)\left(\frac{r_2}{r_3}\right)^{2n+1}\right\} \quad (\text{B. 48})$$

$$CK_3 = \left\{\frac{n}{2n+1} \left(\frac{\sigma_3}{\sigma_2} (n+1)+n\right) + n\left(\frac{n+1}{2n+1}\right) \left(1 - \frac{\sigma_3}{\sigma_2}\right) \left(\frac{r_2}{r_3}\right)^{2n+1}\right\} \quad (\text{B. 49})$$

$$CK_4 = \left\{\left(\frac{r_2}{r_1}\right)^{2n+1} \left(\frac{\sigma_2}{\sigma_1} (n+1)+n\right) + n\left(\frac{\sigma_2}{\sigma_1} - 1\right)\right\} \quad (\text{B. 50})$$

In order to compute Φ_s in terms of the original coordinate system, note that:

$$\cos \theta''' \equiv T(\theta, \phi, \alpha, \beta) = \sin \theta (\cos \phi \sin \beta - \sin \phi \sin \alpha \cos \beta) + \cos \theta \cos \alpha \cos \beta \quad (\text{B. 51})$$

$$\phi''' \equiv P(\theta, \phi, \alpha, \beta, \gamma) = \tan^{-1} y'''/x''' \quad , \quad (\text{B. 52})$$

where, from equation (B. 12),

$$x''' = r_3 [\cos\beta\cos\gamma\sin\theta\cos\phi + (\sin\alpha\sin\beta\cos\gamma + \cos\alpha\sin\gamma)\sin\theta\sin\phi + (\sin\alpha\sin\gamma - \cos\alpha\sin\beta\cos\gamma)\cos\theta] \quad (\text{B. 53})$$

$$y''' = r_3 [-\cos\beta\sin\gamma\sin\theta\cos\phi + (\cos\alpha\cos\gamma - \sin\alpha\sin\beta\sin\gamma)\sin\theta\sin\phi + (\cos\alpha\sin\beta\sin\gamma + \sin\alpha\cos\gamma)\cos\theta] \quad (\text{B. 54})$$

3. Partial Derivatives of the Field with Respect to the Dipole Parameter

The surface potential is again a function of six parameters, i.e.,

M	the dipole strength	
α	}	rotations of coordinate axes
β		
γ		
b	dipole eccentricity (as a fraction of r ₃)	
θ ₀	azimuth of dipole	

For the purpose of estimating these parameters by the program LSQENP, the partial derivatives with respect to each parameter are required.

$$i. \quad \frac{\partial \Phi_s}{\partial M} = \frac{1}{4\pi\sigma_1} \sum_{n=0}^{\infty} \sum_{m=0}^n \frac{(2-\delta_m^0)(n-m)!}{(n+m-1)!} b^{n-1} P_{n-1}^m(\mu_0) K_{mn} P_n^{mn}(\Gamma) \cos mP \quad (\text{B. 55})$$

$$\text{ii. } \frac{\partial \bar{\phi}}{\partial \alpha} = \sum_{n=0}^{\infty} \sum_{m=0}^n M_o K_{mn} [P_{n\alpha}^m(T) \cos m(P) - P_n^m(T) \{m \sin m(P) P_\alpha\}] \quad (\text{B. 56})$$

where

$$\begin{aligned} P_{n\alpha}^m(T) &\equiv \frac{\partial}{\partial \alpha} P_n^m(T) \\ &= \frac{1}{1-T^2} [(n+m)P_{n-1}^m(T) - nTP_n^m(T)] [-\sin\theta \sin\phi \cos\alpha \cos\beta - \cos\theta \sin\alpha \cos\beta] \end{aligned} \quad (\text{B. 57})$$

and

$$\begin{aligned} P_\alpha &\equiv \frac{\partial}{\partial \alpha} P \\ &= \frac{1}{x''^2 + y''^2} [x''' YCA - y''' XCA] \end{aligned} \quad (\text{B. 58})$$

$$\begin{aligned} YCA = \frac{\partial}{\partial \alpha} y''' &= r_3 \{ \sin\theta \sin\phi (-\sin\alpha \cos\gamma - \cos\alpha \sin\beta \sin\gamma) \\ &\quad + \cos\theta (\cos\alpha \cos\gamma - \sin\alpha \sin\beta \sin\gamma) \} \end{aligned} \quad (\text{B. 59})$$

$$\begin{aligned} XCA = \frac{\partial}{\partial \alpha} x''' &= r_3 \{ \sin\theta \sin\phi (\cos\alpha \sin\beta \cos\gamma - \sin\alpha \sin\gamma) \\ &\quad + \cos\theta (\cos\alpha \sin\gamma + \sin\alpha \sin\beta \cos\gamma) \} \end{aligned} \quad (\text{B. 60})$$

$$\text{iii. } \frac{\partial \bar{\phi}}{\partial \beta} = \sum_{n=0}^{\infty} \sum_{m=0}^n M_o K_{mn} [P_{n\beta}^m(T) \cos m(P) - P_n^m(T) \{m \sin m(P) P_\beta\}] \quad (\text{B. 61})$$

where

$$\begin{aligned}
 P_{n\beta}^m(T) &\equiv \frac{\partial}{\partial\beta} P_n^m(T) \\
 &= \frac{1}{1-T^2} [(n+m)P_{n-1}^m(T) - nTP_n^m(T)] [\sin\theta(\cos\phi\cos\beta + \sin\phi\sin\alpha\sin\beta) \\
 &\qquad\qquad\qquad - \cos\theta\cos\alpha\sin\beta] \qquad\qquad\qquad (B. 62)
 \end{aligned}$$

and

$$\begin{aligned}
 P_\beta &= \frac{\partial}{\partial\beta} P \\
 &= \frac{1}{x''^2 + y''^2} [x'''YCB - y'''XCB] \qquad\qquad\qquad (B. 63)
 \end{aligned}$$

$$\begin{aligned}
 YCB &= \frac{\partial}{\partial\beta} y''' \\
 &= r_3 \{ \sin\beta\sin\gamma\sin\theta\cos\phi - \sin\theta\sin\phi\sin\alpha\cos\beta\sin\gamma + \cos\theta\cos\alpha\cos\beta\sin\gamma \} \\
 &\qquad\qquad\qquad (B. 64)
 \end{aligned}$$

$$\begin{aligned}
 XCB &= \frac{\partial}{\partial\beta} x''' \\
 &= r_3 \{ -\sin\beta\cos\gamma\sin\theta\cos\phi + \sin\theta\sin\phi\sin\alpha\cos\beta\cos\gamma - \cos\theta\cos\alpha\cos\beta\cos\gamma \} \\
 &\qquad\qquad\qquad (B. 65)
 \end{aligned}$$

iv. $\frac{\partial\Phi}{\partial\gamma}$, noting that only P is a function of γ ,

$$= - \sum_{n=0}^{\infty} \sum_{m=0}^n m M_o K_{mn} P_n^m(T) \sin m(P) P_\gamma \qquad\qquad\qquad (B. 66)$$

where

$$P_{\gamma} = \frac{\partial}{\partial \gamma} P$$

$$= \frac{1}{x''''^2 + y''''^2} [x'''' YCG - y'''' XCG] \quad (\text{B. 67})$$

$$YCG = \frac{\partial}{\partial \gamma} y''''$$

$$= r_3 \{ -\cos\beta \cos\gamma \sin\theta \cos\phi - \sin\theta \sin\phi (\cos\alpha \sin\gamma + \sin\alpha \sin\beta \cos\gamma) \\ + \cos\theta (\cos\alpha \sin\beta \cos\gamma - \sin\alpha \sin\gamma) \}$$

(B. 68)

$$XCG = \frac{\partial}{\partial \gamma} x''''$$

$$= r_3 \{ -\cos\beta \sin\gamma \sin\theta \cos\phi + \sin\theta \sin\phi (-\sin\alpha \sin\beta \sin\gamma + \cos\alpha \cos\gamma) \\ + \cos\theta (\sin\alpha \cos\gamma + \cos\alpha \sin\beta \sin\gamma) \}$$

(B. 69)

$$\text{v.} \quad \frac{\partial \Phi}{\partial b} \frac{s}{b} = \sum_{n=0}^{\infty} \sum_{m=0}^n (n-1) \frac{M}{b} K_{mn} P_n^m(T) \cos m(P) \quad (\text{B. 70})$$

$$\text{vi.} \quad \frac{\partial \Phi}{\partial \theta_0} \frac{s}{\theta_0} = \sum_{n=0}^{\infty} \sum_{m=0}^n \frac{M}{4\pi\sigma_1} \frac{(2-\delta_m^0)(n-m)!}{(n+m-1)!} b^{n-1} K_{mn} P_n^m(T) \cos m(P) \\ \{ P_{n-1}^m(\mu_0)(-\sin\theta_0) \}$$

(B. 71)

where

$$P_{n-1}^m(\mu_0) = \frac{\partial}{\partial \mu_0} P_{n-1}^m(\mu_0)$$

$$= \frac{1}{1-\mu_0} [n\mu_0 P_{n-1}^m(\mu_0) - (n-m)P_n^m(\mu_0)] \quad (\text{B. 72})$$

4. The Dipole Location

Once an optimum solution for the six parameters is obtained, it is necessary to transform them back into the original coordinate system. Note that the dipole as located in system (d) of Figure B-2 is located at $(b, \theta_o, 0)$ with components $\bar{M}_{z'''} = \bar{M}$, $\bar{M}_{x'''} = \bar{M}_{y'''} = 0$. In rectangular coordinates, the dipole is of course located at

$$\begin{aligned}x''' &= b \sin \theta_o''' \\y''' &= 0 \\z''' &= b \cos \theta_o'''\end{aligned}\tag{B.73}$$

Thus, referring to equation (B.12) and noting that $T^{-1} = T^T$, the location of the dipole in system (a) is given by

$$\begin{bmatrix} x \\ y \\ z \end{bmatrix} = T^T \begin{bmatrix} b \sin \theta_o''' \\ 0 \\ b \cos \theta_o''' \end{bmatrix}\tag{B.74}$$

and the dipole components are given by:

$$\begin{bmatrix} P_x \\ P_y \\ P_z \end{bmatrix} = T^T \begin{bmatrix} 0 \\ 0 \\ M \end{bmatrix}\tag{B.75}$$

The errors in the six parameters $x, y, z, P_x, P_y,$ and P_z can be calculated from the errors in $M, \alpha, \beta, \gamma, b,$ and θ_0 by the relations:

$$\begin{aligned} \Delta x = & \Delta\beta \{ b \cos\beta \cos\theta_0 - b \sin\beta \cos\gamma \sin\theta_0 \} - \Delta\gamma \{ b \cos\beta \sin\gamma \sin\theta_0 \} \\ & + \Delta b \{ \cos\beta \cos\gamma \sin\theta_0 + \sin\beta \cos\theta_0 \} \\ & + \Delta\theta_0 \{ b \cos\beta \cos\gamma \cos\theta_0 - b \sin\beta \sin\theta_0 \} \end{aligned} \quad (B.76)$$

$$\begin{aligned} \Delta y = & \Delta\alpha \{ b \sin\theta_0 (\cos\alpha \sin\beta \cos\gamma - \sin\alpha \sin\gamma) - b \cos\theta_0 \cos\alpha \cos\beta \} \\ & + \Delta\beta \{ b \sin\alpha \cos\beta \cos\gamma \sin\theta_0 + b \sin\alpha \sin\beta \cos\theta_0 \} \\ & + \Delta\gamma \{ b \sin\theta_0 (\cos\alpha \cos\gamma - \sin\alpha \sin\beta \sin\gamma) \} \\ & + \Delta b \{ \sin\theta_0 (\sin\alpha \sin\beta \cos\gamma + \cos\alpha \sin\gamma) - \sin\alpha \cos\beta \cos\theta_0 \} \\ & + \Delta\theta_0 \{ b \cos\theta_0 (\sin\alpha \sin\beta \cos\gamma + \cos\alpha \sin\gamma) + b \sin\alpha \cos\beta \sin\theta_0 \} \end{aligned} \quad (B.77)$$

$$\begin{aligned} \Delta z = & \Delta\alpha \{ b \sin\theta_0 (\sin\alpha \sin\beta \cos\gamma + \cos\alpha \sin\gamma) - b \cos\theta_0 \sin\alpha \cos\beta \} \\ & + \Delta\beta \{ -b \sin\theta_0 \cos\alpha \cos\beta \cos\gamma - b \cos\theta_0 \cos\alpha \sin\beta \} \\ & + \Delta\gamma \{ b \sin\theta_0 (\cos\alpha \sin\beta \sin\gamma + \sin\alpha \cos\gamma) \} \\ & + \Delta b \{ \sin\theta_0 (-\cos\alpha \sin\beta \cos\gamma + \sin\alpha \sin\gamma) + \cos\theta_0 \cos\alpha \cos\beta \} \\ & + \Delta\theta_0 \{ b \cos\theta_0 (-\cos\alpha \sin\beta \cos\gamma + \sin\alpha \sin\gamma) - b \sin\theta_0 \cos\alpha \cos\beta \} \end{aligned} \quad (B.78)$$

$$\Delta P_x = \Delta M \sin\beta + \Delta\beta M \cos\beta \quad (B.79)$$

$$\Delta P_y = -\Delta M \sin\alpha \cos\beta - \Delta\alpha M \cos\alpha \cos\beta + \Delta\beta M \sin\alpha \sin\beta \quad (B.80)$$

$$\Delta P_z = \Delta M \cos\alpha \cos\beta - \Delta\alpha M \sin\alpha \cos\beta - \Delta\beta M \cos\alpha \sin\beta \quad (B.81)$$

5. Programming Notes

Since all of the equations central to the calculations of either the potential or the partial derivatives are in infinite series form, some convergence criteria must be set for the series. It was found by testing the computer implementations of the equations that generally the series achieve reasonable convergence by the time the degree of the Legendre functions becomes about five. After that, successive values of the sum of the series oscillate weakly about the point of convergence. The convergence criterion eventually incorporated was to stop summing the series at the point where three successive terms were smaller than some fraction, δ , of the current value of the series. For the series which evaluated the potential at any point, a satisfactory value of δ was found to be 0.02 or 0.03; for the partial derivatives δ was set at 0.05. These values were determined to be the optimum trade-off between computing time and satisfactory accuracy.

References for Appendix B

1. Smythe, W. R., Static and Dynamic Electricity, McGraw-Hill, New York (1968), p. 238.

APPENDIX C

Details of Preliminary Data Re-Formatting

The data were received from the San Francisco laboratory on punched paper tape; Figure C-1 shows the format of the data as punched on the paper tape. Each channel of the evoked response as averaged by the CAT 1000 computer was registered as 256 samples taken at one ms intervals. Successive samples from the CAT are integers in the range 0-999999, and a calibration factor for each channel is thus required to scale the CAT integers into microvolts.

As shown in Figure C-1, each one of the 256 samples is encoded by three paper tape characters, where each paper tape character contains two decimal digits, written on the tape in 8-4-2-1 BCD code. Note that the 8-4-2-1 code is not strictly followed - decimal "0" was punched on the tape as BCD "10." Preceding the $3 \times 256 = 768$ paper tape characters representing the averaged evoked response for one channel was a six-digit (three tape character) identification sequence consisting of experiment number and channel number.

The paper tapes were read at the Caltech computing facility, producing "images" of contiguous paper tape records on a digital magnetic tape. In order to decode the paper tape images an assembler -- language subroutine (DECODE) was written. This

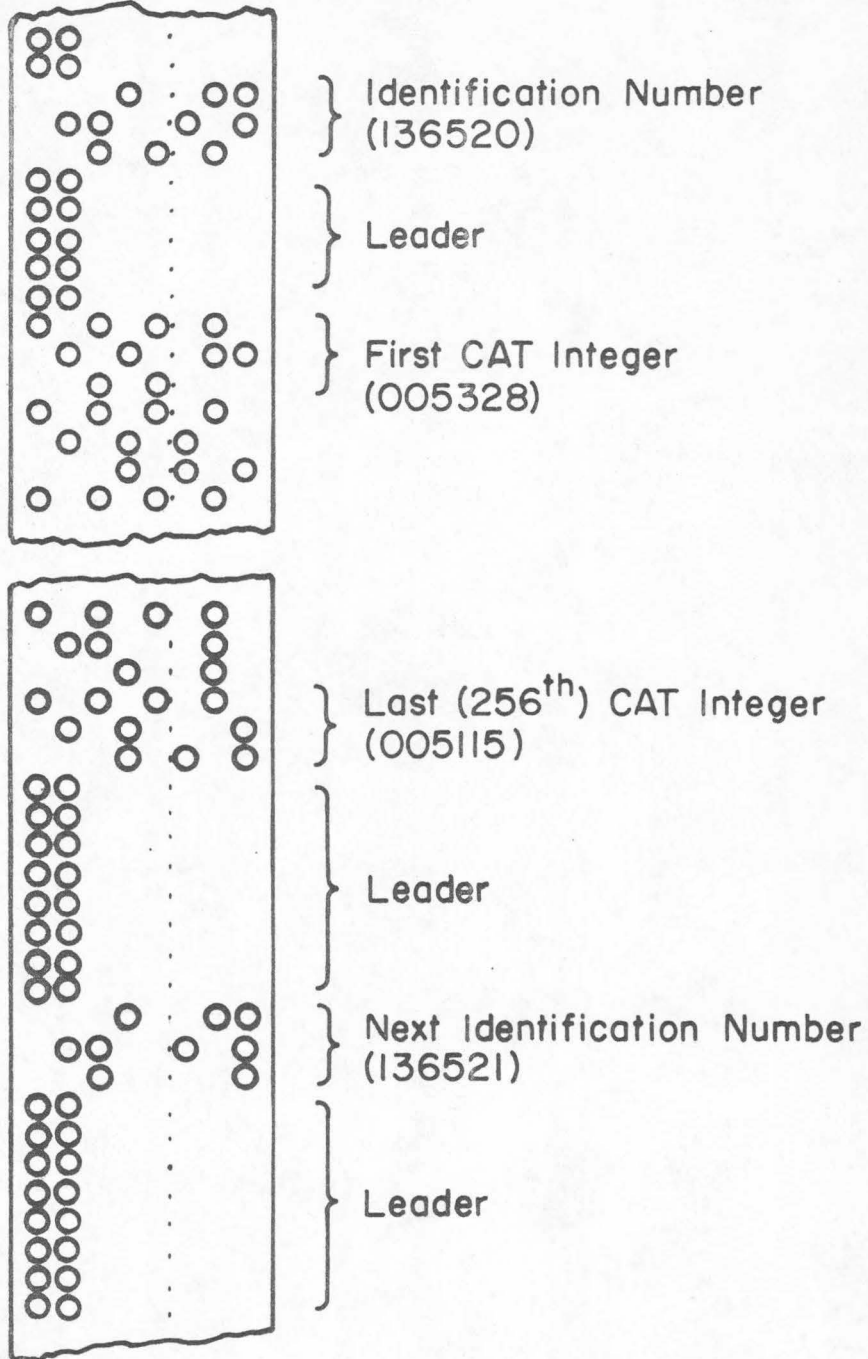


Figure C-1. Format of CAT paper tape. Records of 256 - 6 digit (3 tape characters) integers follow one 6 digit identification number.

routine converted the data from the paper tape format to full word integers and passed them back to the Fortran calling program.

After conversion to Fortran integers, the data were written onto another digital tape. This tape was subsequently read by a calibration program which scaled the data to have units of microvolts, encoded as Fortran "real" numbers. Again a new tape was written, containing the calibrated data.

This last operation thus produced, for each subject, a tape containing three replications of N channels of responses to three experimental conditions. This tape of $3 \times 3 \times N$ records was processed by a program which produced the final "raw" data tape for each subject. The format of this tape is shown in Figure C-2.

Since there were three replications of each experiment for each subject, a "mean" response for each channel was derived by averaging over replications. Thus, for each channel for some condition, the 256 potential values have some mean value and a standard deviation of this mean value. The mean response and the standard deviations of the mean response for each channel occupy the first $2 \times 256 = 512$ words of the record shown in Figure C-2.

Sometimes it is of course possible to suffer spurious conversion and sampling errors which produce "maverick" data values. The effects of these erroneous points are minimized by smoothing the mean curve with a smoothing function shown in Figure C-3. As indicated, a second order polynomial is fitted in a least-squares sense to seven consecutive data points. Each data

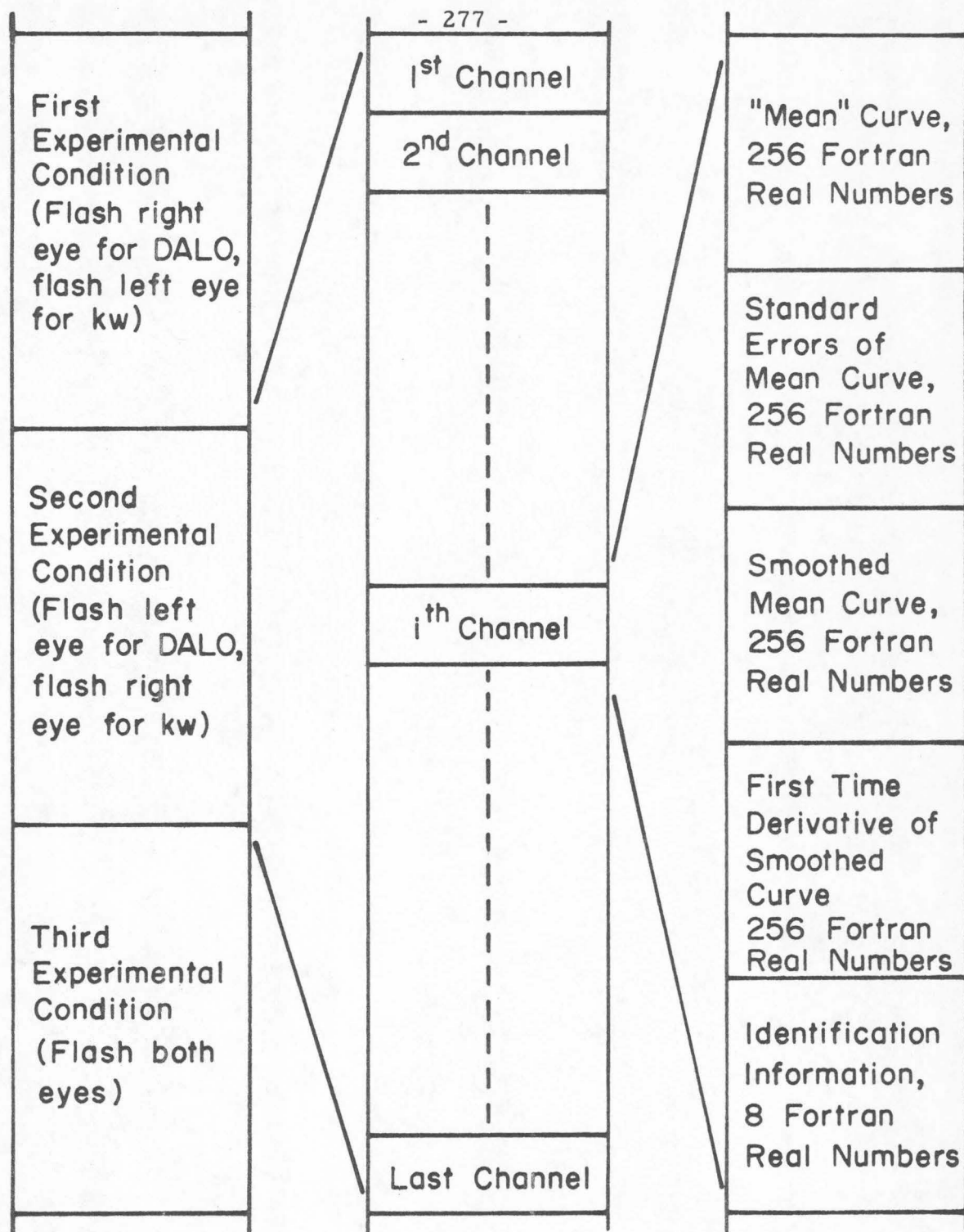


Figure C-2. Format of digital magnetic tape of "raw" data for each subject.

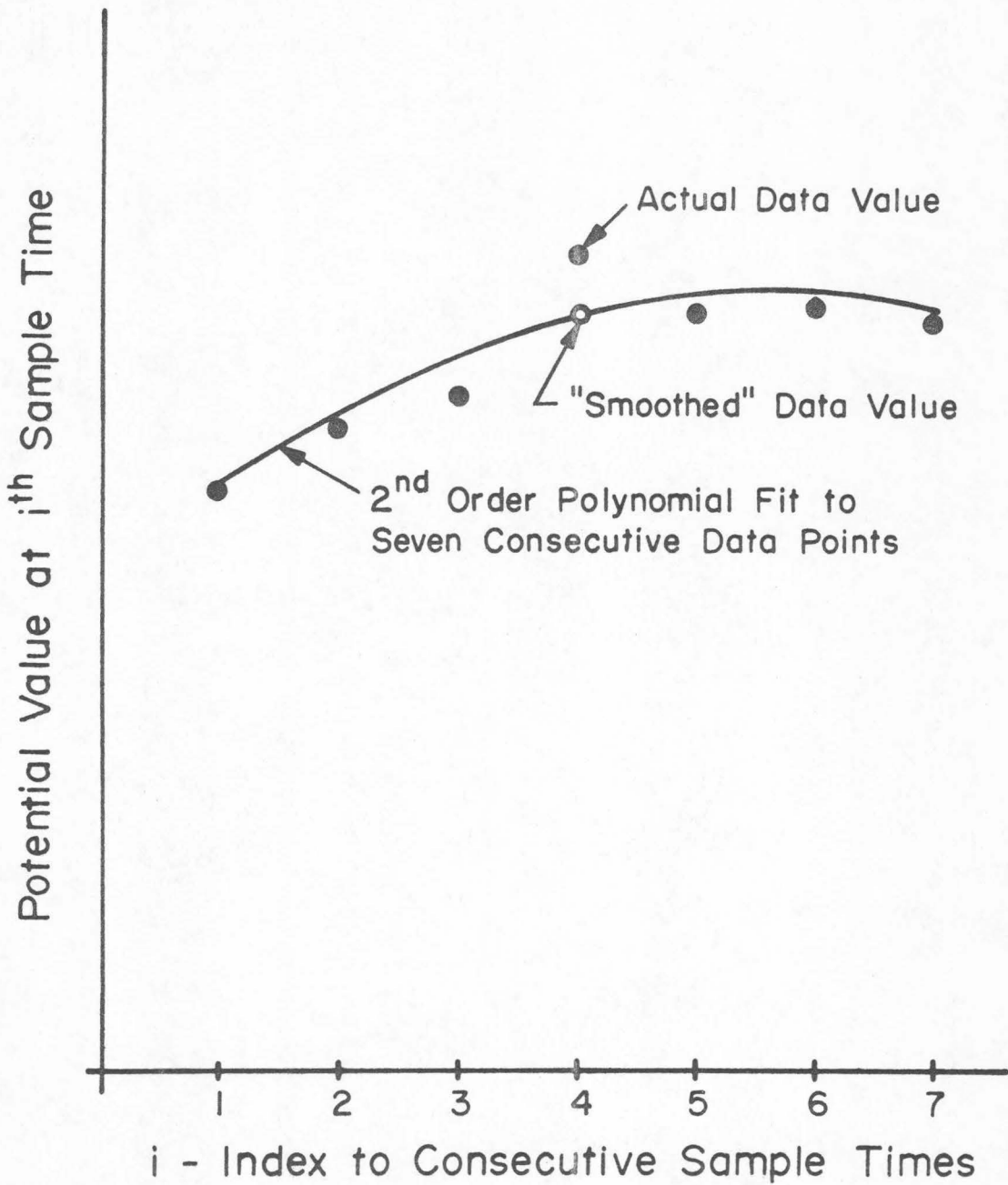


Figure C-3. Smoothing of evoked responses by fitting second order polynomial to seven data points and calculating smoothed value at middle point.

point is weighted inversely according to its standard deviation in determining the coefficients of the polynomial. After fitting the second order curve, a new value for the middle point is calculated from the polynomial expression. This point does not replace the original data value in storage, but a new, smoothed curve is constructed entirely from seven unsmoothed values at a time. The first and last values of the smoothed curve are constrained to be identically those of the original trace. The second and third and the second last and third last values of the smoothed curve are derived from fitting the polynomial to only three and five ordinate values respectively. This smoothed curve is found in the third group of 256 real numbers in the record pertinent to one channel of one condition.

It was desired at one stage to produce not only a smoothed curve for each response but also the first time derivative of that response. This is easily derived at the same time that the responses are smoothed, by also evaluating the slope of the polynomial, at the point which was smoothed. This group of values of the slope of the mean curve fills the fourth 256 positions of each record of Figure C-2.

Finally, the record which describes the response in one channel for one condition is concluded by some eight words of information such as channel number and label information. The data tape thus formed contains $3 \times N$ records, one for each of N channels

- 280 -

for each of three conditions. It is this tape for each subject which is used in all subsequent analyses.